Synthesis and structure-activity studies of well-defined nickel complexes as catalysts for cross coupling of alkyl electrophiles

THÈSE Nº 6729 (2015)

PRÉSENTÉE LE 28 AOÛT 2015
À LA FACULTÉ DES SCIENCES DE BASE
LABORATOIRE DE SYNTHÈSE ET DE CATALYSE INORGANIQUE
PROGRAMME DOCTORAL EN CHIMIE ET GÉNIE CHIMIQUE

ÉCOLE POLYTECHNIQUE FÉDÉRALE DE LAUSANNE

POUR L'OBTENTION DU GRADE DE DOCTEUR ÈS SCIENCES

PAR

Pablo Marcelo PEREZ GARCIA

acceptée sur proposition du jury:

Dr R. Hovius, président du jury
Prof. X. Hu, directeur de thèse
Prof. C. Saouma, rapporteuse
Prof. M.-E. Moret, rapporteur
Prof. S. Gerber, rapporteuse

ÉCOLE POLYTECHNIQUE
FÉDÉRALE DE LAUSANNE

Suisse
2015

Acknowledgments

First, I would like to express all my gratitude to my advisor, Prof. Xile Hu, for all his never-ending and positive support and his guidance during the last four years. I am very grateful for his trust having given me the opportunity to become part of his research group to work on such interesting project. The lessons that I received during all our instructive discussions have become cornerstones in my professional life as chemist.

I would to thank my thesis jury: Prof. Sandrine Gerber, Prof. Caroline Saouma, Prof. Marc-Etienne Moret and Dr. Ruud Hovius, who kindly accepted to review this manuscript.

I would like to thank all past and present co-workers of the LSCI. Either friends or colleagues, I will always remember them for the nice work environment and the enjoyable moments outside from the lab. I am especially grateful to Thomas, Peng and Alessio for all the academic collaborations. I would like to thank Nicolas and Alexander for all the experimental help. I will also like to give a big thanks to Dr. Heron Vrubel, Dr. Dafa Chen and Dr. Oleg Vechorkin for all their technical and academic guidance when I arrived to the group.

I cannot forget to thank all the people working at EPFL: Annelise Carrupt, Gladys Pache, Benjamin Kronenberg and Giovanni Petrucci from the BCH-magasin; Dr. Rosario Scopelliti and Dr. Euro Solari for the X-Ray and elemental analysis; Martial Rey, Anto Barisic and Dr. Pascal Miéville for their NMR technical support; Dr. Luc Patiny for his academic guidance for 2D NMR analysis; Christina Zamanos-Epremian and Anne-Lene Odegaard for their kind support for the administrative work; Donald Zbinden and Patrick Favre for the IT support. And a special thanks to my mentor, Dr. Anne-Sophie Chauvin, for all her advices and positive support.

Abstract

Cross coupling reactions have become ubiquitous tools for chemists in fundamental research and industrial production. During the last years, significant efforts are devoted to develop methods for cross coupling of alkyl electrophiles. These substrates are challenging to cross couple because they are less prone to oxidative addition, and because unproductive β-hydride elimination often competes favorably with the cross coupling. β-hydride elimination tends to be slower when nickel based catalysts are used compared to palladium based ones. Besides the economic advantage of nickel, its chemistry involving radical mechanisms gives a wide range of possibilities, e.g. higher reactivity for the coupling of secondary alkyl electrophiles. The catalytic activity of nickel complexes can be electronically and sterically modulated by a judicious design of the ancillary ligands. This dissertation is devoted to the development of well-defined nickel complexes as catalysts for cross coupling processes of alkyl electrophiles.

In chapter one, we summarize recent cross coupling methodologies of alkyl electrophiles using nickel based catalysts. The description of each study includes the coupling conditions, the substrate scope and the mechanistic considerations.

In chapter two, we report the development of high diastereoselective alkyl-alkyl Kumada coupling method for 1,3- and 1,4-substituted cyclohexyl halides and tetrahydropyrans using an amido bis(amine) nickel complex "Nickamine" as catalyst. The stereochemical properties of the starting materials and of the coupling products were determined by NMR techniques. The mechanistic investigations of the coupling provided evidence of a reversible activation of the alkyl halide.

In chapter three, we present the synthesis of new bidentate amido – amine ligands derived from 2,5-dimethylpyrrolidine or α-methylbenzylamine. The ligands were used to synthesize well-defined bidentate nickel complexes by transmetallation from the corresponding lithium complexes. A complex having an α-methylbenzylamine derived ligand and 2,4-lutidine as co-ligand was an effective catalyst for the coupling of non-activated secondary iodides with alkyl Grignard reagents. An enantiomerically pure version of this complex was synthesized and no racemization was observed during the synthesis. The chiral complex showed no asymmetric induction capacity as a cross coupling catalyst.

In chapter four, the synthesis of new amido bis(amine) pincer ligands derived from α-methylbenzylamine or pyrrolidine are described. The metallation of a NNN ligand derived from α-methylbenzylamine was not possible by transmetallation from the corresponding lithium complex or by oxidative addition from the corresponding chloroamine. A well-defined pincer nickel complex was synthesized by Li – Ni transmetallation using a NNN ligand having dimethyl amino and pyrolidine donors. Crystal structure analysis shows that the pyrrolidine donor is slightly less hindered. This complex is an effective catalyst for alkyl-alkyl and alkyl-aryl Kumada coupling of non-activated primary and secondary alkyl halides. The coupling process shows good functional group tolerance. This is the first time that a well-defined nickel pincer complex shows high catalytic activity for Kumada coupling reactions of sterically hindered alkyl substrates.

In chapter 5, a well-defined nickel pincer complex bearing an alkyl amine donor is synthesized. The complex is able to catalyzed direct coupling of non-activated primary halides with terminal alkynes at room temperature. The catalysis has a good substrate scope and high functional group tolerance. Kinetic data suggest that the new pincer ligand is hemilabile, and the dissociation of the alkyl amine donor is the turnover-determining step of the catalysis. An intermediate Ni-alkynyl species has been isolated and structurally characterized. The reactivity of this species gives insight into the nature of the active species for the activation of alkyl halide.

Keywords: nickel, Kumada coupling, Grignard reagent, diastereoselective, alkynylation, Sonogashira coupling, hemilabile ligands, kinetics, pincer ligands, alkyl electrophiles.

Résumé

Les réactions de couplage sont devenues des outils omniprésents pour les chimistes dans la recherche fondamentale et la production industrielle. Ces dernières années, des efforts considérables ont été consacrés pour le développement de méthodologies pour les réactions de couplage des électrophiles alkyles. Ces substrats sont difficiles à faire réagir car ils sont moins sujets à l'addition oxydante et parce que la réaction d'élimination de β-hydrure rivalise fortement avec la réaction de couplage. L'élimination de β-hydrure a tendance à être plus lente dans un catalyseur à base de nickel comparé à un catalyseur à base de palladium. Hormis les avantages économiques du nickel, sa chimie impliquant des mécanismes radicalaires donne un large éventail de possibilités comme les réactions de couplage des électrophiles alkyle secondaires. L'activité catalytique du nickel peut être modulée électroniquement et stériquement par une conception judicieuse des ligands auxiliaires. Cette dissertation est consacrée au développement de complexes de nickel bien définis utilisés comme catalyseurs pour les réactions de couplage des électrophiles alkyles.

Dans le premier chapitre, nous résumons les méthodologies récemment développées pour les réactions de couplage des électrophiles alkyle utilisant des catalyseurs à base de nickel. La description de chaque étude inclue les conditions de couplage, l'étendue des substrats ayant réagi et les considérations mécanistiques.

Dans le deuxième chapitre, nous rapportons le développement d'une méthodologie de couplage de Kumada hautement diastereosélective pour des halogénures de cyclohexyle 1,3- et 1,4-substitués et pour des dérivés de tetrahydropyranes en utilisant un complexe de nickel amido bis(amine) "Nickamine" comme catalyseur. Les propriétés stéréochimiques des produits de départ et des produits de couplage ont été déterminées par des techniques d'analyse RMN. L'étude mécanistique de ces couplages a mis en évidence une activation réversible de l'halogénure d'alkyle.

Dans le troisième chapitre, nous présentons la synthèse de nouveaux ligands bidentés amido – amine dérivés de la 2,5-diméthylepyrrolidine ou de la α-méthylebenzylamine. Les ligands ont servi ensuite à synthétiser des complexes de nickel bidentés bien définis par transmétallation à partir des complexes de lithium correspondants. Un complexe ayant un ligand dérivé de la α-méthylebenzylamine et de la 2,4-lutidine comme co-ligand s'est avéré être un catalyseur

efficace pour le couplage d'iodures d'alkyle secondaires non-activés avec des réactifs des organomagnésiens de type alkyle. Une version énantiomèriquement pure de ce complexe a été synthétisée sans racémisation. Le complexe chiral n'a pas montré de capacité d'induction asymétrique en tant que catalyseur de réactions de couplage.

Dans le quatrième chapitre, nous décrivons la synthèse de nouveaux ligands "pincer" amido bis(amine) dérivés de la α-méthylebenzylamine et de la pyrrolidine. La métallation d'un ligand NNN dérivé de la α-méthylebenzyleamine n'a pas été possible par transmétallation à partir du complexe de lithium correspondant ou par addition oxydante à partir de la chloroamine correspondante. Un complexe de nickel bien défini a été synthétisé par transmétallation Li – Ni à partir d'un ligand portant des groupes donneurs diméthyle amino et pyrrolidine. L'analyse de la structure cristalline montre que le groupe donneur pyrrolidine est légèrement moins encombré stériquement. Ce complexe est un catalyseur efficace pour le couplage de Kumada alkyle-alkyle ou alkyle-aryle des halogénures d'alkyle primaires et secondaires non-activés. La réaction de couplage présente une bonne tolérance pour différents types de groupes fonctionnels. Ce complexe "pincer" de nickel bien défini est le premier dans la littérature à montrer une activité catalytique élevée dans les réactions de couplage de Kumada de substrats alkyles stériquement encombrés.

Dans le cinquième chapitre, un complexe "pincer" de nickel bien défini ayant un groupe donneur amino alkyle est synthétisé. Le complexe est capable de catalyser le couplage direct entre des halogénures d'alkyle non-activés et des alcynes terminaux à température ambiante. La catalyse est efficace avec une grande variété de substrats et tolère un nombre élevé de groupes fonctionnels. Des données cinétiques suggèrent que le nouveau complexe "pincer" est hémilabile, et que la dissociation du groupe donneur amino alkyle est l'étape cinétiquement déterminante de la catalyse. Une espèce intermédiaire Ni-alcynyl a été isolée et caractérisée structurellement. La réactivité de cet intermédiaire donne un aperçu des espèces actives pour l'activation de l'halogénure d'alkyle.

Mots - clés: nickel, couplage de Kumada, organomagnésien, diastereosélectif, alcynylation, couplage de Sonogashira, ligand hemilabile, cinétique, ligand "pincer", électrophiles alkyle.

List of symbols and abbreviations

Å	angstrom
acac	acetylacetonate
ax.	axial
BBN	9-borobicyclo[3.3.1]-nonane
BOC	tert-butyloxycarbonyl
bpy	bipyridine
cat.	catalyst
COD	1,5-cyclooctadiene
d	doublet
dba	dibenzylideneacetone
deg	degrees
diglyme	bis(2-methoxyethyl) ether
diop	(2,3-O-isopropylidene-2,3-dihydroxy-1,4-bis(diphenylphosphino)butane)
DMA	N,N-dimethylacetamide
dme	1,2-dimethoxyethane
DMF	N,N-dimethylformamide
DMI	1,3-Dimethyl-2-imidazolidinone
DMSO	dimethyl sulfoxide
dppf	1,1'-bis(diphenylphosphino)ferrocene
dr	diastereoselective ratio
ee	enantiomeric excess
eq.	equatorial
equiv.	equivalent
Et_2O	diethyl ether
EtOH	ethanol
GC	gas chromatography
GC – MS	gas chromatography – mass spectrometry
glyme	1,2-dimethoxyethane
HMPA	Hexamethylphosphoramide
HPLC	high-performance liquid chromatography

HRESI – MS	High-resolution electrospray ionisation mass spectrometry
HSQC	Heteronuclear Single Quantum Correlation
^{i}BuOH	isobutanol
^{i}PrOH	isopropanol
K	Kelvin degrees
k_{cat}	catalyst rate constant
k_{OBS}	observed rate constant
LiHMDS	Lithium bis(trimethylsilyl)amide
LiO^{t}Bu	lithium tert-butoxyde
m	multiplet
M	molar
MeI	methyl iodide
MeLi	methyl lithium
mg	milligram
mL	milliliter
μL	microliter
mmol	millimol
mol	mol
MS	mass spectrometry
NaHMDS	sodium bis(trimethylsilyl)amide
^{n}Bu	n-butyl
^{n}BuLi	n-butyl lithium
NCS	N-Chlorosuccinimide
NEP	N-ethylpyrrolidone
NMP	N-Methylpyrrolidone
NMR	nuclear magnetic resonance
O-TMDEA	bis[2-(N,N-dimethylaminoethyl)]ether
Pd$_2$(dba)$_3$	tris(dibenzylideneacetone)dipalladium(0)
Ph	phenyl
ppm	parts per million
py	pyridine
Pybox	2,6-bis[(4R)-4-phenyl-2-oxazolinyl]pyridine
QTOF	quadrupole time of flight

Ruphos   [[3-(diethoxyphosphinothioylthio)-1,4-dioxan-2-yl]thio]-diethoxy-
                  thioxophosphorane

rt   room temperature

^{s}Bu   sec-butyl

t   triplet

TBAI   tetrabutylammonium iodide

^{t}BuOH   tert-butanol

TEMPO   (2,2,6,6-Tetramethylpiperidin-1-yl)oxyl

THF   tetrahydrofuran

TMDEA   tetramethylethylenediamine

Table of Contents

Chapter 1 : Introduction

1.1 Cross coupling reactions of alkyl electrophiles with organometallic reagents

Transition metal catalyzed cross coupling reactions have become an ubiquitous tool of organic chemists for selective carbon – carbon bond formation.[1,2] The pioneering work of Heck[3-7] describing the addition of *in situ* formed methyl and phenylpalladium halides to olefins was a cornerstone for the development of this field. Several coupling methods have been discovered using transition metals as catalysts to couple the nucleophilic carbon of an organometallic reagent with an electrophilic carbon typically coming from a carbon – halide bond. These reactions have been categorized by the nature of organometallic reagent and the name of the discoverer. In this way, the Kumada,[8] Sonogashira,[9] Negishi,[10] Suzuki,[11] Stille[12] and Hiyama[13] couplings have become permanent terms in the vocabulary of chemists. The relevance of these intellectual contributions was recognized by the Nobel Prize in chemistry awarded in 2010 to Richard F. Heck, Ei-ichi Negishi and Akira Suzuki. Figure 1 shows the organometallic species involved for each type of coupling reaction.

Kumada-Corriu-Tamao:

$$R^1-X \quad + \quad R^2-MgY \quad \xrightarrow{\text{cat.}} \quad R^1-R^2$$
Organomagnesium

Sonogashira:

$$R^1-X \quad + \quad R^2\!\!=\!\!\!=\!\!CuY \quad \xrightarrow{\text{cat.}} \quad R^1\!\!=\!\!\!=\!\!R^2$$
Organocuprate
in situ formed

Negishi:

$$R^1-X \quad + \quad R^2-ZnY \text{ or } (R^2)_2Zn \quad \xrightarrow{\text{cat.}} \quad R^1-R^2$$
Organozinc

Suzuki-Miyaura:

$$R^1-X \quad + \quad R^2-B(YZ)_2 \quad \xrightarrow{\text{cat.}} \quad R^1-R^2$$
Organoborane

Stille:

$$R^1-X \quad + \quad R^2-Sn(R^3)_2 \quad \xrightarrow{\text{cat.}} \quad R^1-R^2$$
Organostannane

Hiyama:

$$R^1-X \quad + \quad R^2-Si(YR^3)_2 \quad \xrightarrow{\text{cat.}} \quad R^1-R^2$$
Organosilane
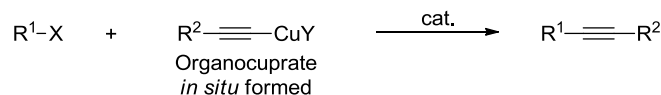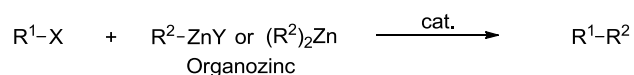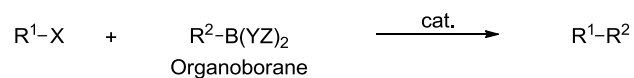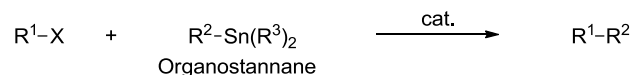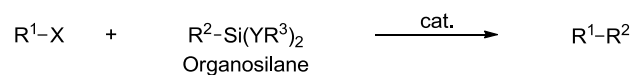
Figure 1. General classification of cross coupling reactions involving organometallic reagents.

The catalytic cycle of the above described processes generally involves three steps around the metal center: (i) the oxidative addition of the electrophilic reagent, (ii) the transmetallation of

the organometallic reagent and (iii) the reductive elimination of the coupling product. A challenging category of electrophile reagents are the alkyl halides or pseudohalides. These substrates are more electron rich than their aryl or alkenyl analogous, therefore, they go slowly through the oxidative addition to the metal center.[14] Once the alkyl halide is added to the metal center, the formed alkyl − metal complex is not stable due to the lack of π electrons of the alkyl ligand to interact with the empty d orbitals of the metal center. This instability made the alkyl − metal complex prone to suffer a fast β-hydride elimination preventing the formation of the desired coupled product. Figure 2, shows a typical catalytic cycle involving the coupling of an alkyl halide.
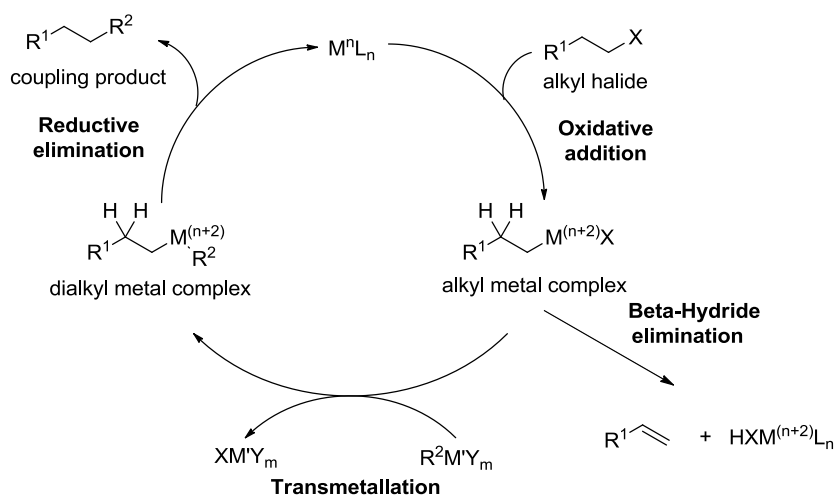
Figure 2. General catalytic cycle of a transition metal catalyzed cross coupling of an alkyl halide with an organometallic reagent.

1.2 Nickel as catalyst for cross coupling reactions

Nickel is placed in the group 10 of the periodic table just above palladium and platinum. Among these three transition metals, nickel is highly more abundant and less expensive.[15] Nevertheless, this economic advantage could put under the shadow all the interesting chemical properties of nickel in catalysis research. Several reviews have described the utility of nickel in general organic reactions,[15] reductive coupling,[16] and cross coupling process.[2] More recently, two reviews have highlighted the utility of nickel in homogenous catalysis for cross coupling reactions.[17,18] The oxidative addition in a nickel metal center tends to occurs readily[19] because its relative electropositive character. Compared to palladium, the β-hydride elimination is more difficult in a nickel center because of a higher energy barrier of the rotation of the Ni − C bond to arrange the structure before the elimination process.[20] On the

other hand, reductive elimination can be more difficult.[21] Furthermore, nickel can have access to oxidation states untypical for palladium as Ni(I) and Ni(III), which opens the possibility to radical reaction modes. For all the above discussed properties, nickel is generally chosen as catalyst for the development of cross coupling methodologies involving alkyl electrophiles.[22]

The next sections of this chapter resumes recent research works of nickel-catalyzed cross coupling processes between alkyl electrophiles and organometallic reagents.

1.3 Ni-catalyzed Kumada-Corriu-Tamao coupling

The coupling of aryl/alkenyl chlorides with alkyl/aryl Grignard reagents was reported in 1972 by Kumada and Tamao using NiCl$_2$(dppe) (dppe = 1,2-bis(diphenylphosphino)ethane) as catalyst.[8] The same year, Corriu reported the formation of trans-stilbene from the coupling of β-bromostyrene with phenylmagnesium bromide catalyzed by Ni(acac)$_2$ (acac=acetylacetonate).[23] Kumada-Corriu-Tamao coupling methodologies for alkyl electrophiles have been actively developed during the last years using different metals centers as catalysts, e.g. cobalt,[24,25] copper[26-29] and iron.[30-33]

Kambe and coworkers reported the first coupling of non-activated primary bromides or tosylates with alkyl Grignard reagents using NiCl$_2$/1,3-butadiene as catalyst.[34] The coupling yields reported were good (56-100 %), but the tolerance of the catalysis to functional groups was not studied. The mechanism of the process was rationalized by experiments. A negative radical clock experiment excluded the possibility of a radical mechanism and Ni(COD)$_2$ (COD = 1,5-cyclooctadiene) demonstrated to be also an efficient catalyst excluding oxidative addition as starting point of the catalytic cycle. The cycle starts with a Ni(0) center formed from the reaction with the Grignard reagent followed by a formation of a bis-π-allyl nickel (0) complex. The reaction of this bis-π-allyl nickel (0) complex with the Grignard reagent forms a η^1,η^3-octadiene-diylnickelate. The alkyl halide is then oxidatively added and the coupling product is formed by reductive elimination. In a parallel study, the authors also proved that NiCl$_2$/1,3-butadiene was a catalyst for the coupling of non-activated primary fluorides with alkyl Grignard reagents.[29] Scheme 1 shows typical reaction conditions of this method.

(A)

(B)
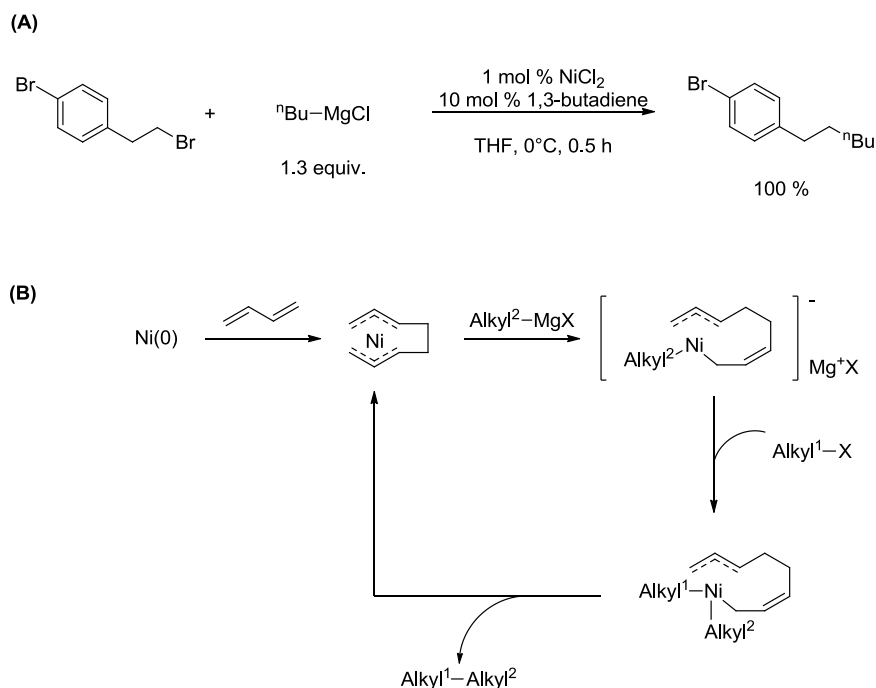
Scheme 1. (A) Typical reaction conditions and (B) catalytic cycle of the Kumada coupling of alkyl electrophiles catalyzed by $NiCl_2$/1,3-butadiene.

Cardenas and co-workers recently developed and efficient coupling system of non-activated primary and secondary alkyl iodides with alkyl Grignard reagents using $Ni(acac)_2$/TMEDA (TMEDA = Tetramethylethylenediamine) as catalyst.[35] The coupling yields were good (51 – 98 %) and the catalysis was not interfered in presence of several functional groups, including esters, carbamates, nitriles, alkoxides and acetals. Scheme 2 shows typical reaction conditions of this method.
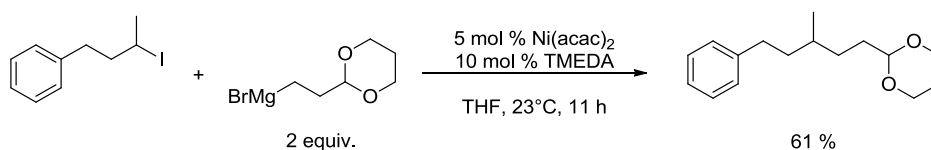
Scheme 2. Typical reaction conditions of the Kumada coupling of alkyl halides using $Ni(acac)_2$/TMEDA as catalyst.

Our group developed a well-defined amido bis(amine) nickel pincer complex "Nickamine". This complex[36] has demonstrated to be a very efficient catalyst for the coupling of non-activated primary halides with alkyl,[37] aryl,[38] alkynyl[39] Grignard reagents (Scheme 3). A plethora of substrates containing functional groups as ester, amide, ether, acetal, nitrile, thioether, keto and several heterocycles were tolerated.

5

(A)

(B)

(C)
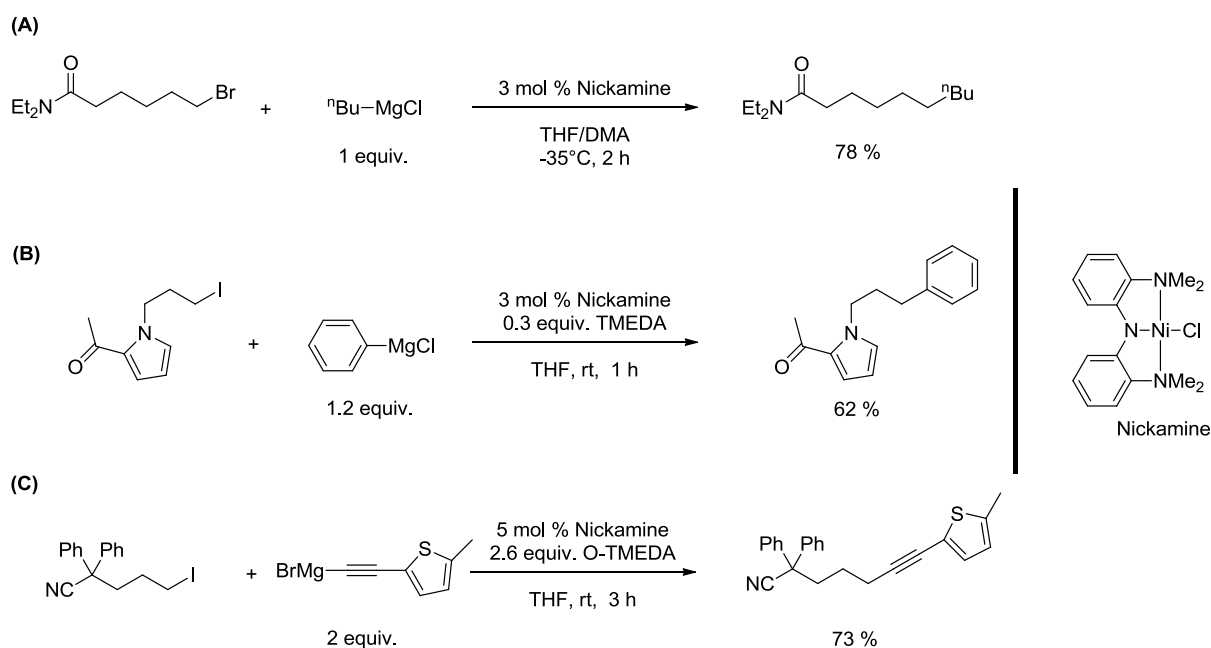
Scheme 3. Typical reaction conditions of the Kumada coupling of alkyl halides using Ni(acac)$_2$/TMEDA as catalyst.

The mechanism of alkyl-alkyl Kumada coupling process catalyzed by Nickamine was studied. A first mechanistic study showed that β-hydride elimination is kinetically accessible during the catalytic cycle but it is avoided due to a high thermodynamic barrier.[40] Some years after, a more extensive mechanistic investigation revealed several features.[41] Nickamine coordinated to the Grignard reagent seems to be the active species (Figure 3). The oxidative addition of the alkyl halide occurs through a bimetallic process involving consecutive reactions with two different Ni(II)-alkyl[2] species to form two different Ni(III) complexes. The Ni(III) complex containing the two alkyl coupling parts undergoes reductive elimination forming the coupling product and an unstable Ni(I) complex. The comproportionation between the Ni(I) complex and the remaining Ni(III) complex form two Ni(II) complexes, which rejoin the catalytic cycle. Similar mechanistic conclusions were obtained for the alkyl-aryl coupling process catalyzed by Nickamine.[42]
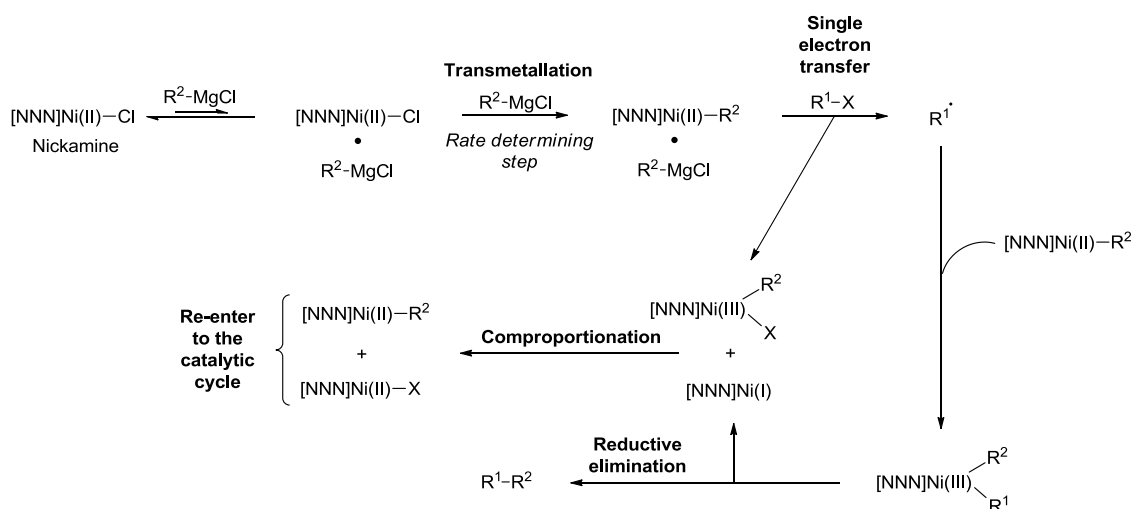
Figure 3. Catalytic cycle of the alkyl – alkyl Kumada coupling reaction catalyzed by Nickamine.

The Kumada coupling of acyclic non-activated alkyl halides is a limitation for Nickamine. Our group developed a series of amido – amine nickel complexes to test their catalytic activity for alkyl – alkyl Kumada coupling of non-activated secondary halides.[43] Two complexes were highly active as catalysts (Scheme 4). One had 2,4-lutidine as co-ligand and the other PPh$_3$. The origin of the efficiency of these complexes as catalysts was related to the dissociation of the co-ligands during the catalysis processes forming active 3-coordinated species. The study did not include a functional group tolerance.

(A)

(B)

(C)
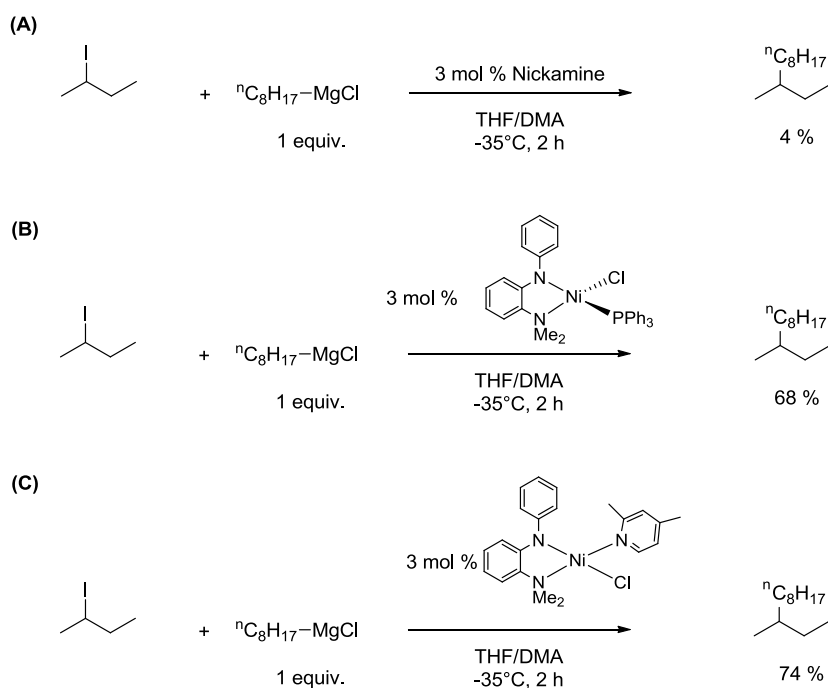
Scheme 4. Amido – amine nickel complexes as catalysts for alkyl – alkyl Kumada coupling of non-activated secondary alkyl halides.

Enantioselective cross coupling reactions remain under-developed. Some useful reviews can be found in the literature.[44-46] Enantioselective catalyst-controlled Kumada coupling was first studied using racemic secondary alkyl Grignard reagents. Kumada[47] and Consiglio[48] have independely reported the enantioselective coupling of secondary Grignard reagents with vinyl and aryl halides using $Ni[(-)-diop]Cl_2$ as catalyst (diop = 2,3-O-isopropylidene-2,3-dihydroxy-1,4-bis(diphenylphosphino)butane). The enantioselectivities reported were around 15 %. The process seems to proceed through a dynamic-kinetic resolution. Scheme 5 shows typical reaction conditions of this method.

(A)

(B)
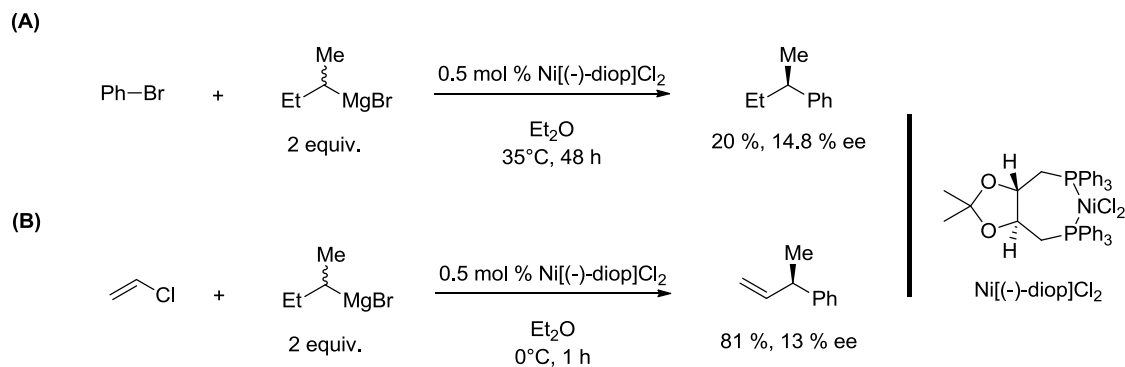
Scheme 5. Typical reaction conditions for the asymmetric cross coupling of racemic secondary Grignard reagents with (A) aryl halides and (B) vinyl halides catalyzed by $Ni[(-)-diop]Cl_2$.

8

Asymmetric coupling methods have been developed for the reaction of vinyl bromides with racemic secondary Grignard reagents using catalysts consisting of mixtures of different chiral ligands and nickel or palladium precursors.[44] Scheme 6 shows the reaction conditions for the coupling between bromostyrene and *sec*-butylmagnesium bromide using a nickel based catalyst combined to a chiral ferrocenylphosphine[49] or a palladium based catalyst combined to a N–Ar axially chiral mimetic-type ligand.[50] The enantioselectivities reported were good but the scope of this reaction is very narrow.
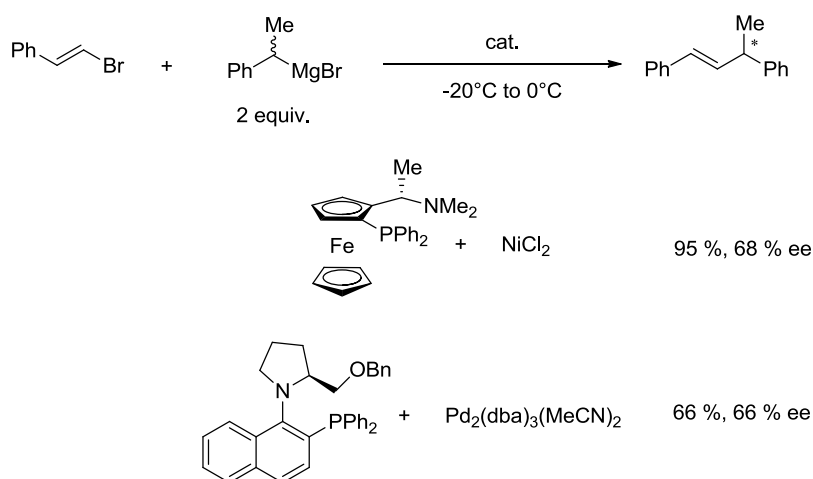
Scheme 6. Typical reaction conditions for the asymmetric cross coupling of bromostyrene with *sec*-butylmagnesium bromide.

Fu and co-workers reported asymmetric Kumada coupling of α-bromoketones with aryl Grignard reagents catalyzed by $NiCl_2 \cdot$glyme combined with bis(oxazoline) chiral ligands.[51] The method allowed coupling functionalized Grignard reagents, e.g. ester, ether, fluoro and chloro. The coupling yields (73 – 91 %) as well the enantiomeric excess (80 – 95 %) were good. Scheme 7 shows typical reaction conditions of this method.
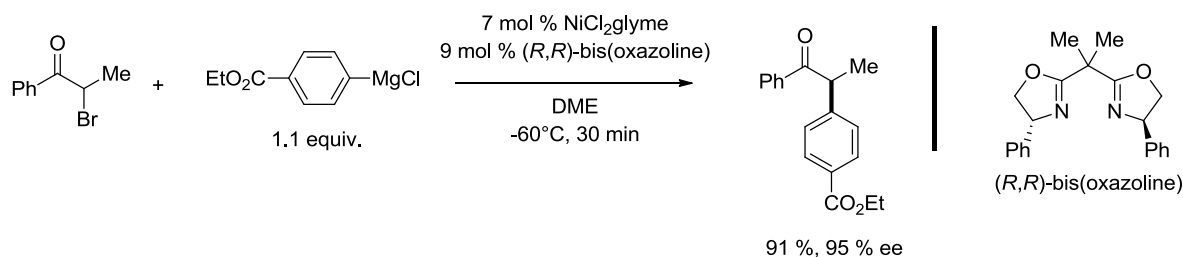
Scheme 7. Typical reaction conditions for the aryl – alkyl asymmetric Kumada coupling of α-bromoketones catalyzed by $NiCl_2 \cdot$glyme/(*R*,*R*)-bis(oxazoline).

1.4 Ni-catalyzed Negishi coupling

The coupling process involving zinc nucleophiles with nickel catalyst is economically convenient and compared to other process like Stille coupling is environmentally advantageous too.[52] Several recent studies have described palladium-catalyzed Negishi couplings of alkyl electrophiles.[53-56] Cardenas and co-workers wrote an excellent review for general nickel catalyzed Negishi couplings.[52] In this section, we resume nickel-catalyzed Negishi couplings of alkyl electrophiles.

Knochel and coworkers developed a group tolerant coupling system between non-activated primary iodides and diorgano zinc compounds using $Ni(acac)_2$ as catalyst and 1-(trifluoromethyl)-4-vinylbenzene as co-catalyst.[57] The coupling process showed a high group tolerance including: ketone, ester, amide and thioacetal. The coupling yields were good with values between 66 % and 78 %. The co-catalyst had an acceleration effect on the rate of the coupling process and suppressed the iodine – zinc exchange side reaction. The catalytic system $Ni(acac)_2$/1-(trifluoromethyl)-4-vinylbenzene was also active for the coupling of polyfunctional aryl zinc reagents with non-activated primary alkyl iodides.[58] The group tolerance and the coupling yields were similar for both processes. Scheme 8 shows representative reactions of this coupling method.
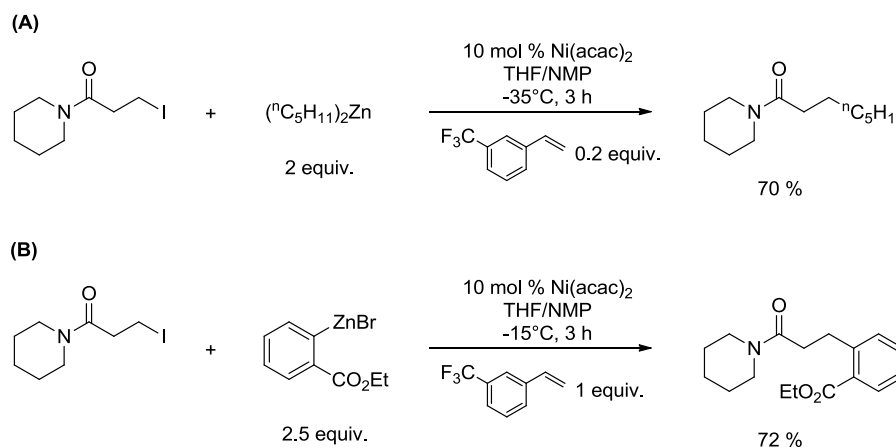
Scheme 8. Representative Negishi coupling reactions of non-activated primary iodides with (A) dialkyl zinc or (B) aryl zinc reagents using $Ni(acac)_2$/1-(trifluoromethyl)-4-vinylbenzene as catalyst.

Another example of a nickel active catalyst for Negishi alkyl – alkyl coupling is the well-defined $[tpy]NiCH_3$ complex (tpy = terpyridine) developed by Vicic and coworkers.[59] The catalyst has a stable Ni(I) center because the unpaired electron is accepted on the π orbitals of the ligand. Cyclohexyl iodide was effectively coupled to alkyl zinc reagents in

correct yields. The homocoupling byproducts led the authors to suggest a radical pathway for the coupling process. The catalytic cycle starts with the homolytically cleavage of the alkyl[1]-I bond by the [tpy]Ni-alkyl[2] complex to create a Ni(II) complex [tpy]Ni(alkyl[2])(I) which releases an alkyl[2] radical by single electron transfer and the Ni(I) complex [tpy]Ni-I. The two released alkyl radicals react to form the coupling product alkyl[1]-alkyl[2] and the catalyst is regenerated by transmetallation reaction between alkyl[2]ZnX and [tpy]Ni-I. Scheme 9 represents the catalytic cycle of this process.
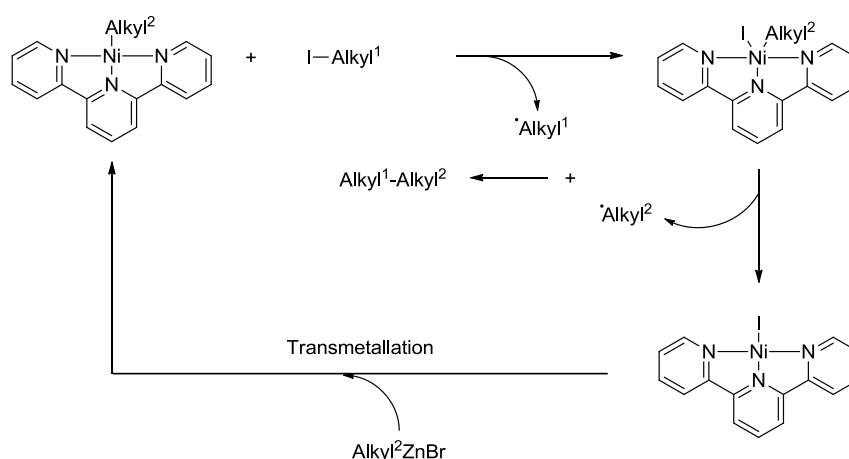
Scheme 9. Catalytic cycle for Negishi coupling catalyzed by a [tpy]Ni(alkyl[2]) well-defined complex.

A similar catalytic system involving a Ni(I) active center was proposed by Cardenas and coworkers.[60] This group developed an efficient coupling system of aryl iodides with primary and secondary alkyl zinc halides using $NiCl_2(py)_4$/(bpy) as catalyst (py = pyridine and bpy = bipyridine). The reported coupling yields were good (43 − 89 %) and the catalysis showed excellent functional group tolerance for fluorides, ketones, nitriles, esters, amines, acetals, carboxylic acids and aldehydes. The authors also proposed a Ni(I)-Ni(III) catalytic cycle based on DFT studies. The Ni(I) center is stabilized by the bipyridine and readily reacts with the alkyl zinc halide to form a pentacoordinated Ni(III) complex, which undergoes though reductive elimination producing the coupling product. Scheme 10 shows representative reaction conditions and the proposed catalytic cycle. It is noteworthy to mention that other nickel based systems were developed for coupling between aryl halides and alkyl zinc halides. Biscoe and co-workers proposed a method using $NiCl_2$/terpyridine[61] as catalyst and Love and co-workers demonstrated that $NiCl_2(PEt_3)_2$ is an effective catalyst to couple aryl fluorides and in situ formed alkyl zinc halides.[62]

(A)

(B)
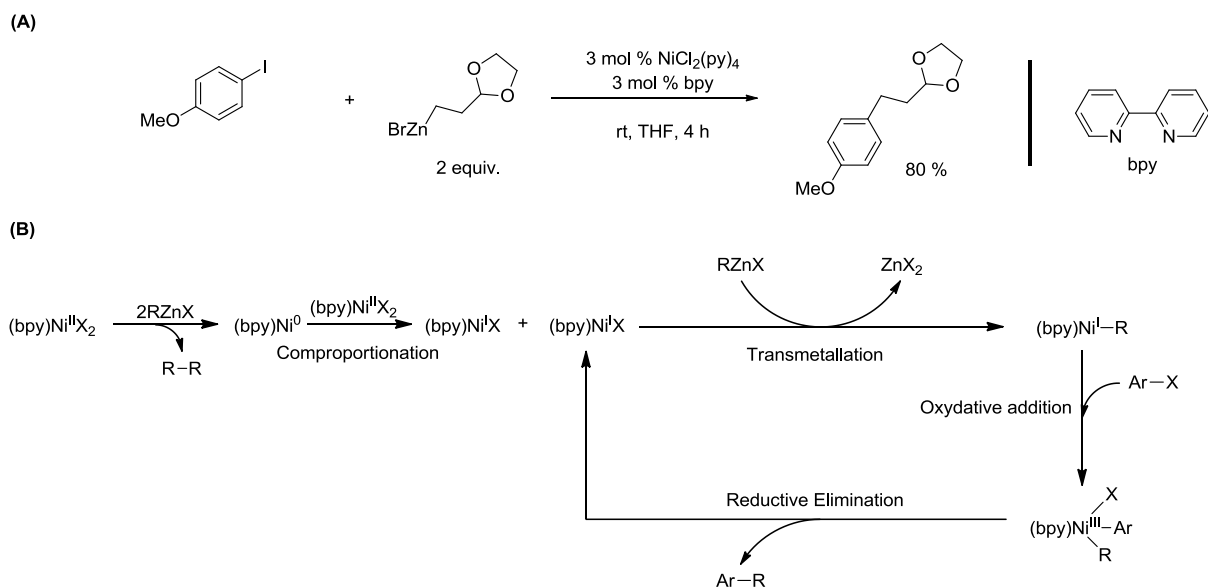
Scheme 10. Cross coupling of aryl halides with alkyl zinc reagents catalyzed by $NiCl_2(py)_4$/(bpy). (A) Representative experimental conditions and (B) proposed catalytic cycle.

Fu and coworkers developed efficient coupling systems between alkyl electrophiles and alkyl zinc reagents using catalysts composed by nickel precursors and oxazoline based ligands. As starting point, the authors developed an effective coupling system of non-activated primary and secondary alkyl halides with organozinc compounds using $Ni(COD)_2$/s-Bu-Pybox as catalyst.[63] Compounds containing reactive functional groups as: acetals, esters, amides and ketones were successfully coupled in good yields (62 − 88 %). Scheme 11 shows typical reaction conditions of this method.
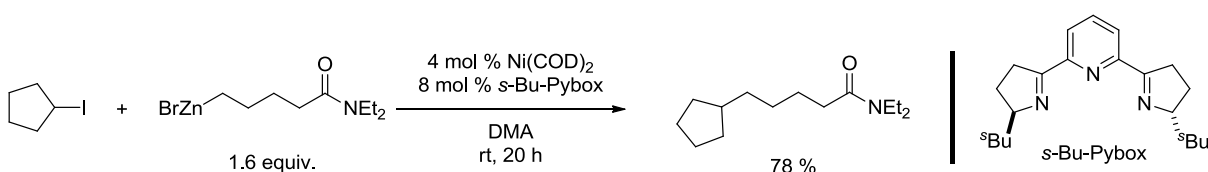
Scheme 11. Representative reaction conditions for Negishi coupling reaction catalyzed by $Ni(COD)_2$/s-Bu-Pybox.

As next step, the $Ni(COD)_2$/s-Bu-Pybox coupling system was tested for asymmetric Negishi coupling of secondary α-bromo amides,[64] the coupling yield was low but the enantiomeric excess (ee) of the product was high. The authors optimized the coupling process using $NiCl_2$·glyme/(R)-(i-Pr)-Pybox as catalyst. The coupling yields were good (51 − 90 %) and the enantiomeric excesses excellent (77 − 98 %). The functional group tolerance of the coupling

process included: alkenes, acetals and nitriles. Scheme 12 shows typical reaction conditions of this method.
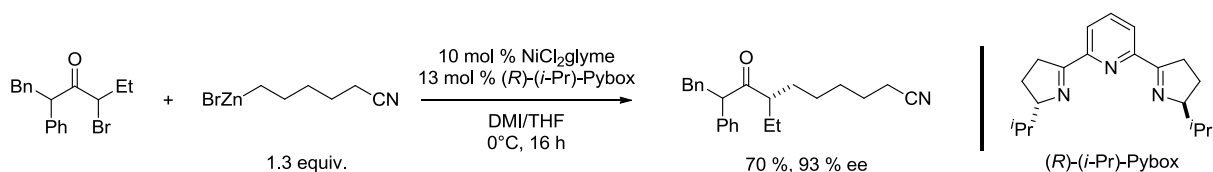
Scheme 12. Representative reaction conditions for asymmetric Negishi coupling reaction catalyzed by NiCl$_2$·glyme/(*R*)-(*i*-Pr)-Pybox.

The results described in the last paragraph allowed developing similar nickel based/Pybox catalysts for the coupling of different types of alkyl halides with organo zinc compounds. NiBr$_2$·diglyme/(*R*)-(*i*-Pr)-Pybox was successfully used as catalyst for the enantioselective coupling of secondary benzylic halides with functionalized primary organo zinc reagents[65]. Secondary benzylic bromides were also enantioselectively coupled to achiral alkylzinc reagents using NiBr$_2$·diglyme/(*S,S*)-(*i*-Pr)-Pybox as catalyst.[66] The coupling of alkylzinc reagents with secondary allylic chlorides was achieved using NiCl$_2$·glyme/(*S*)-BnCH$_2$-Pybox as catalyst.[67]

The enantioselective Negishi arylation of propargylic bromides was effectively catalyzed by NiCl$_2$·glyme/Indanyl-Pybox[68] or by NiBr$_2$·DME/(*S*)-*i*-Pr-pybox,[69] The second catalyst was used to carry on systematic mechanistic studies of the coupling process. The studies showed evidence of a radical pathway involving the formation of a [(*S*)-*i*-Pr-pybox]Ni(I)Br chain-carrying radical, which homolytically cleaves the C-Br bond of the propargylic bromide forming the propargylic radical and [(*S*)-*i*-Pr-pybox]Ni(II)Br$_2$ complex. [(*S*)-*i*-Pr-pybox]Ni(II)Br$_2$ forms [(*S*)-*i*-Pr-pybox-Ni(II)Ar]Br by transmetallation with ArZnBr. [(*S*)-*i*-Pr-pybox-Ni(II)Ar]Br reacts with the propargylic radical to form a Ni(III) species, which undergoes through reductive elimination to form the coupling product and [(*S*)-*i*-Pr-pybox]Ni(I)Br, which re-enters to the catalytic cycle. Scheme 13 shows the reaction conditions and the catalytic cycle of this method.

(A)

(B)
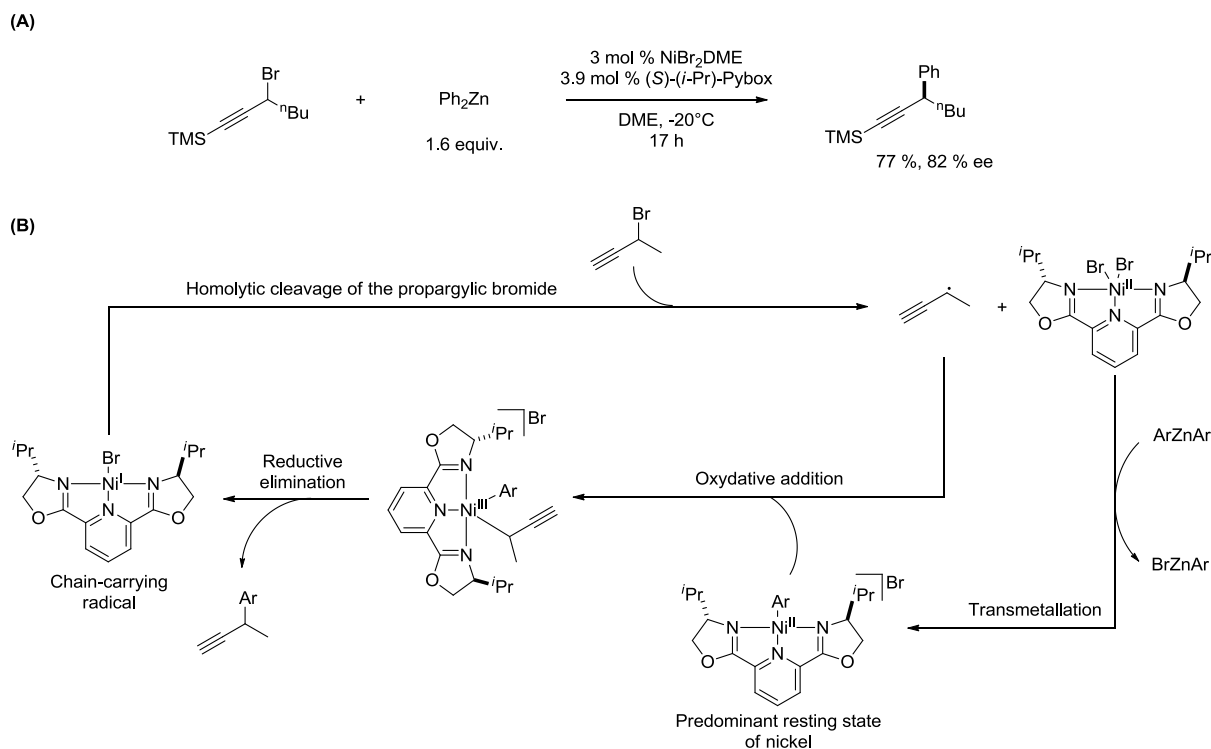
Scheme 13. Asymmetric coupling of propargylic bromides with aryl zinc reagents catalyzed by NiBr$_2$·DME/(S)-(i-Pr)-Pybox.(A) Representative reaction conditions and (B) suggested catalytic cycle.

1.5 Ni-catalyzed Suzuki – Miyaura coupling

Organoboron reagents are relatively stable, readily prepared and normally environmental benign compared to Grignard reagents and other Grignard reagents. The weak nucleophilicity of these reagents made them tolerant to functional groups.[70] Several types of organoboron reagents have been used for Suzuki – Miyaura coupling, e.g. alkenylboranes, cathecol boronic acids, boranes, etc.[71]

The first nickel-catalyzed Suzuki coupling of non-activated secondary halides was reported by Fu and co-workers.[72] The method used aryl boronic acids as coupling partners and Ni(COD)$_2$/bathophenanthroline as catalyst. Non-activated primary halides and alkenyl boronic acids were also successfully used as coupling partners. The tolerance of some functional groups on the organoboron reagents was successfully tested, e.g. ether, nitrile and fluoro. Scheme 14 shows typical reaction conditions of this method.

(A)

(B)
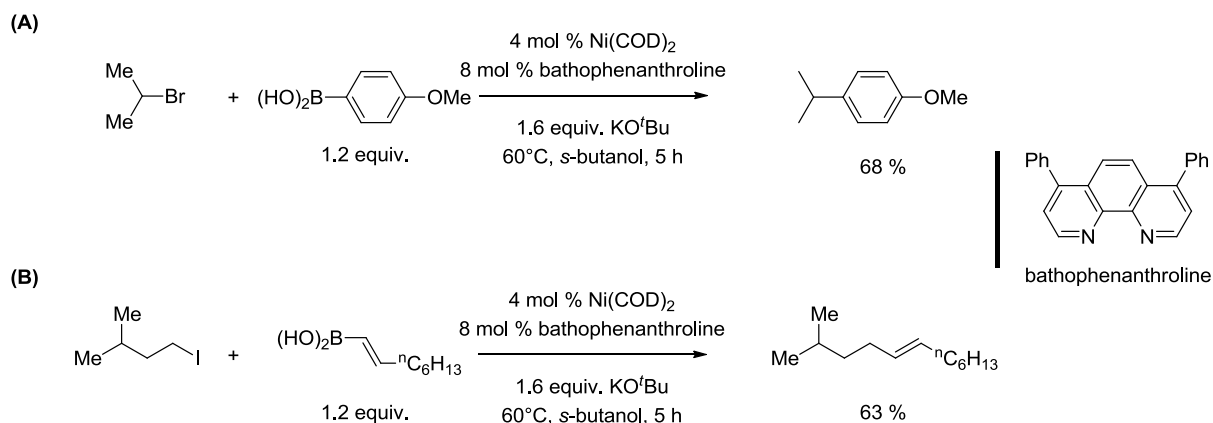
Scheme 14. Representative coupling of (A) secondary and (B) primary non-activated halides with organic boronic acids catalyzed by Ni(COD)$_2$/bathophenanthroline.

In 2007, Fu and co-workers reported the first nickel-catalyzed alkyl − alkyl Suzuki coupling. The catalyst was composed by NiCl$_2$·glyme and trans-N,N′-dimethyl-1,2-cyclohexanediamine **L1**. The method allowed coupling non-activated primary and secondary alkyl halide with alkyl-(9-BBN) reagents (9-BBN = 9-Borabicyclo(3.3.1)nonane). The coupling yields were good (64 − 93 %) and ester, ether, amide functional groups were tolerated. The authors showed evidence of the activation of the alkylborane by the alkoxyde (KO^{t}Bu) for the transmetallation to the nickel center. The use of this method was extended to the coupling of non-activated alkyl chlorides with alkyl-(9-BBN) reagents using NiBr$_2$·diglyme/(R,R)-**L2** as catalyst.[73] This catalyst was also effective to couple alkyl bromides or iodides. The functional group tolerances of both methods are similar. Mechanistic investigations demonstrated that the rate law of the process is first order on the catalyst, first order on the alkylborane and zeroth order on the alkyl halide (first order in case of alkyl chlorides). Scheme 15 shows typical reaction conditions of this method.

(A)

(B)
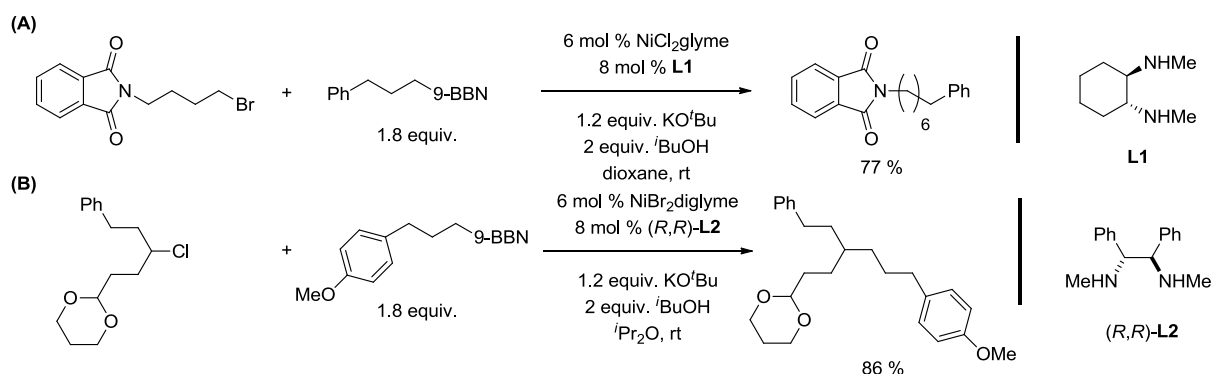
Scheme 15. Representative nickel catalyzed couplings of (A) bromo and (B) chloro alkyl reagents with alkyl-(9-BBN) reagents.

15

Fu and co-workers successfully tested the nickel/chiral diamine catalyst system for asymmetric Suzuki coupling of alkyl electrophiles.[74-77] In a recent study, the authors demonstrated that non-activated secondary bromides and chlorides are asymmetrically coupled to alkyl-(9-BBN) reagents using $NiBr_2 \cdot diglyme/(R,R)$-**L2** as catalyst.[77] Carbamate- and sulfonamide protected haloamines were used as alkyl electrophiles. The coupling yields (54 – 89 %) and the enantiomeric excesses (72 – 90 %) were good. Mechanistic studies demonstrated that the rate law of the process is first order for the catalyst and for the organoborane and zeroth order for the electrophile. The transmetallation seems to be the rate determining step. DFT studies of this coupling method were reported.[78] The catalytic cycle starts with a $L_nNi(I)$-X complex formed by disproportionation of the $L_nNi(II)X_2$ pre-catalyst. $L_nNi(I)$-X undergoes through transmetallation with the alkyl borane to form $L_nNi(I)$-alkyl^2. The oxidative addition of the electrophile (alkyl^1-X) happens in two times, first $L_nNi(II)(X)(alkyl^2)$ is formed with an alkyl^1 radical in the outer coordination sphere and secondly $L_nNi(III)(X)(alkyl^2)(alkyl^1)$ is formed by insertion of the alkyl^1 radical to the nickel center. Finally, the coupling product alkyl^1-alkyl^2 and $L_nNi(I)$-X are formed by reductive elimination from $L_nNi(III)(X)(alkyl^2)(alkyl^1)$. Scheme 16 shows typical reaction conditions of this method and the description of the catalytic cycle.

(A)

(B)
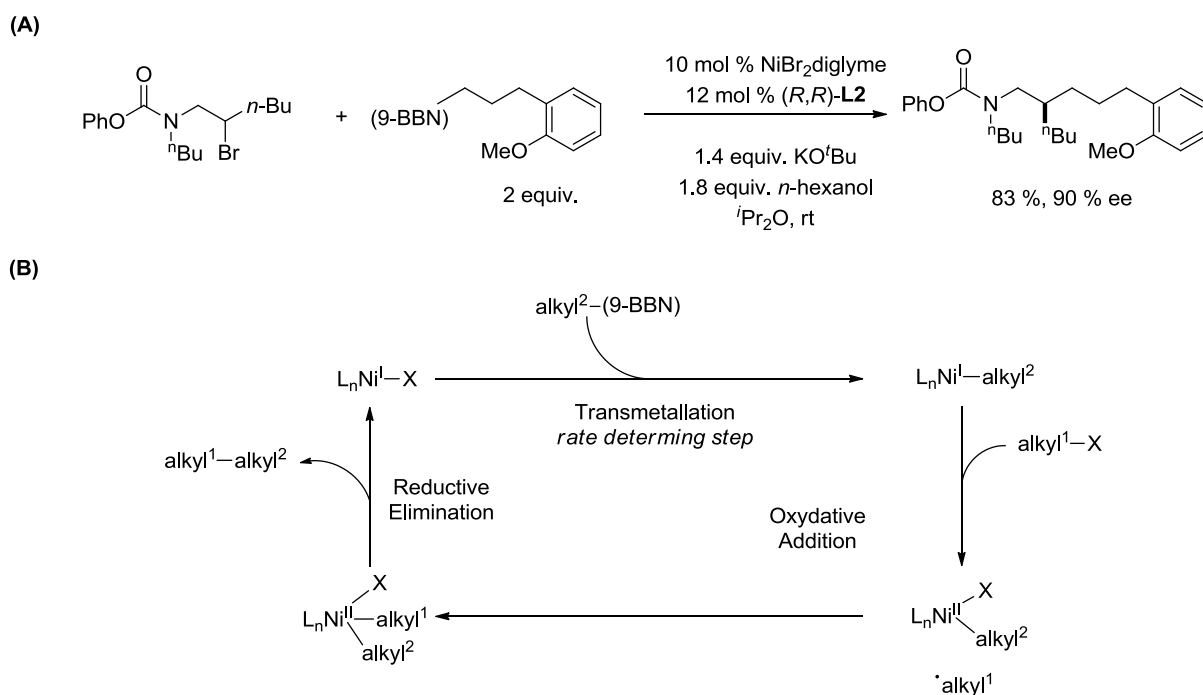
Scheme 16. Asymmetric coupling of non-activated secondary bromides with alkyl-(9-BBN) reagents catalyzed by $NiBr_2 \cdot diglyme/(R,R)$-**L2**.(A) Representative reaction conditions and (B) suggested catalytic cycle.

Molander and co-workers reported the coupling of non-activated primary halides with potassium aryl- and heteroaryltrifluoroborates catalyzed by NiBr$_2$·glyme/ bathophenanthroline.[79] The coupling was set up using stoichiometric quantities of both coupling partners. The catalysis tolerated several functional groups and heterocycles, including ester, acetal, ether, alkene, ketone, alcohol, furans, pyridine, pyrimidines, thiophenes, indole and imidazole. For the heteroaryl cross coupling the synthesis could be carried out on gram scale with only 1 mol % of catalyst. The catalyst NiBr$_2$·glyme/ bathophenanthroline was effective to couple alkyl bromides or iodides but NiCl$_2$·glyme/L-Prolinol was necessary to couple alkyl chlorides. Scheme 17 presents typical reaction conditions of these methods.
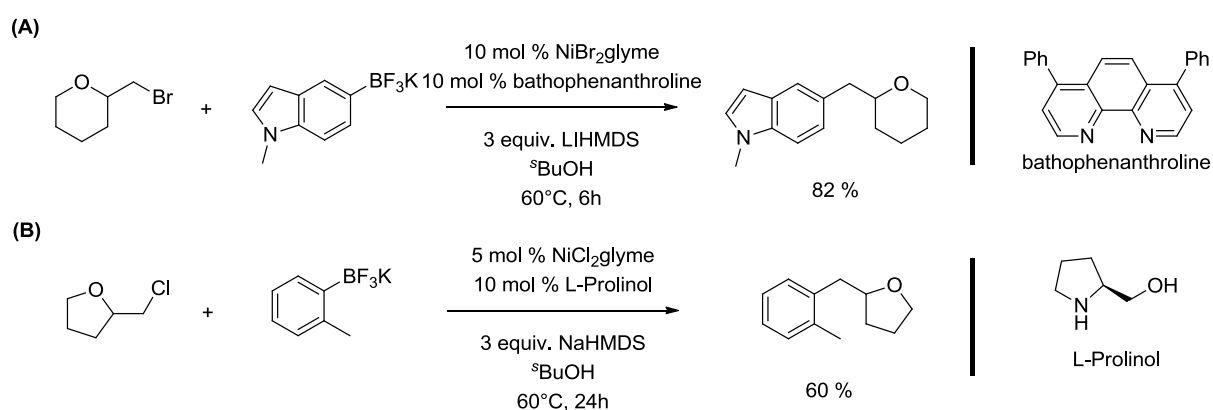
Scheme 17. Representative nickel catalyzed coupling of (A) bromo and (B) chloro alkyl reagents with organotrifluoroborates.

Our group reported that Nickamine is an effective catalyst for coupling of non-activated alkyl halides with alkyl-(9-BBN) or aryl-(9-BBN) reagents.[80] The coupling method tolerated a variety of functional groups including ester, ether, furan, thioether, acetal and amide. The coupling yields were good (49 – 87%). The study shows promising results for the alkyl – aryl Suzuki coupling for phenylboronic acids. Radical – clock experiments showed evidence of a radical mechanism for the coupling process. Scheme 18 shows representative reaction conditions of this method.
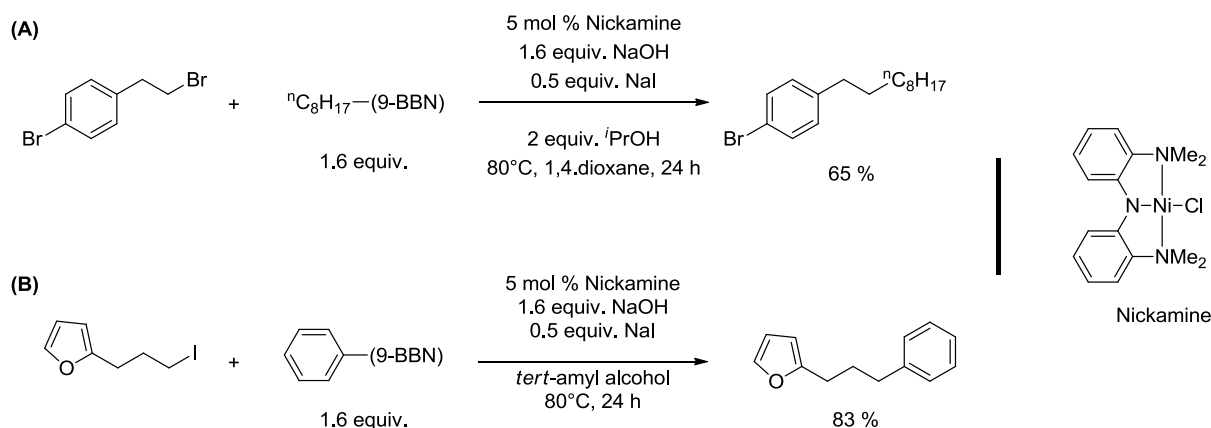
Scheme 18. Representative coupling conditions of non-activated alkyl halides with (A) alkyl-(9-BBN) and (B) aryl-(9-BBN) reagents using Nickamine as catalyst.

1.6 Ni-catalyzed Hiyama coupling

Organosilicon coupling partners are interesting due to their readily reactivity, low toxicity and high group tolerance.[2] Palladium-catalyzed Hiyama coupling is well-documented.[81,82] Nickel-catalyzed coupling of alkyl electrophiles with organosilicon reagents was mostly developed by Fu and co-workers. At first, [83] they developed an air-stable efficient coupling methodology using NiBr$_2$.diglyme/bathophenanthroline as catalyst for the reaction of organosilicon aryls with primary and secondary non activated bromides or iodides. The coupling method showed a high functional group tolerance including: ether, imide, keto, carbamate, acetal and nitrile. Scheme 19 shows representative coupling conditions for this method.
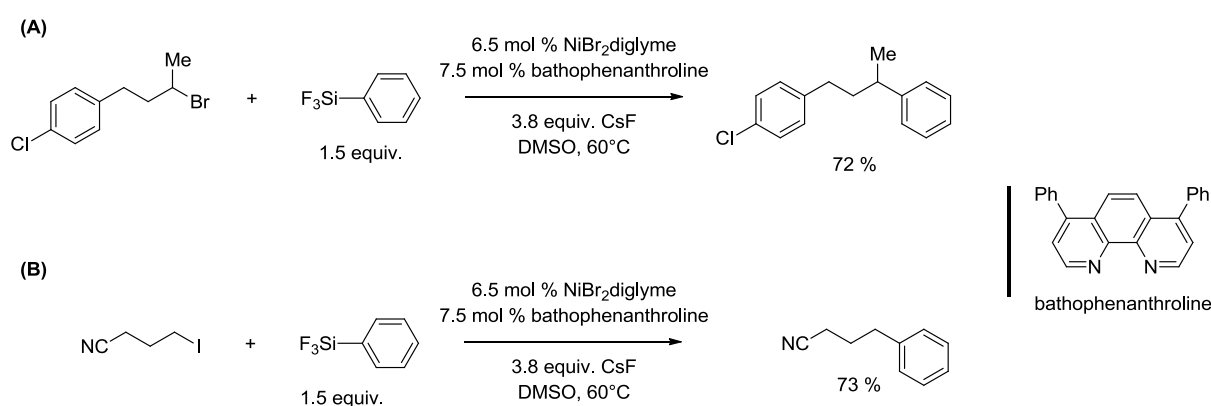
Scheme 19. Representative Hiyama coupling reactions of non-activated (A) secondary or (B) primary halides using NiBr$_2$·diglyme/bathophenanthroline as catalyst.

Three years after the authors modified the coupling methodology using NiCl$_2$·glyme/(*R,S*)-norephedrine as catalyst.[84] The method was efficient to couple aryl silanes reagents with non-

activated and activated secondary halides. α-Brominated ketones, esters, amides, phosphonates and nitriles were successfully coupled in good yields (65 - 92 %). Asymmetric induction was not possible despite the catalyst included a chiral ligand. To overcome this limitation, the authors developed a methodology for asymmetric Hiyama cross couplings for the production of α-aryl esters in good enantiomeric excess (above 89 % ee).[85] The catalyst was composed by $NiCl_2$·glyme and the chiral diamine (*S,S*)-**L2**. The catalytic system was effective for the asymmetric coupling of α-bromo esters with substituted aryl or alkenyl silanes (yields above 66 %). Scheme 20 shows representative reactions for the Hiyama coupling process using $NiCl_2$·glyme/(*R,S*)-norephedrine or $NiCl_2$·glyme/(*S,S*)-**L2** as catalyst.
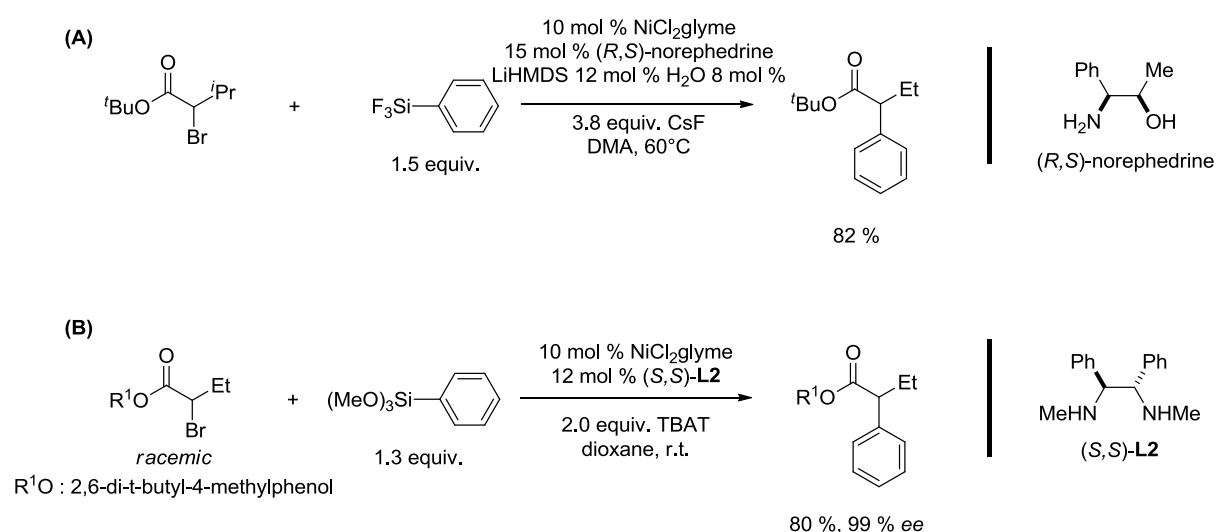
Scheme 20. Representative Hiyama coupling conditions using (A) $NiCl_2$·glyme/norephedrine or (B) $NiCl_2$·glyme/(*S,S*)-**L1** as catalysts.

1.7 Ni-catalyzed Stille coupling

Alkyltin compounds can be easily absorbed by the skin therefore they are highly toxic.[86] Moreover trialkyl tin species are difficult to separate from the products at the end of the process.[87] Despite these difficulties organotin compounds are actively used in bioactive compounds. [88,89] Alkyl Stille coupling is poorly developed even using palladium based catalysts.[90,91]

Fu and co-workers developed a method to couple non-activated primary and secondary halides with aryltrichlorotin reagents using $NiCl_2$/2,2'-bipyridine as catalyst.[92] Cyclic and acyclic secondary halides were coupled to in good yields (47 − 83 %). Ether and pyrrole functional groups did not interfere with the catalysis. Aryl and alkenyltributylstannanes could

be used as coupling partner but a previous reaction with $SnCl_4$ was necessary. Scheme 21 shows the representative reaction conditions of this method.
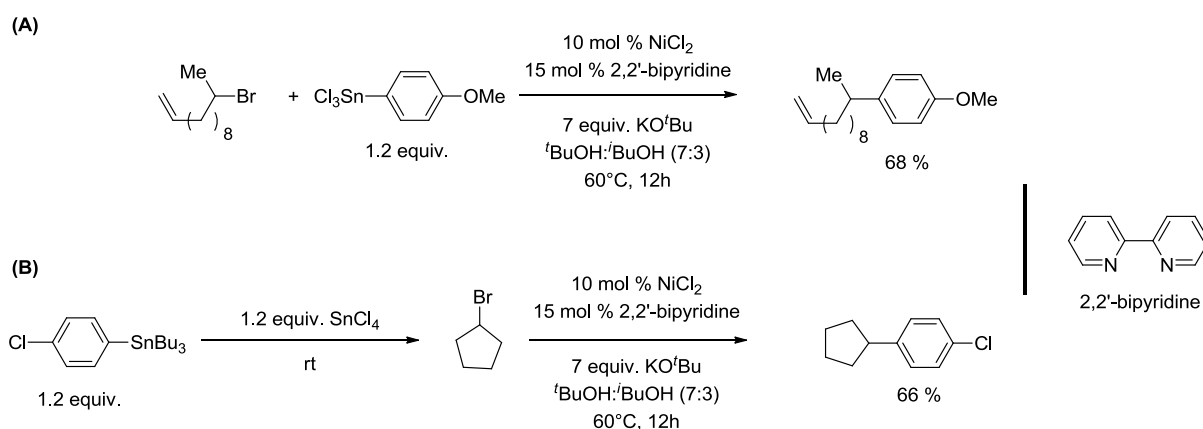
Scheme 21. Representative Stille coupling reactions of non-activated secondary bromides with (A) aryltrichlorotin or (B) aryltributylstannane reagents using $NiCl_2$/2,2'-bipyridine as catalyst.

1.8 Ni-catalyzed Sonogashira coupling

The coupling of terminal alkynes with aryl electrophiles have become an important procedure for the pharmaceutical industry.[93] Literature offers excellent recent reviews about Sonogashira type coupling methodologies.[94-96] Only few works implying nickel homogenous catalytic systems have been reported,[97-99] the cause is most likely the deactivation of the nickel center by a stable coordination of the triple bond.[100] We will focus our discussion on two recent works involving the coupling of non-activated alkyl halides with terminal alkynes.

Our group demonstrated that Nickamine is an excellent catalyst for the coupling between non-activated alkyl halides and terminal alkynes.[98] The coupling needed CuI as co-catalyst and caesium carbonate as base. The coupling process occurred at high temperature (>100°C) and it was effective for primary iodides, bromides and chlorides, the last two required an *in situ* halogen exchange in presence of NaI or tetrabutylammonium idode (TBAI) respectively. A variety of functional groups as ester, amide, aromatic enone, keto, acetal, nitrile, tetramethylsilyl and heterocycle did not interfere with the coupling. The yields obtained were excellent between 61 – 89 %. Scheme 22 shows typical reaction conditions of this process.
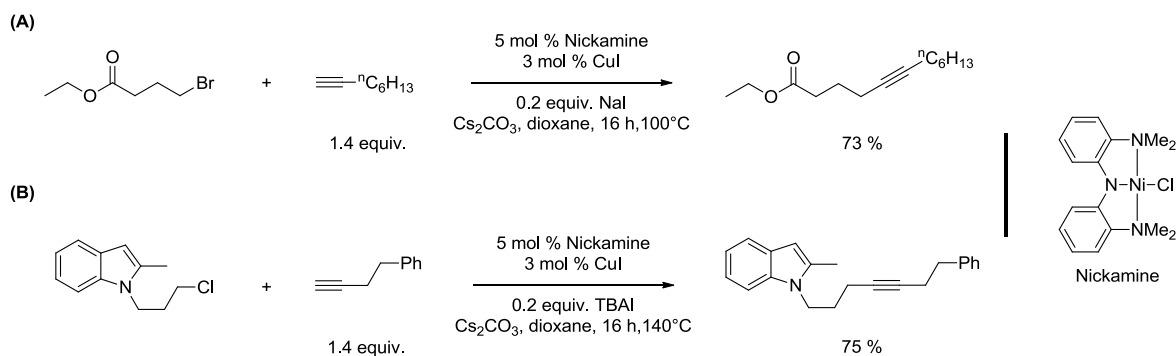
Scheme 22. Sonogashira coupling of alkyl halides catalyzed by Nickamine.

Liu and co-workers developed a highly active catalyst system for the coupling of non-activated primary and secondary halides with terminal alkynes using $Ni(COD)_2$/Pybox as catalyst.[99] The coupling occurred at room temperature, needed CuI as co-catalyst and LiO^tBu as base. Primary or secondary halides containing functional groups, e.g. ester, acetal, amino, nitrile, amido, hydroxyl, borate, fluoro ,tetramethylsilyl and heterocycle, were successfully coupled. It is noteworthy to mention that the coupling method was highly diastereoselective for substituted cyclohexyl iodides obtaining diastereoselective ratios (dr) higher than 91:9. Scheme 23 highlights representative examples of this method.
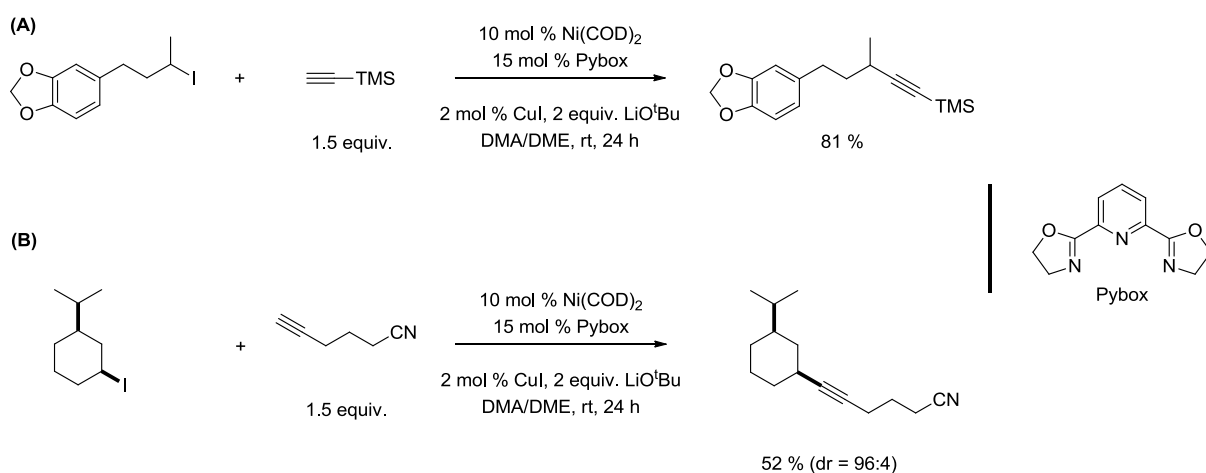
Scheme 23. Room temperature Sonogashira coupling of alkyl halides catalyzed by $Ni(COD)_2$/Pybox.

1.9 Aim of the project

This work is devoted to the development and the structure activity of well-defined nickel complexes as catalysts for cross coupling reactions of alkyl electrophiles. In previous studies,[37] our group demonstrated that Nickamine was an effective catalyst for the alkyl – alkyl Kumada coupling of cyclohexyl iodides and tetrahydropyrans. In chapter two, we will

demonstrate how the bulky structure of Nickamine can be exploited to catalyze highly diastereoselective Kumada coupling reactions of 1,3 and 1,4-disubstituted cyclohexyl halides and tetrahydropyranes.

The second generation of amido – amide nickel catalysts developed by our group demonstrated to be highly active catalysts for coupling non-activated secondary alkyl halides with alkyl Grignard reagents.[43] Creation of chiral tertiary carbon centers by a catalyst controlled enantioselective Kumada coupling is a non-existent method. This issue could be overcome by the development of well-defined chiral nickel complexes. In chapters three and four, we will present the synthesis of potentially chiral amido – amine ligands and the synthesis of their corresponding nickel complexes. The study of the catalyst activity of these complexes for Kumada coupling reactions of non-activated secondary halides will be also presented.

Our group studied the mechanism of alkyl – alkyl[40,41] and alkyl – aryl[42] Kumada coupling reactions catalyzed by Nickamine. On the other side, the study of the mechanism of alkyl – alkynyl Sonogashira[98] coupling catalyzed by Nickamine is not obvious due to the high temperature requirements of the coupling process. In chapter five, we will present the synthesis of a NNN pincer complex having an ethyl amino donor. This complex is an effective catalyst for alkyl – alkynyl Sonogashira coupling at room temperature, which allowed us studying the coupling mechanism in detail.

1.10 References

(1)   Hartwig, J. F. *Organotransition Metal Chemistry - From Bonding to Catalysis*; University Science Books: Sausalito, CA, 2010.

(2)   Meijere, A. d.; Diederich, F. *Metal-Catalyzed Cross-Coupling Reactions*; 2nd ed.; Wiley-VCH: Weinheim, Germany, 2004.

(3)   Heck, R. F. *J. Am. Chem. Soc.* **1968**, *90*, 5526.

(4)   Heck, R. F. *J. Am. Chem. Soc.* **1968**, *90*, 5531.

(5)   Heck, R. F. *J. Am. Chem. Soc.* **1968**, *90*, 5518.

(6)   Heck, R. F. *J. Am. Chem. Soc.* **1968**, *90*, 5538.

(7)   Heck, R. F. *J. Am. Chem. Soc.* **1968**, *90*, 5542.

(8)   Tamao, K.; Sumitani, K.; Kumada, M. *J. Am. Chem. Soc.* **1972**, *94*, 4374.

(9)   Sonogashira, K.; Tohda, Y.; Hagihara, N. *Tetrahedron Lett.* **1975**, *16*, 4467.

(10)   Negishi, E. *Acc. Chem. Res.* **1982**, *15*, 340.

(11)   Miyaura, N.; Yamada, K.; Suzuki, A. *Tetrahedron Lett.* **1979**, *36*, 3437.

(12)   Stille, J. K. *Ang. Chem. Int. Ed.* **1986**, *25*, 508.

(13)   Hatanaka, Y.; Hiyama, T. *J. Org. Chem.* **1988**, *53*, 918.

(14)   Ariafard, A.; Lin, Z. *Organometallics* **2006**, *25*, 4030.

(15)   Tamaru, Y. *Modern Organonickel Chemistry*; Wiley-VCH, 2005.

(16)   Montgomery, J. *Angew. Chem. Int. Ed.* **2004**, *43*, 3890.

(17)   Hu, X. *Chem. Sci.* **2011**, *2*, 1867.

(18)   Tasker, S. Z.; Standley, E. A.; Jamison, T. F. *Nature* **2014**, *509*, 299.

(19)   Tsou, T. T.; Kochi, J. K. *J. Am. Chem. Soc.* **1979**, *101*, 6319.

(20)   Lin, B.; Liu, L.; Fu, Y.; Lu, S.; Chen, Q.; Guo, Q. *Organometallics* **2004**, *23*, 3890

(21)   Lanni, E. L.; McNeil, A. J. *J. Am. Chem. Soc.* **2009**, *131*, 16573.

(22)   Rudolph, A.; Lautens, M. *Angew. Chem. Int. Ed.* **2009**, *48*, 2656.

(23)   Corriu, R. J. P.; Masse, J. P. *J. Chem. Soc.: Chemical Communications* **1972**, 144a.

(24)   Cahiez, G.; Chaboche, C.; Duplais, C.; Giulliani, A.; Moyeux, A. *Adv. Synth. Catal.* **2008**, *350*, 1484.

(25)   Cahiez, G.; Gager, O.; Buendia, J. *Angew. Chem. Int. Ed.* **2010**, *49*, 1278.

(26)   Gérard, C.; Christophe, C.; Michelle, J. *Tetrahedron* **2000**.

(27)   Gérard, C.; Olivier, G.; Julien, B. *Synlett* **2010**.

(28)   Ren, P.; Stern, L.; Hu, X. *Angew. Chem. Int. Ed.* **2012**, *51*, 9110.

(29)   Terao, J.; Ikumi, A.; Kuniyasu, H.; Kambe, N. *J. Am. Chem. Soc.* **2003**, *125*, 5646.

(30)   Bauer, G.; Cheung, C. W.; Hu, X. *Synthesis* **2015**, *in press*.

(31)   Cheung, C. W.; Ren, P.; Hu, X. *Org. Lett.* **2014**, *16*, 2566.

(32)   Dongol, K. G.; Koh, H.; Sau, M.; Chai, C. L. L. *Adv. Synth. Cat.* **2007**, *349*, 1015.

(33)   Nakamura, M.; Matsuo, K.; Ito, S.; Nakamura, E. *J. Am. Chem. Soc.* **2004**, *126*, 3686.

(34)   Terao, J.; Watanabe, H.; Ikumi, A.; Kuniyasu, H.; Kambe, N. *J. Am. Chem. Soc.* **2002**, *124*, 4222.

(35)   Guisán-Ceinos, M.; Soler-Yanes, R.; Collado-Sanz, D.; Phapale, V. B.; Buñuel, E.; Cárdenas, D. J. *Chem. Eur. J.* **2013**, *19*, 8405.

(36)   Csok, Z.; Vechorkin, O.; Harkins, S. B.; Scopelliti, R.; Hu, X. *J. Am. Chem. Soc.* **2008**, *130*, 8156.

(37)   Vechorkin, O.; Hu, X. *Angew. Chem. Int. Ed.* **2009**, *48*, 2937.

(38)   Vechorkin, O.; Proust, V.; Hu, X. *J. Am. Chem. Soc.* **2009**, *131*, 9756.

(39)   Vechorkin, O.; Godinat, A.; Scopelliti, R.; Hu, X. *Angew. Chem. Int. Ed.* **2011**, *50*, 11777.

(40)   Breitenfeld, J.; Vechorkin, O.; Corminboeuf, C.; Scopelliti, R.; Hu, X. *Organometallics* **2010**, *29*, 3686.

(41)   Breitenfeld, J.; Ruiz, J.; Wodrich, M. D.; Hu, X. *J. Am. Chem. Soc.* **2013**, *135*, 12004.

(42)   Breitenfeld, J.; Wodrich, M. D.; Hu, X. *Organometallics* **2014**, *33*, 5708.

(43)   Ren, P.; Vechorkin, O.; Allmen, K. v.; Scopelliti, R.; Hu, X. *J. Am. Chem. Soc.* **2011**, *133*, 7084.

(44)   Swift, E. C.; Jarvo, E. R. *Tetrahedron* **2013**, *69*, 5799.

(45)   Hayashi, T. *J. of Organomet. Chem.* **2002**, *653*, 41.

(46)   Glorius, F. *Angew. Chem. Int. Ed.* **2008**, *47*, 8347.

(47)   Kiso, Y.; Tamao, K.; Miyake, N.; Yamamoto, K.; Kumada, M. *Tetrahedron Lett.* **1974**, *15*, 3.

(48)   Consiglio, G.; Botteghi, C. *Helv. Chim. Acta.* **1973**, *56*, 460.

(49)   Hayashi, T.; Konishi, M.; Fukushima, M.; Mise, T.; Kagotani, M.; Tajika, M.; Kumada, M. *J. Am. Chem. Soc.* **1982**, *104*, 180.

(50)   Horibe, H.; Fukuda, Y.; Kondo, K.; Okuno, H.; Murakami, Y.; Aoyama, T. *Tetrahedron* **2004**, *60*, 10701.

(51)   Lou, S.; Fu, G. C. *J. Am. Chem. Soc.* **2010**, *132*, 1264.

(52)   Phapale, V. B.; Cardenas, D. J. *Chem. Soc. Rev.* **2009**, *38*, 1598.

(53)   Zhou, J.; Fu, G. C. *J. Am. Chem. Soc.* **2003**, *125*, 12527.

(54)   Hadei, N.; Kantchev, E. A. B.; O'Brie, C. J.; Organ, M. G. *Org. Lett.* **2005**, *7*, 3805.

(55)   Gioria, E.; Martínez-Ilarduya, J. M.; Espinet, P. *Organometallics* **2014**, *33*, 4394.

(56)   Achonduh, G. T.; Hadei, N.; Valente, C.; Avola, S.; O'Brien, C. J.; Organ, M. G. *Chem. Comun..* **2010**, *46*, 4109.

(57)   Giovannini, R.; Stüdemann, T.; Dussin, G.; Knochel, P. *Angew. Chem. Int. Ed.* **1998**, *37*, 2387.

(58)   Giovannini, R.; Knochel, P. *J. Am. Chem. Soc.* **1998**, *120*, 11186.

(59)   Anderson, T. J.; Jones, G. D.; Vicic, D. A. *J. Am. Chem. Soc.* **2004**, *126*, 8100.

(60)   Phapale, V. B.; Guisán-Ceinos, M.; Buñuel, E.; Cárdenas, D. J. *Chem. Eur. J.* **2009**, *15*, 12681.

(61)   Joshi-Pangu, A.; Ganesh, M.; Biscoe, M. R. *Org. Lett.* **2011**, *13*, 1218.

(62)   Sun, A. D.; Leung, K.; Restivo, A. D.; LaBerge, N. A.; Takasaki, H.; Love, J. A. *Chem. Eur. J.* **2014**, *20*, 3162.

(63)   Zhou, J.; Fu, G. C. *J. Am. Chem. Soc.* **2003**, *125*, 14726.

(64)   Fischer, C.; Fu, G. C. *J. Am. Chem. Soc.* **2005**, *127*, 4594.

(65)   Arp, F. O.; Fu, G. C. *J. Am. Chem. Soc.* **2005**, *127*, 10482.

(66)   Binder, J. T.; Cordier, C. J.; Fu, G. C. *J. Am. Chem. Soc.* **2012**, *134*, 17003.

(67)   Son, S.; Fu, G. C. *J. Am. Chem. Soc.* **2008**, *130*, 2756.

(68)   Smith, S. W.; Fu, G. C. *J. Am. Chem. Soc.* **2008**, *130*, 12645.

(69)   Schley, N. D.; Fu, G. C. *J. Am. Chem. Soc.* **2014**, *136*, 16588.

(70)   Norio, M.; Akira, S. *Chem. Rev.* **1995**.

(71)   Lennox, A. J. J.; Lloyd-Jones, G. C. *Chem. Soc. Rev.* **2014**, *43*, 412.

(72)   Zhou, J.; Fu, G. C. *J. Am. Chem. Soc.* **2004**, *126*, 1340.

(73)   Lu, Z.; Fu, G. C. *Angew. Chem. Int. Ed.* **2010**, *49*, 6676.

(74)   Cong, H.; Fu, G. C. *J. Am. Chem. Soc.* **2014**, *136*, 3788.

(75)   Han, F.S. *Chem. Soc. Rev.* **2013**, *42*, 5270.

(76)   Saito, B.; Fu, G. C. *J. Am. Chem. Soc.* **2007**, *129*, 9602.

(77)   Wilsily, A.; Tramutola, F.; Owston, N. A.; Fu, G. C. *J. Am. Chem. Soc.* **2012**, *134*, 5794.

(78)   Li, Z.; Jiang, Y.-Y.; Fu, Y. *Chem. Eur. J.* **2012**, *18*, 4345.

(79)   Molander, G. A.; Argintaru, O. A.; Aron, I.; Dreher, S. D. *Org. Lett.* **2010**, *12*, 5783.

(80)   Di Franco, T.; Boutin, N.; Hu, X. *Synthesis* **2013**, *45*, 2949.

(81)   Nakao, Y.; Hiyama, T. *Chem. Soc. Rev.* **2011**, *40*, 4893.

(82)   Sore, H. F.; Galloway, W. R. J. D.; Spring, D. R. *Chem. Soc. Rev.* **2012**, *41*, 1845.

(83)   Powell, D. A.; Fu, G. C. *J. Am. Chem. Soc.* **2004**, *126*, 7788.

(84)   Strotman, N. A.; Sommer, S.; Fu, G. C. *Angew. Chem. Int. Ed.* **2007**, *46*, 3556.

(85)   Dai, X.; Strotman, N. A.; Fu, G. C. *J. Am. Chem. Soc.* **2008**, *130*, 3302.

(86)   *Handbook on the Toxicology of Metals*; 3th ed.; Elsevier, 2007.

(87)   Gallagher, W. P.; Terstiege, I.; Maleczka, R. E. *J. Am. Chem. Soc.* **2001**, *123*, 3194.

(88)   Deng, H.; Jung, J.-K. K.; Liu, T.; Kuntz, K. W.; Snapper, M. L.; Hoveyda, A. H. *J. Am. Chem. Soc.* **2003**, *125*, 9032.

(89)   Magano, J.; Dunetz, J. R. *Chem. Rev.* **2011**, *111*, 2177.

(90)   Menzel, K.; Fu, G. C. *J. Am. Chem. Soc.* **2003**, *125*, 3718.

(91)   Tang, H.; Menzel, K.; Fu, G. C. *Angew. Chem. Int. Ed.* **2003**, *42*, 5079.

(92)   Powell, D. A.; Maki, T.; Fu, G. C. *J. Am. Chem. Soc.* **2005**, *127*, 510.

(93)   King, A.; Yasuda, N. In *Organometallics in Process Chemistry*; Springer Berlin Heidelberg: 2004; Vol. 6, p 205.

(94)   Chinchilla, R.; Najera, C. *Chem. Soc. Rev.* **2011**, *40*, 5084.

(95)   Chinchilla, R.; Nájera, C. *Chem. Rev.* **2007**, *107*, 874.

(96)   Doucet, H.; Hierso, J. C. *Angew. Chem. Int. Ed.* **2007**, *46*, 834.

(97)   Beletskaya, I. P.; Latyshev, G. V.; Tsvetkov, A. V.; Lukashev, N. V. *Tetrahedron Lett.* **2003**, *44*, 5011.

(98)   Vechorkin, O.; Barmaz, D.; Proust, V.; Hu, X. *J. Am. Chem. Soc.* **2009**, *131*, 12078.

(99)   Yi, J.; Lu, X.; Sun, Y. Y.; Xiao, B.; Liu, L. *Angew. Chem. Int. Ed.* **2013**, *52*, 12409.

(100)   Cassar, L. *J. Organomet. Chem.* **1975**, *93*, 253.

Chapter 2 : Nickel-Catalyzed Diastereoselective Alkyl-Alkyl Kumada Coupling Reactions

2.1 Introduction

Current advances in transition metal catalysis have transformed the challenging alkyl-alkyl cross coupling into a synthetically applicable method for construction new C – C bonds.[1,2] Since stereogenic centers are ubiquitous in bioactive molecules,[3] the exploration of the stereoselective capacities of a synthetic methodology is mandatory to increase its academic or industrial value. While remarkable progress has been made in enantioselective alkyl – alkyl coupling,[4-9] diastereoselective cross – coupling of this type is largely unexplored. The conformational preference of the substituents close to the coupling carbons are determinant for the stereoselectivity of the coupling. For this reason, the reports of highly diastereoselective coupling was mostly reported for 1,2-substituted cyclic substrates.[10-14]

Knochel and co-workers developed highly diastereoselective Negishi coupling of 1,3- and 1.4-substituted cyclohexylzinc reagents with aryl, hetereoaryl, and alkynyl halides.[15-18] These pioneering studies demonstrated powerful diasterocontrol using the conformational preference of Pd-cyclohexyl intermediates, which were produced by transmetallation of a Pd catalyst with cyclohexyl zinc reagents (Scheme 1).
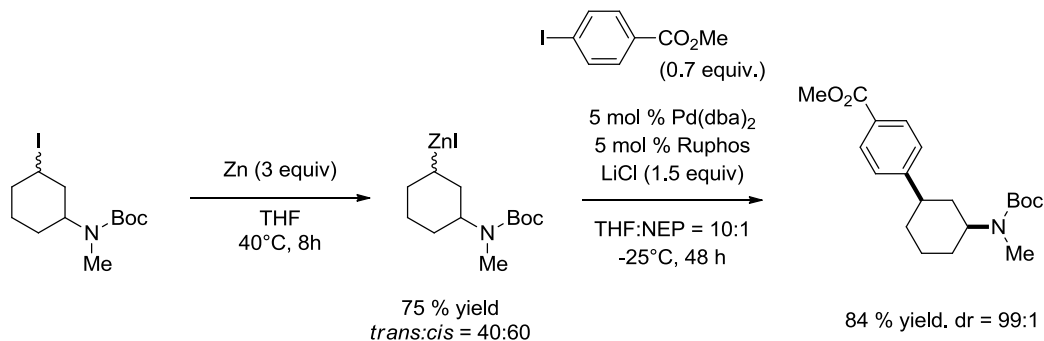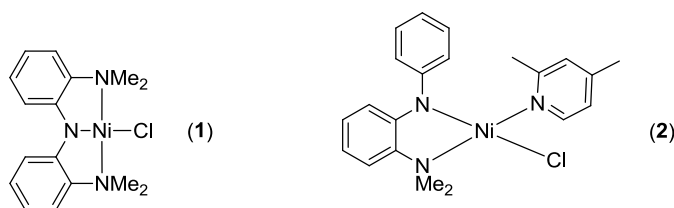

Scheme 1: Representative example of a high diastereoselective Negishi cross-coupling developed by Knochel and co-workers.[15]
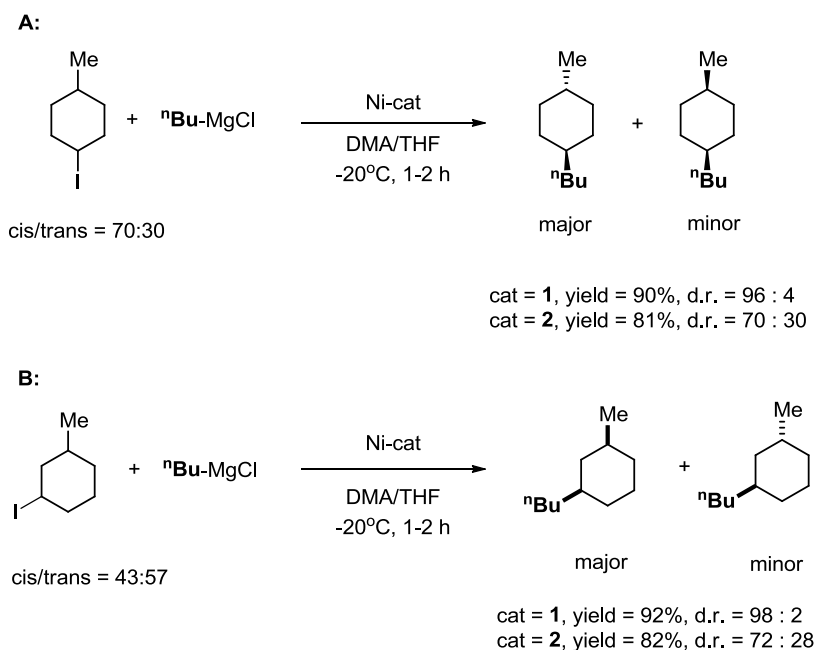
We reasoned that analogous nickel cyclohexyl intermediates might be generated through oxidative addition of cyclohexyl halides on a nickel catalyst. Herein we report high diastereoselective nickel-catalyzed cross-coupling of 1,3- and 1,4-substituted cyclohexyl halides and tetrahydropyrans with alkyl Grignard reagents. These structural units are important building blocks of Liquid Crystal Display (LCD) materials[19] or biologically active molecules[20].

2.2 Test reactions

Complexes **1** and **2** were chosen as catalysts after we previously showed them to be efficient for alkyl – alkyl Kumada coupling reactions[21-25] (Figure 1). The coupling of 4-methylcyclohexyl iodide with ^{n}BuMgCl was examined using the previously published protocols (Scheme 2). Catalyst **2** was more efficient for the coupling of secondary alkyl halides, and a 3 mol % loading was sufficient for a high coupling yield. Comparatively, a 9 mol % loading of **1** was required for a similar coupling yield. *trans*-1-Butyl-4-methylcyclohexane was produced as the major isomer using either catalyst. The diastereoselectivity of the reaction was excellent using **1** as the catalyst (dr = 96:4) but was modest with **2** as the catalyst (dr = 70:30). The pincer $^{Me}N_2N$ ligand in **1** seems to be sufficiently bulky to induce high diastereoselectivity, while it was shown that the lutidine ligand dissociated from **2** during catalysis[23]. The ligand environment of the nickel center might be considered less sterically hindered in **2** than in **1**, which could lead to a lower diastereoselectivity. The coupling of 3-methylcyclohexyl iodide with ^{n}BuMgCl was also examined. *cis*-1-Butyl-3-methylcyclohexane was the major isomer of the product using either catalyst. Catalyst **1** again enabled excellent diastereoselectivity (dr = 98:2), while catalyst **2** resulted in modest diastereoselectivity (dr = 72:28). It is noteworthy to mention that the geometric isomerism of the starting materials and the coupling products were determined by NMR techniques, which are fully explained in the experimental section.

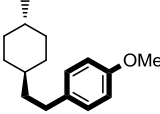**Figure 1.** Amino – amide nickel complexes developed by our group.

A:

cis/trans = 70:30

major   minor

cat = **1**, yield = 90%, d.r. = 96 : 4
cat = **2**, yield = 81%, d.r. = 70 : 30

B:

cis/trans = 43:57

major   minor

cat = **1**, yield = 92%, d.r. = 98 : 2
cat = **2**, yield = 82%, d.r. = 72 : 28
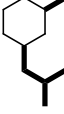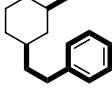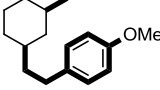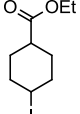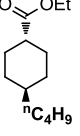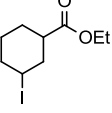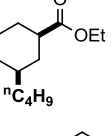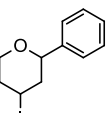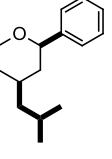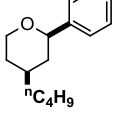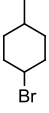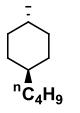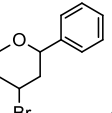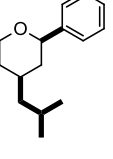
Scheme 2. Test Reactions in Diastereoselective Alkyl-Alkyl Kumada Coupling.
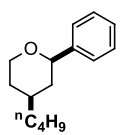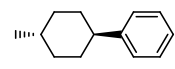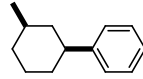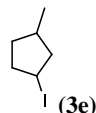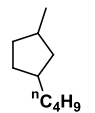
2.3 Scope of the diastereoselective alkyl-alkyl Kumada coupling

The scope of the diastereoselective alkyl-alkyl Kumada coupling was explored using **1** as the catalyst (Table 1).

Table 1. Scope of Nickel-Catalyzed Diastereoselective Kumada Coupling of Alkyl Halides.

Entry	Alkyl-x	Product	Yield (%)	d.r.
1	(3a)	$^nC_5H_{11}$	80[b]	96:4
2	**3a**	$^nC_8H_{17}$	80[b]	96:4
3	**3a**		87[b]	96:4
4	**3a**		65[c,d]	94:6

5	**3a**		$81^{c,d}$	94:6
6	(3b)	$^nC_5H_{11}$	77^b	98:2
7	**3b**	$^nC_8H_{17}$	93^b	98:2
8	**3b**		87^b	97:3
9	**3b**		$79^{c,d}$	>99:1
10	**3b**	OMe	$69^{c,d}$	96:4
11		$^nC_4H_9$	74^c	90:10
12		$^nC_4H_9$	52^c	90:10
13	(3c)		80^c	>99:1
14	**3c**	$^nC_4H_9$	65^c	>99:1
15		$^nC_4H_9$	77^b	94:6
16		$^nC_4H_9$	$79^{b,f}$	95:5
17	(3d)		$83^{b,f}$	95:5

18	**3d**		$88^{b,f}$	95:5
19	**3a**		$62^{b,g}$	94:6
20	**3b**		$91^{b,g}$	95:5
21	**(3e)**		87^{b}	55:45

^{a}Standard conditions: The Grignard reagent (0.6 mmol) in THF (3.5 mL) was added by Syringe pump over 2 h to a solution of **1** (15 mg, 9 mol %) and alkyl halide (0.5 mmol) in DMA (0.75 mL) at -20°C. Reaction time: 30 min. ^{b}GC yield. ^{c}Isolated yield. ^{d}Modified conditions: The Grignard reagent was added to a solution of **1** (15 mg, 9 mol %), TMEDA (25 μL), and alkyl halide (0.5 mmol) in THF (1 mL) at -20°C. ^{e}The other isomer was not observed by NMR. ^{f}Standard Conditions except at rt. ^{g}Modified conditions except at rt.

A large number of alkyl Grignard reagents could be used, with generally high yields. For 1,4-substituted substrates, the major product is always the *trans*-isomer; for 1,3-substituted substrates, the major product is always the *cis*-isomer. The diastereoselective ratio was nearly independent of the nature of the Grignard reagent. The coupling of ^{n}PentylMgCl and ^{n}OctylMgCl compared to the coupling of ^{n}BuMgCl gave identical dr values, that is, 96:4 with 4-methylcyclohexyl iodide (entries 1 – 2, Table 1) and 98:2 with 3-methylcyclohexyl iodide (entries 6 – 7, Table 1). ^{i}BuMgCl was coupled with similar dr values (entries 3 and 8, Table 1). Grignard reagents with an aryl group were successfully coupled, although a modification of experimental conditions was required to obtain reasonable isolated yields (entries 4, 5, 9, 10, Table 1). An ester was able to control the conformation of the nickel-cyclohexyl intermediates as well. Thus, coupling of ethyl 4-iodocyclohexanecarboxylate and 3-iodocyclohexanecarboxylate gave a dr of 90:10 (entries 11 and 12, Table 1). The lower dr compared to those of methyl-substituted derivatives is consistent with a lower A value of ester (A = 1.2 -1.3) than for CH_3 (A = 1.74)^{26}. This result confirms that the diastereoselectivity of the coupling reactions is linked to the conformational preference of remote substituents. Gratifyingly, the coupling of tetrahydropyran derivatives was also successful (entries 13, 14, 17, 18, Table 1). The dr reached >99:1 for the coupling of **3c**, which is consistent with the high A value of the C_6H_5 group (A = 2.8 on cyclohexane and even larger on tetrahydropyran).^{26} Alkyl bromides could be coupled with high dr values (≥94:6, entries 15 – 18, Table 1). These reactions were conducted at rt to ensure high yields, and as a result the

yields are slightly lower than those from the corresponding alkyl iodides at -20°C. While this work focuses on alkyl-alkyl coupling, the method described here could be modified[27] for diastereoselective alkyl-aryl[16,18,28,29] coupling as well. Coupling of **3a** and **3b** with PhMgCl was achieved in good yields and high dr (entries 19 – 20, Table 1). When 3-methyl-1-iodocyclopentane was coupled to ^{n}BuMgCl, the yield was 87 %, but the dr was only 55:45 (entry 21, Table 1). The low diastereoselectivity is consistent with the similar energies of different conformers for cyclopentane derivatives.[26]

2.4 Understanding the diastereoselectivity

The origin of the diastereoselectivity was probed by several experiments. The diastereoselectivity was independent of the dr ratio of the substrates. When an 80:20 *cis/trans* mixture of 4-methylcyclohexyl iodide was coupled to ^{n}BuMgCl, the dr of the product was 96:4, the same as that of the coupling of a 70:30 *cis/trans* mixture of 4-methylcyclohexyl iodide. Likewise, when a 20:80 *cis/trans* mixture of 3-methylcyclohexyl iodide was coupled to ^{n}BuMgCl, the dr of the product was the same (98:2) as that of the coupling of a 43:57 *cis/trans* mixture of 3-methylcyclohexyl iodide.

2.4.1 Reaction profile

The coupling of 3-methylcyclohexyl iodide with ^{n}BuMgCl was followed at partial conversions. ^{n}BuMgCl was slowly added by a syringe pump over 1 h to the reaction mixture, and the quantities of substrates and products were determined by GC (Figure 2). The dr of the product was 98:2 throughout the reaction. Interestingly, the amount of *cis*-3-methylcyclohexyl iodide increased initially before the eventual decrease to give the coupling product. The initial increase, albeit small, was always observed in multiple reaction trials. The amount of *trans*-3-methylcyclohexyl iodide decreased at all times.
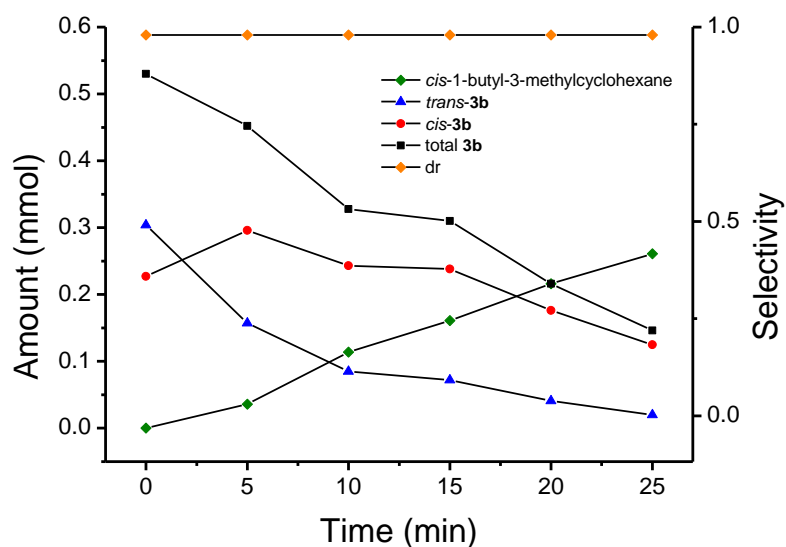
Figure 2. Reaction profile of the coupling of 3-methylcyclohexyl iodide with ^{n}BuMgCl.

To further confirm the initial increase of the amount of *cis*-3-methylcyclohexyl iodide, the kinetic profile of the coupling of 3-methylcyclohexyl iodide with ^{n}BuMgCl was followed in the first 5 min (Figure 3). Because the coupling was fast and completed quickly after the addition of the Grignard reagent, a 3-fold dilution in the initial concentrations of the reagents was necessary to enable measurements. Again, the amount of *cis*-3-methylcyclohexyl iodide was found to increase during this time. Control experiments showed that $MgBr_2$ and NaI do not mediate the isomerization, pointing to an essential role of the nickel catalyst in the isomerization.
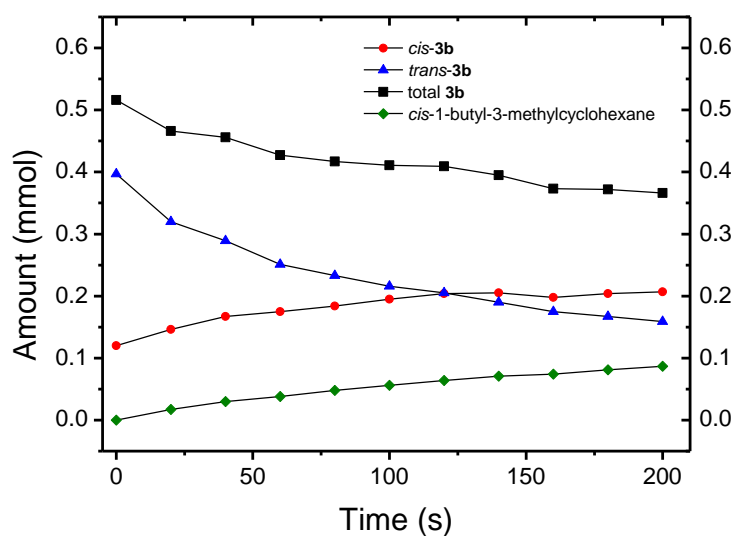
Figure 3. Kinetic profile of the coupling of 3-methylcyclohexyl iodide with ^{n}BuMgCl.

2.4.2 A rationale of the diastereoselective process

The abovementioned observations suggested that the activation of 3-methylcyclohexyl iodide was reversible in the current catalytic system. The reverse reaction, however, gave *cis*-3-methylcyclohexyl iodide as the major product because it is thermodynamically more stable. Therefore, at low conversion, an increase in the quantity of *cis*-3-methylcyclohexyl iodide could be observed. These observations all point the independence of the diastereoselectivity on the dr ratio of the substrates. We have reported evidence that the alkyl-alkyl Kumada coupling reactions catalyzed by **1** and **2** occurred via a radical process.[23,30] A radical-based mechanism would be consistent with the results described here. It is noted that in the presence of a radical inhibitor, TEMPO, the yields of the coupling of 4-methylcyclohexyl iodide and 3-methyl-cyclohexyl iodide with ^{n}BuMgCl catalyzed by **1** decreased to ca. 46 %, but the dr remained the same. This result is consistent with that the reaction occurs via a radical process. Figure 4 depicts a rationale for the diastereoselectiviy of the coupling reactions, using **3a** and **3b** as examples. The activation of cyclohexyl halides by a nickel catalyst generated a cyclohexyl radical. The substituents would prefer an equatorial position. When the carbon radical recombines with a nickel center, the nickel-ligand fragment might take either the axial of the equatorial position. In general, the equatorial position is preferred, and the ratio of axially and equatorially bound nickel intermediates depends on the steric property of the catalyst. A concerted C – C reductive elimination in known to be stereo-conservative[1,31,32] and would lead to the enrichment of the *trans*-product in the 1,4-substituted substrates and the *cis*-product in the 1,3-substituted substrates.

1,4-control

1,3-control
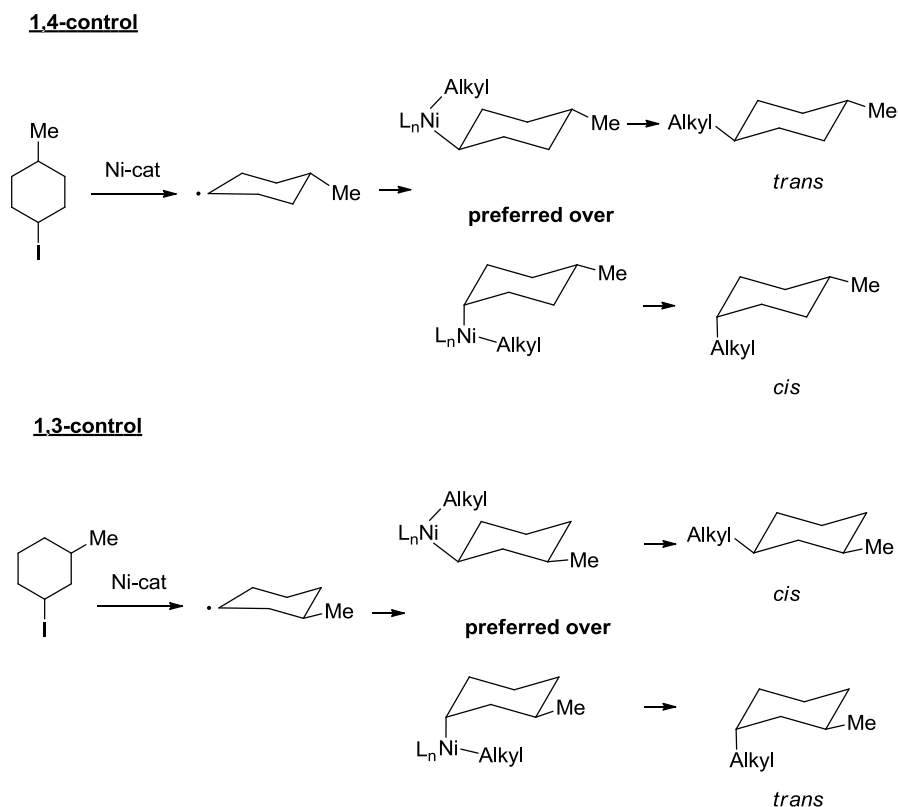
Figure 4. A rationale for observed diastereoselectivity.

2.5 Conclusion

In summary, we have developed a nickel-catalyzed diastereoselective alkyl-alkyl Kumada coupling method for 1,3- and 1,4-substituted cyclohexyl halides and tetrahydropyrans. Excellent diastereoselectivity is achieved using the nickel pincer catalyst **1**. The diastereoselectivity is controlled by the conformational preference of the nickel-alkyl intermediates. Fortuitously, we have also obtained evidence for the reversible activation of alkyl halide in the nickel catalysis, which provides significant information for mechanistic considerations of the nickel-catalyzed cross-coupling of non-activated halides.

2.6 Experimental section

2.6.1 Chemical reagents

All manipulations were carried out under an inert $N_2(g)$ atmosphere using standard Schlenk or glovebox techniques. Solvents were purified using a two-column solid-state purification system (Innovative Technology, NJ, USA) and transferred to the glove box without exposure to air. Deuterated solvents were purchased from Cambridge Isotope Laboratories, Inc., and were degassed and stored over activated 3 Å molecular sieves. Unless otherwise noted, all other reagents and starting materials were purchased from commercial sources and used without further purification. Liquid compounds were degassed by standard freeze-pump-thaw procedures prior to use. The following chemicals were prepared according to literature procedure: complex **1**,[24] complex **2**,[23] 4-methylcyclohexyl iodide (**3a**),[23] 3-methylcyclohexyl iodide (**3b**),[23] 4-iodocyclohexanecarboxylate,[23] 3-iodocyclohexanecarboxylate,[23] tetrahydropyran (**3c**),[33] tetrahydropyran (**3d**).[34]

2.6.2 Physical methods

The ^1H and ^{13}C NMR spectra were recorded at 293 K on a Bruker Avance 400 spectrometer. ^1H NMR chemical shifts were referenced to residual solvent as determined relative to Me_4Si (δ = 0 ppm). The $^{13}C\{^1H\}$ chemical shifts were reported in ppm relative to the carbon resonance of $CDCl_3$ (77.0 ppm). GC-MS measurements were conducted on a Perkin-Elmer Clarus 600 GC equipped with Clarus 600T MS. HRESI-MS measurements were conducted at the EPFL ISIC Mass Spectrometry Service with a Micro Mass QTOF Ultima spectrometer.

2.6.3 Determination of the diastereomeric ratios of the starting materials

The values of the diastereoisomeric ratios of 4-methylcyclohexyl iodide and 3-methylcyclohexyl iodide were calculated by GC − MS analysis and their identification was made by ^1H NMR analysis. For these compounds the hydrogen germinal to the iodine is easily identifiable at low field chemical shift (4 − 5 ppm), and the coupling structure can indicate its geometric position (Figure 5). More specifically, an axial proton should show a higher coupling structure than an equatorial.[35] Figure 1 shows the ^1H NMR spectra of 4-methylcyclohexyl iodide and 3-methylcyclohexyl iodide and the signals corresponding to their geometric isomers.
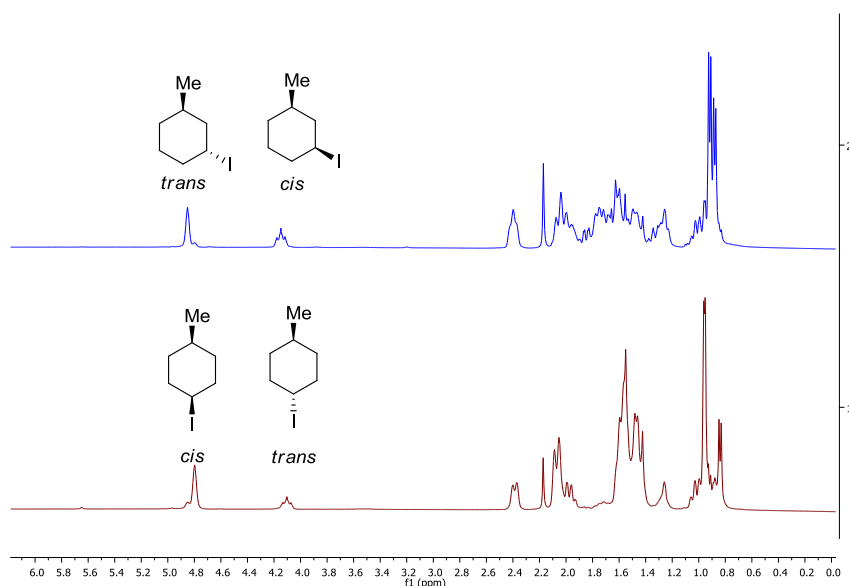
Figure 5. ^{1}H NMR spectra of the 3-methylcyclohexyl iodide (blue spectrum) and of 4-methylcyclohexyl iodide (red spectrum).

2.6.4 Determination of the diastereomeric ratios of the coupling products.

The diastereoisomeric ratios of the coupling products were determined by NMR techniques. The analysis of 1-butyl-4-methylcyclohexane and 1-butyl-3-methylcyclohexane is used as examples here. Jensen *et al.*[36] reported that the ^{1}H NMR spectrum of cyclohexane recorded at low temperature shows different chemical shifts for the axial and equatorial protons. The axial protons are around 0.5 ppm ($\Delta\delta_{eq\text{-}ax}$) upfield. We decided to use this information to determine the spatial conformation of the coupling product 1-butyl-4-methylcyclohexane. Figure 6 shows the conformational analysis of this molecule. The *trans*-isomer having both substituents in equatorial position is thermodynamically much more favorable. Therefore, the methylene protons (marked in blue and red in Figure 6) will basically have well-defined axial or equatorial positions due to the almost absent chair-flipping conversion. On the other hand, the *cis*-isomer has not a thermodynamically preferential conformer, therefore the methylene protons are in constant exchange between an axial and an equatorial position. Hence, the $\Delta\delta_{eq\text{-}ax}$ should be higher in the case of the *trans*-isomer.
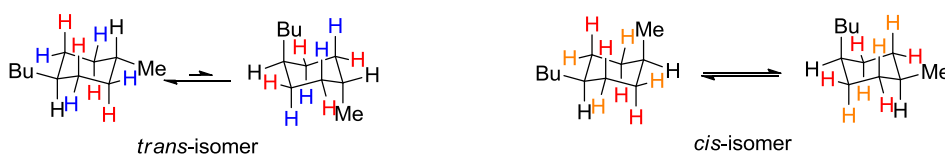
Figure 6. Conformational analysis of 1-butyl-4-methylcyclohexane.

We decided then to apply the Heteronuclear Single Quantum Correlation NMR (HSQC) to identify the isomers *trans* and *cis* of the 1-butyl-4-methylcyclohexane. As reference reaction, we analyzed first the isomer mixture produced using **2** as the catalyst. The dr of this reaction is low, 70:30, so it should be possible to observe both isomers. To our delight, the isomers *trans* and *cis* were clearly identifiable (Figure 7) and the non-substituted methylene signals of the *trans*-isomer showed indeed a higher $\Delta\delta_{eq-ax}$.
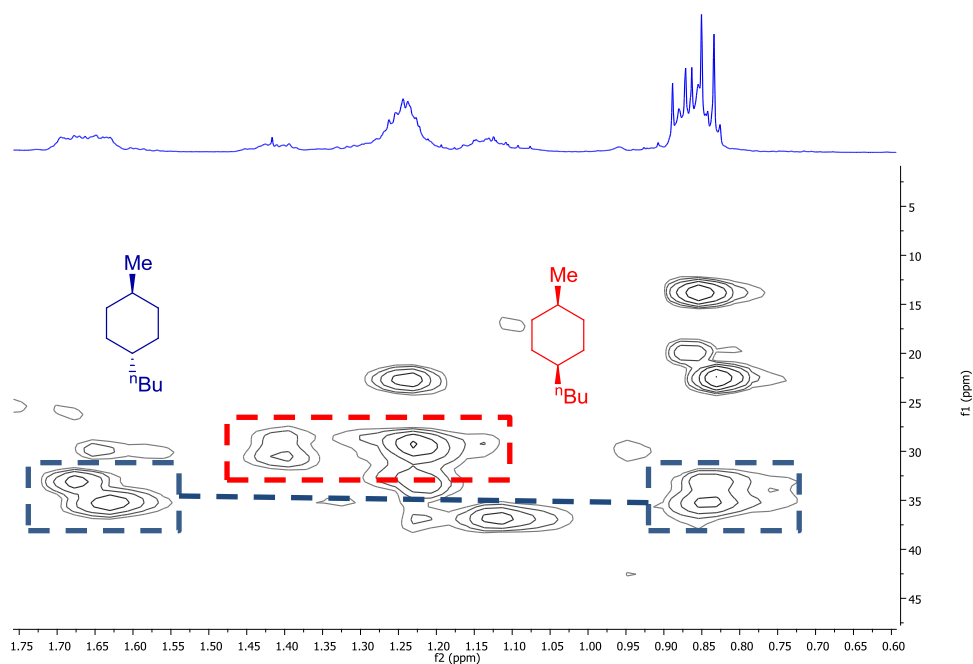
Figure 7. HSQC of cross-coupling product 1-butyl-4-methyl-cyclohexane obtained using complex **2** as the catalyst**.**

Figure 8 shows the HSQC spectrum of the 1-butyl-4-methylcyclohexane isomer mixture produced using **1** as the catalyst. The signals corresponding to the *cis*-isomer almost disappeared showing that the reaction is selective producing the thermodynamically most stable *trans*-isomer.
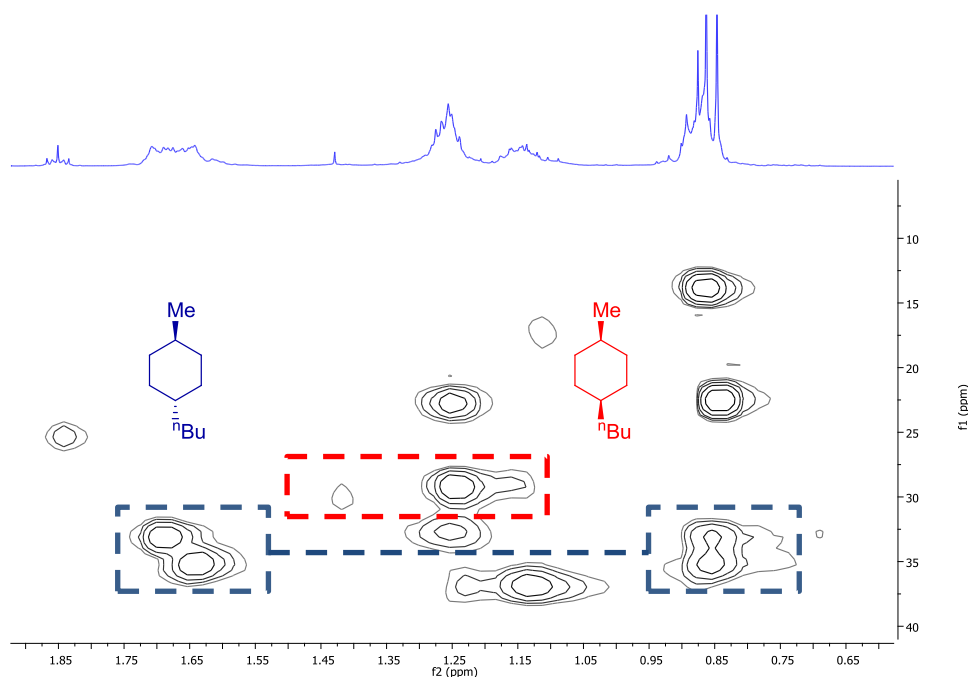
Figure 8. HSQC of cross-coupling product 1-butyl-4-methyl-cyclohexane obtained using complex **1** as the catalyst.

We did a similar conformational analysis for the coupling product 1-butyl-3-methylcyclohexane (Figure 9). The thermodynamically most stable conformer of the *cis*-isomer has both substituents in equatorial position. So the methylene hydrogens of this isomer will have a well-defined position as axial or equatorial. If this is true, the axial proton (red colored in Figure 9) of the methylene between the two substituents is present in a very shielding environment.[37] Consequently, the ^{1}H NMR signal of this hydrogen constitutes a "fingerprint" signal of the *trans*-1-butyl-3-methylcyclohexane. On the other hand, the *trans*-isomer does not have any preferential conformer and therefore the protons are in constant exchange between the axial and equatorial position. Figure 10 shows the superposition of ^{1}H NMR spectra of the pre-purified reaction mixtures containing 1-butyl-3-methylcyclohexane as coupling product obtained using complex **1** or **2** as catalysts. Both spectra contain a clear quadruplet at high field showing around 0.45 ppm as chemical shift. Considering the high dr determined by GC-MS analysis, it can be unambiguously concluded that the major product for this reaction is the *cis*-isomer.
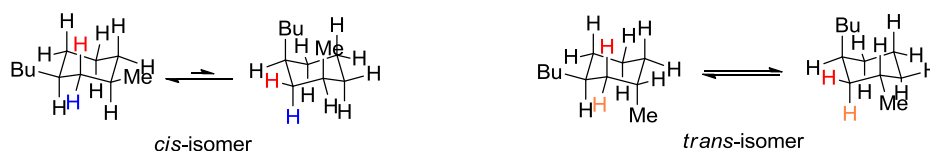
Figure 9. Conformational analysis of 1-butyl-3-methylcyclohexane
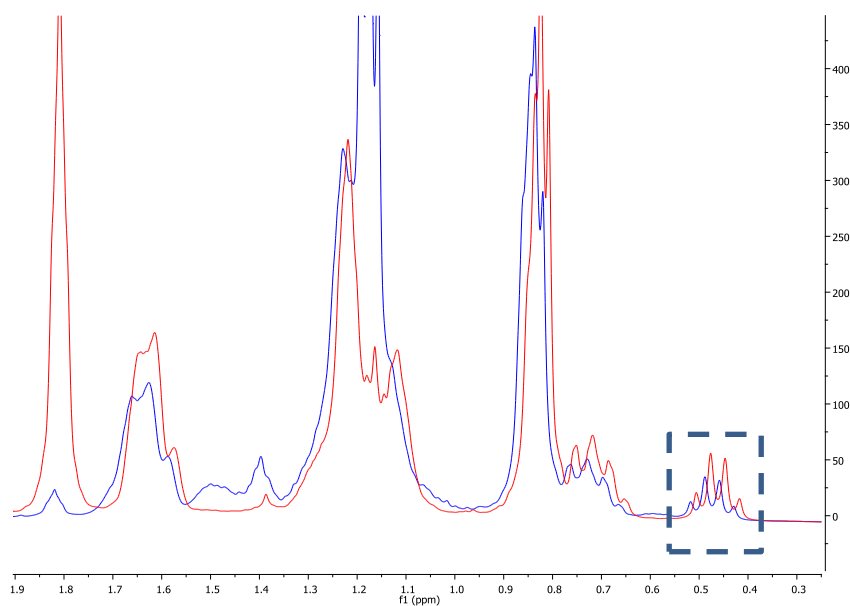
Figure 10. ^{1}H NMR spectra of 1-butyl-4-methylcyclohexane produced using **1** (red spectrum) or **2** (blue spectrum) as catalyst.

2.6.5 General procedures for Scheme 2 and Table 1

A solution of alkyl-MgCl (commercially available, 0.6 mmol) was diluted to 3.5 mL with THF. The solution was then slowly added by the syringe pump over 2 h to a solution containing [(^{Me}N$_2$N)Ni-Cl] (15 mg, 0.043 mmol), 0.75 mL of DMA, and the iodide (0.5 mmol) at -20°C. After the addition, the solution was still stirred for 30 min at -20°C. It was then quenched by the addition of 5 mL of a saturated solution of NH$_4$Cl and 5 mL of water. The organic phase in the resulting solution mixture was extracted with ether (3 times, 10 mL each), dried over Na$_2$SO$_4$, filtered, and subject to GC analysis. 60 μL of decane (0.31 mmol) was used as an internal standard.

- *Note for the entries 15, 16, 17 and 18*

The same procedure described in the last paragraph was applied, with the change that the addition was made at room temperature.

- *Note for the entries 4, 5, 9, 10, 19 and 20*

A solution of alkyl-MgCl or aryl-MgCl (commercially available, 0.6 mmol) was diluted to 3.5 mL with THF. The solution was then slowly added by the syringe pump over 2 h to a solution containing [($^{Me}N_2N)Ni-Cl$] (15 mg, 0.043 mmol), 1 mL of THF, TMDEA (25 µL, 0.17 mmol), and the iodide or bromide (0.5 mmol) at room temperature. After the addition, the solution was still stirred for 30 min at -20°C. It was then quenched by the addition of 5 mL of a saturated solution of NH_4Cl and 5 mL of water. The organic phase in the resulting solution mixture was extracted with ether (3 times, 10 mL each), dried over Na_2SO_4, filtered, and subject to GC analysis. 60 µL of decane (0.31 mmol) was used as an internal standard.

- *Note for entry 21*

The dr of the starting material was determined by ^{1}H NMR analysis (55:45, *cis*:*trans*). It must be considered that in a cyclopentane system, the energetic difference between an "equatorial" substituent and an "axial" substituent is small, which leads to a low d.r. of the coupling product.

- *Determination of the dr value*

The determination of the dr values was made by GC-MS analysis (except for entries 13, 14, 17 and 18 for where the dr values were determined by ^{1}H NMR analysis).

2.6.6 TEMPO-test

The coupling reaction of ^nBu-MgCl with 4-methylcyclohexyl iodide and with 3-methylcyclohexyl iodide were also conducted in the presence of one equivalent of a radical inhibitor ((2,2,6,6-tetramethylpiperidin-1-yl)oxidanyl, TEMPO). The yield of the reaction decreased to 47 % and 46 %, respectively. However the dr of the coupling products was exactly the same as given in Scheme 2.

2.6.7 Time dependent analysis

- *Reaction profile (Figure 1)*

A 2 M solution of ^nButyl-MgCl (commercially available, 0.6 mmol) was diluted to 3.5 mL with THF. The solution was then slowly added by the syringe pump (programmed for a total time of addition of 1 h) to a solution containing [($^{Me}N_2N)Ni-Cl$] (15 mg, 0.043 mmol), 0.75

mL of DMA, 60 μL of decane as internal standard (0.31 mmol) and the 3-methylcyclohexyl iodide (0.5 mmol) at -20°C. Small aliquots of 20 μL of the reaction mixture were taken each 5 minutes during the first 25 minutes of the addition. Each one of the aliquots was quenched with 1.5 mL of acetonitrile and analyzed then by GC-MS.

- *Kinetic profile (Figure 2)*

A 2 M solution of ^{n}Butyl-MgCl (commercially available, 0.6 mmol) was diluted to 3.5 mL with THF. The solution was then one time added to a solution containing [(^{Me}N$_2$N)Ni-Cl] (15 mg, 0.043 mmol), 2.25 mL of DMA, 60 μL of decane as internal standard (0.31 mmol), 7 mL of THF and the 3-methylcyclohexyl iodide (0.5 mmol) at -20°C. Small aliquots of the reaction mixture were taken each 20 seconds, leading to a total of 10 samples. Each one of the aliquots was quenched with acetonitrile and analyzed then by GC-MS.

2.6.8 Test for a possible role of MgBr$_2$ and NaI in the isomerization

The same conditions described for the general procedure were used to run two separated tests, replacing the Grignard reagent by stoichiometric quantities of anhydrous NaI and anhydrous MgBr$_2$ respectively. The reaction mixtures were stirred during 2 hours at -20°C. There was no isomerization observed for both tests.

2.6.9 Characterization of entries of Table 1

(2-(4-methylcyclohexyl)ethyl)benzene, entry 4
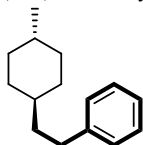
Purified by column (SiO$_2$, Hexane), 65% yield as a transparent liquid.
^{1}H NMR (400 MHz, CDCl$_3$): 7.36-7.26 (m, 2H), 7.25-7.16 (m, 3H), 2.65 (t, *J* = 8 Hz, 2H), 1.82-1.62 (m, 4H), 1.52-1.42 (m, 2H), 1.35-1.10 (br, 2H), 1.02-0.8 (m, 7H).
^{13}C NMR (100 MHz, CDCl$_3$): 143.2, 128.4, 128.3, 125.4, 39.3, 37.0, 35.3, 33.4, 33.3, 32.8, 22.8.
MS-APPI: calculated for (C$_{15}$H$_{22}$, M), 212.17160; found, 212.17177.
Anal. Calcd. C, 89.0; H, 11.0; Found: C, 89.2; H, 10.9.

1-methoxy-4-(2-(4-methylcyclohexyl)ethyl)benzene, entry 5
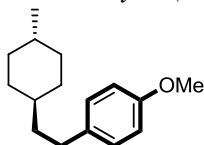
Purified by column (SiO$_2$, Hexane:EtOAc 50:1), 81% yield as a transparent liquid.

^{1}H NMR (400 MHz, CDCl$_3$): 7.10 (d, J = 8 Hz, 2H), 6.83 (d, J = 8.4 Hz, 2H), 3.80 (s, 3H), 2.57 (t, J = 7.6 Hz, 2H), 1.85-1.75 (m, 4H), 1.60-1.50 (m, 2H), 1.40-1.15 (br, 2H), 1.05-0.8 (m, 7H).
^{13}C NMR (100 MHz, CDCl$_3$): 157.5, 135.3, 129.2, 113.7, 55.3, 39.6, 37.0, 35.3, 33.3, 32.9, 32.4, 22.8.
HRESI-MS: calculated for (C$_{16}$H$_{25}$O, M+H), 233.1905; found, 213.1886
Anal. Calcd. C, 82.7; H, 10.4; Found: C, 82.4; H, 10.2.

(2-(3-methylcyclohexyl)ethyl)benzene, entry 9

Purified by column (SiO$_2$, Hexane), 79% yield as a transparent liquid.
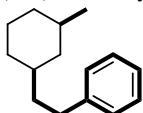**^{1}H NMR** (400 MHz, CDCl$_3$): 7.37-7.30 (m, 2H), 7.28-7.20 (m, 3H), 2.70 (t, J = 8 Hz, 2H), 1.90-1.70 (m, 4H), 1.62-1.50 (m, 2H), 1.45-1.3 (br, 3H), 1.00-0.8 (m, 5H), 0.70-0.60 (m, 1H).
^{13}C NMR (100 MHz, CDCl$_3$): 143.2, 128.4, 128.3, 125.6, 42.3, 39.7, 37.4, 35.4, 33.3, 33.0, 32.7, 26.4, 23.1.
MS-APPI: calculated for (C$_{15}$H$_{22}$, M), 212.17160; found, 212.17167.

1-methoxy-4-(2-(3-methylcyclohexyl)ethyl)benzene, entry 10
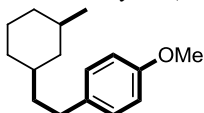
Purified by column (SiO$_2$, Hexane:EtOAc 50:1), 69% yield as a transparent liquid.
^{1}H NMR (400 MHz, CDCl$_3$): 7.10 (d, J = 8 Hz, 2H), 6.82 (d, J = 7.6 Hz, 2H), 3.79 (s, 3H), 2.57 (t, J = 8 Hz, 2H), 1.80-1.62 (m, 4H), 1.52-1.42 (m, 2H), 1.36-1.16 (br, 3H), 0.95-0.75 (m, 5H), 0.65-0.50 (m, 1H).
^{13}C NMR (100 MHz, CDCl$_3$): 157.5, 135.3, 129.2, 113.7, 55.2, 42.3, 39.8, 37.2, 35.4, 32.8, 32.6, 32.2, 26.2, 23.0.
HRESI-MS: calculated for (C$_{16}$H$_{25}$O, M+H), 233.1905; found, 213.1927
Anal. Calcd. C, 82.7; H, 10.4; Found: C, 83.1; H, 10.2

ethyl 4-butylcyclohexanecarboxylate, entry11
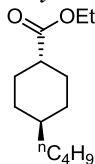
Purified by column (SiO$_2$, Hexane:EtOAc 50:1), 74% yield as a transparent liquid.
^{1}H NMR (400 MHz, CDCl$_3$): 4.17-4.07 (m, 2H), 2.20 (t, J = 12 Hz, 1H), 1.95 (d, J = 12 Hz, 2H), 1.80 (d, J = 12 Hz, 2H), 1.59-1.45 (m, 1H), 1.43-1.32 (m, 2H), 1.30-1.10 (m, 10H), 0.98-0.82 (m, 4H).
^{13}C NMR (100 MHz, CDCl$_3$): 176.2, 60.0, 43.6, 37.0, 37.0, 32.3, 29.1, 29.0, 23.0, 14.2, 14.1.
HRESI-MS: calculated for (C$_{13}$H$_{25}$O$_2$, M+H), 213.1855; found, 213.1865.

ethyl 3-butylcyclohexanecarboxylate, entry 12
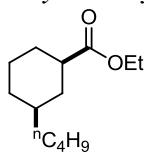
Purified by column (SiO$_2$, Hexane:EtOAc 50:1), 52% yield as a transparent liquid.
^{1}H NMR (400 MHz, CDCl$_3$): 4.15-4.05 (m, 2H), 2.26 (t, J = 9.6 Hz, 1H), 2.00-1.90 (m, 2H), 1.82-1.65 (m, 2H), 1.35-1.15 (m, 12H), 1.10-0.95 (m, 1H), 0.93-0.78 (m, 4H).
^{13}C NMR (100 MHz, CDCl$_3$): 176.2, 60.1, 43.6, 37.0, 37.0, 35.6, 32.5, 29.1, 29.0, 25.5, 23.0, 14.3, 14.1.
HRESI-MS: calculated for (C$_{13}$H$_{25}$O$_2$, M+H), 213.1855; found, 213.1865.

4-isobutyl-2-phenyltetrahydro-2H-pyran, entry 13
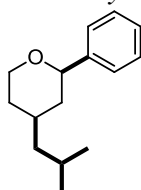
Purified by column (SiO$_2$, Hexane:EtOAc 50:1), 80% yield as a transparent liquid.
^{1}H NMR (400 MHz, CDCl$_3$): 7.44-7.17 (m, 5H), 4.30 (d, J = 11.2 Hz, 1H), 4.19-4.13 (m, 1H), 3.61 (t, J = 11.2 Hz, 1H), 1.93-1.51 (m, 4H), 1.41-1.10 (m, 4H), 0.89 (t, J = 4.8 Hz, 6H).
^{13}C NMR (100 MHz, CDCl$_3$): 143.2, 128.4, 127.4, 125.9, 80.0, 68.6, 46.5, 41.2, 33.3, 32.9, 24.3, 22.9, 22.84.
HRESI-MS: calculated for (C$_{15}$H$_{23}$O, M+H), 219.1749; found, 219.1750.

4-butyl-4-methyl-2-phenyltetrahydro-2H-pyran, entry 14
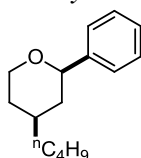
Purified by column (SiO$_2$, Hexane:EtOAc 50:1), 65% yield as a transparent liquid.
^{1}H NMR (400 MHz, CDCl$_3$): 7.44-7.17 (m, 5H), 4.32 (d, J = 10.8 Hz, 1H), 4.25-4.1 (m, 1H), 3.60 (t, J = 12 Hz, 1H), 1.95 (m, J = 12 Hz, 1H), 1.80-1.57 (m, 2H), 1.43-1.15 (m, 8H), 0.95-0.84 (m, 3H).
^{13}C NMR (100 MHz, CDCl$_3$): 143.3, 128.3, 127.3, 125.9, 80.0, 68.6, 41.1, 36.8, 35.7, 32.8, 28.7, 22.9, 14.2.
HRESI-MS: calculated for (C$_{15}$H$_{23}$O, M+H), 219.1749; found, 219.1750.

2.7 References

(1)   Hartwig, J. F. *Organotransition Metal Chemistry - From Bonding to Catalysis*; University Science Books: Sausalito, CA, 2010.

(2)   Marsden, J. A.; Haley, M. M.; Meijere, A. D., Diedrich, F., Eds.; Wiley-VCH: Weinheim: 2004; Vol. 1.

(3)   Mori, K. *Chirality* **2011**, *23*, 449.

(4)   Glorius, F. *Angew. Chem. Int. Ed.* **2008**, *47*, 8347.

(5)   Lu, Z.; Wilsily, A.; Fu, G. C. *J. Am. Chem. Soc.* **2011**, *133*, 8154.

(6)   Lundin, P. M.; Fu, G. C. *J. Am. Chem. Soc.* **2010**, *132*, 11027.

(7)   Rudolph, A.; Lautens, M. *Ang. Chem. Int. Ed.* **2009**, *48*, 2656.

(8)   Saito, B.; Fu, G. C. *J. Am. Chem. Soc.* **2008**, *130*, 6694.

(9)   Zultanski, S. L.; Fu, G. C. *J. Am. Chem. Soc.* **2011**, *133*, 15362.

(10)   Gong, H.; Gagné, M. R. *J. Am. Chem. Soc.* **2008**, *130*, 12177.

(11)   Hammann, J. M.; Steib, A. K.; Knochel, P. *Org. Lett.* **2014**, *16*, 6500.

(12)   Lu, Z.; Fu, G. C. *Ang. Chem. Int. Ed.* **2010**, *49*, 6676.

(13)   Saito, B.; Fu, G. C. *J. Am. Chem. Soc.* **2007**, *129*, 9602.

(14)   Yu, X.; Yang, T.; Wang, S.; Xu, H.; Gong, H. *Org. Lett.* **2011**, *13*, 2138.

(15)   Moriya, K.; Knochel, P. *Org. Lett.* **2014**, *16*, 924.

(16)   Seel, S.; Thaler, T.; Takatsu, K.; Zhang, C.; Zipse, H.; Straub, B. F.; Mayer, P.; Knochel, P. *J. Am. Chem. Soc.* **2011**, *133*, 4774.

(17)   Thaler, T.; Guo, L.-N.; Mayer, P.; Knochel, P. *Angew. Chem. Int. Ed.* **2011**, *50*, 2174.

(18)   Thaler, T.; Haag, B.; Gavryushin, A.; Schober, K.; Hartmann, E.; Gschwind, R. M.; Zipse, H.; Mayer, P.; Knochel, P. *Nat. Chem.* **2010**, *2*, 125.

(19)   Pauluth, D.; Tarumi, K. *J. Mater. Chem.* **2004**, *14*, 1219.

(20)   Kang, E. J.; Lee, E. *Chem. Rev.* **2005**, *105*, 4348.

(21)   Vechorkin, O.; Hu, X. *Angew. Chem. Int. Ed.* **2009**, *48*, 2937.

(22)   Vechorkin, O.; Csok, Z.; Scopelliti, R.; Hu, X. *Chem. Eur. J.* **2009**, *15*, 3889.

(23)   Ren, P.; Vechorkin, O.; Allmen, K. v.; Scopelliti, R.; Hu, X. *J. Am. Chem. Soc.* **2011**, *133*, 7084.

(24)   Csok, Z.; Vechorkin, O.; Harkins, S. B.; Scopelliti, R.; Hu, X. *J. Am. Chem. Soc.* **2008**, *130*, 8156.

(25)   Breitenfeld, J.; Vechorkin, O.; Corminboeuf, C.; Scopelliti, R.; Hu, X. *Organometallics* **2010**, *29*, 3686.

(26)   Anslyn, E. V.; Dougherty, D. A. *Modern Physical Organic Chemistry*; University Science Books: Sausalito, CA, 2006.

(27)   Vechorkin, O.; Proust, V.; Hu, X. *J. Am. Chem. Soc.* **2009**, *131*, 9756.

(28)   Steib, A. K.; Thaler, T.; Komeyama, K.; Mayer, P.; Knochel, P. *Angew. Chem. Int. Ed.* **2011**, *50*, 3303.

(29)   Nakamura, M.; Matsuo, K.; Ito, S.; Nakamura, E. *J. Am. Chem. Soc.* **2004**, *126*, 3686.

(30)   Breitenfeld, J.; Ruiz, J.; Wodrich, M. D.; Hu, X. *J. Am. Chem. Soc.* **2013**, *135*, 12004.

(31)   Wilsily, A.; Tramutola, F.; Owston, N. A.; Fu, G. C. *J. Am. Chem. Soc.* **2012**, *134*, 5794.

(32)   Taylor, B. L. H.; Jarvo, E. R. *J. Org. Chem.* **2011**, *76*, 7573.

(33)   Sabitha, G.; Reddy, K. B.; Reddy, G. S. K. K.; Fatima, N.; Yadav, J. S. *Synlett* **2005**, *2005*, 2347.

(34)   Clarisse, D.; Pelotier, B.; Piva, O.; Fache, F. *Chem. Comm.* **2012**, *48*, 157.

(35)   Karplus, M. *J. Am. Chem. Soc.* **1963**, *85*, 2870.

(36)   Jensen, F. R.; Noyce, D. S.; Sederholm, C. H.; Berlin, A. J. *J. Am Chem. Soc.* **1962**, *84*, 386.

(37)   Danneels, D.; Anteunis, M. *Organic Magnetic Resonance* **1974**, *6*, 617.

Chapter 3 : Design and synthesis of bidentate amido – amine ligands and their nickel complexes: initial studies for stereoconvergent alkyl – alkyl Kumada coupling.

3.1 Introduction

Among metal catalyzed cross coupling methodologies,[1] the coupling of alkyl electrophiles is still challenging due to the slow oxidative addition of alkyl electrophiles to the metal center, and the tendency of metal alkyl species for β-hydride elimination.[2] Recently a number of catalytic methodologies have been developed to overcome these difficulties, using: nickel,[3-7] palladium,[8,9] copper,[10,11] iron[12-14] and cobalt[15-18] as transition metal centers and Grignard reagents as carbon nucleophiles. In the previous chapters, we discussed the possible application of cross coupling methodologies to the construction of stereogenic centers. To accomplish this purpose, the first condition is that the metal based catalytic system should be effective for the coupling of secondary or tertiary carbon substrates. The use of secondary or tertiary carbon electrophiles in metal catalyzed coupling reactions is difficult; the electronic richness and the steric hindrance of these compounds make them reluctant to undergo oxidative addition to the metal center.[19] Once a metal based catalytic system is active to create tertiary or quaternary carbons centers, the asymmetric induction of cross coupling reaction could be envisaged to be accomplished in two ways:[20] by substrate-control or by catalyst-control. In a substrate-controlled stereoselective reaction, or simply referred as stereospecific, the stereochemical information is transferred by one of the coupling moieties (Scheme 1A). On the other hand, in a catalyst-controlled stereoselective reaction, also referred as stereoconvergent, the coupling stereoselectivity is controlled by the chirality of the ligands on the catalytic metal center (Scheme 1B).
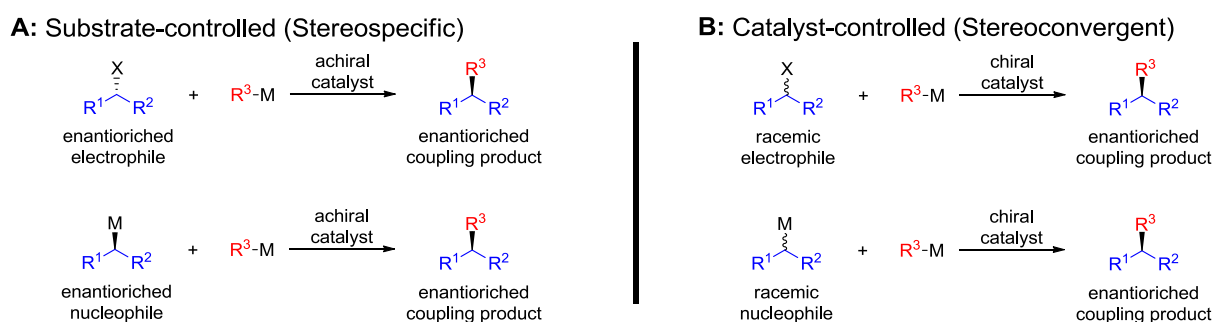
Scheme 1. General types of asymmetric induction in cross-coupling reactions.

The stereoconvergent reactions have the advantage that only catalytic quantities of a chiral compound are required to couple racemic substrates. Despite the initial successful studies for enantioselective Kumada coupling induced by chiral catalysts,[21,22] this domain remains largely unexplored. To the best of our knowledge only two examples of stereoconvergent

Kumada coupling were developed in the last decade. The pioneering work of Fu and co-workers[6] established that a Ni/bis(oxazoline) catalyst achieves at low temperature (-60°C) enantioselective cross coupling of α-bromoketones with aryl Grignard reagents in excellent yields and good enantiomeric excess (Scheme 2A). Similar studies were carried out by Walsh and co-workers[17] extending the use of chiral bis(oxazoline) ligands to Co catalyzed Kumada coupling of α-bromo esters with aryl Grignard reagents (Scheme 2B). Walsh's methodology required higher catalyst loading than Fu's methodology but higher enantiomeric excess were obtained. Furthermore, the Co catalyzed coupling methodology was successfully used for a total synthesis of a nonsteroidal anti-inflamatory drug (*S*)-ar-tumerone demonstrating its versatility.

A: Stereoconvergent nickel catalyzed Kumada coupling
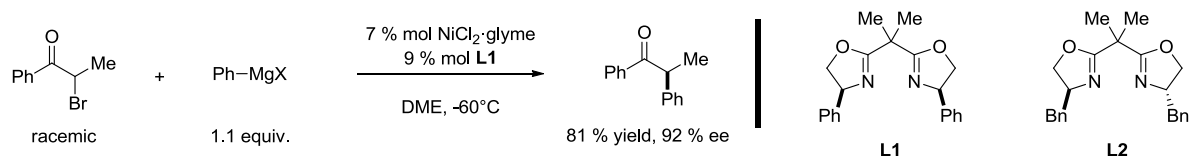
B: Stereoconvergent cobalt catalyzed Kumada coupling
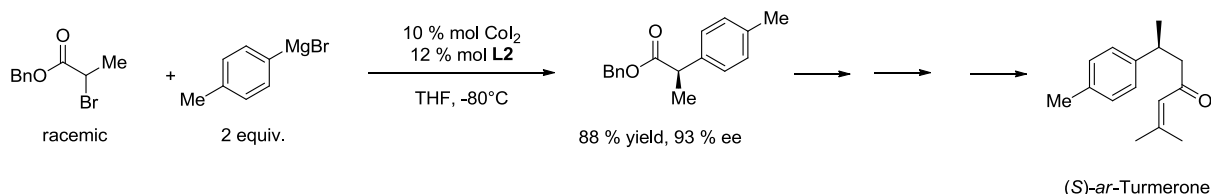
Scheme 2. Representative examples of stereoconvergent nickel and cobalt catalyzed Kumada coupling.

The above mentioned studies points to new opportunities in asymmetric catalysis. The alkyl – alkyl Kumada coupling is still unexplored for stereoconvergent coupling. Our group developed effective nickel amido – amine bidentate catalysts for alkyl – alkyl Kumada coupling of non-activated secondary halides.[5] Asymmetric modifications of our amido – amine ligands could be used to synthesize well-defined nickel chiral complexes. We hypothesize that a chiral amido – amine nickel complex might catalyze asymmetric alkyl – alkyl Kumada coupling reactions of non-activated secondary halides.

Herein, we present the synthesis of two new amido - amine bidentate ligands containing racemic tertiary carbons and a new enantiomeric pure amido – amine bidentate ligands. Their nickel complexes demonstrated good catalytic activity for the alkyl – alkyl Kumada coupling

non-activated secondary alkyl halides and allowed us to perform initial studies of stereoconvergent Kumada coupling by a well-defined catalyst.

3.2 Synthesis of bidentate amido – amine ligands

The synthesis of the amido – amine ligand "Pengamine" **4**, was previously developed by our group.[5] Figure 1 shows the retrosynthetic route of ligand **4**. The ligand was synthesized by Buchwald – Hartwig coupling between aniline and 2-bromo-N,N-dimethylaniline. Ligand **4** was used to develop active nickel bidentate catalysts for cross – coupling reactions of unactivated secondary halides with Grignard reagents. A similar synthetic route could be used to synthesize amido – amine ligands from readily available starting material containing racemic or chiral carbon centers. Taking into account structural similarities, we decided to use the α-methylbenzylamine and the 2,5-dimethyl-pyrrolidine as starting materials for the synthesis of two new amido – amine ligands described in the following sections.
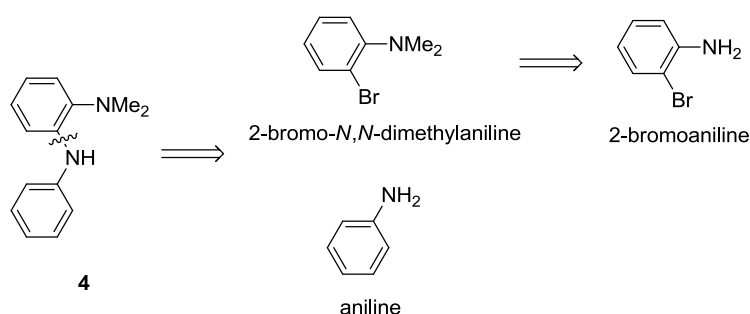
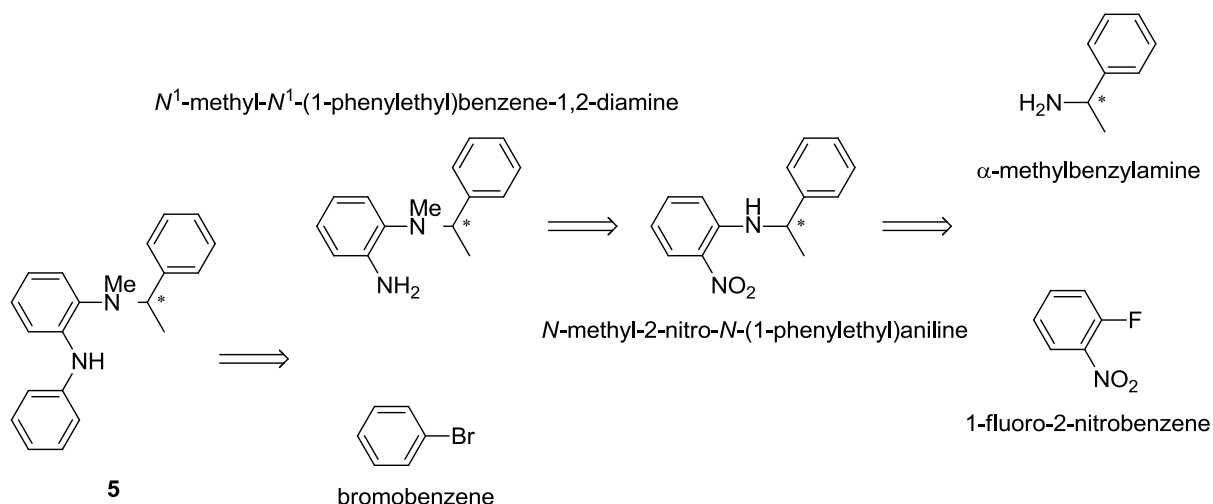

Figure 1. Retrosynthetic route of Pengamine ligand **4**.

3.2.1 A ligand derived from α-methylbenzylamine.

Figure 2 shows the retrosynthetic route of a new bidentate ligand **5**. Compared to ligand **4**, one of the methyl substituents of the amine donor is replaced by a racemic (1-ethyl)benzyl substituent in ligand **5**.

Figure 2. Retrosynthetic route of a new bidentate ligand **5**.

Racemic and *S* enantiomeric forms of α-methylbenzylamine were used to synthesize *rac*-**5** and (*S*)-**5**, respectively. The synthesis of the enantiomeric pure ligand (*S*)-**5** is described here. The synthesis started by aromatic nucleophilic substitution between (*S*)-α-methylbenzylamine and 1-fluoro-2-nitrobenzene in DMSO in the presence of K_2CO_3. The reaction resulted in the formation of (*S*)-2-nitro-*N*-(1-phenylethyl)aniline in a good yield. This substrate was then methylated in THF by MeI in the presence of NaH and HMPA as additive. The nitro group of the methylated substrate (*S*)-*N*-methyl-2-nitro-*N*-(1-phenylethyl)aniline was reduced to amine group in hydrogen atmosphere in presence of Pd/C. Scheme 3 shows the experimental conditions of these three reactions.
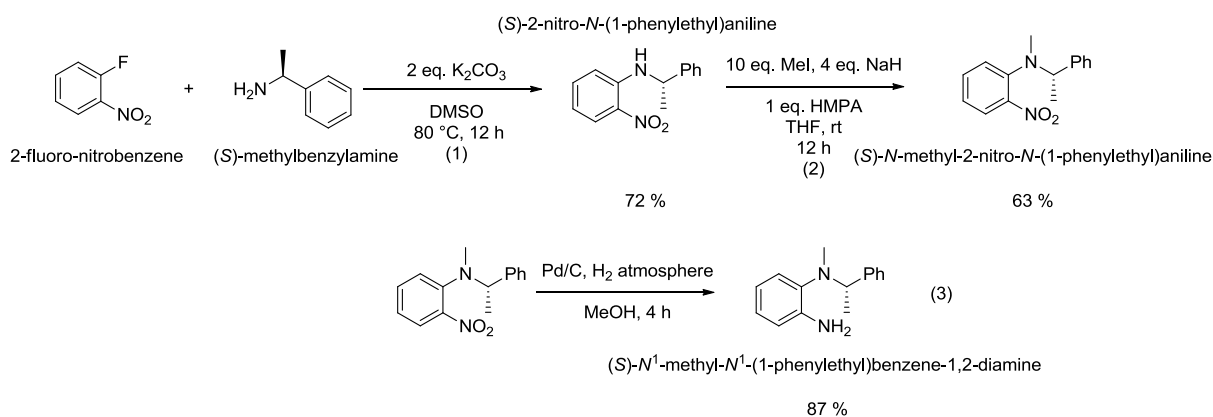
Scheme 3. Synthesis of (*S*)-*N¹*-methyl-*N¹*-(1-phenylethyl)benzene-1,2-diamine.

Ligand (*S*)-**5** was finally obtained, in an excellent yield, by C/N coupling between (*S*)-N^1-methyl-N^1-(1-phenylethyl)benzene-1,2-diamine and bromobenzene catalyzed by Pd^0 in presence of dppf (Scheme 4). The total yield at the end of the four steps synthesis was 36 % for both racemic and enantiomeric versions of ligand **5**. It is noteworthy to mention that (*S*)-**5** did not suffer any racemization during the synthesis; chiral HPLC analysis demonstrated that the enantiomeric purity of 99.5 % ee of the commercial (S)-α-methylbenzylamine was maintained for (*S*)-**5**.
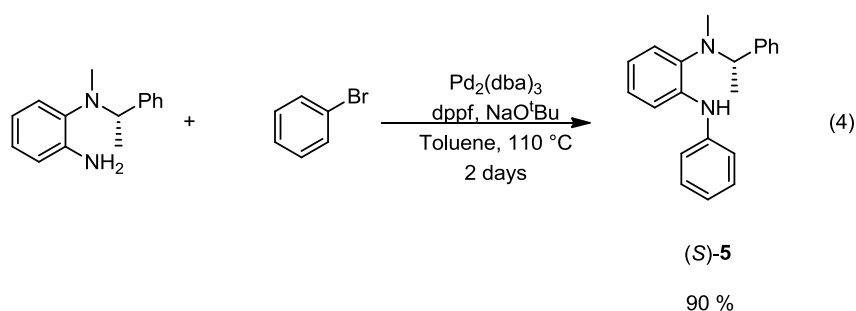
Scheme 4. Synthesis of ligand (*S*)-**5** by Pd^0 catalyzed C-N coupling.

3.2.2 A pyrrolidine derived ligand

Figure 3 shows the retrosynthetic route of a new bidentate ligand **6**, where the dimethyl amine donor in **4** is replaced by a 2,5-dimethylpyrrolidine group.
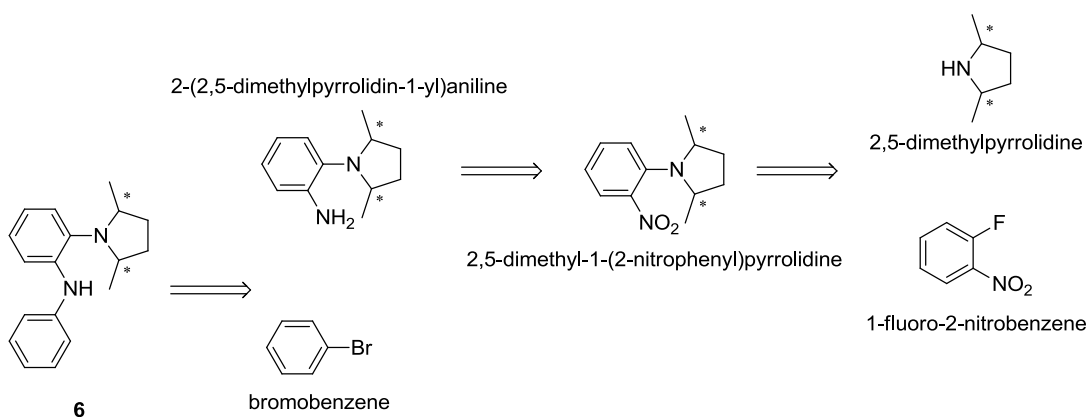
Figure 3. Retrosynthetic route of a new bidentate ligand **6**.

The synthesis started by the aromatic nucleophilic substitution between the 2,5-dimethylpyrrolidine and the 1-fluoro-2-nitrobenzene in DMSO in presence of K_2CO_3 producing 2,5-dimethyl-1-(2-nitrophenyl)pyrrolidine in good yield. The nitro group of this

substrate was then hydrogenated under hydrogen atmosphere in presence of Pd/C catalyst, giving 2-(2,5-dimethylpyrrolidin-1-yl)aniline in excellent yield. This substrate was coupled with bromobenzene in good yield using Pd-catalyzed Buchwald – Hartwig C – N coupling method. The ligand **6** was obtained with an overall yield of 48 %. Scheme 5 shows the reaction conditions of this three step synthesis.
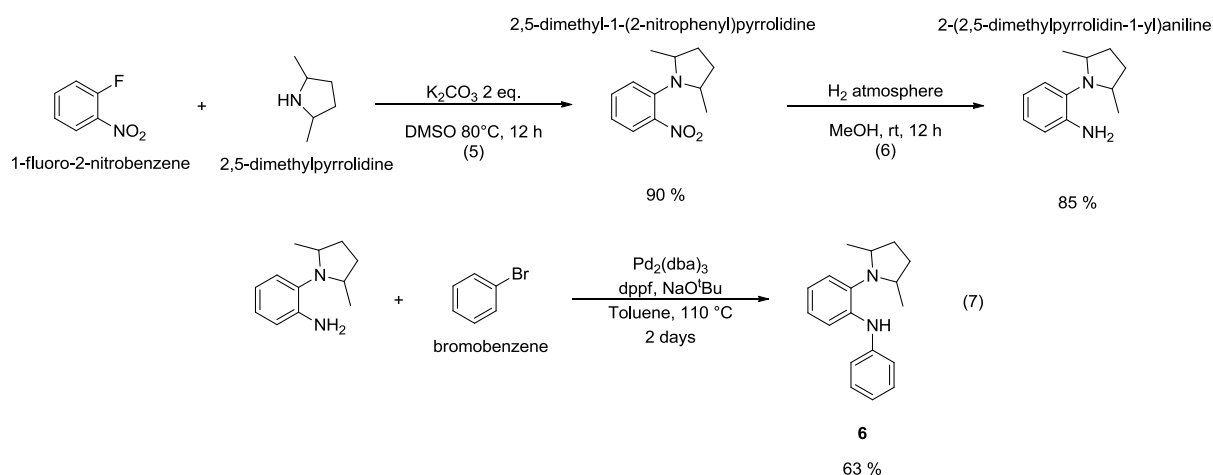
Scheme 5. Synthesis of ligand **6**.

3.3 Metalation trials

Previous studies have shown that an effective method to metalate amido – amine ligands is through lithium salt of the ligand. If the ligand is bidentate, the choice of nickel precursors containing strong co-ligands is primordial. The compounds $NiCl_2(2,4\text{-lutidine})_2$ and $NiCl_2(PPh_3)_2$ were previously used[5] for the successful synthesis of complexes derived from ligand **4** so we decided to employ them as nickel precursors for metalation trials with new ligands **5** and **6**.

3.3.1 α-Methylbenzylamine derived ligand

Our metalation studies started by the synthesis of the lithium salt *rac*-**5** obtained by direct reaction of *rac*-**5** with ^{n}BuLi in toluene (eq. 8, Scheme 6). The reaction of the lithium salt *rac*-**7** with $NiCl_2(PPh_3)_2$ didn't produce an identifiable compound (eq. 9, Scheme 6).
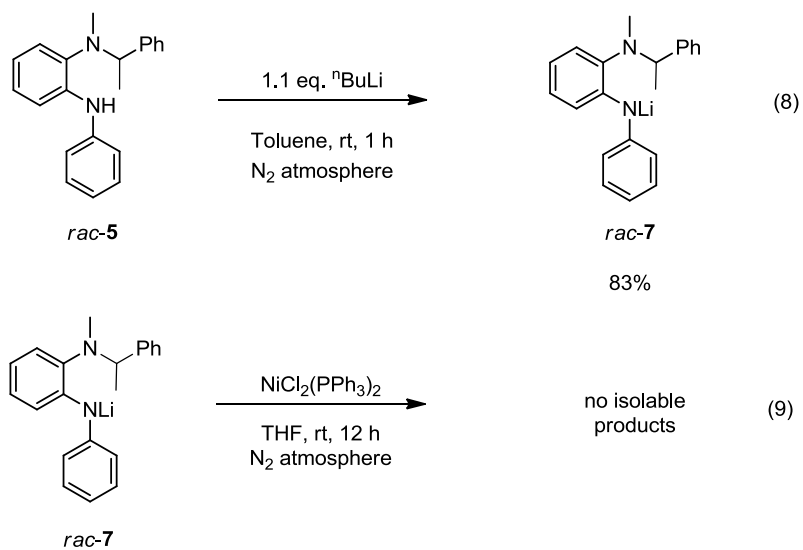
Scheme 6. Synthesis of lithium salt *rac*-**7** and reaction trial with NiCl$_2$PPh$_3$ precursor.

On the other hand, lithium salt *rac*-**7** reacted successfully with NiCl$_2$(2,4-lutidine)$_2$ producing a new bidentate nickel complex *rac*-**8** (Scheme 7). The X-Ray analysis of complex *rac*-**8** revealed a square planar structure (Figure 4). Encouraged by these results, the enantiomeric version of this new complex (*S*)-**8** was also synthesized in similar yields.
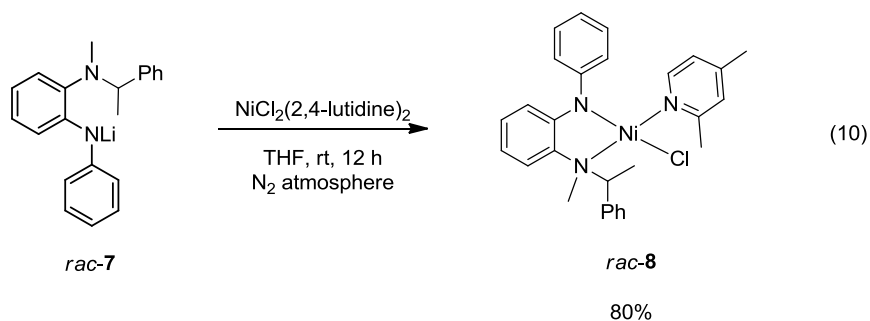
Scheme 7. Synthesis of a new bidentate complex *rac*-**8**.
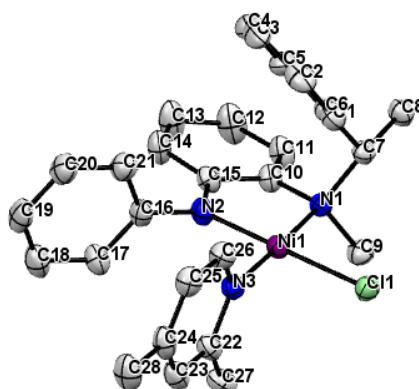
Figure 4. Crystal structure of complex *rac*-**8**. Hydrogen atoms are omitted for clarity. The thermal ellipsoids are displayed in a 50% probability. Selected lengths (Å) and angles (deg): Ni1-N1, 1.988(2); Ni1-N2, 1.859(3); Ni1-N3, 1.900(3); Ni1-Cl1, 2.2176(10); N1-Ni1-N2, 86.02(11); N2-Ni1-N3, 91.49(11); N3-Ni1-N1, 177.26(11).

3.3.2 Pyrrolidine derived ligand

Ligand **6** was also tested for the synthesis of new bidentate complexes. The corresponding lithium salt **9** was prepared by deprotonation with ^{n}BuLi in toluene in good yield (eq. 11, Scheme 8). The lithium salt **6** was then reacted with $NiCl_2(2,4\text{-lutidine})_2$ producing a blue compound **10** (eq. 12, Scheme 8) recovered and characterized by X-Ray analysis (Figure 5). The crystal structure of **10** revealed a dimeric nickel complex containing two μ^2 bridging chlorides but no 2,4-lutidine as co-ligand.
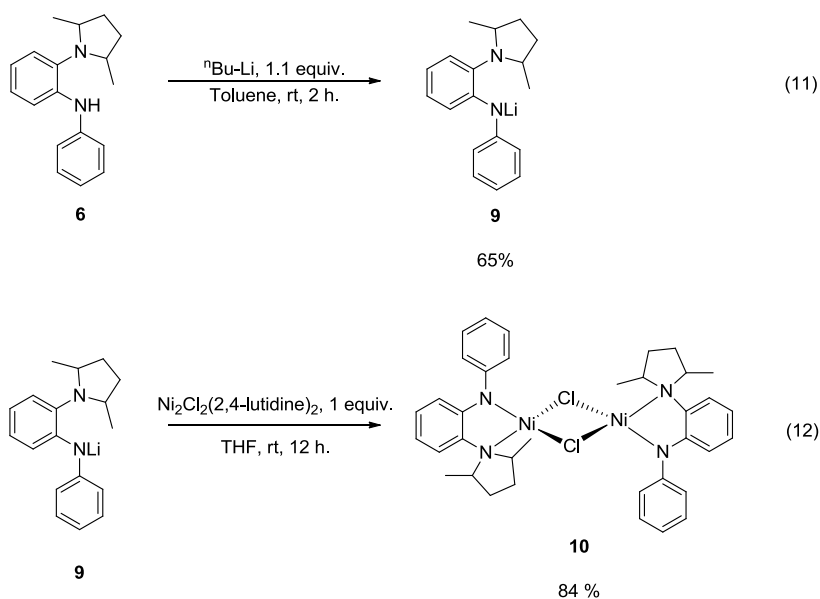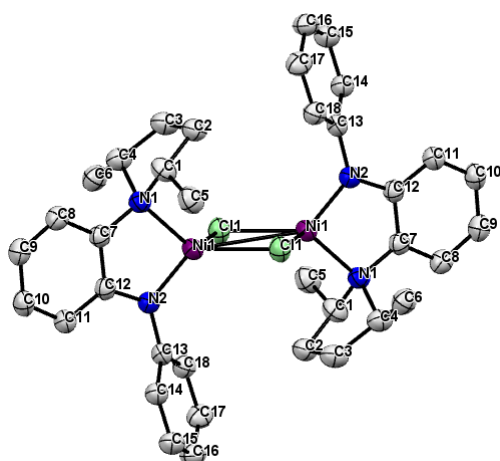

Scheme 8. Synthesis of dimeric nickel complex **10**.
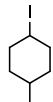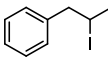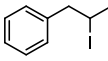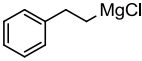
Figure 5. Crystal structure of complex **10**. Hydrogen atoms are omitted for clarity. The thermal ellipsoids are displayed in a 50% probability. Selected lengths (Å) and angles (deg): Ni1-N1, 2.099(3); Ni1-N2, 1.870(3); Ni1-Cl1, 2.349(11); N1-Ni1-N2, 84.83(12); N1-Ni1-Cl1, 122.04(8); Cl1-Ni1-N1, 86.01(4).

3.4 Catalyst activity screening

We tested the catalytic activity of complexes **8** and **10** for the Kumada coupling of non-activated secondary halides using previously described optimized conditions.[5] We started the screening of the catalyst activity of complex *rac*-**8** for the alkyl − alkyl Kumada coupling of non-activated secondary iodides. The reaction conditions, the coupling substrates and the obtained coupling yields are described in Table 1. Complex *rac*-**8** resulted being a good catalyst for the cross coupling process of cyclic (entries 1-3, Table 1) and acyclic secondary iodides (entries 4-6, Table 1).

Table 1. Kumada coupling activity of complex *rac*-**8** for non-activated iodides.
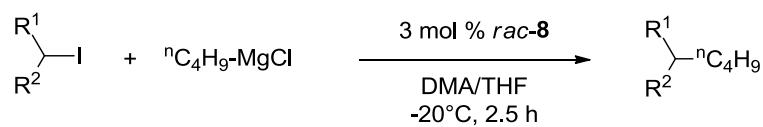
Entry	Iodide	Grignard reagent	Yield[a] %
1		^nBu-MgCl	78
2		^nBu-MgCl	60 d.r. 80:20
3		^nBu-MgCl	80 d.r. 80:20
4		^nOctyl-MgCl	75
5		^nBu-MgCl	80
6			75

[a]GC yields referred to the alkyl halide.
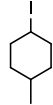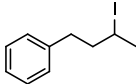
The obtained good coupling yields motivated us to test the enantioselective activity of chiral pure (*S*)-**8**. We decided to use as model reaction the coupling between (2-iodopropyl)benzyl and phenethyl magnesium chloride (entry 6, Table 1). Unfortunately, even though the coupling yield was high 75 %, the enantiomeric excess was only around 7 % (Scheme 9).
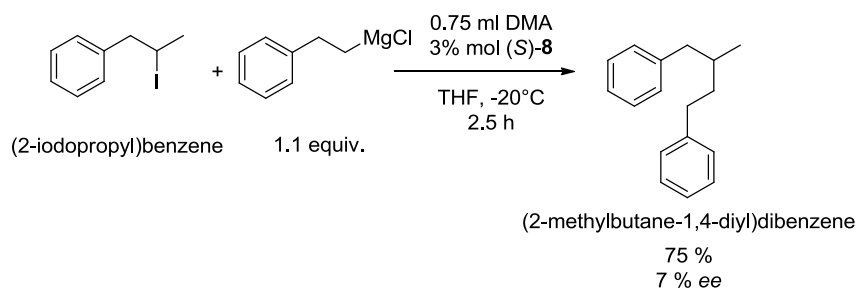
Scheme 9. Enantioselective Kumada coupling using (*S*)-**8** as catalyst.

The catalyst activity of complex **10** was also tested for the alkyl – alkyl Kumada coupling of cyclic (entries 1-2, Table 2) or acyclic iodides (entry 3, Table 2). Unfortunately, the obtained coupling yields were low or null.

Table 2. Kumada coupling activity of complex **10** for non-activated iodides.
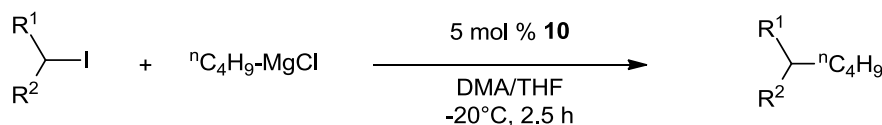
Entry	Iodide	Yield[a] %	Byproduct
1		15	Homocoupling halide
2		17 d.r. 81:19	Homocoupling halide
3		No rxn.	Homocoupling halide

[a]GC yields referred to the alkyl halide.

3.5 Discussion

We successfully synthesized a new chiral bidentate nickel complex (*S*)-**8** which effectively catalyzes alkyl – alkyl cross coupling reactions between non activated secondary alkyl halides and Grignard reagents. The precursor ligand (*S*)-**8** was designed using (*S*)-α-methylbenzylamine (99.5 % ee) as readily available starting material. The ligand synthesis involved 4 steps and no racemization was observed by chiral HPLC analysis of the final product. The synthetic sequence ligand lithiation – metalation was effective for the synthesis of complex **8** from $NiCl_2$(2,4-lutidine) precursor. The use of PPh_3 as co-ligand was nevertheless not possible; we suspect that the high steric hindrance of the phosphine co-ligands prevents the formation of the complex. It is noteworthy to mention that the catalyst activity of complex *rac*-**8** for the Kumada non-activated secondary halides is equal to our reported most active system.[5] Unfortunately, low asymmetric induction was observed when we tested complex (*S*)-**8** as catalyst for the coupling of (2-iodopropyl)benzene and phenethyl magnesium chloride (Scheme 9). We hypothesized that the bond between the nitrogen linker (N1) and the benzylic secondary carbon (C7) freely rotates in solution (Figures 4 and 6),

which represents a drawback for the transmission of the stereogenicity. Subsequently, the ligand structure should be as fixed as possible to avoid any movement of the bonds connected to the sterogenic centers.
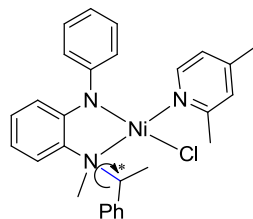
(*S*)-**8**

Figure 6. Schematic rotation of C12 – N1 bond (blue color) of chiral complex (*S*)-**8**.

Ligand **6** presents a more fixed structure around its tertiary carbon centers. Nevertheless, this steric feature appears to be a pitfall for the metalation of the ligand. The dimethylpyrrolidine linker seems to be too steric hindered to allow including a bulky co-ligand in the structure of the bidentate nickel complex. The formation of the μ^2 bichloride nickel dimer **10** is consistent with this hypothesis. Dimer **10** didn't show good catalytic activity for the coupling of non-activated iodides with alkyl Grignard reagents (Table 2).

3.6 Conclusions

In summary, we successfully synthesized a well-defined chiral bidentate amido – amine nickel complex having high catalytic activity for the coupling of non-activated secondary iodides with alkyl Grignard reagents. Even though the asymmetric induction during the coupling process was not successful, to the best of our knowledge, our approach using well-defined chiral complexes is a worthy starting point to understand the catalyst structural features determining the transfer of the stereochemical information. To accomplish this purpose, the rigidity of the ligand structure is crucial. Therefore, a pincer type ligand is probably more suitable as catalyst for stereoconvergent Kumada coupling. In the next chapter, we present the development of new pincer complexes and their catalyst activity study for the creation of tertiary carbon centers through Kumada coupling reactions.

3.7 Experimental Part

3.7.1 Chemicals and Reagents

The inert atmosphere manipulations were carried out under $N_2(g)$ atmosphere using standard Schlenk or glovebox techniques. Solvents were purified using a two-column solid-state purification system (Innovative Technology, NJ, USA) and transferred to the glove box without exposure to air. Deuterated solvents were purchased from Cambridge Isotope Laboratories, Inc., and were degassed and stored over activated 3 Å molecular sieves. Unless otherwise noted, all other reagents and starting materials were purchased from commercial sources and used without further purification. Liquid compounds were degassed by standard freeze-pump-thaw procedures prior to use. The nickel precursors $NiCl_2(2,4\text{-lutidine})_2$,[23] $NiCl_2(PPh_3)_2$[24] were prepared according to literature procedures. The iodides substrates from Table 1 and Table 2 were prepared form the corresponding alcohols.[5] The studies presented in this chapter are intermediate results, therefore the new synthesized compounds were only but univocally characterized by one physical method.

3.7.2 Physical methods

The ^1H spectra were recorded at 293 K on a Bruker Avance 400 spectrometer. ^1H NMR chemical shifts were referenced to residual solvent as determined relative to Me_4Si ($\delta = 0$ ppm). GC-MS measurements were conducted on a Perkin-Elmer Clarus 600 GC equipped with Clarus 600T MS. HRESI-MS measurements were conducted at the EPFL ISIC Mass Spectrometry Service with a Micro Mass QTOF Ultima spectrometer. HPLC analyses were carried out on an Agilent 1260 series system with Daicel CHIRALPAK ® columns (internal diameter 4.6 mm, column length 250 mm, particle size 5 μ).

3.7.3 Synthetic procedures for the synthesis of complex 8

- *Synthesis of (S)-2-nitro-N-(1-phenylethyl)aniline (Reaction 1)*

1-Fluoro-2-nitrobenzene (2 g, 14.2 mmol) and K_2CO_3 (2 equiv) are dissolved in 40 mL of DMSO in a 250 mL round necked 250 mL flask at room temperature. Once all the solids are dissolved, *S*-(-)-α-methylbenzylamine (1.7 g, 14.2 mmol) is slowly added under stirring. After the addition, the mixture is heated until 80°C and stirred overnight. The resulting mixture is extracted 3 times with 50 mL of CH_2Cl_2. The combined organic layer was washed 4 times with 50 mL of brine and dried with anhydrous Na_2SO_4. Once the solvent was evaporated, the

crude product was purified by flash chromatography obtaining the pure product as orange oil. (SiO$_2$, Hexane:EtOAc 10:1). Yield: 2.5 g, 72 %

^{1}H NMR (400 MHz, CDCl$_3$, δ in ppm) 8.45 (s.br, 1H), 8.2 (d, *J* = 8.4 Hz, 1H), 7.4-7.24 (m, 6H), 6.68-6.58 (m, 2H), 4.83-4.55 (m, 1H), 1.67 (d, *J* = 6.7 Hz, 3H).

- *Synthesis of (S)-N-methyl-2-nitro-N-(1-phenylethyl)aniline (Reaction 2)*

(*S*)-2-nitro-N-(1-phenylethyl)aniline (4 g, 16.5 mmol) was dissolved in 100 ml of dry THF in an 250 mL oven dried round necked 250 mL flask. Once the solution was completely homogenous, NaH in mineral dispersion was slowly added (2.7 g, 66 mmol). MeI (23.4 g, 165 mmol) and HMPA (2.95 g, 16.5 mmol) were then successively added drop by drop under N$_2$ atmosphere. The final mixture was stirred overnight at room temperature. THF was then carefully evaporated, and the residue was carefully dissolved in water. The resulting aqueous solution was extracted 3 times with 50 mL of CH$_2$Cl$_2$. The combined organic layer was then washed with brine and dried with anhydrous Na$_2$SO$_4$. Once the solvent was evaporated, the crude product was purified by flash chromatography as yellow oil. (SiO$_2$, Hexane:EtOAc 10:1). Yield: 2.7 g, 63 %.

^{1}H NMR (400 MHz, CDCl$_3$, δ in ppm) 7.74 (d, *J* = 8 Hz, 1H), 7.45-7.25 (m, 6H), 7.11 (d, *J* = 8 Hz, 1H), 6.97 (t, *J* = 7.2 Hz, 1H), 4.68 (q, *J* = 6.5 Hz, 1H), 2.57 (s, 3H), 1.57 (d, *J* = 6.5 Hz, 3H).

- *Synthesis of (S)-N^1-methyl-N^1-(1-phenylethyl)benzene-1,2-diamine (Reaction 3)*

(*S*)-N-methyl-2-nitro-N-(1-phenylethyl)aniline (1 g, 3.9 mmol) was dissolved in 50 mL of methanol in a 250 mL round necked flask, and Pd/C (100 mg) was then added. The mixture was stirred during 3 hours under a H$_2$ atmosphere. The Pd/C was then taken out from the solution by filtration. Methanol was then evaporated, affording 0.76 g of the pure product as brown oil. Yield 87 %

^{1}H NMR (400 MHz, CDCl$_3$, δ in ppm) 7.4-7.25 (m, 5H), 7.05-6.95 (m, 2H), 6.82-6.65 (m, 2H), 4.25-4.15 (m, 3H), 2.46 (s, 3H), 1.33 (d, *J* = 6.4 Hz, 3H).

- *Synthesis of ligand (S)-5 (Reaction 4)*

A 250 mL reaction vessel was charged with Pd$_2$(dba)$_3$ (41 mg, 0.045 mmol), bis(diphenylphosphino)-ferrocene (dppf) (50 mg, 0.09 mmol), NaO^{t}Bu (300 mg, 3 mmol) and toluene (50 mL) under a dinitrogen atmosphere. (*S*)-N^1-methyl-N^1-(1-phenylethyl)benzene-1,2-diamine (500 mg, 2.2 mmol) and bromobenzene (345 mg, 2.2 mmol) were added to the reaction mixture. The resulting brown solution was vigorously

stirred for 2 days at 110 °C. The solution was then cooled to room temperature and filtered through Celite. Removal of the solvent yielded a black liquid which was then purified by flash chromatography to afford the product as light brown oil. (SiO$_2$, Hexane/ EtOAc 30:1).Yield: 0.6 g, 90 % with 99.5% ee (HPLC analysis of the product: Daicel CHIRALPAK IA column; solvent system: 1% i-PrOH in hexane; 0.6 mL/min).

^{1}H NMR (400 MHz, CDCl$_3$, δ in ppm) 7.4-6.8 (m, 14H), 4.2-4.1 (m, 2H), 2.5 (s, 3H), 1.32 (d, J = 6.8 Hz, 3H).
MS: calculated for (C$_{21}$H$_{22}$N$_2$, M+H), 303.42; found, 303.78

- *Synthesis of lithium salt (S)-7*

A solution of (*S*)-**2** (5 g, 16.5 mmol) was prepared in toluene (50 mL) under inert atmosphere. A solution of ^{n}BuLi (11 mL, 17.36 mmol, 1.6 M in hexane) was carefully added. The solution turned gray-white. The reaction mixture was stirred for 2 h until the presence of a white solid. The solvent was then evaporated, and 20 mL of pentane were added. The product was recovered under vacuum filtration as a white power. Yield: 4.2 g, 83 %

^{1}H NMR (400 MHz, C$_6$D$_6$, δ in ppm) 7.63-6.63 (br, 14H), 4.25-3.97 (br, 1H), 2.6-2.25 (br, 3H), 1.42-1.16 (br, 3H).

- *Synthesis of complex (S)-8*

Under an inert atmosphere, a THF solution (2 mL) of (*S*)-**4** (0.5 g, 1.8 mmol) was added to a THF suspension (5 mL) of NiCl$_2$(2,4-lutidine)$_2$ (0.62 g, 1.8 mmol). The reaction mixture was stirred overnight at room temperature. After removal of solvent, the residue was dissolved with a very small quantity of toluene and filtered through a glass fiber filter. The toluene was then evaporated and the resulting solid was washed with pentane. The product was obtained as a yellow brown solid. Yield: 0.6 g, 80 %. Diffusion of pentane into a toluene solution of (*S*)-**4** afforded brown crystals suitable for X-ray analysis.

- *Crystallographic data of complex rac-8*

A total of 50673 reflections (-12 ≤ h ≤ 11, -18 ≤ k ≤ 18, -29 ≤ l ≤ 29) were collected at T = 100(2) K of which 6862 were unique (Rint = 0.0506); Mo$_{K\alpha}$ radiation (λ= 0.71073 Å). The structure was solved by the direct methods. All non-hydrogen atoms were refined anisotropically, and hydrogen atoms were placed in calculated idealized positions. The residual peak and hole electron densities were 0.604 and –0.360 eA^{-3}, respectively. The absorption coefficient was 0.760 mm^{-1}. The least squares refinement converged normally with residuals of R(F) = 0.0333, wR(F2) = 0.0785 and a GOF = 1.085 (I>2σ(I)). C$_{33}$H$_{42}$ClN$_3$Ni,

Mw = 574.86, space group $P2_12_12_1$, Orthorhombic, a = 9.4014(6), b = 14.215(2), c = 22.500(3) Å, $\alpha = 90°$, $\beta = 90°$, $\gamma = 90°$, V = 3007.1(7) Å^3, Z = 4, ρ_{calcd} = 1.27 Mg/m^3.

3.7.4 Synthetic procedures for the synthesis of complex 10

- *Synthesis of 2,5-dimethyl-1-(2-nitrophenyl)pyrrolidine (Reaction 5)*

1-fluoro-2-nitrobenzene (1.04 g, 7.4 mmol) was dissolved in 20 mL of DMSO and K_2CO_3 (2.04 g, 14.7 mmol) was added. 2,5-dimethyl-pyrrolidine (0.73 g, 7.4 mmol) was added under stirring to the resulted mixture. After the addition was finished, the reaction was heated at reflux during 3 h. Then the reaction was stirred overnight at r.t. 30 mL of water were added to the reaction mixture and the product was extracted with DCM (3 times, 30 mL each) and the organic phase was washed with brine (2 times, 30 mL each) and with distilled water (2 times, 20 mL each). The organic phase was then dried over Na_2SO_4, filtered and the solvent was evaporated under vacuum to give the product as orange oil. Yield: 1.5 g, 90 %. The purity of the compound was verified by GC – MS analysis.

- *Synthesis of 2-(2,5-dimethylpyrrolidin-1-yl)aniline (Reaction 6)*

2,5-dimethyl-1-(2-nitrophenyl)pyrrolidine (1.5 g, 6.8 mmol) was dissolved in 50 mL of methanol and 100 mg of Pd/C (6.6 % w/w) was added. The reaction flask was degassed and flushed with hydrogen twice and stirred overnight under hydrogen (1.5 bar) at r.t. The Pd catalyst was filtered off, and the solvent was removed under a reduced pressure. The pure compound was obtained as dark yellow oil. Yield: 85% (1.1 g). The purity of the compound was verified by GC – MS analysis.

- *Synthesis of ligand 6*

A 250 mL reaction vessel was charged with $Pd_2(dba)_3$ (113 mg, 0.12 mmol), bis(diphenylphosphino)-ferrocene (dppf) (137 mg, 0.25 mmol), NaO^{t}Bu (780 mg, 8.1 mmol) and toluene (50 mL) under a N_2 atmosphere. 2-(2,5-dimethylpyrrolidin-1-yl)aniline (1.1 g, 6.05 mmol) and bromobenzene (0.95 g, 6.05 mmol) were added to the reaction mixture. The resulting brown solution was vigorously stirred for 2 days at 110 °C. The solution was then cooled to room temperature and filtered through Celite. Removal of the solvent yielded a black liquid which was then purified by flash chromatography to afford the product as light brown oil. (SiO$_2$, Hexane/ EtOAc 30:1).Yield: 1 g, 63 %. The purity of the compound was verified by GC – MS analysis.

- *Synthesis of lithium salt 9*

A solution of **3** (1 g, 3.7 mmol) was prepared in toluene (30 mL) under inert atmosphere. A solution of ^{n}BuLi (2.5 mL, 4.1 mmol, 1.6 M in hexane) was carefully added. The solution turned gray-white. The reaction mixture was stirred for 2 h until the presence of a white solid. The solvent was then carefully evaporated, and 20 mL of pentane were added. The product was recovered under vacuum filtration as a white power. Yield: 0.6 g, 65 %

- *Synthesis of complex 10*

Under an inert atmosphere, a THF solution (2 mL) of **6** (0.5 g, 1.8 mmol) was added to a THF suspension (5 mL) of $NiCl_2(2,4-lutidine)_2$ (0.62 g, 1.8 mmol). The reaction mixture was stirred overnight at room temperature. After removal of solvent, the residue was dissolved with a very small quantity of toluene and filtered through a glass fiber filter. The toluene was then evaporated and the resulting solid was washed with pentane. The product was obtained as a dark blue solid. Yield: 0.52 g, 80 %. Diffusion of pentane into a toluene solution of **7** afforded blue crystals suitable for X-ray analysis.

- *Crystallographic data of complex 10*

A total of 7076 reflections ($-15 \leq h \leq 15$, $-17 \leq k \leq 17$, $-26 \leq l \leq 26$) were collected at T = 140(2) K of which 7076 were unique (Rint = 0.0233); $Mo_{K\alpha}$ radiation (λ= 0.71073 Å). The structure was solved by the direct methods. All non-hydrogen atoms were refined anisotropically, and hydrogen atoms were placed in calculated idealized positions. The residual peak and hole electron densities were 0.659 and -0.543 eA^{-3}, respectively. The absorption coefficient was 1.361 mm^{-1}. The least squares refinement converged normally with residuals of R(F) = 0.0605, wR(F2) = 0.1619 and a GOF = 1.095 (I>2σ(I)). $C_{18}H_{21}ClN_2Ni$, Mw = 359.53, space group P_{bca}, Orthorhombic, a = 11.937(3), b = 13.215(2), c = 20.529(4) Å, α = 90°, β = 90°, γ = 90°, V = 3238.4(11) $Å^3$, Z = 8, ρ_{calcd} = 1.475 Mg/m^3.

3.7.5 Typical procedure for the coupling reactions described in Table 1 and Table 2

0.5 mmol (1 eq.) of Grignard reagent was diluted in THF (3 mL), and then was added dropwise via syringe pump during 2 h to a DMA (0.75 mL) solution containing the nickel catalyst (0.015 mmol, 3 mol %) and alkyl iodide (0.5 mmol) at -20°C. After addition, the reaction mixture was further stirred for 30 min at -20°C and then the solution was taken out from the cooling system and stirred for some minutes to warm up to room temperature. 15 mL

of distilled water, 1 mL of hydrochloric acid (25 %) and decane (internal standard, 60 µL, 0.31 mmol) were successively added to the reaction mixture. The resulting solution was extracted with diethyl ether (3 × 10 mL) and the combined organic phase was separated, dried over anhydrous Na_2SO_4, and filtered. The organic products were identified and quantified by GC-MS.

Note for entry 6 in Table 1: (2-methylbutane-1,4-diyl)dibenzene was separately produced using *rac*-**8** and (*S*)-**8** as catalysts. The enantiomeric excess of this coupling product was measured by HPLC analysis performed with a Daicel CHIRALPAK IA column; solvent system: hexane; 0.5 mL/min).

3.8 References

(1)   Hartwig, J. F. *Organotransition Metal Chemistry - From Bonding to Catalysis*; University Science Books: Sausalito, CA, 2010.
(2)   Frisch, A. C.; Beller, M. *Angew. Chem. Int. Ed.* **2005**, *44*, 674.
(3)   Terao, J.; Watanabe, H.; Ikumi, A.; Kuniyasu, H.; Kambe, N. *J. Am. Chem. Soc.* **2002**, *124*, 4222.
(4)   Terao, J.; Ikumi, A.; Kuniyasu, H.; Kambe, N. *J. Am. Chem. Soc.* **2003**, *125*, 5646.
(5)   Ren, P.; Vechorkin, O.; von Allmen, K.; Scopelliti, R.; Hu, X. L. *J. Am. Chem. Soc.* **2011**, *133*, 7084.
(6)   Lou, S.; Fu, G. C. *J. Am. Chem. Soc.* **2010**, *132*, 1264.
(7)   Csok, Z.; Vechorkin, O.; Harkins, S. B.; Scopelliti, R.; Hu, X. L. *J. Am. Chem. Soc.* **2008**, *130*, 8156.
(8)   Terao, J.; Naitoh, Y.; Kuniyasu, H.; Kambe, N. *Chem. Lett.* **2003**, *32*, 890.
(9)   Frisch, A. C.; Shaikh, N.; Zapf, A.; Beller, M. *Angew. Chem. Int. Ed.* **2002**, *41*, 4056.
(10)   Ren, P.; Stern, L. A.; Hu, X. L. *Angew. Chem. Int. Ed.* **2012**, *51*, 9110.
(11)   Iwasaki, T.; Imanishi, R.; Shimizu, R.; Kuniyasu, H.; Terao, J.; Kambe, N. *J. Org. Chem.* **2014**, *79*, 8522.
(12)   Guisan-Ceinos, M.; Tato, F.; Bunuel, E.; Calle, P.; Cardenas, D. J. *Chem. Sci.* **2013**, *4*, 1098.
(13)   Dongol, K. G.; Koh, H.; Sau, M.; Chai, C. L. L. *Ad. Synth. Catal.* **2007**, *349*, 1015.
(14)   Cheung, C. W.; Ren, P.; Hu, X. *Org. Lett.* **2014**, *16*, 2566.
(15)   Cahiez, G.; Chaboche, C.; Duplais, C.; Giulliani, A.; Moyeux, A. *Ad. Synth. Catal.* **2008**, *350*, 1484.
(16)   Iwasaki, T.; Takagawa, H.; Singh, S. P.; Kuniyasu, H.; Kambe, N. *J. Am. Chem. Soc.* **2013**, *135*, 9604.
(17)   Mao, J.; Liu, F.; Wang, M.; Wu, L.; Zheng, B.; Liu, S.; Zhong, J.; Bian, Q.; Walsh, P. J. *J. Am. Chem. Soc.* **2014**, *136*, 17662.
(18)   Ohmiya, H.; Yorimitsu, H.; Oshima, K. *Org. Lett.* **2006**, *8*, 3093.
(19)   Rudolph, A.; Lautens, M. *Angew. Chem. Int. Ed.* **2009**, *48*, 2656.
(20)   Swift, E. C.; Jarvo, E. R. *Tetrahedron* **2013**, *69*, 5799.
(21)   Kiso, Y.; Tamao, K.; Miyake, N.; Yamamoto, K.; Kumada, M. *Tetrahedron Lett.* **1974**, *15*, 3.
(22)   Consiglio, G.; Botteghi, C. *Helv. Chim. Acta.* **1973**, *56*, 460.
(23)   Wiencko, H. L.; Kogut, E.; Warren, T. H. *Inorg. Chim. Acta.* **2003**, *345*, 199.
(24)   Venanzi, L. M. *J. Chem. Soc.* **1958**, 719.

Chapter 4 : New nickel pincer complexes as catalysts for Kumada coupling of alkyl halides

4.1 Introduction

Stability, high selectivity and high activity are the three desirable characteristics of an ideal catalyst.[1] In the case of organometallic catalysis, the fine-tuning of the catalytic properties of the metal center is made through a rational design of the ligand. The catalytic process is largely influenced by the electronic and the steric properties of the ligand.[2] The pincer structural motif is often used for the development of catalyst for coupling process.[3] Figure 1 shows a typical EZE architecture of pincer complexes where the three binding sites are coplanar and meridional oriented.
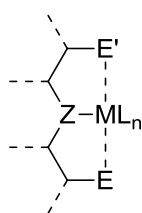
Figure 1. General representation of Pincer complex architecture.

Pincer complexes can be classified by their donor atoms. For instance, if the central atom is a carbon and the side arms are amino ligands, then the ligand is abbreviated as NCN ;with phosphines at the side arms, the ligand is abbreviated as PCP. The two side arms are not necessarily the same. This can foster an improvement of the catalytic activity of the complex, but the synthetic design of the ligands might be challenging.[4,5]

We can find few examples of well-defined nickel pincer complexes used as catalysts for Kumada coupling process.[6] Liang and co-workers reported a group of amido diphosphine PNP nickel complexes that are active for aryl – aryl coupling.[7] Wang and co-workers compared the activity of unsymmetrical PNP, NNP and NNN amido nickel complexes as catalysts for coupling of aryl chlorides with aryl Grignard reagents[8,9] and they recently succeeded to couple aryl fluorides with aryl Grignard reagents using a PNN amido phosphine-amine nickel complex.[10]   Our group developed Nickamine using an NNN amido bis(amine) pincer ligand.[11] This complex is an extremely versatile catalyst for coupling of non-activated alkyl halides with alkyl, aryl or alkynyl Grignard reagents. Figure 2 shows the structure of the above described complexes.

**11**, Liang, 2006   **12**, Wang, 2013   **13**, Wang, 2014   **1**, Hu, 2008
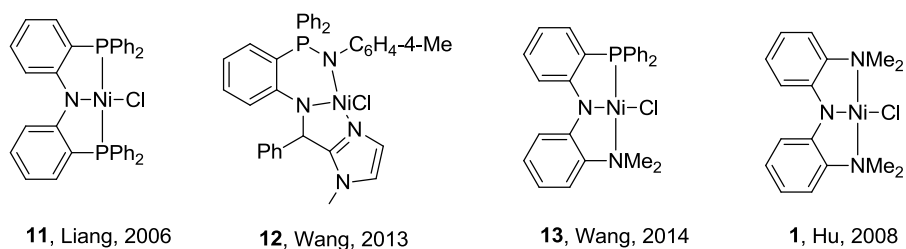
Figure 2. Well-defined nickel pincer complexes active for Kumada coupling.

As described earlier, we are interested in developing asymmetric cross coupling reactions of secondary alkyl halides. Our strategy is to first develop racemic catalysts that are efficient for the coupling of secondary alkyl halides, and then transform the catalysts into chiral versions. Herein, we describe the synthesis of two new pincer ligands and a new nickel pincer complex. The complex has good catalytic activity for Kumada coupling of non-activated primary and secondary halides. The reactivity of this new nickel complex gave important insights for the design of catalysts for the cross-coupling of bulky alkyl halides. The work also paves the way for future development of chiral catalysts.

## 4.2 Synthesis and metalation trials of a new ligand derived from α-methylbenzylamine

We designed a new amido bis(amine) pincer ligand **14** using α-methylbenzylamine as readily available starting material. Figure 3 shows the retrosynthetic route of ligand **14**. One of the considerations for our design is that the ligand might be made chiral if chiral α-methylbenzylamine is used.
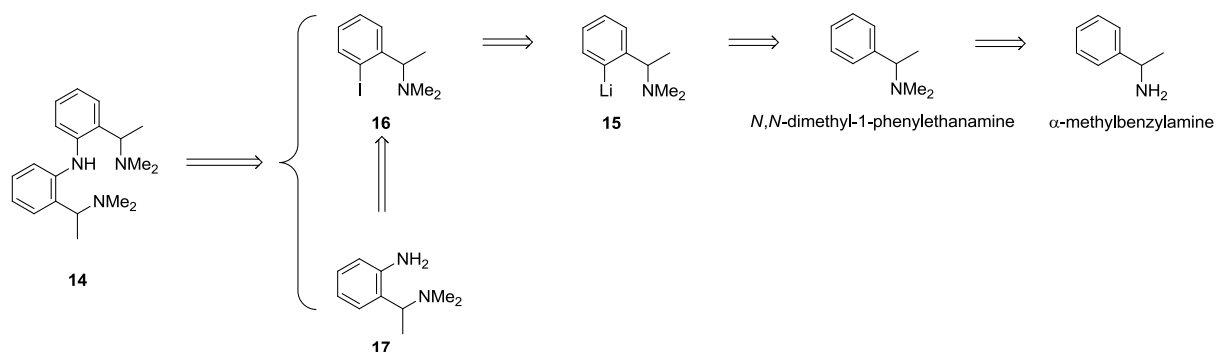

Figure 3. Retrosynthetic route of ligand **14**.

We started the synthesis by the Echweiler – Clark methylation of α-methylbenzylamine.[12] The reaction produced *N,N*-dimethyl-1-phenylethanamine in a good yield. Lithiated compound **15**

was then formed by reaction with *sec*-butyllithium deprotonation in pentane. The reaction of **15** with iodide produced iodinated substrate **16** in a decent yield. Compound **16** was submitted to the Fe_2O_3/CuI catalyzed amination, developed by Darcel and co-workers,[13] producing substrate **17** in a good yield. Scheme 1 shows the experimental conditions of the above described reactions.
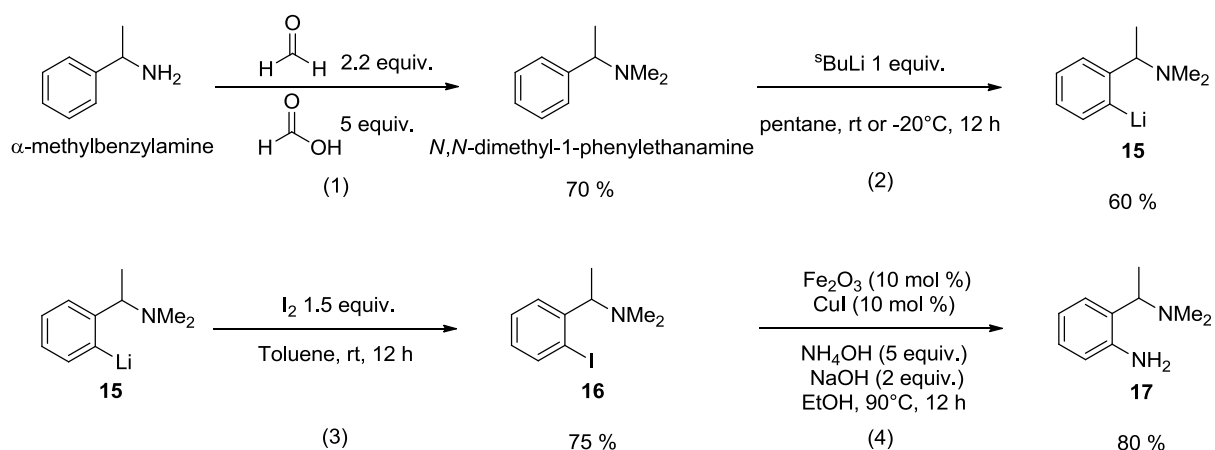
**Scheme 1.** Synthesis of compounds **15**, **16** and **17**.

Compounds **16** and **17** were C/N coupled using Buchwald – Harwtig catalytic methodology obtaining ligand **14** in a good yield (Scheme 2). The overall yield of the five step synthesis was 23 %.
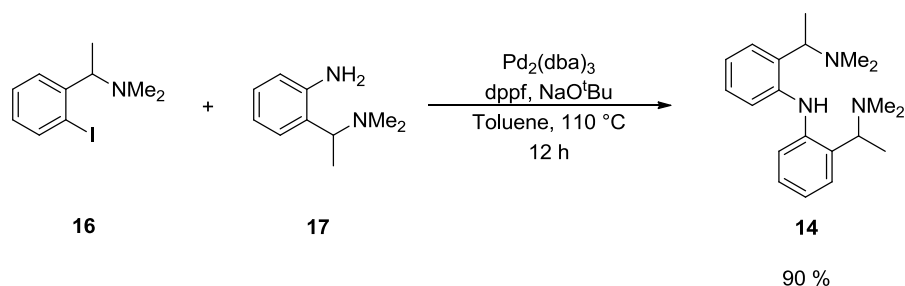
Scheme 2. Synthesis of ligand **14** by Pd^0 catalyzed C-N coupling.

Lithiation of ligand **14** by MeLi produced lithium salt **18** in a good yield. The Li – Ni transmetallation reaction of **18** was tried using several Ni precursors (Table 1). The reaction of **18** with NiCl$_2$dme in THF produced a black powder non characterizable (entry 1, Table 1). When **18** was dissolved in THF and the solvent evaporated, the ^{1}H NMR analysis of the residue showed only the presence of ligand 1 (entry 2, Table 1). It seems that lithium salt **18** is

too basic and readily reacts with any proton source. NiCl₂dme and other nickel precursors were tested by reaction with **18** in benzene (entries 3 – 6, Table 1). Unfortunately, none of the reactions allowed giving the desired complex.
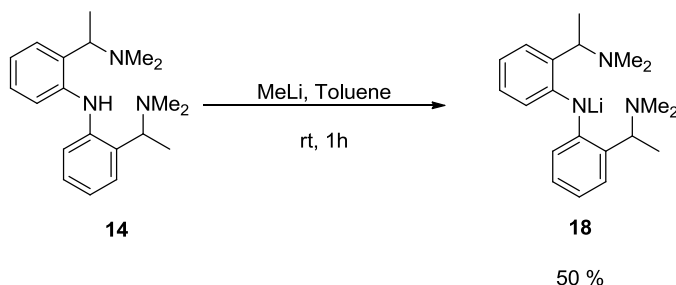
Scheme 3. Synthesis of lithium salt **18** by MeLi reaction.

Table 1. Transmetalation trials of lithium salt **18**.

| Entry	Solvent	Ni precursor	Observations
1	THF	NiCl₂dme	Decomposition
2	THF	----	Return to **14**
3	Benzene	NiCl₂dme	Decomposition
4	Benzene	NiCl₂(2,4-lutidine)₂	Decomposition
5	Benzene	NiCl₂(PPh₃)₂	Decomposition
6	Benzene	NiCl₂(pyridine)₄	Decomposition

Other synthetic routes were tested for the synthesis of a Ni complex using ligand **14**. We decided to set up reactions by *in situ* addition of the nickel precursor after the deprotonation process. Table 2 shows the experimental conditions for those experiments. The reaction of **14** with NiCl₂dme using MeLi as base and THF as solvent was set up at -50°C produced again a black residue. The use of Et₃N as base was tested to avoid the formation of the apparently very reactive lithium salt **18**, two unsuccessful trials were carried out at room and elevated temperature using THF as solvent (entries 2 – 3, Table 2). Two reactions were carried out without base in benzene producing also negative results (entries 4 – 5, Table 2).

Finally, two reactions were conducted using $PdCl_2$ as metal precursor and MeLi as base, the result was unfortunately also negative (entries 7 – 8, Table 2).

Table 2. Transmetalation trials of ligand **14**.

Entry	Solvent	Metal precursor	Temperature	Base	Observations
1	THF	$NiCl_2$dme	-50°C	MeLi	Decomposition
2	THF	$NiCl_2$dme	rt	Et_3N	Decomposition
3	THF	$NiCl_2$dme	70°C	Et_3N	Decomposition
4	Benzene	$NiCl_2$dme	rt	----	Decomposition
5	Benzene	Ni(COD)$_2$	rt	----	Decomposition
6	Benzene	$NiClMe(PPh_3)_2$	rt	----	Decomposition
7	Benzene	$PdCl_2$	rt	MeLi	Decomposition
8	THF	$PdCl_2$	rt	MeLi	Decomposition

The results described in table 1 and table 2 drive us to design the metalation of ligand **14** by another synthetic approach. It is known that secondary amines could be easily transformed in chloroamines by oxidation with N-chlorosuccinimide (NCS). Ligand **1** could be chlorinated by this methodology and the formed N – Cl bond was inserted to a Ni^0 center by oxidative addition.[14] The feasibility of this methodology was firstly tested for the synthesis of Nickamine **1**. The *in situ* sequence NCS chlorination – Ni(COD)$_2$ oxidative addition was indeed successful for the synthesis of Nickamine (reaction 7, Scheme 4). Regrettably, the metalation of ligand **14** was not possible by this methodology (reaction 8, Scheme 4).
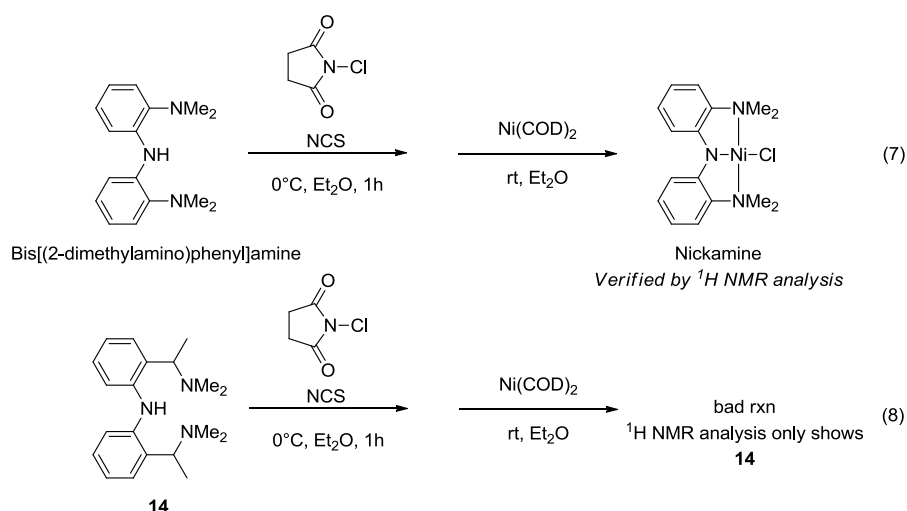
Scheme 4. Metalation tests by oxidative addition.

All the above mentioned results seem to indicate that the structural feature of Nickamine with (dimethylamino)phenyl linkers is important to stabilize the formation of amido – amine nickel complexes. In the next section, we show how a ligand combining moieties of the Bis[(2-dimethylamino)phenyl]amine and ligand **14** could be used to synthesize a new stable nickel pincer complex.

4.3 Synthesis and catalytic activity study of a new pincer Ni complex derived from the α-methylbenzylamine.

We decided to combine the stability of the (dimethylamino)phenyl moiety of Nickamine ligand with the novelty of the α-methylbenzylamine derived moiety of ligand **14**. A new amido bis(amine) ligand **19** was synthesized from C/N Buchwald – Harwtig coupling between compound **6** and N^1,N^1-dimethylbenzene-1,2-diamine. Scheme 5 shows the experimental conditions of this reaction.
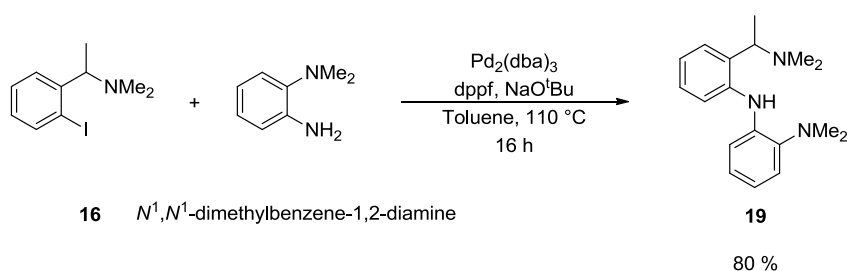

Scheme 5. Synthesis of ligand **19** by Pd^0 catalyzed C-N coupling.

The lithiation of **19** by [n]BuLi in toluene produced lithium salt **20** in a good yield and the addition of Ni(dme)Cl$_2$ to **20** in THF produced complex **21**. Scheme 6 shows the experimental conditions of these reactions. Single –crystal diffraction analysis confirmed the structure of complex **21** (Figure 4).
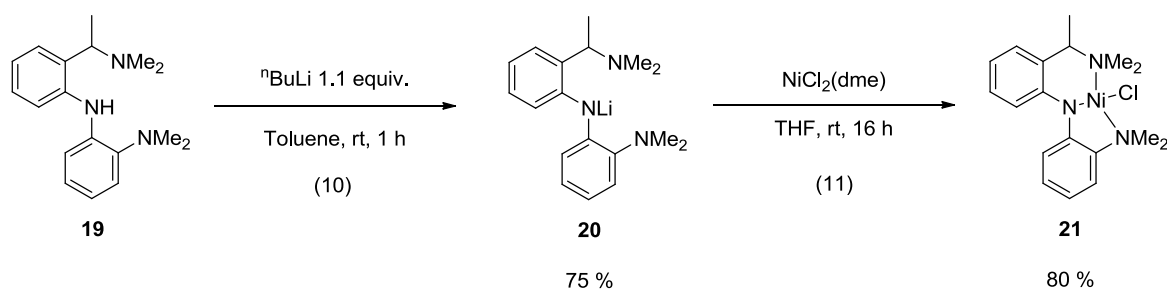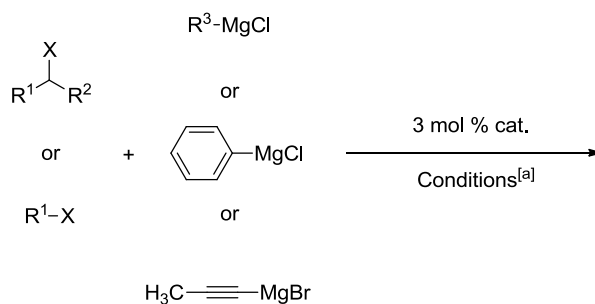

Scheme 6. Synthesis of complex **21**.
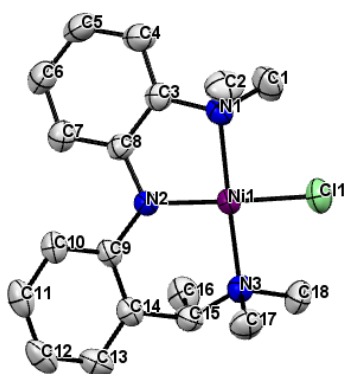
Figure 4. Crystal structure of complex **21**. Hydrogens atoms are omitted for clarity. Selected lengths (Å) and angles (deg): Ni1 – N1, 1.9877(11); Ni1 – N2, 1.8678(11); Ni1 – N3, 1.9797(11); Ni1 – Cl1, 2.2144(4); N1 – Ni1 – N2, 85.79(4); N2 – Ni1 – N3, 93.15(4); N3 – Ni1 – N1, 169.78(5).
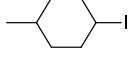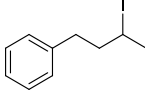
The catalytic activity of new complex **21** was tested for Kumada coupling reactions. Representative coupling reactions between non-activated iodides and alkyl, aryl or alkynyl Grignard reagents were set up under reported conditions.[15-17] Table 3 shows the comparison of coupling yields using complex **21** or Nickamine as catalysts. Octyl iodide was successful coupled to propynyl magnesium bromide and phenyl magnesium chloride (entries 1 – 2, Table 3). 1,4- and 1,3-methylcyclohexyl iodide was coupled in good yields and with high diastereoselective ratios to butyl magnesium chloride (entries 3 – 4, Table 3). The acyclic secondary iodide (3-iodobutyl)benzene was coupled to octyl magnesium chloride in low but encouraging yield (entry 5, Table 3). The coupling of secondary iodides was carried out using

7 mol %.[18] The coupling of secondary alkyl halides with aryl or alkynyl Grignard reagents was not possible by either catalysts.

Table 3. Comparison of Kumada coupling yields using Nickamine or new complex **21** as catalysts.

Entry	Alkyl Halide	Grignard Reagent	Yield[b] cat. 1	Yield[b] cat. 21
1	nOctyl- I	BrMg$\equiv$CH$_3$	93	70
2	nOctyl- I	ClMg—(phenyl)	83	70
3	(methylcyclohexyl iodide)	nButyl-MgCl	90[c] (98:2)	78[c] (93:7)
4	(cyclohexyl iodide)	nButyl-MgCl	92[c] (96:4)	76[c] (94:6)
5	(secondary iodide)	nOctyl-MgCl	Trace	38[c]

[a] Conditions described in experimental section. [b] GC yields relative to alkyl halide. [c] 7 mol % catalyst.

The catalytic activities of Nickamine and new nickel pincer complex **21** are apparently comparable. Nevertheless, complex **21** only showed a slightly better coupling activity for acyclic non-activated secondary iodides. In the next section, a new Ni pincer complex is presented as a good catalyst for the coupling creation of acyclic tertiary carbon centers.

4.4 Synthesis and catalytic activity study of a new pincer Ni complex having a pyrrolidine side linker.

In the previous chapter, we synthesized a nickel dimer complex from a new amido – amine bidentate ligand derived from the 2,5-dimethylpyrrolidine. We wanted to conserve the pyrrolidine building block because its structural feature was before used for the development chiral ligands effective for metal catalyzed Kumada coupling.[19] We designed a new amide(bisamino) ligand **22** having a pyrrolidine amine linker. Figure 5 shows the retrosynthetic route for the new ligand **22**.
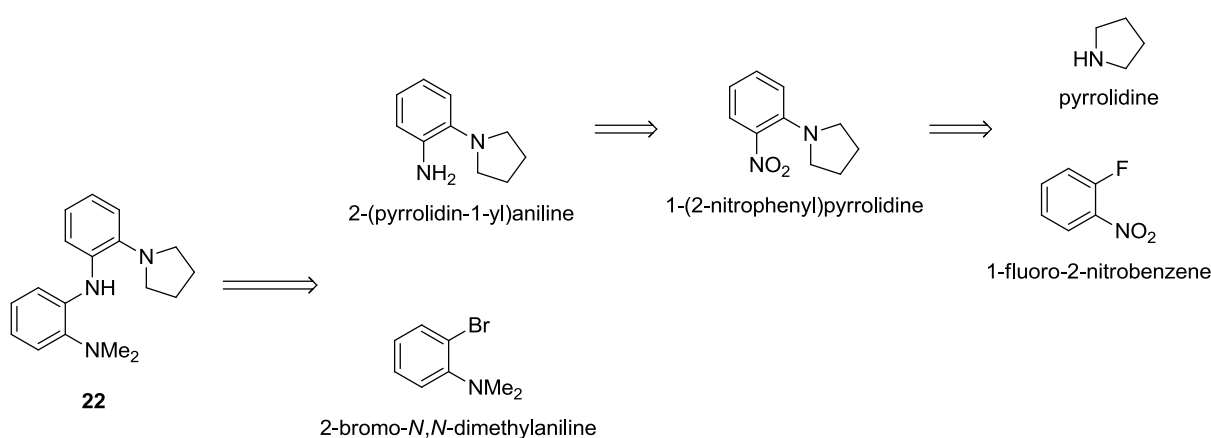
Figure 5. Retrosynthetic route of ligand **22**.

The synthesis started by the aromatic nucleophilic substitution between pyrrolidine and 1-fluoro-2-nitrobenzene in acetonitrile in presence of K_2CO_3 producing 1-(2-nitrophenyl)pyrrolidine in a good yield. The nitro group of this substrate was then hydrogenated under hydrogen atmosphere in presence of Pd/C catalyst, giving 2-(pyrrolidin-1-yl)aniline in an excellent yield. This substrate was coupled with 2-bromo-*N,N*-dimethylaniline in a good yield using Pd-catalyzed Buchwald – Hartwig C – N coupling method. Ligand **22** was obtained with an overall yield of 76 %. Scheme 7 shows the reaction conditions of this three step synthesis.
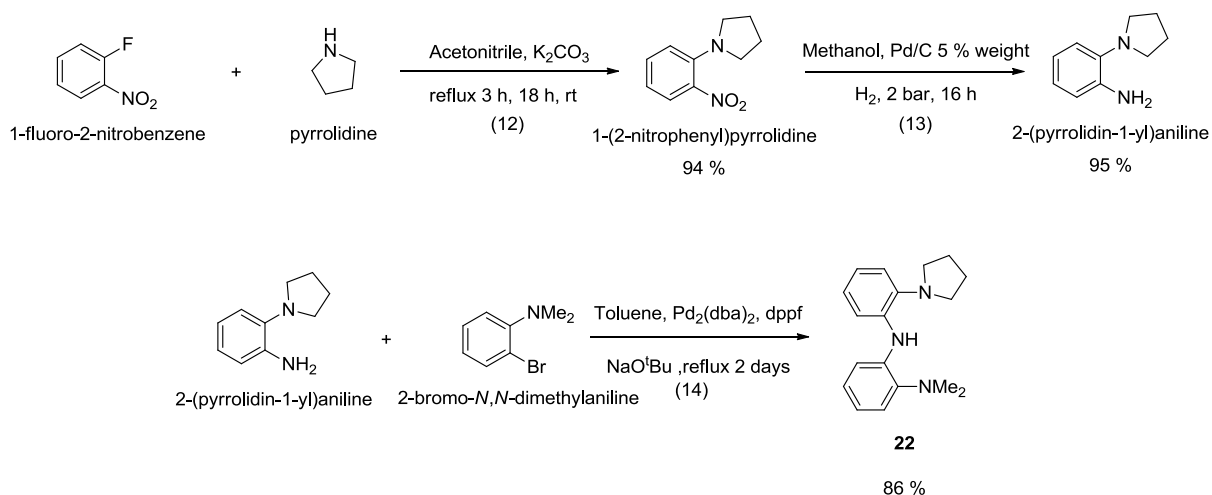
Scheme 7. Synthesis of ligand **22**.

The lithiation of **22** by ^{n}BuLi followed by *in situ* addition of Ni(dme)Cl$_2$ produced complex **23** in a good yield (Scheme 8). The structure of complex **23** was confirmed by single − crystal diffraction study (Figure 6). A noteworthy structural feature is the opening angle C − N − C of the pyrrolidine linker which is 5 degrees smaller than the C − N − C angle of the dimethyl amine linker.
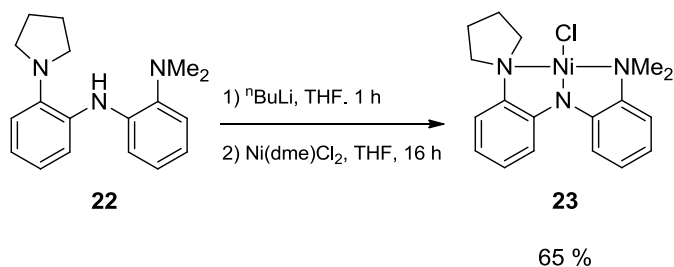
Scheme 8. Synthesis of the new pincer complex **23**.
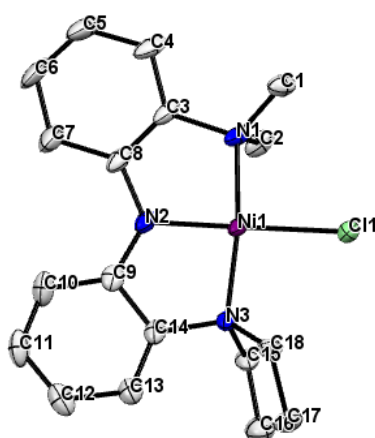
Figure 6. Crystal structure of complex **23**. Hydrogens atoms are omitted for clarity. Selected lengths (Å) and angles (deg): Ni1 – N1, 1.963(4); Ni1 – N2, 1.854(4); Ni1 – N3, 1.968(4); Ni1 – Cl1, 2.2130(13); N1 – Ni1 – N2, 86.76(18); N2 – Ni1 – N3, 86.02(17); N3 – Ni1 – N1, 169.83(16); C2 – N1 – C1, 108.1(4); C15 – N3 – C18, 104.7 (4).

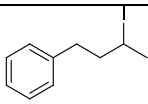The catalytic activity of complex **23** was tested for Kumada coupling using representative alkyl iodides. Table 4 shows the comparison of coupling yields using complex **23** or Nickamine as catalysts. 1-Iodooctane was coupled to butylmagnesium chloride and 1-iododecane was coupled to phenylmagnesium chloride (entries 1 – 2, Table 4) obtaining similar coupling yields for both catalysts. Surprisingly, the complex was also active for the coupling of the acyclic secondary iodide (3-iodobutyl)benzene with octylmagnesium chloride (entry 3, Table 4). This result indicates that complex **23** is an active pincer catalyst for the creation of tertiary carbon centers by Kumada coupling.

Table 4. Comparison of Kumada coupling yields using Nickamine or new complex **23** as catalysts.
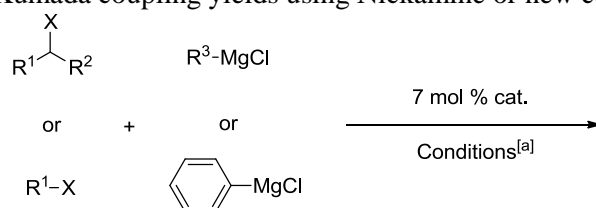
Entry	Alkyl Halide	Grignard Reagent	Yield[b] cat. 1	Yield cat. 23
1	^{n}Octyl- I	^{n}Butyl-MgCl	90	96[b]
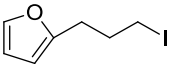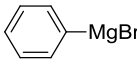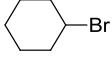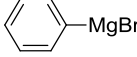
2	nDecyl- I	ClMg—⟨benzene⟩	83	80[c]
3	⟨PhCH₂CH₂CH(CH₃)⟩	nOctyl-MgCl	Trace	80[c]

[a] Conditions described in experimental section. [b] GC yields relative to alkyl halide.
[c] Isolated yield

Encouraged by the above mentioned results, we decided to study more the reactivity of complex **23**. Firstly, we screened the scope of the catalysis for the aryl and alkyl Kumada coupling of suitable substrates for Nickamine.[15-17] Several compounds containing interesting functional groups were successfully coupled to alkyl or aryl Grignard substrates. Table 5 compares the coupling yields obtained by catalysis using Nickamine and **23**. The ester group was tolerated (entry 1, Table 5), and so nitrile or fluoro groups (entries 2 − 3, Table 5). Heterocyclic groups as tetrahydropyrane and furane were also coupled in good isolated yields (entries 4 − 5 and 8, Table 5). Six membered ring secondary halides were also successfully coupled with excellent diastereoselectivity (entries 6-7 and 9, Table 5). All the coupling yields were similar for both catalysts, showing that **23** had a similar functional group tolerance as Nickamine.

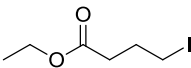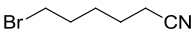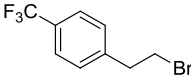**Table 5.** Coupling yields of substrates having similar reactivity through catalysis with **1** or **23**.
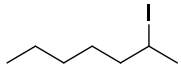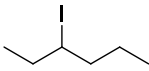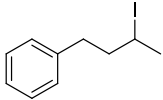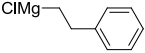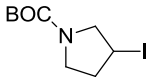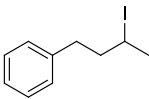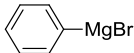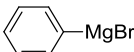
Entry	Alkyl Halide	Grignard Reagent	Yield cat. 1	Yield cat. 23
1	⟨ethyl ester with I⟩	nOctyl-MgCl	85[b]	70[b]
2	Br⟨chain⟩CN	nButyl-MgCl	77[b]	60[b]
3	F₃C⟨aryl⟩Br	nOctyl-MgCl	18[a]	63[b]
4	⟨O-Ph pyran with I⟩	nButyl-MgCl	79[b]	80[b]

5		^{n}Octyl-MgCl	99[b]	79[b]
6		^{n}Butyl-MgCl	90[a] (98:2)	80[a] (97:3)
7		^{n}Butyl-MgCl	92[a] (96:4)	74[a] (95:5)
8		—MgBr	80[b]	80[b]
9	—Br	—MgBr	65[a]	70[b]

[a] GC yields relative to alkyl halide [b] Isolated yields relative to alkyl halide

Nickamine has a reported low activity for Kumada coupling of acyclic or high member ring non-activated halides.[17,20] The successful coupling of (3-iodobutyl)benzene reported in Table 4 (entry 3), suggests that complex **23** could overcome Nickamine catalytic limitations. Coupling substrates normally showing low or null reactivity with Nickamine were chosen to compare the catalyst activity between the two complexes (Table 6). The chosen catalyst loading was 7 % mol to ensure high coupling yields. 2-Iodoheptane was coupled in excellent yield (entry 1, Table 6) and 3-iodohexane was coupled in lower but still good yield (entry 2, Table 6). (3-Iodobutyl)benzene was coupled in good isolated yields with alkyl and aryl Grignard reagents (entries 3 and 9, Table 6) and 2-iodopropane was successfully coupled to phenylmagnesium chloride (entry 11, Table 6). The coupling yields of simple or functionalized five membered ring iodides were slightly improved (entries 4 – 5 and 8, Table 6) using **23** as catalyst as well for the case of bromocyclopropane (entry 6, Table 6). Iodocycloheptane was also successfully coupled to alkyl or aryl Grignard reagents (entries 7 and 10, Table 6).

Table 6. Coupling yields of substrates showing higher reactivity using **23** as catalyst.

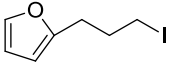| Entry	Alkyl Halide	Grignard Reagent	Yield cat. C1	Yield cat. 2
1		[n]Octyl-MgCl	Trace	87[a]
2		[n]Octyl-MgCl	Trace	50[a]
3		[n]Octyl-MgCl	Trace	70[b]
4		[n]Octyl-MgCl	82[a]	92[a]
5		ClMg—⟋⟍ Ph	40[a]	72[b]
6	Br⟍▷	[n]Butyl-MgCl	52[a]	65[a]
7		[n]Butyl-MgCl	Trace	78[a]
8	BOC–N⟍⟋–I	[n]Butyl-MgCl	67[a]	81[a]
9		Ph—MgBr	Trace	60[b]
10		Ph—MgBr	5[a]	50[b]

| 11 | | | 18[a] | 62[a] |

[a] GC yields relative to alkyl halide [b] Isolated yields relative to the alkyl halide
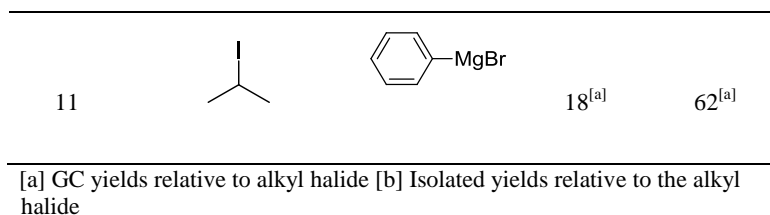
The molecular basis of the catalytic activity of complex **23** for the Kumada coupling of non-activated secondary halides is still unclear. A plausible explanation is the smaller $C - N - C$ angle of the pyrrolidine linker in complex **23**, which could suggest less steric hinderance compared to the dimethyl amino linker. This structural feature probably gives more accessibility to the nickel center allowing the activation of sterically hindered halides.

4.5 Conclusion

In summary, we developed the synthesis of two new amido bis(amine) ligands and the synthesis of a new well-defined nickel pincer complex. Compared to previously reported Nickamine, new complex **23** is not only an effective catalyst for alkyl – alkyl and alkyl – aryl Kumada coupling of primary alkyl halides but also extends its applicability to acyclic secondary alkyl halides. To the best of our knowledge this system constitutes the first well-defined pincer nickel catalyst able to couple steric hindered non-activated alkyl halides with alkyl or aryl Grignard reagents in good yields. Moreover, the chemical architecture of complex **23** constitutes an important structural paradigm for the design of active chiral pincer complexes.

It is noteworthy to remark how modification of pincer NNN ligands can be very useful to extend the versatility of these catalytic systems. In the next chapter, we present a complete mechanistic study of the room temperature performed Sonogashira coupling process catalyzed by a previously reported[21] nickel NNN pincer complex.

4.6 Experimental Part

4.6.1 Chemicals and Reagents

All manipulations were carried out under an inert $N_2(g)$ atmosphere using standard Schlenk or glovebox techniques. Solvents were purified using a two-column solid-state purification system (Innovative Technology, NJ, USA) and transferred to the glove box without exposure to air. Deuterated solvents were purchased from Cambridge Isotope Laboratories, Inc., and were degassed and stored over activated 3 Å molecular sieves. Unless otherwise noted, all other reagents and starting materials were purchased from commercial sources and used without further purification. Liquid compounds were degassed by standard freeze-pump-thaw procedures prior to use. The following chemicals were prepared according to literature procedure: 2-bromo-N,N.dimethylaniline,[11] 1-iodo-3-methylcyclohexane[20] (entry 3, Table 3), 1-iodo-4-methylcyclohexane[20] (entry 4, Table 3), (3-iodobutyl)benzene (entry 5, Table 3), 5-iodopentyl acetate[22] (entry 1, Table 5), tetrahydropyran[23] (entry 4, Table 5), 2-(3-iodopropyl)furan[24] (entries 5 and 8, Table 5), 2-iodoheptane[20] (entry 1, Table 6), 3-iodohexane[20] (entry 2, Table 6), 1-iodocycloheptane[20] (entries 7 and 10, Table 6) and *tert*-butyl 3-iodopyrrolidine-1-carboxylate[20] (entry 8, Table 6).

4.6.2 Physical methods

The ^1H and ^{13}C NMR spectra were recorded at 293 K on a Bruker Avance 400 spectrometer. ^1H NMR chemical shifts were referenced to residual solvent as determined relative to Me_4Si (δ = 0 ppm). The $^{13}C\{^1H\}$ chemical shifts were reported in ppm relative to the carbon resonance of $CDCl_3$ (77.0 ppm). GC-MS measurements were conducted on a Perkin-Elmer Clarus 600 GC equipped with Clarus 600T MS. HRESI-MS measurements were conducted at the EPFL ISIC Mass Spectrometry Service with a Micro Mass QTOF Ultima spectrometer.

4.6.3 Synthesis of Ligand 19

- *Synthesis of N,N-dimethyl-1-phenylethanamine*

A 250-ml flask was fitted with a reflux condenser, then α-methylbenzylamine (12.1 g, 0.1 mol) was added and the flask cooled in an ice bath. Cold 98% formic acid (25 g, 0.54 mol) was slowly added through the condenser under well stirring speed. Then 18 g (19 mL, 0.25 mol) of 37% formaldehyde solution were added and the solution was slowly heated to room temperature. The reaction mixture was then heated to reflux for 3 hours. The solution

was slowly cooled to room temperature, then 9 mL of concentrated hydrochloric acid were added and the excess of formaldehyde was evaporated in vacuo. The resulting solution was cooled and made basic adding a solution 25 % NaOH. The mixture was then extracted 3 times with 50 mL of diethyl ether and the organic phase was dried over powdered KOH. The solvent was evaporated and the product was distilled (bp 183 – 184°C). The pure product was obtained as transparent oil in a yield of 70 % (10.4 g).

^{1}H NMR (400 MHz, CDCl$_3$): 7.35 – 7.25 (m, 5H), 3.26 (q, *J* = 6.4 Hz 1H), 2.22 (s, 6H), 1.39 (d, *J* = 6.6 Hz, 1H).
HRESI-MS: calculated for (C$_{10}$H$_{16}$N, M+H), 150.1283; found, 150.1291.

- *Synthesis of lithium salt* **15**[25]

A solution of *N,N*-dimethyl-1-phenylethanamine (6 g, 40.3 mmol) in 80 mL of pentane was cooled to -20°C under N$_2$ atmosphere. To this solution, 28.8 mL (1.4 M, 40.3 mmol) of a solution of *sec*-butyllithium were carefully and slowly added. The resulting solution was stirred for 30 minutes at -20°C and for 16 h at room temperature. At the end of the stirring time, a cream colored suspension was formed. The solid material was filtered off and washed with 50 mL of pentane. The resulting lithium salt **2** was obtained as a white solid in a yield of 60 % (3.8 g).

- *Synthesis of compound* **16**

A solution of lithium salt **2** (5.4 g, 34.9 mmol) in 70 mL of toluene was cooled to 0°C under N$_2$ atmosphere. To the cold solution, solid iodine (10.6 g, 41.7 mmol) was slowly added. The resulting solution was stirred for 30 minutes at 0°C and for 16 h at room temperature. After the stirring time, the solvent was vacuum evaporated and the product extracted with 200 mL CH$_2$Cl$_2$. The organic phase was then washed with a saturated Na$_2$S$_2$O$_3$ solution and with distilled water. After drying the organic phase over anhydrous Na$_2$SO$_4$, the solvent was vacuum evaporated and the pure product was recovered as transparent oil in a yield of 75 % (7.2 g).

^{1}H NMR (400 MHz, CDCl$_3$): 7.83 (d, *J* = 7.7 Hz, 1H), 7.49 (d, *J* = 7.3 Hz, 1H), 7.34 (t, *J* = 7.2 Hz, 1H), 6.94 (t, *J* = 7.0 Hz, 1H), 3.52 (q, *J* = 6.0 Hz, 1H), 2.26 (s, 6H), 1.28 (d, *J* = 6.3 Hz, 3H).
^{13}C NMR (100 MHz, CDCl$_3$): 147.18, 139.52, 128.63, 128.24, 100.58, 69.51, 43.74, 20.64.
HRESI-MS: calculated for (C$_{10}$H$_{15}$NI, M+H), 276.0249; found, 276.0241.

- *Synthesis of compound* **17**

Commercially available red iron oxide Fe_2O_3 (64 mg, 10 mol%) and CuI (76 mg, 10 mol %) were added to a solution of compound **16** (1.1 g, 4 mmol) in ethanol (4 mL). Aqueous ammonia (20 mmol, 25 % in water) and NaOH (320 mg, 8 mmol) were successively added to the reaction mixture. The reaction tube was sealed and then heated at 90 °C for 16 h. The reaction mixture was cooled to room temperature, extracted 3 times with 10 mL of diethyl ether and the solvent was vacuum evaporated. The pure product was recovered as brown oil in a yield of 80 % (0.53 g).

¹H NMR (400 MHz, $CDCl_3$): 7.03 (dd, J = 13.5, 6.0 Hz, 1H), 6.99 (d, J = 7.3 Hz, 1H), 6.66 (t, J = 7.2 Hz, 1H), 6.61 (d, J = 7.7 Hz, 1H), 4.95 − 4.85 (br, 1H), 3.35 (q, J = 6.3 Hz, 1H), 2.21 (s, 6H), 1.38 (d, J = 6.6 Hz, 3H).
¹³C NMR (100 MHz, $CDCl_3$): 146.23, 128.36, 127.62, 117.57, 116.08, 65.45, 42.72, 14.48.
HRESI-MS: calculated for ($C_{10}H_{16}N_2$, M+H), 165.1392; found, 165.1392.

- *Synthesis of ligand* **14**

A 50 mL reaction vessel was charged with $Pd_2(dba)_3$ (94 mg, 0.1 mmol), bis(diphenylphosphino)-ferrocene (DPPF) (115 mg, 0.2 mmol), NaO^tBu (650 mg, 6.8 mmol) and toluene (20 mL) under N_2 atmosphere. Iodinated substrate **16** (1.4 g, 5 mmol) and compound **17** (0.8 g, 5 mmol) were added to the reaction mixture. The resulting brown solution was vigorously stirred for 16 h at 110 °C. The solution was then cooled to room temperature and filtered through Celite. Removal of the solvent yielded a black liquid which was then dissolved in hexane and filtered through celite, the vacuum evaporation of the solvent afforded the pure compound as brown oil in a yield of 90% (1.4 g).

¹H NMR (400 MHz, $CDCl_3$): 9.16 (s, 1H), 9.05 (s, 1H), 7.52 (dd, J = 11.3, 4.3 Hz, 2H), 7.36 − 7.30 (m, 2H), 7.21 − 7.13 (m, 2H), 7.00 − 6.94 (m, 2H), 3.51 (q, J = 6.7 Hz, 1H), 3.39 (q, J = 6.7 Hz, 1H), 2.17 (s, 12H), 1.41 (d, J = 6.7 Hz, 3H), 1.37 (d, J = 6.7 Hz, 3H).

- *Synthesis of lithium salt* **5**

A solution of **14** (1 g, 3.4 mmol) was prepared in toluene (20 mL) under inert atmosphere. A solution of MeLi (2.3 mL, 3.7 mmol, 1.6 M in diethyl ether) was carefully added. The solution turned gray-white. The reaction mixture was stirred for 2 h until the presence of a white solid. The solvent was then carefully vacuum evaporated, and 20 mL of pentane were added. The product was recovered under vacuum filtration as a white power in a yield of 50% (0.54 g).

4.6.4 Metalation trials of ligand 14

- *Synthetics trials starting from lithium salt 15 (Table 1)*

A solution of lithium salt **15** (50 mg, 0.16 mmol) in 2 mL of solvent was added to a suspension of 0.16 mmol of Ni precursor in 3 mL of solvent under N_2 atmosphere. The resulting solution was stirred for 16 hours at room temperature. The solution was filtered was filtered through PTFE (0.22 µm pore size) filters and the solvent was evaporated. The recovered solid was ^{1}H NMR analyzed in benzene-d^6. In the case of entries indicating decomposition the solution became black and the ^{1}H NMR spectra were not interpretable.

- *Synthetics trials starting from ligand 14 (Table 2)*

A solution of ligand **14** (100 mg, 0.34 mmol) in 2 mL of solvent was added to a suspension of 0.34 mmol of metal precursor in 3 mL of solvent under N_2 atmosphere. After 10 minutes of stirring at the temperature indicated in Table 2, 0.34 mmol of base were added. The resulting solution was stirred for 16 hours at temperature indicated in Table 2. The solution was filtered was filtered through PTFE (0.22 µm pore size) filters and the solvent was evaporated. The recovered solid was ^{1}H NMR analyzed in benzene-d^6. In the case of entries indicating decomposition the solution became black and the ^{1}H NMR spectra were not interpretable.

- *Synthesis of Nickamine by oxidative addition*

A stirred solution of Bis[(2-dimethylamino)phenyl]amine (50 mg, 0.2 mmol) in 5 mL of ether was cooled to 0°C under N_2 atmosphere. A suspension of NCS (26 mg, 0.2 mmol) was then slowly added. The solution was stirred for 1 hour and a precooled suspension of Ni(COD)$_2$ (54 mg, 0.2 mmol) was slowly added. The solution became brown and was stirred for 2 hours at room temperature. The resulting solution was filtered through PTFE (0.22 µm pore size) filters and the solvent was evaporated. The recovered brown solid was ^{1}H NMR analyzed verifying the formation of Nickamine.

^{1}H NMR (400 MHz, CDCl$_3$): 7.43 (d, J = 8.3 Hz, 2H), 7.06 – 6.91 (m, 4H), 6.48 (t, J = 7.5 Hz, 2H), 2.91 (s, 12H).

- *Synthesis trial of a nickel complex by oxidative addition from ligand 14*

Ligand **14** was submitted to the same experimental procedure described in the previous paragraph. The ^{1}H NMR analysis of the residue only revealed the presence of ligand **14**.

4.6.5 Synthesis of complex 21

- *Synthesis of ligand* **19**

A 100 mL reaction vessel was charged with Pd$_2$(dba)$_3$ (132 mg, 0.14 mmol), bis(diphenylphosphino)-ferrocene (DPPF) (160 mg, 0.29 mmol), NaO^{t}Bu (915 mg, 9.5 mmol) and toluene (30 mL) under N$_2$ atmosphere. Iodinated substrate **16** (1.9 g, 7 mmol) and N^1,N^1-dimethylbenzene-1,2-diamine (960 mg, 7 mmol) were added to the reaction mixture. The resulting brown solution was vigorously stirred for 16 h at 110 °C. The solution was then cooled to room temperature and filtered through Celite. Removal of the solvent yielded a black liquid which was then dissolved in hexane and filtered through celite, the vacuum evaporation of the solvent afforded the pure compound as brown oil in a yield of 80% (1.6 g).

^{1}H NMR (400 MHz, CDCl$_3$): 9.29 (s, 1H), 7.73 (d, J = 7.9 Hz, 1H), 7.66 (d, J = 7.8 Hz, 1H), 7.18 (d, J = 7.4 Hz, 2H), 7.09 (t, J = 7.0 Hz, 2H), 6.96 (dd, J = 14.9, 7.4 Hz, 1H), 6.59 (d, J = 7.3 Hz, 1H), 3.50 (q, J = 6.4 Hz, 1H), 2.59 (s, 6H), 2.14 (s, 6H), 1.27 (d, J = 6.7 Hz, 3H).

- *Synthesis of lithium salt* **20**

A solution of **19** (0.7 g, 2.5 mmol) was prepared in toluene (20 mL) under inert atmosphere. A solution of ^{n}BuLi (1.7 mL, 2.8 mmol, 1.6 M in hexane) was carefully added. The solution turned gray-white. The reaction mixture was stirred for 2 h until the presence of a white solid. The solvent was then carefully vacuum evaporated, and 20 mL of pentane were added. The product was recovered under vacuum filtration as a white power in a yield of 75% (0.6 g).

- *Synthesis of complex* **21**

Under an inert atmosphere, a THF solution (2 mL) of **20** (0.5 g, 1.7 mmol) was added to a THF suspension (5 mL) of NiCl$_2$dme (0.38 g, 1.7 mmol). The reaction mixture was stirred overnight at room temperature. After removal of solvent, the residue was dissolved in 5 mL toluene and filtered through PTFE (0.22 μm pore size) filters. The toluene was then vacuum evaporated and the resulting solid was washed with pentane. The product was obtained as a red solid in a yield of 80% (0.51 g). Diffusion of pentane into a toluene solution of **21** afforded blue crystals suitable for X-ray analysis. Figure 7 shows the ^{1}H NMR spectrum of isolated complex **21**.

^{1}H NMR (400 MHz, C$_6$D$_6$): 7.75 − 6.94 (br, 1H), 6.80 − 6.65 (br, 4H), 6.55 − 6.40 (br, 2H), 6.25 − 6.15 (br, 1H), 3.15 − 3.05 (br, 1H), 2.70 (s, 3H), 2.47 (s, 3H), 2.23 (s, 3H), 1.96 (s, 3H), 1.74 − 1.55 (br, 3H).
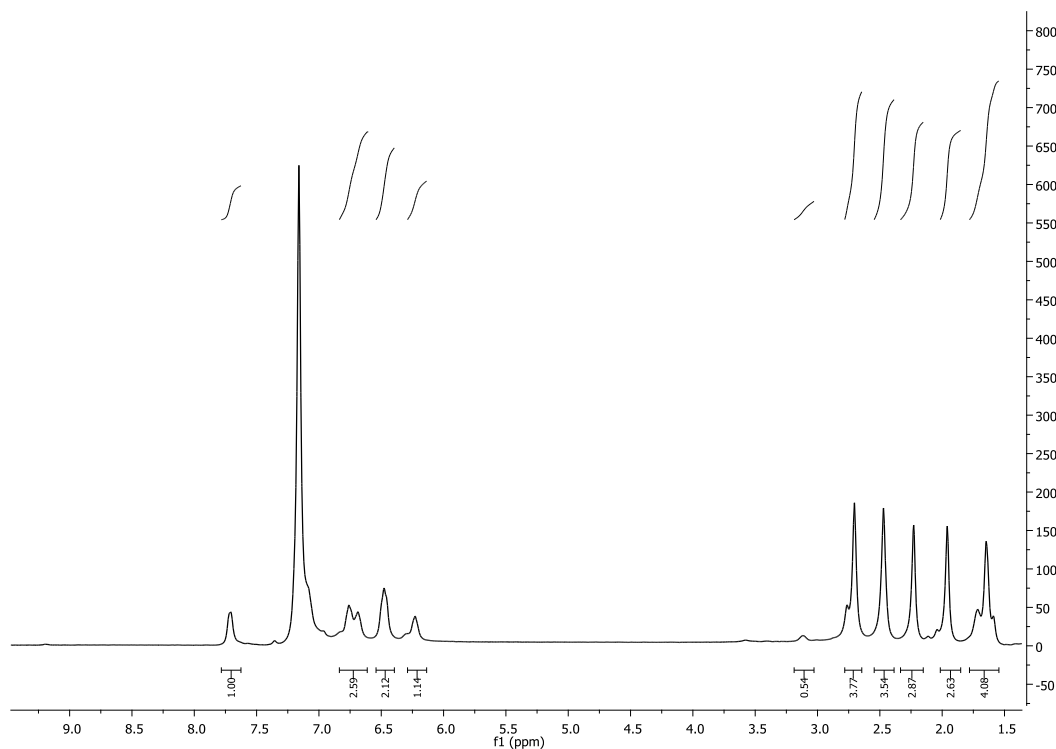
Figure 7. ^{1}H NMR spectrum of complex **21**.

- *Crystallographic details for complex 21*

A total of 56419 reflections (-12 ≤ h ≤ 12, -14 ≤ k ≤ 18, -45 ≤ l ≤ 45) were collected at T = 100(2) K of which 5186 were unique (Rint = 0.0322); $Mo_{K\alpha}$ radiation (λ= 0.71073 Å). The structure was solved by the direct methods. All non-hydrogen atoms were refined anisotropically, and hydrogen atoms were placed in calculated idealized positions. The residual peak and hole electron densities were 0.438 and –0.421 eA^{-3}, respectively. The absorption coefficient was 1.238 mm^{-1}. The least squares refinement converged normally with residuals of R(F) = 0.0269, wR(F2) = 0.0633 and a GOF = 1.135 (I>2σ(I)). $C_{18}H_{24}ClN_3Ni$, Mw = 376.55, space group P*bca*, Orthorhombic, a = 8.5780(12), b = 12.8882(10), c = 32.326(4) Å, α = 90°, β = 90°, γ = 90°, V = 3573.9(8) $Å^3$, Z = 8, ρ_{calcd} = 1.400 Mg/m^3.

4.6.6 Catalytic trials of complex 21 (Table 3)

- *Alkyl – Alkyl Kumada coupling*

0.6 mmol (1.2 equiv.) of alkyl Grignard reagent was diluted in THF (3 mL), and then was added dropwise via syringe pump during 2 h to a DMA (0.75 mL) solution containing the nickel catalyst (0.015 mmol, 3 mol%) and alkyl iodide (0.5 mmol) at -20°C. After addition, the reaction mixture was further stirred for 30 min at -20°C and then the solution was taken

out from the cooling system and stirred for some minutes to warm up to room temperature. The reaction mixture was quenched with 10 mL of water and extracted with 15 mL of ether each time. The yields of the reactions were calculated by GC analysis using decane as internal standard (60 µL, 0.31 mmol).

- *Alkyl – Aryl Kumada coupling*

0.6 mmol (1.2 equiv.) of aryl Grignard reagent was diluted in THF (3 mL), and then was added dropwise via syringe pump during 2 h to a THF (1 mL) solution containing the nickel catalyst (0.015 mmol, 3 mol%), alkyl iodide (0.5 mmol) and TMEDA (10 µL, 0.22 equiv.) at room temperature. After addition, the reaction mixture was further stirred for 30 min. The reaction mixture was quenched with 10 mL of water and extracted with 15 mL of ether each time. The yields of the reactions were calculated by GC analysis using decane as internal standard (60 µL, 0.31 mmol).

- *Alkyl – Alkynyl coupling*

0.6 mmol (1.2 equiv.) of alkynyl Grignard reagent was diluted in THF (3 mL), and then was added dropwise via syringe pump during 2 h to a THF (1 mL) solution containing the nickel catalyst (0.015 mmol, 3 mol%), alkyl iodide (0.5 mmol) and O-TMEDA (250 µL, 2.7 equiv.) at room temperature. After addition, the reaction mixture was further stirred for 30 min. The reaction mixture was quenched with 10 mL of water and extracted with 15 mL of ether each time. The yields of the reactions were calculated by GC analysis using decane as internal standard (60 µL, 0.31 mmol).

4.6.7 Synthesis of complex 23

- *Synthesis of 1-(2-nitrophenyl)pyrrolidine*

1-fluoro-2-nitrobenzene (4 g, 28.4 mmol) was dissolved in 40 mL of acetonitrile and K_2CO_3 (2.2 g, 16 mmol) was added. Pyrrolidine (2 g, 28.4 mmol) was added under stirring to the resulted mixture. After the addition was finished, the reaction was heated at reflux during 3 h. Then the reaction was stirred overnight at r.t. 60 mL of water were added to the reaction mixture and the product was extracted with DCM (3 times, 60 mL each) and the organic phase was washed with brine (2 times, 60 mL each) and with distilled water (2 times, 50 mL each). The organic phase was then dried over Na_2SO_4, filtered and the solvent was evaporated under vacuum to give the product as orange oil in a yield of 94% (5.1 g).

^{1}H NMR (400 MHz, CDCl$_3$): 7.73 (d, J = 8.2 Hz, 1H), 7.35 (m, J = 7.6 Hz, 1H), 6.90 (d, J = 8.6 Hz, 1H), 6.70 (t, J = 7.6 Hz, 1H), 3.25 – 3.16 (m, 4H), 2.10 – 1.95 (m, 4H).
^{13}C NMR (100 MHz, CDCl$_3$): 142.81, 137.08, 133.03, 126.77, 115.95, 115.49, 50.43, 25.79.
HRESI-MS: calculated for (C$_{10}$H$_{12}$N$_2$O$_2$, M+H), 193.0977; found, 193.0979.

- *Synthesis of 2-(pyrrolidin-1-yl)aniline*

1-(2-nitrophenyl)pyrrolidine (3 g, 15.6 mmol) was dissolved in 100 mL of methanol and 150 mg of Pd/C (5% of Pd) was added. The reaction flask was degassed and flushed with hydrogen twice and stirred overnight under hydrogen (1.5 bar) at room temperature. The Pd catalyst was filtered off, and the solvent was removed under a reduced pressure. The pure compound was obtained as dark yellow oil in a yield of 95% (2.4 g).

^{1}H NMR (400 MHz, CDCl$_3$): 7.07 – 6.97 (m, 1H), 6.97 – 6.84 (m, 1H), 6.77 – 6.72 (m, 2H), 3.86 (br, 2H), 3.10 – 3.00 (m, 4H), 2.01 – 1.85 (m, 4H).
^{13}C NMR (100 MHz, CDCl$_3$): 141.41, 137.82, 123.51, 118.75, 118.65, 115.53, 50.96, 24.21.
HRESI-MS: calculated for (C$_{10}$H$_{14}$N$_2$, M+H), 163.1235; found, 163.1236.

- *Synthesis of N1,N1-dimethyl-N2-(2-(pyrrolidin-1-yl)phenyl)benzene-1,2-diamine (**22**).*

A 250 mL reaction vessel was charged with Pd$_2$(dba)$_3$ (229 mg, 0.25 mmol), bis(diphenylphosphino)-ferrocene (DPPF) (278 mg, 0.5 mmol), NaO^{t}Bu (1.6 g, 16.64 mmol) and toluene (50 mL) under a dinitrogen atmosphere. 2-Bromo-*N,N*-dimethylaniline (2.5 g, 12.3 mmol) and 2-(pyrrolidin-1-yl)aniline (2 g, 12.3 mmol) were added to the reaction mixture. The resulting brown solution was vigorously stirred for 2 days at 110 °C. The solution was then cooled to room temperature and filtered through Celite. Removal of the solvent yielded a black liquid which was then dissolved in hexane and filtered through Celite, the removal of the solvent by vacuum evaporation afforded the pure compound as brown oil in a yield of 86% (3 g).

^{1}H NMR (400 MHz, CDCl$_3$): 7.55 – 7.47 (m, 1H), 7.34 (dd, J = 8.0, 1.2 Hz, 1H), 7.26 (dd, J = 7.6, 2 Hz, 1H), 7.19 – 7.05 (m, 4H), 7.01 – 6.91 (m, 2H), 3.29 – 3.23 (m, 4H), 2.85 (s, 6H), 2.06 – 1.99 (m, 4H).
^{13}C NMR (100 MHz, CDCl$_3$): 142.53, 141.84, 139.22, 134.76, 124.22, 121.99, 121.41, 120.39, 119.51, 118.77, 117.51, 113.31, 50.76, 44.18, 24.69.
HRESI-MS: calculated for (C$_{18}$H$_{23}$N$_3$, M+H), 282.1970; found, 282.1970.

- *Synthesis of complex **23***

^{n}BuLi (11.07 mmol, 1.6 M in hexane) was slowly added to a THF solution (80 mL) of the ligand **22** (2.83 g, 10.06 mmol) at room temperature. The reaction mixture was stirred for 2 h, and then NiCl$_2$(dme) (2.2 g, 10.06 mmol, dme = dimethoxyethane) was added. The resulting solution was stirred overnight and then evaporated in vacuum. The residue was extracted with toluene, and then was concentrated to ca. 5 mL. Addition of pentane (20 mL) afforded a

reddish precipitate, which was filtered, washed with additional pentane, and dried in vacuo. Yield: 2.4g (65%). Diffusion of pentane into a toluene solution of **23** afforded red crystals suitable for X-ray analysis. Figures 8 and 9 shows the ^{1}H and ^{13}C NMR spectra of isolated complex **23**.

^{1}H NMR (400 MHz, CDCl$_3$): 7.38 (d, J = 8.3 Hz, 1H), 7.06 – 6.88 (m, 2H), 6.68 (d, J = 8.0 Hz, 1H), 6.47 (t, J = 7.6 Hz, 1H), 6.39 (t, J = 7.6 Hz, 1H), 4.54 – 4.39 (m, 1H), 3.16 (dd, J = 11.7, 5.6 Hz, 1H), 2.88 (s, 3H), 1.98 – 1.87 (m, 2H).
^{13}C NMR (100 MHz, CDCl$_3$): 128.21, 127.47, 121.50, 120.28, 116.09, 116.03, 114.29, 113.60, 61.82, 51.44, 24.76.
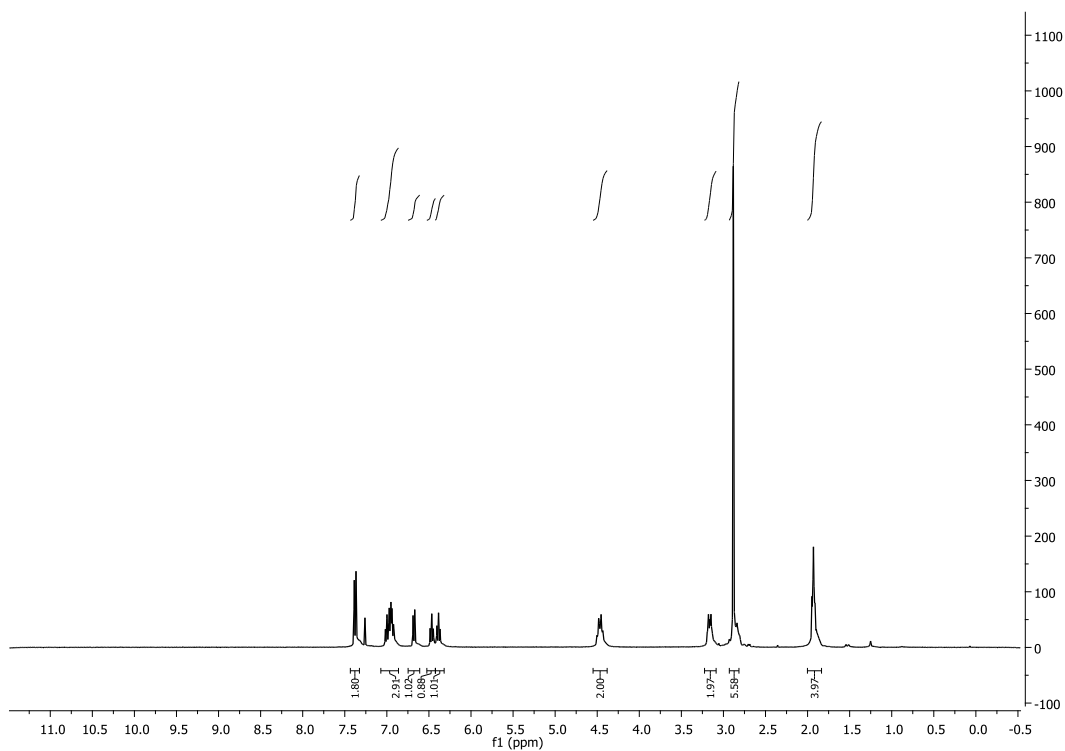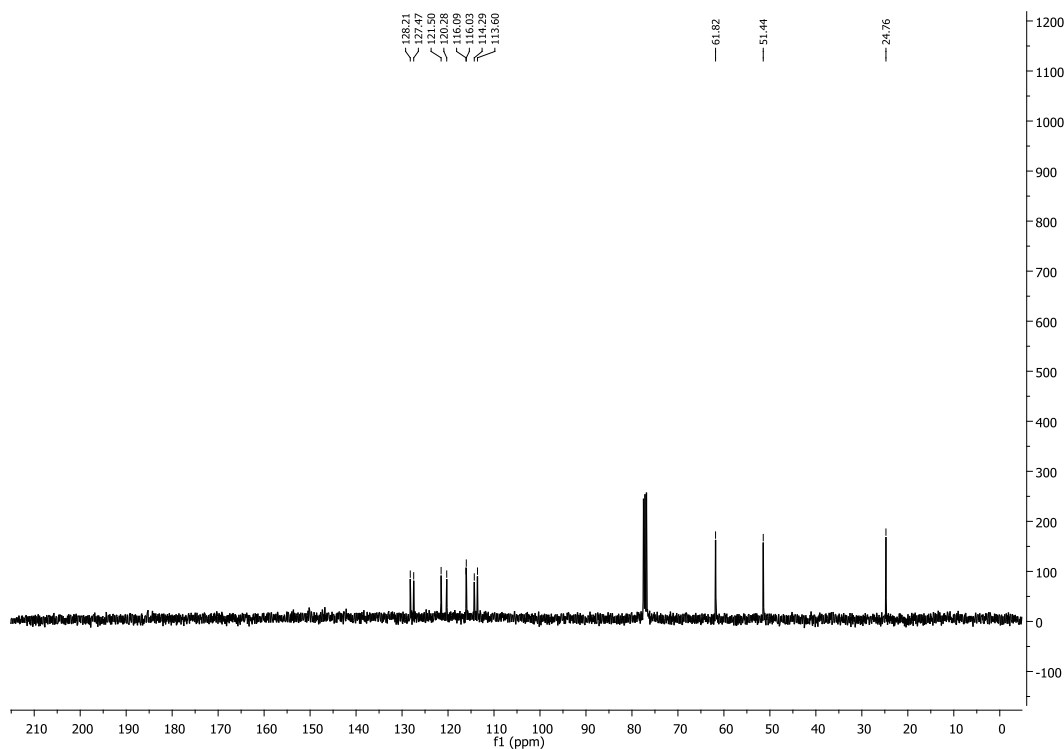**Anal. Calcd for C$_{18}$H$_{22}$ClN$_3$Ni:**   C: 57.94; H: 5.92; N: 11.17 Found: C: 57.74; H: 5.99; N: 11.20.

Figure 8. ^{1}H NMR spectrum of complex **23**.

91

Figure 9. ^{1}H NMR spectrum of complex **23**.

- *Crystallographic details of complex* **23**

A total of 53852 reflections (-24 ≤ h ≤ 24, -14 ≤ k ≤ 14, -26 ≤ l ≤ 26) were collected at T = 100(2) K of which 9750 were unique (Rint = 0.0576); Mo$_{K\alpha}$ radiation (λ= 0.71073 Å). The structure was solved by the direct methods. All non-hydrogen atoms were refined anisotropically, and hydrogen atoms were placed in calculated idealized positions. The residual peak and hole electron densities were 1.524 and −1.275 eA^{-3}, respectively. The absorption coefficient was 1.319 mm^{-1}. The least squares refinement converged normally with residuals of R(F) = 0.0815, wR(F2) = 0.1670 and a GOF = 1.299 (I>2σ(I)). C$_{18}$H$_{22}$ClN$_3$Ni, Mw = 374.55, space group P2$_1$/*c*, Monoclinic, a = 17.067(4), b = 10.4806(18), c = 18.8193(14) Å, α = 90°, β = 95.005(11)°, γ = 90°, V = 3353.5(20) Å^3, Z = 8, ρ$_{calcd}$ = 1.484 Mg/m^3.

4.6.8 Catalytic trials of complex 10 (Tables 4, 5 and 6)

- *Alkyl – Alkyl Kumada coupling.*

0.6 mmol (1.2 equiv..) of alkyl Grignard reagent was diluted in THF (3 mL), and then was added dropwise via syringe pump during 2 h to a DMA (0.75 mL) solution containing the nickel catalyst (0.035 mmol, 7 mol%) and alkyl iodide (0.5 mmol) at -20°C. After addition,

the reaction mixture was further stirred for 30 min at -20°C and then the solution was taken out from the cooling system and stirred for some minutes to warm up to room temperature. The reaction mixture was quenched with 10 mL of water and extracted with 15 mL of ether each time. The solvent was evaporated in vacuo and the crude product was purified by SiO_2 chromatographic column.

- *Alkyl – Aryl Kumada coupling*

0.6 mmol (1.2 equiv.) of aryl Grignard reagent was diluted in THF (3 mL), and then was added dropwise via syringe pump during 2 h to a THF (1 mL) solution containing the nickel catalyst (0.035 mmol, 7 mol%), alkyl iodide (0.5 mmol) and TMEDA (10 μL, 0.22 equiv.) at room temperature. After addition, the reaction mixture was further stirred for 30 min. The reaction mixture was quenched with 10 mL of water and extracted with 15 mL of ether each time. The solvent was evaporated in vacuo and the crude product was purified by SiO_2 chromatographic column.

4.6.9 Detailed description for coupling products.

decylbenzene (entry 2, Table 4):
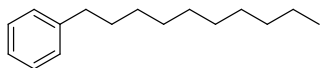
Purified by column (SiO_2, Hexane), 80% yield as a transparent oil.
^{1}H NMR (400 MHz, $CDCl_3$): 7.36 – 7.30 (m, 2H), 7.26 – 7.17 (m, 3H), 2.66 (t, J = 8 Hz, 2H), 1.71 – 1.62 (m, 2H), 1.42 – 1.22 (m, 14H), 0.94 (t, J = 6.8 Hz, 3H).
^{13}C NMR (100 MHz, $CDCl_3$): 143.10, 128.54, 128.35, 125.67, 36.16, 32.08, 31.72, 29.80, 29.78, 29.70, 29.52, 22.86, 14.29.
HRAPCI-MS: calculated for ($C_{16}H_{26}$), 218.2035; found, 218.2030.

ethyl dodecanoate (entry 1, Table 5):
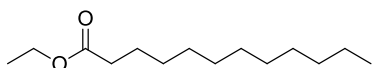
Purified by column (SiO_2, 90:10 Hexane:Ethyl acetate), 70% yield as a transparent oil.
^{1}H NMR (400 MHz, $CDCl_3$): 4.11 (q, J = 7.1 Hz, 2H), 2.27 (t, J = 7.6 Hz, 2H), 1.69 – 1.51 (m, 2H), 1.39 – 1.11 (m, 19H), 0.87 (t, J = 6.8 Hz, 3H).
^{13}C NMR (100 MHz, $CDCl_3$): 174.06, 60.27, 34.53, 32.05, 29.74, 29.60, 29.48, 29.41, 29.29, 25.13, 22.83, 14.38, 14.25.
HRESI-MS: calculated for ($C_{14}H_{28}O_2$, M+H), 229.2168; found, 229.2171.

decanenitrile (entry 2, Table 5):
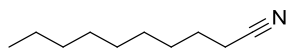
Purified by column (SiO$_2$, 90:10 Hexane:Ethyl acetate), 60% yield as a yellowish oil.
^{1}H NMR (400 MHz, CDCl$_3$): 2.33 (t, *J* = 7.1 Hz, 2H), 1.65 (q, *J* = 7.6 Hz, 2H), 1.47 − 1.37 (m, 2H), 1.35 − 1.17 (m, 10), 0.87 (t, *J* = 6.8 Hz, 3H).
^{13}C NMR (100 MHz, CDCl$_3$): 120.00, 31.91, 29.37, 29.27, 28.87, 28.77, 25.48, 22.74, 17.23, 14.20.
HRESI-MS: calculated for (C$_{10}$H$_{19}$N, M+H), 154.1596; found, 154.1592.

1-decyl-4-(trifluoromethyl)benzene (entry 3, Table 5):

Purified by column (SiO$_2$, Hexane), 63% yield as a yellowish oil.
^{1}H NMR (400 MHz, CDCl$_3$): 7.52 (d, *J* = 8.1 Hz, 2H), 7.28 (d, *J* = 8.0 Hz, 2H), 2.65 (t, *J* = 8.0 Hz, 2H), 1.67 − 1.57 (m, 2H), 1.37 − 1.14 (m, 14H), 0.88 (t, *J* = 6.8 Hz, 3H).
^{13}C NMR (100 MHz, CDCl$_3$): 147.04, 128.68, 128.57, 125.16, 125.12, 35.81, 31.91, 31.23, 29.61, 29.57, 29.46, 29.34, 29.23, 22.70, 14.13.
HRESI-MS: calculated for (C$_{17}$H$_{25}$F$_3$, M-F), 267.1924; found, 267.1922.

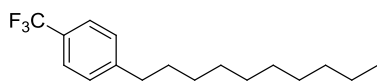*4-butyl-2-phenyltetrahydro-2H-pyran (entry 4, Table 5):*
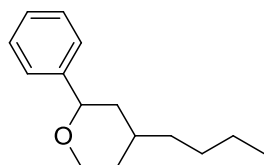
Purified by column (SiO$_2$, 90:10 Hexane:Ethyl acetate), 80% yield as a transparent oil.
^{1}H NMR (400 MHz, CDCl$_3$): 7.41 − 7.23 (m, 5H), 4.34 (dd, J = 11.3, 2.0 Hz, 1H), 4.19 (dd, J = 11.2, 3.9 Hz, 1H), 3.68 − 3.56 (m, 1H), 1.97 − 1.85 (m, 1H), 1.76 − 1.58 (m, 2H), 1.45 − 1.18 (m, 8H), 0.96 − 0.86 (m, 3).
^{13}C NMR (100 MHz, CDCl$_3$): 143.43, 128.43, 127.42, 125.98, 80.08, 68.73, 41.14, 36.84, 35.83, 32.85, 28.73, 22.99, 14.25.
HRAPCI-MS: calculated for (C$_{15}$H$_{22}$O), 218.1621; found, 218.1618.

2-undecylfuran (entry 5, Table 5):
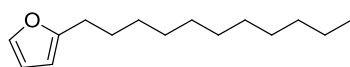
Purified by column (SiO$_2$, 90:10 Hexane:Ethyl acetate), 79% yield as a transparent oil.

¹H NMR (400 MHz, CDCl₃): 7.32 – 7.28 (m, 1H), 6.30 – 6.26 (m, 1H), 5.99 – 5.96 (m, 1H), 2.62 (t, J = 7.6 Hz, 2H), 1.70 – 1.60 (m, 2H), 1.37 – 1.17 (m, 16), 0.89 (t, J = 6.8 Hz, 3H).
¹³C NMR (100 MHz, CDCl₃): 156.78, 140.74, 110.15, 104.63, 32.08, 29.80, 29.79, 29.72, 29.54, 29.51, 29.36, 28.20, 28.13, 22.85, 14.28.
HRESI-MS: calculated for ($C_{15}H_{26}O$, M+H), 223.2062; found, 223.2063.

2-(3-phenylpropyl)furan (entry 8, Table 5):

Purified by column (SiO₂, 90:10 Hexane:Ethyl acetate), 80% yield as a transparent oil.
¹H NMR (400 MHz, CDCl₃): 7.37 – 7.30 (m, 2H), 7.27 – 7.19 (m, 3H), 6.35 – 6.31 (m, 1H), 6.07 – 6.02 (m, 1H), 2.76 – 2.67 (m, 4H), 2.03 (q, J = 7.6 Hz, 2H).
¹³C NMR (100 MHz, CDCl₃): 156.11, 142.08, 140.94, 128.62, 128.46, 125.95, 110.20, 105.02, 35.36, 29.78, 27.56.
HRESI-MS: calculated for ($C_{13}H_{15}$, M+H), 187.1123; found, 187.1120.
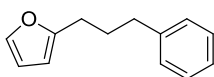
cyclohexylbenzene (entry 9, Table 5):
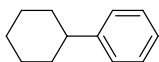
Purified by column (SiO₂, Hexane), 70% yield as a transparent oil.
¹H NMR (400 MHz, CDCl₃): 7.39 – 7.32 (m, 2H), 7.31 – 7.16 (m, 3H), 2.60 – 2.52 (m, 1H), 2.03 – 1.72 (m, 6H), 1.58 – 1.21 (m, 6H).
¹³C NMR (100 MHz, CDCl₃): 148.22, 128.40, 126.96, 125.90, 44.74, 34.60, 27.06, 26.31.
HRAPCI-MS: calculated for ($C_{12}H_{16}$), 160.1252; found, 160.1244.

(3-methylundecyl)benzene (entry 3, Table 6):
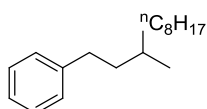
Purified by column (SiO₂, Hexane), 70% yield as a transparent oil.
¹H NMR (400 MHz, CDCl₃): 7.35 – 7.27 (m, 2H), 7.26 – 7.18 (m, 3H), 2.75 – 2.55 (m, 2H), 1.74 – 1.61 (m, 1H), 1.55 – 1.43 (m, 2H), 1.43 – 1.14 (m, 14H), 0.97 (d, J = 6.3 Hz, 3H), 0.94 (t, J = 6.8 Hz, 3H).
¹³C NMR (100 MHz, CDCl₃): 143.26, 128.37, 128.27, 125.53, 39.02, 36.96, 33.54, 32.54, 31.97, 30.05, 29.72, 29.41, 27.02, 22.74, 19.66, 14.17.
HRAPCI-MS: calculated for ($C_{18}H_{30}$), 246.2342; found, 246.2334.

(2-cyclopentylethyl)benzene (entry 5, Table 6):
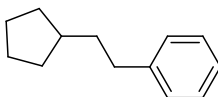
Purified by column (SiO$_2$, Hexane), 72% yield as a transparent oil.
^{1}H NMR (400 MHz, CDCl$_3$): 7.43 – 7.11 (m, 5H), 2.65 (dd, J = 15.8, 7.7 Hz, 2H), 1.90 – 1.72 (m. 3H), 1.75 – 1.47 (m, 6H), 1.25 – 1.07 (m, 2H).
^{13}C NMR (100 MHz, CDCl$_3$): 143.22, 128.49, 128.36, 125.65, 39.79, 38.30, 35.28, 32.79, 25.37.
HRAPCI-MS: calculated for (C$_{13}$H$_{18}$), 174.1409; found, 174.1403.

tert-butyl 3-butylpyrrolidine-1-carboxylate (entry 8, Table 6):
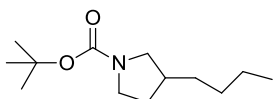
^{1}H NMR (400 MHz, CDCl$_3$): 3.60 – 3.32 (m, 2H), 3.31 – 3.06 (m, 1H), 2.92 – 2.62 (m, 1H), 2.18 – 1.83 (m, 2H), 1.54 – 1.10 (m, 16H), 0.92 – 0.82 (m, 3H).
^{13}C NMR (100 MHz, CDCl$_3$): 154.78, 78.99, 51.86, 51.42, 45.93, 45.60, 39.28, 38.42, 33.07, 32.07, 31.33, 30.55, 28.69, 22.90, 14.16.
HRESI-MS: calculated for (C$_{13}$H$_{25}$NO$_2$, M+Na), 250.1783; found, 250.1782.

butane-1,3-diyldibenzene (entry 9, Table 6):
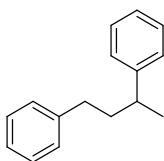
Purified by column (SiO$_2$, Hexane), 60% yield as a transparent oil.
^{1}H NMR (400 MHz, CDCl$_3$): 7.42 – 7.15 (m, 10H), 2.85 – 2.73 (m, 1H), 2.64 – 2.51 (m, 2H), 2.06 – 1.90 (m, 2H), 1.35 (d, *J* = 6.9 Hz, 3H).
^{13}C NMR (100 MHz, CDCl$_3$): 147.33, 142.59, 128.46, 128.43, 128.32, 127.13, 126.02, 125.70, 40.05, 39.56, 33.99, 22.59.
HRAPCI-MS: calculated for (C$_{16}$H$_{18}$), 210.1409; found, 210.1402.

phenylcycloheptane (entry 10, Table 2):
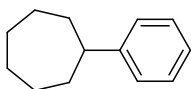
Purified by column (SiO$_2$, Hexane), 50% yield as a transparent oil.
^{1}H NMR (400 MHz, CDCl$_3$): 7.43 – 7.06 (m, 1H), 2.75 – 2.65 (m, 1H), 2.07 – 1.50 (m, 3H).
^{13}C NMR (100 MHz, CDCl$_3$): 150.16, 128.42, 126.82, 125.63, 47.20, 36.96, 28.09, 27.37.
HRAPCI-MS: calculated for (C$_{13}$H$_{28}$), 174.1409; found, 174.1402.

4.7 References

(1)   Selander, N.; J. Szabó, K. *Chem. Rev.* **2011**, *111*, 2048.
(2)   Hu, X. *Chem. Sci.* **2011**, *2*, 1867.
(3)   Morales-Morales, D.; Jensen, C. M. *The Chemistry of Pincer Compounds*; Elsevier: Amsterdam, 2007.
(4)   Lindner, R.; van den Bosch, B.; Lutz, M.; Reek, J. N. H.; van der Vlugt, J. I. *Organometallics* **2011**, *30*, 499.
(5)   Braunstein, P.; Naud, F. *Angew. Chem. Int. Ed.* **2001**, *40*, 680.
(6)   Wang, Z.-X.; Liu, N. *Eur. J. Inorg. Chem.* **2012**, *2012*, 901.
(7)   Liang, L.-C.; Chien, P.-S.; Lin, J.-M.; Huang, M.-H.; Huang, Y.-L.; Liao, J.-H. *Organometallics* **2006**, *25*, 1399.
(8)   Zhang, X.-Q.; Wang, Z.-X. *Synlett* **2013**, *24*, 2081.
(9)   Wang, Z.-X.; Wang, L. *Chem. Commun.* **2007**, 2423.
(10)   Wu, D.; Wang, Z.-X. *Org. Biomol. Chem.* **2014**, *12*, 6414.
(11)   Csok, Z.; Vechorkin, O.; Harkins, S. B.; Scopelliti, R.; Hu, X. *J. Am. Chem. Soc.* **2008**, *130*, 8156.
(12)   Pine, S. H. *J. Chem. Ed.* **1968**, *45*, 118.
(13)   Wu, X.-F.; Darcel, C. *Eur. J. Org. Chem.* **2009**, *2009*, 4753.
(14)   Wenschuh, E.; Zimmering, R. *Zeitschrift für Chemie* **1987**, *27*, 448.
(15)   Vechorkin, O.; Proust, V.; Hu, X. *J. Am. Chem. Soc.* **2009**, *131*, 9756.
(16)   Vechorkin, O.; Godinat, A.; Scopelliti, R.; Hu, X. *Angew. Chem. Int. Ed.* **2011**, *50*, 11777.
(17)   Vechorkin, O.; Barmaz, D.; Proust, V.; Hu, X. *J. Am. Chem. Soc.* **2009**, *131*, 12078.
(18)   Perez Garcia, P. M.; Di Franco, T.; Orsino, A.; Ren, P.; Hu, X. *Org. Lett.* **2012**, *14*, 4286.
(19)   Horibe, H.; Fukuda, Y.; Kondo, K.; Okuno, H.; Murakami, Y.; Aoyama, T. *Tetrahedron* **2004**, *60*, 10701.
(20)   Ren, P.; Vechorkin, O.; Allmen, K. v.; Scopelliti, R.; Hu, X. *J. Am. Chem. Soc.* **2011**, *133*, 7084.
(21)   Ren, P., PhD. Thesis, Ecole Polytechnique Fédérale de Lausanne, 2012.
(22)   Oku, A.; Harada, T.; Kita, K. *Tetrahedron Lett.* **1982**, *23*, 681.
(23)   Sabitha, G.; Reddy, K. B.; Reddy, G. S. K. K.; Fatima, N.; Yadav, J. S. *Synlett* **2005**, *2005*, 2347.
(24)   Gómez, G.; Rivera, H.; García, I.; Estévez, L.; Fall, Y. *Tetrahedron Lett.* **2005**, *46*, 5819.
(25)   van Koten, G.; Jastrzebski, J. T. B. H. *Tetrahedron* **1989**, *45*, 569.

Chapter 5 : Nickel-Catalyzed Direct Alkylation of Terminal Alkynes at Room Temperature: A Hemilabile Pincer Ligand Enhances Catalytic Activity

5.1 Introduction

Alkynes are ubiquitous synthetic intermediates and precursors to biologically active molecules and organic materials;[1,2] therefore, methods that provide a streamlined access to alkynes are highly desirable. The synthesis of aryl- and alkenyl-substituted alkynes has become routine, largely thanks to the development of Sonogashira coupling of aryl and alkenyl halides with terminal alkynes;[3-6] however, the synthesis of alkyl-substituted alkynes is less straightforward. The traditional method of reacting alkali metal acetylides, in particular lithium acetylides, with alkyl electrophiles has a limited scope, is intolerant to sensitive functional groups, and needs a low temperature. Organometallic coupling reactions of alkynyl halides with metal-alkyl reagents[7,8] or alkyl halides with metal-alkynyl reagents[9-12] are more general and tolerant, but they require the pre-activation of alkynes, a reactive organometallic reagent, or both. Compared with these methods, the direct coupling of alkyl halides with terminal alkynes involves fewer steps, is operationally simpler, and often costs less. On the other hand, such coupling is challenging not only due to the general difficulty in the coupling of alkyl electrophiles, but also due to a low concentration of metal alkynyl intermediate in the reaction mixture.

Until now, there are only four metal-ligand combinations that are capable of catalyzing the direct alkylation of terminal alkynes with non-activated alky electrophiles. The groups of Fu[13] and Glorius[14] introduced the first two systems (Figure 1), which were both based on Pd and a N-heterocyclic carbene ligand. Our group reported the first Ni catalyst for this transformation:[15] the catalyst is a nickel pincer complex, Nickamine (**1**). The group of Liu[16] then developed a system based on $Ni(cod)_2$ and a pyridine bisoxazoline (Pybox) ligand. This system is the most active catalyst to date, and it catalyzes the coupling of both primary and secondary non-activated alkyl halides at room temperature.
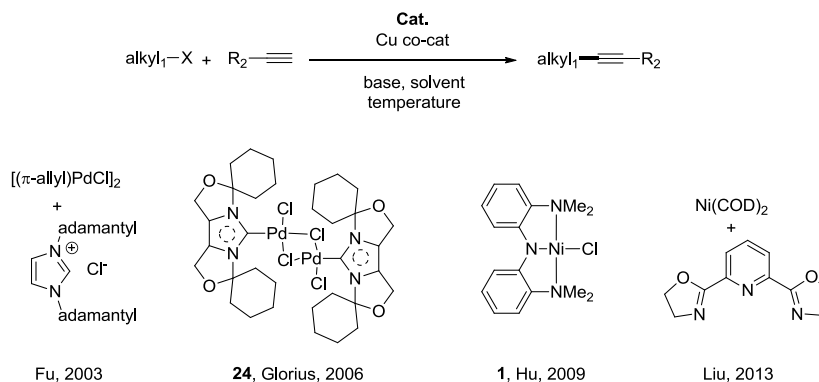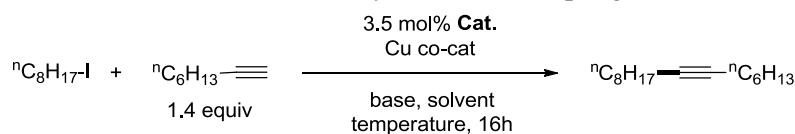
Figure 1. Reported catalyst systems/precatalysts for direct alkylation of alkynes.

Despite the progress in method development, the mechanism of the coupling of alkyl halides with terminal alkynes remains largely unclear. The catalysis by Nickamine seems appropriate for in-depth mechanistic investigations because the catalyst is well-defined. In comparison, the coordination environment of the active catalyst in the Liu system is unidentified. Nevertheless, Nickamine only catalyzes the coupling at an elevated temperature (100°C-140°C) which is inconvenient for both synthetic applications and mechanistic study. Herein, we describe the development of a new nickel pincer complex that catalyzes direct alkylation of terminal alkynes at room temperature. The new catalytic system was subject to a kinetics study, which revealed the hemilabile nature of the new pincer ligand as a key factor for the improved catalytic efficiency. A catalytically relevant Ni alkynyl complex was synthesized and structurally characterized. The reactivity of this Ni alkynyl complex gave important insights into the active species for the activation of alkyl halide.

5.2 A new nickel pincer catalyst for direct alkylation of alkynes

The coupling between 1-iodooctane and oct-1-yne was used as the test reaction for the optimization of reaction conditions. It was reported that Nickamine catalyzed this reaction efficiently at 100°C[15]; the reaction was best carried out using 5 mol% **1** as catalyst, 3 mol% CuI as co-catalyst, 1.4 equivalent Cs_2CO_3 as base, dioxane as solvent, the reaction time was 16 h. We found that replacing Cs_2CO_3 with LiO^{t}Bu led to successful coupling at 60°C (entry 1, Table 1). However, the yield of the reaction decreased to only 10 % at 50°C (entry 2, Table 1). The use of more polar solvents such as acetonitrile (MeCN) or dimethylformamide (DMF) allowed the coupling at room temperature, but the best yield was 43% in DMF (entries 3 and 4, Table 1).

Table 1. Optimization of Conditions for Ni-catalyzed Direct Coupling of 1-iodooctane with oct-1-yne

$$^nC_8H_{17}\text{-}I \ + \ ^nC_6H_{13}\text{---}\equiv \quad \xrightarrow[\substack{\text{base, solvent} \\ \text{temperature, 16h}}]{\substack{3.5 \text{ mol\% } \textbf{Cat.} \\ \text{Cu co-cat}}} \quad ^nC_8H_{17}\text{---}\equiv\text{---}^nC_6H_{13}$$

$$1.4 \text{ equiv}$$

Entry	CuI (mol %)	Base (1.4 equiv)	Solvent	Catalyst	Temperature [°C]	Yield [%][b]
1	CuI	LiOtBu	Dioxane	1	60	Quant.
2	9	LiO^{t}Bu	Dioxane	1	50	10
3	9	LiO^{t}Bu	MeCN	1	20	8
4	9	LiO^{t}Bu	DMF	1	20	43
5	9	LiO^{t}Bu	DMF	2	20	13
6	9	LiO^{t}Bu	DMF	25	20	74
7	0	LiO^{t}Bu	DMF	25	20	13
8	4.5	LiO^{t}Bu	DMF	25	20	74
9	9	Cs$_2$CO$_3$	DMF	25	20	10

[a] General reaction conditions: 0.5 mmol of 1-iodooctane and other reagents according to Table 1 in 2 mL of solvent.
[b] Yields are determined by GC and are relative to alkyl halide.

The above mentioned results showed that Nickamine is not suitable to be used as catalyst for this process at room temperature. We decided then to test other Ni complexes from the vast library of nickel complexes developed in our group.[17-19] Complex **2** (Figure 2) was previously shown to have improved efficiency for the coupling of secondary alkyl halides with alkyl Grignard reagents;[18] however, the coupling yield was only 15% when **2** was used as catalyst (entry 5, Table 1). At the same time, heterogeneous black particles were observed in the reaction using **2** as catalyst. We suspected that complex **2**, having only a bidentate chelate, was unstable under the reaction conditions and decomposed to nickel particles.
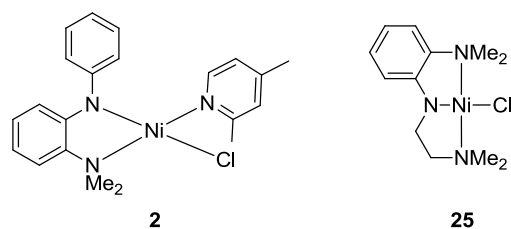
Figure 2. Structural formula for complexes **2** and **25**.

A pincer ligand seems to be more suitable for this process to maintain the stability of the Ni complex. Complex **25** was previously designed and synthesized[19] to test its activity vis-à-vis complex **2** for Kumada cross coupling reactions. One of the two aryl linkers in the N_2N ligand of Nickamine was replaced by a simple ethylene linker. This unsymmetrical NNN pincer ligand was expected to be more labile, which rendered the resulting Ni complex more reactive. The crystal structure of **6** was determined, showing Ni in the expected square planar ligand environment (Figure 3). The Ni-N and Ni-Cl bond distances in **25** are nearly identical to those in **1**,[19,20] except that the Ni1-N1 distance is 0.04 Å longer in **25**. Taking into account these structural features, we decided to test complex **25** for the alkylation of terminal alkynes at room temperature.
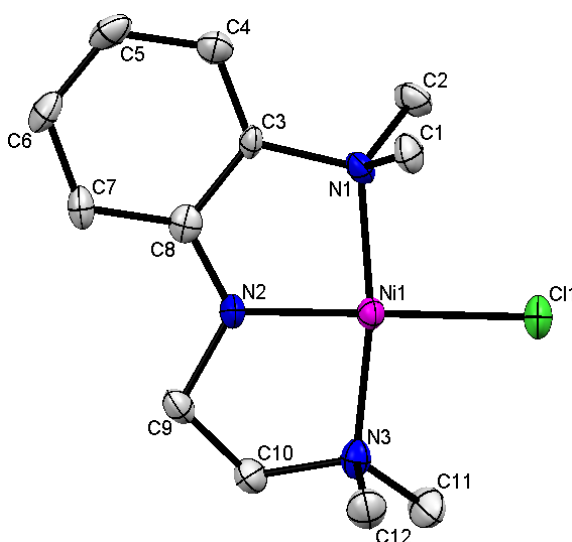
Figure 3. Crystal structure of complex **25**. Only one of the two molecules in the asymmetric unit is shown. Hydrogen atoms are omitted for clarity. The thermal ellipsoids are displayed in a 50% probability. Selected lengths (Å) and angles (deg): Ni1-N1, 1.995(3); Ni1-N2, 1.832(3); Ni2-N3, 1.962(4); Ni1-Cl1, 2.2102(11); N1-Ni1-N2, 85.60(14); N2-Ni1-N3, 84.74(13); N3-Ni1-N1, 169.04(13).

To our delight, complex **25** is indeed a better catalyst than Nickamine for the reaction in Table 1. At room temperature, a coupling yield of 74% was obtained when **25** was used as the catalyst (entry 6, Table 1). CuI was important for the coupling. Without CuI, the yield was only 13 % (entry 7, Table 1). The loading of CuI could be decreased to 4.5 mol% while maintaining the same yield (entry 8, Table 1). For convenience in weighting, a 9 mol% loading of CuI was applied in small scale reactions. LiOBu^t was the best base; use of Cs_2CO_3 as base decreased the yield to 10% (entry 9, Table 1). Under the optimized conditions (entry 6, Table 1), the main side products were 1-tert-butoxyoctane and 1-octene
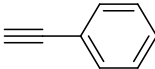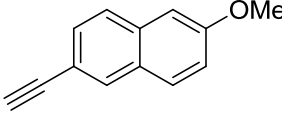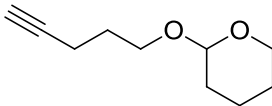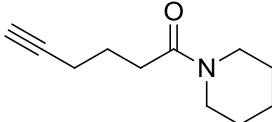
(Experimental Part). The former was produced by the attack of tert-butoxide anion on 1-iodooctane, while the latter was produced by base-induced HI elimination of octyl iodide or reductive elimination from a Ni-octyl intermediate. The excess amount of oct-1-yne was unreacted.
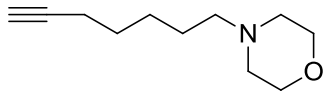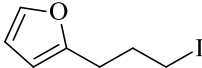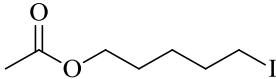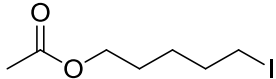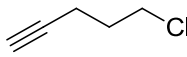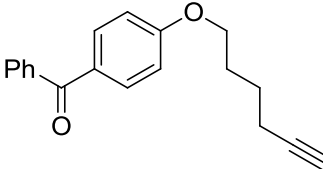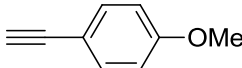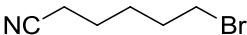
5.3 Scope of direct alkylation of alkynes

The optimized conditions in Table 1 were then applied for the coupling of more elaborate substrates (Table 2).

Table 2. Scope of Direct Alkylation of Alkynes Using **25** as Catalyst[a]

Entry	Alkyl-X	Alkyne	Yield [%]
1	Octyl-I	≡—$^nC_6H_{13}$	60[c](82)[d]
2	Octyl-I		60[c](69)[d]
3	Decyl-I	≡—TMS	58[c]
4	Octyl-I		60[c]
5	Octyl-I		64[b]
6	Octyl-I		63[b]

7	Octyl-Br		60^c
8		$\equiv\!-^nC_6H_{13}$	65^c
9		$\equiv\!-^nC_6H_{13}$	52^b
10			50^c
11	Octyl-I		65^c
12	Octyl-Br		57^b
13		$\equiv\!-^nC_6H_{13}$	60^c

[a] For coupling of iodides, no NaI was added; for coupling of bromides, 20 mol % NaI was added. [b] Isolated yields relative to alkyl halide, the reaction was set-up using 2 mL DMF for every 0.5 mmol of alkyl halide. [c] Isolated yields relative to alkyl halide; the reaction was set-up using 1 mL DMF for every 0.5 mmol of alkyl halide. [d] Calibrated GC yields are shown in parenthesis.

For some substrates, increasing the concentrations of the reactants led to slightly higher yields (about 10%). Alkyl, aryl, and silyl-substituted alkynes could be coupled (entries 1-3, Table 2). The isolated yields of some products were significantly lower than calibrated GC yields (entry 1, Table 2), which was probably due to the difficulty in isolation of these products. Modest to good isolated yields were obtained for the coupling of substrates containing acetal (entry 5, Table 2), amide (entry 6, Table 2), amine (entry 7, Table 2), furan (entry 8, Table 2), ester (entries 9 and 10, Table 2), alkyl chloride (entry 10, Table 2), ketone (entry 11, Table 2), and nitrile (entry 13, Table 2). The conditions could be applied to the coupling of alkyl bromides

if 20 mol % of NaI was used for a presumable Br/I exchange (entries 7, 12-13, Table 2). The coupling of alkyl chlorides was not successful, likely due to a more inert C-Cl bond. Unfortunately the system is not efficient for the alkynylation of secondary alkyl halides which seems to be a general limitation of the most part of the Ni(II) pincer systems. Overall, the scope and yields for the alkynylation of primary alkyl halides are comparable to those catalyzed by the Ni(cod)$_2$/Pybox system developed by Liu and co-workers.[16] The current system, therefore, is well suited for an in-depth mechanistic study due to the defined nature of the catalyst and the mild reaction conditions.

5.4 Kinetics of direct alkylation of alkynes

The reaction profile of the coupling of 1-iodooctane with oct-1-yne was measured by gas chromatography (GC). Figure 4 shows the conversion of reagent and formation of product during a period of 3 hours. The formation of product followed a linear line, indicating a constant reaction rate. Due to the detection limit of the FID detector of GC, only the data collected after 20 minutes could be reliably used. This gave the false impression of an induction period in the reaction profiles produced from GC data. However, following reactions by NMR indicates that there is no induction period. For example, the coupling of 1-iodooctane with phenylacetylene was followed by ^{1}H-NMR in d_7-DMF. The formation of the coupling product from the beginning of the reaction was confirmed by NMR (Figure 5). Moreover, the yields of the coupling product determined by NMR were identical to the yields determined by GC analysis (Figure 5). For experimental convenience, we chose GC as the analytical tool for further kinetic measurements.
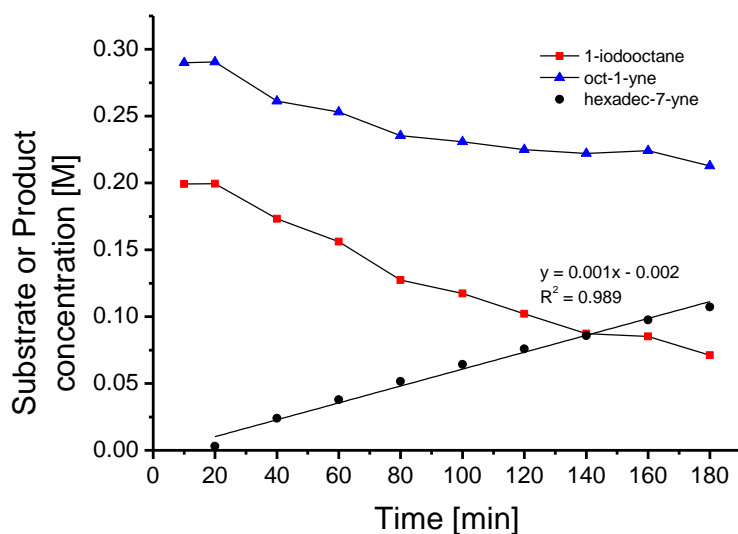
Figure 4. Reaction profile for the coupling of 1-iodooctane with oct-1-yne. At the end of this period, the conversion of 1-iodooctane is 72%, the conversion of oct-1-yne is 39%, and the yield of hexadec-7-yne is 43%.
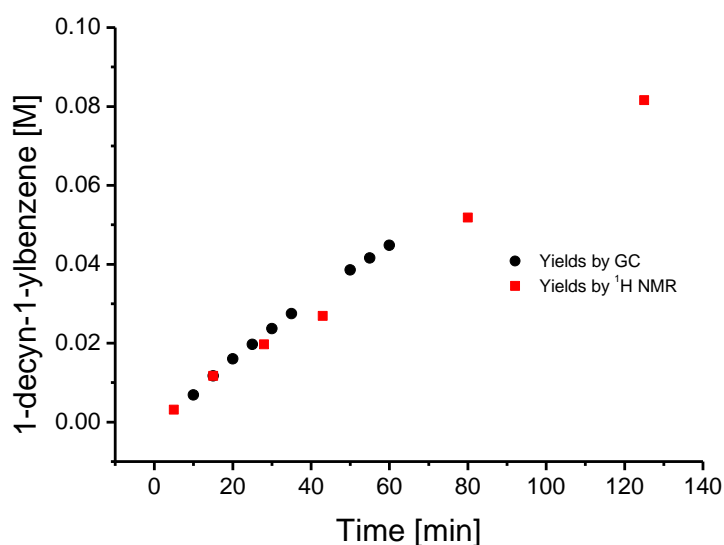
Figure 5. Comparison of time-dependent yields of coupling determined by NMR and GC

The kinetics of the coupling of 1-iodooctane and oct-1-yne was further studied by determining the rates of the coupling reaction using the initial rate approximation. Figure 6A shows the reaction is 0th order in the concentration of 1-iodooctane. The rates of the reaction are nearly constant at different concentrations of 1-iodooctane. Figure 6B shows that the reaction is also 0th order in the concentration of oct-1-yne. Figure 6C shows the coupling is independent of

the loading of CuI. On the other hand, Figure 6D shows that the reaction is first order in the concentration of catalyst **25**. The reaction rate is also independent of the loading of LiO^{t}Bu as it is showed in Figure 18 (Experimental Part).
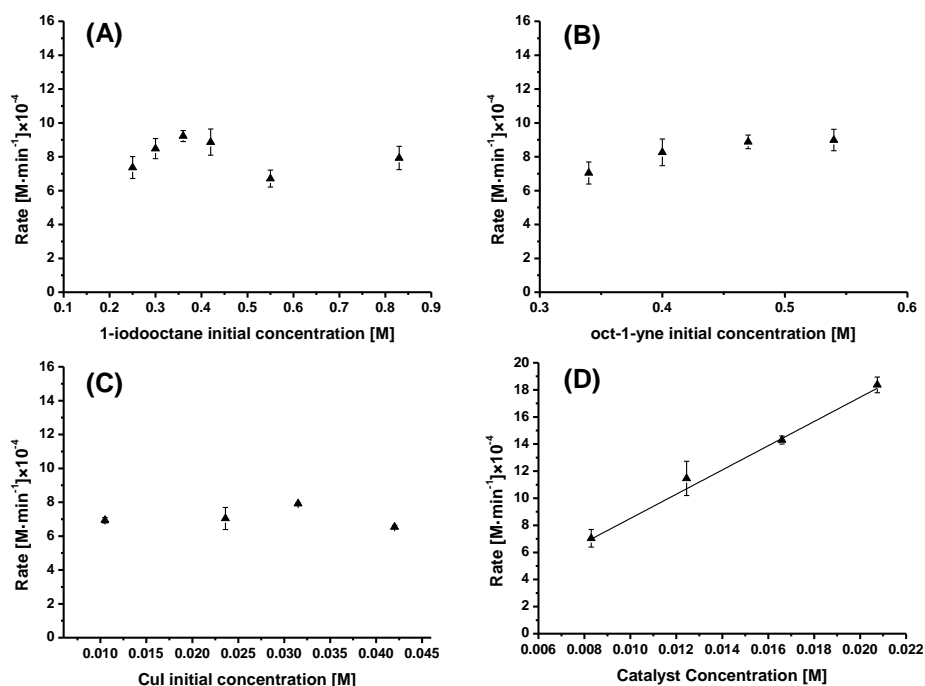
Figure 6. (A) The dependence of initial reaction rates on the initial concentration of 1-iodooctane. (B) The dependence of initial reaction rates on the initial concentration of oct-1-yne. (C) The dependence of initial reaction rates on the loading of CuI. (D) The dependence of initial reaction rates on the loading of catalyst. The rates were averaged over three independent measurements. The error bar represents the standard deviation of the results from three independent measurements.

Therefore, a simple rate law can be drawn for the catalysis (eq. 1) which can be used to determine the rate constant (k_{cat}). Table 3 lists the values determined from different set of experiments. The averaged value is 1.6×10^{-3} s^{-1}.

$$\frac{d[P]}{dt} = k_{cat}[\mathbf{25}] = k_{OBS} \rightarrow k_{cat} = \frac{k_{OBS}}{[\mathbf{25}]} \qquad (1)$$

Table 3. The Rate Constants of Coupling of 1-iodooctane with oct-1-yne.

Set of Experiment	k_{cat} [s⁻¹]	Error[a] [%]
Varying [1-iodooctane]	1.8×10^{-3}	10
Varying [oct-1-yne]	1.8×10^{-3}	7
Varying [CuI]	1.5×10^{-3}	10
Varying [Catalyst]	1.5×10^{-3}	10
Overall reaction profile	1.8×10^{-3}	16
Average	1.6×10^{-3}	-

[a]The error is calculated as the standard deviation of three independent measurements.

To probe possible catalyst deactivation, a reaction progress analysis[21] at same excess conditions was performed for the coupling of 1-iodooctane and the oct-1-yne (Figure 7). The reaction rates are nearly identical for three runs with the same excess, precluding significant catalyst deactivation. Additionally, the catalytic system was subject to a recycling experiment (Scheme 1). After a catalytic run of the coupling between 1-iodooctane and oct-1-yne (yield = 80 %), new samples of the same substrates and base, but not the Ni catalyst nor Cu co-catalyst, were added to the reaction mixture. The coupling proceeded again to give the product in 80% yield. This result again suggests that there was no significant catalyst deactivation.
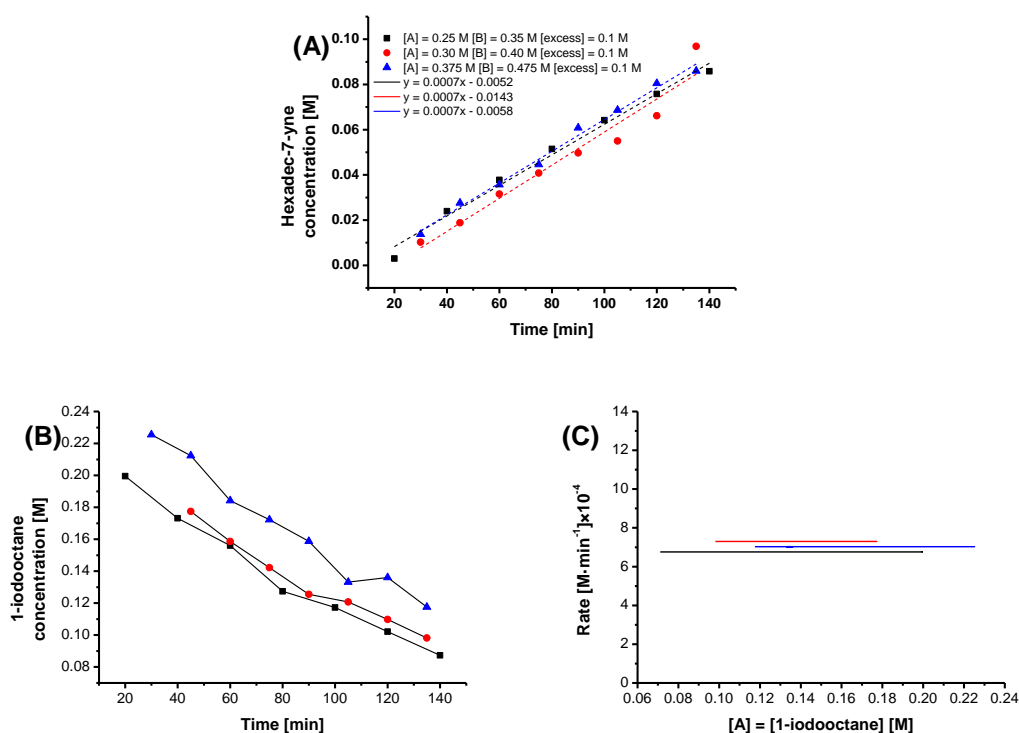
Figure 7. (A) Time-dependent yields of coupling runs under same excess conditions; the concentrations of reagents are noted and the rates are calculated from the reaction profile. (B) Kinetic profiles of 1-iodooctane during three coupling reactions under same excess. (C) Representation of the rate of the reactions vs. substrate concentration.
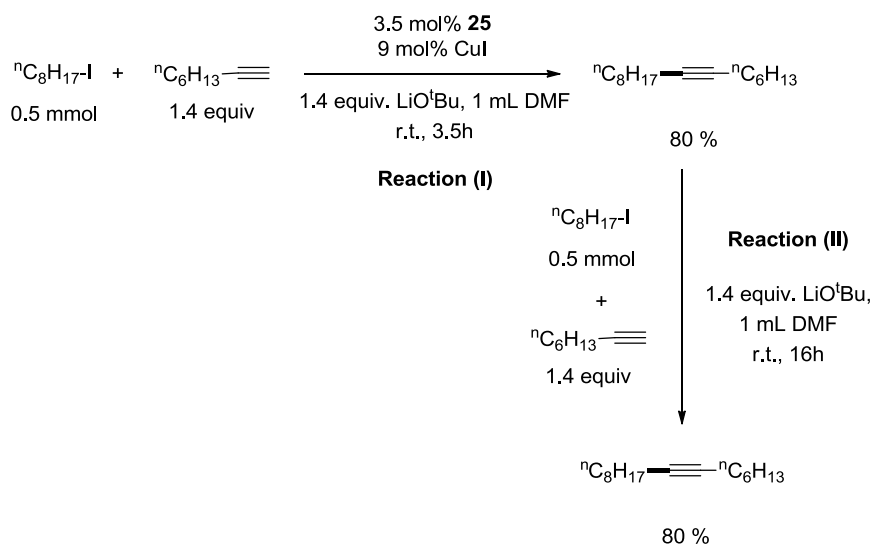
Scheme 1. Recycling experiment for catalyst **25**.

5.5 Turnover determining step

The kinetic studies show that the catalysis is 0th order in CuI, LiO^{t}Bu, alkyl halide, and alkyne and 1st order in catalyst. One possible explanation is that reductive elimination is the turnover determining step. If this is true, the reaction rate should be influenced by the electronic properties of substrates.[22] Thus, the reaction rates of the coupling of 1-iodooctane with substituted phenylacetylenes were measured. These rates are compared with the rate of the coupling of 1-iodooctane with oct-1-yne (Figure 8). The rates of the coupling of oct-1-yne, phenylacetylene, and 4-ethynylanisol are similar despite difference in the electronics. With electron-withdrawing CF$_3$ and F groups, the rates decrease. These results suggest reductive elimination is unlikely the turnover determining step because reductive elimination would favor more electron-poor substrates.
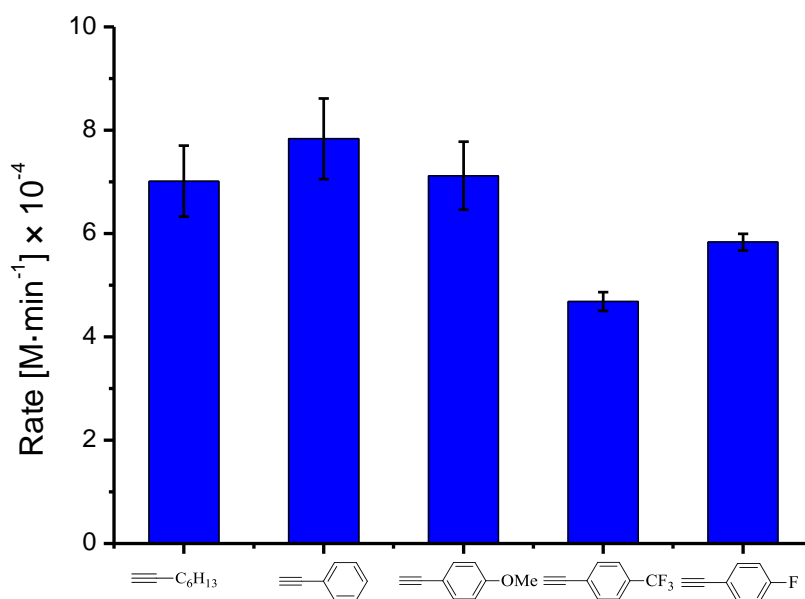
Figure 8. Comparison of coupling rates when different alkynes are used as coupling partners; the rates were averaged over three independent measurements. The error bar represents the standard deviation of the results from independent measurements.

A possible turnover determining step that does not involve either substrate or Cu is an intramolecular rearrangement of the catalyst. Judging from the ligands of complex **6**, we suspected that exchange of the flexible ethylenylamine nitrogen by another ligand from the Ni center was likely during catalysis. The dissociation of the nitrogen will create an open

coordination site necessary for the coupling reaction. If the dissociation is the slowest step, then the catalysis would only depend on Ni, but not any other reagent. The different catalytic efficiency of complexes **1**, **2**, and **25** provides circumstantial evidence for this hypothesis. Complex **3** has a more rigid pincer ligand, so dissociation of an amine donor would be more difficult especially at room temperature. Complex **3** has a more labile lutidine ligand and its dissociation is more facile. However, the favorable ligand dissociation also makes the complex unstable. Complex **25** has the best catalytic activity which might be a result of having a stable "pincer" form and a hemilabile amine ligand. To further support this hypothesis, the coupling reaction of 1-iodooctane and oct-1-yne was conducted in the presence of 30 mol% coordinating ligands. Figure 9 shows that the rates of the coupling were decreased in the presence of these ligands. Among pyridine derivatives, the least bulky ligand pyridine slowed down most the reaction. The less bulky 2,4-lutidine slowed down less, and the most bulky 2,6-lutidine slowed down the least. This result is consistent with the inhibition of catalytically active, amine-decoordinated nickel species by the exogenous ligands. The coupling was also slowed down in the presence of internal alkynes such as hexadec-7-yne and 4-octyne, which suggests that product inhibition might occur to some degree. However, product inhibition has little effect on the kinetic data which were collected at the early or middle stage of catalysis.
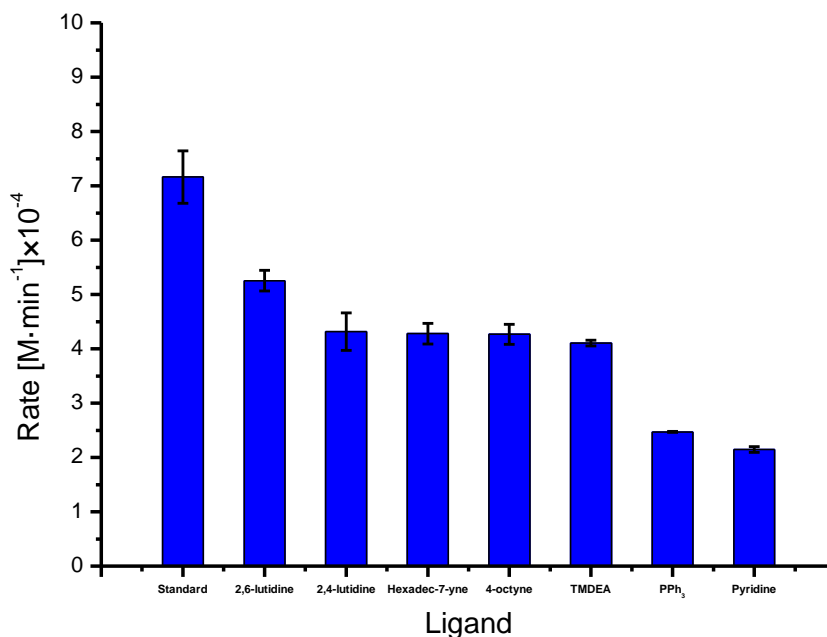
Figure 9. Comparison of coupling rates in the presence of different exogenous ligands. The rates were averaged over three independent measurements. The error bar represents the standard deviation of the results from independent measurements.

5.6 Active species for alkylation

Literature suggests that organometallic Ni complexes are responsible for the oxidative addition of alkyl halides in a large number of Ni-catalyzed cross coupling reactions of alkyl halides.[12,15,20,23-28] For the reactions described here, a ligated Ni-alkynyl species might be proposed as the active intermediate. To take advantage of the well-defined nature of catalyst **6**, we attempted to identify and isolate such an intermediate.

When complex **6** was treated with equal amounts of CuI, LiOBu[t], and phenylacetylene in DMF at room temperature, a NNN-Ni-phenylacetylide complex **26** was formed as the only detectable metal-containing product (Figure 10, ^{1}H NMR blue spectrum), with an isolated yield of 60%. Complex **26** was independently synthesized by treating complex **25** with phenylethynylmagnesium bromide (Figure 10, ^{1}H NMR red spectrum). The structure of **26** was determined by X-ray crystallography (Figure 11). The replacement of Cl with phenylacetylide leads to no significant change in the structural parameters of the Ni-NNN fragment (compare Figures 3 and 11). The Ni-N2 bond distance is identical in complexes **25** and **26**. This is surprising considering the different trans-influence property of Cl and acetylide. A possible explanation is that the Ni-N2 distance is dictated by the structure of the

pincer ligands. The overall structure of **26** is also similar to that of an analogous nickel pincer alkynyl complex.[12]
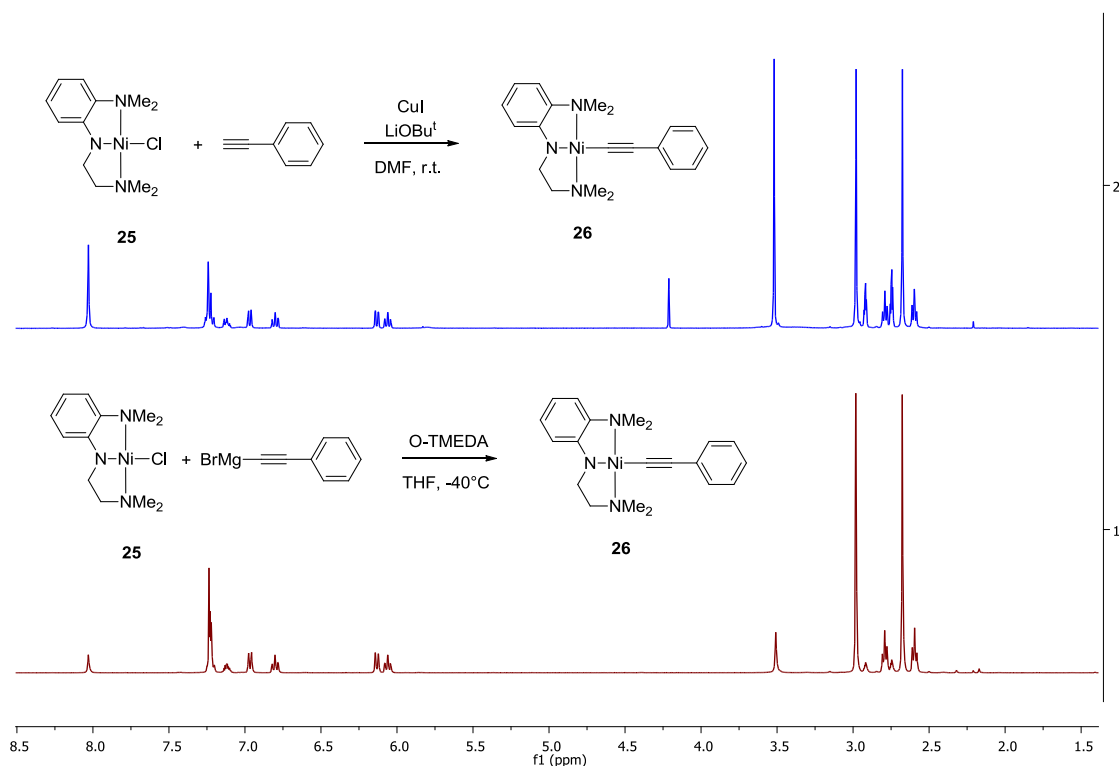
Figure 10. Synthetic methodologies for the Ni-acetylide complex **26** and their corresponding ^{1}H NMR spectrum. *Upper blue spectrum:* synthesis of complex **26** using Sonogashira type conditions. *Lower red spectrum:* synthesis of complex **26** using an alkynyl Grignard reagent.
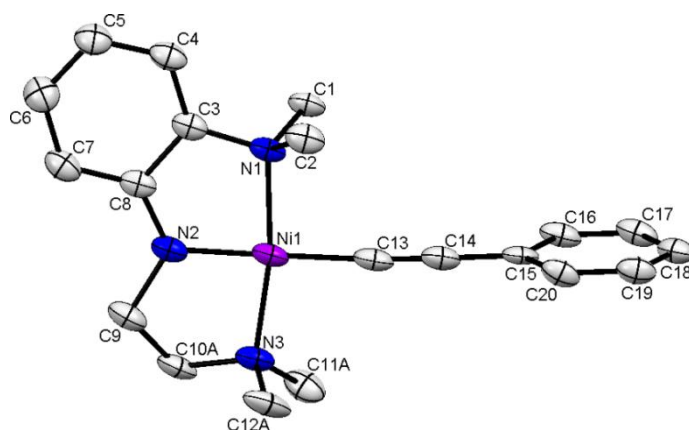
Figure 11. Crystal structure of complex **26**. Hydrogen atoms are omitted for clarity. The thermal ellipsoids are displayed in a 50% probability. Selected lengths (Å) and angles (deg): Ni1-N1, 1.965(3); Ni1-N2, 1.832(3); Ni2-N3, 1.958(3); Ni1-Cl3, 1.876(5); C13-C14, 1.219(6); N1-Ni1-N2, 85.39(13); N2-Ni1-N3, 85.13(14); N3-Ni1-N1, 170.52(14); N2-Ni1-C13, 179.22(14); Ni-C13-C14, 175.8(3).

Complex **26** had the same efficiency as complex **25** for the coupling of 1-iodooctane with phenylacetylene (Scheme 2). Furthermore, the reaction profiles of the coupling using **26** or **25** as catalyst are identical (Figure 12).
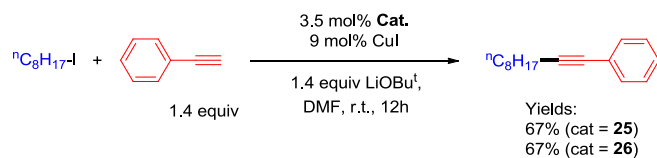
Scheme 2. Comparison of catalytic efficiency of complexes **25** and **26**.
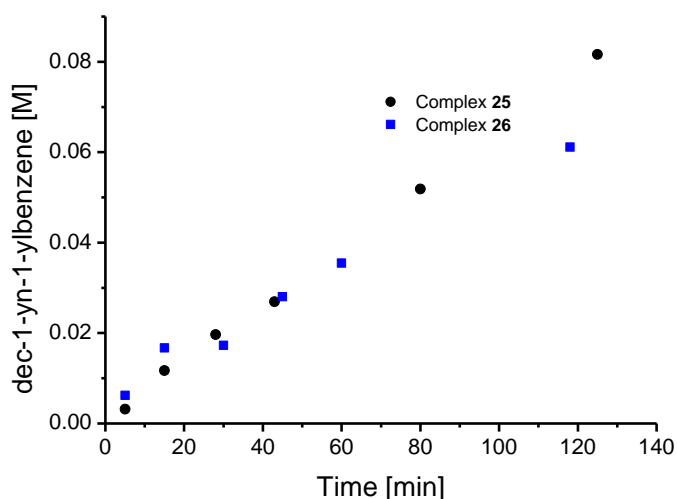
Figure 12. Comparison of ^{1}H NMR time-dependent yields of coupling using complex **25** or complex **26** as catalyst.

The reactivity of **26** towards alkyl iodide was probed. Under catalytically relevant conditions (room temperature in DMF), **26** reacted with 1-iodooctane to give the coupling product, 1-decyn-1-ylbenzene. However, after 6 h, the yield was only 15%, much lower than that of catalysis (eq. 2, Scheme 3). When 9 mol% CuI was added to this reaction, the yield was again only 10% (eq. 3, Scheme 3). However, if this reaction was carried out in the presence of 1 equivalent of phenylacetylene and 9 mol% of CuI, then after 6 h, the coupling yield was 76% which was similar to that of catalysis (eq. 4, Scheme 3). When eq. 4 was conducted without LiOBu^t or phenylacetylene, no product was formed. When it was conducted without CuI, a reduced yield of 43% was obtained. These results suggested that complex **26** need to be activated by an acetylide species to form a Ni bis(acetylide) complex which was the species

that reacted with alkyl halide in the catalysis. Cu-acetylide was more efficient than Li-acetylide for the formation of the bis(acetylide) complex. When 1 equivalent of 1-iodooctane, **26**, and oct-1-yne was mixed together with 9 mol% of CuI and 1.4 equivalent of LiOBu^t, both 1-decyn-1-ylbenzene and hexadec-7-yn were formed in similar yields, with an overall coupling yield of 60% (eq. 5, Scheme 3). This result showed that the acetylide fragments from complex **7** and oct-1-yne could be coupled in a similar probability.

To verify whether the phenylacetylide ligand in complex **26** could be exchanged by a different acetylide ligand ligated on Cu under catalytically relevant conditions, **26** was reacted with 1 equivalent of oct-1-yne in the presence of 1 equivalent of CuI and LiOBu^t. A new nickel complex (**27**) was formed and it was present in a roughly 1:1 ratio to complex **26** in the reaction mixture (eq. 6, Scheme 3, Figure 13 – ^{1}H NMR black spectrum). Complex **27** was also tentatively synthesized in solution and could be assigned to the Ni octynyl complex (Figure 13, ^{1}H NMR red spectrum). This result indicates that the acetylide ligand on Ni is exchangeable during catalysis, which explains the outcome of eq. 5. The exchange reaction likely proceeds via the Ni bis(acetylide) intermediate. Altogether, the outcomes of reactions 2-6 provide indirect support to the formation of a Ni bis(acetylide) complex, possibly connected to a Cu(I) ion, as the active species for alkylation in the catalysis.
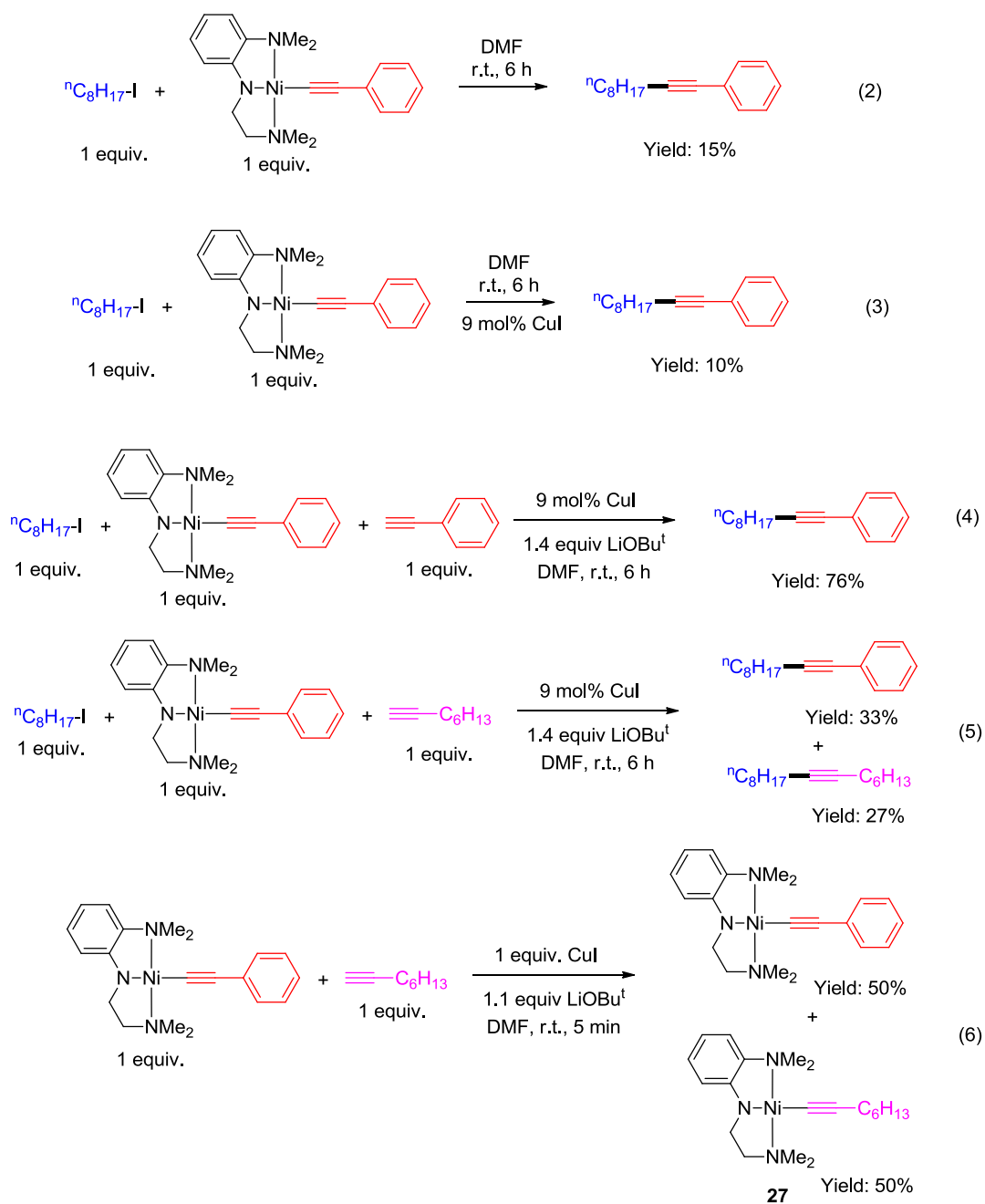
Scheme 3. Reactivity of Ni-alkynyl complex **26**.
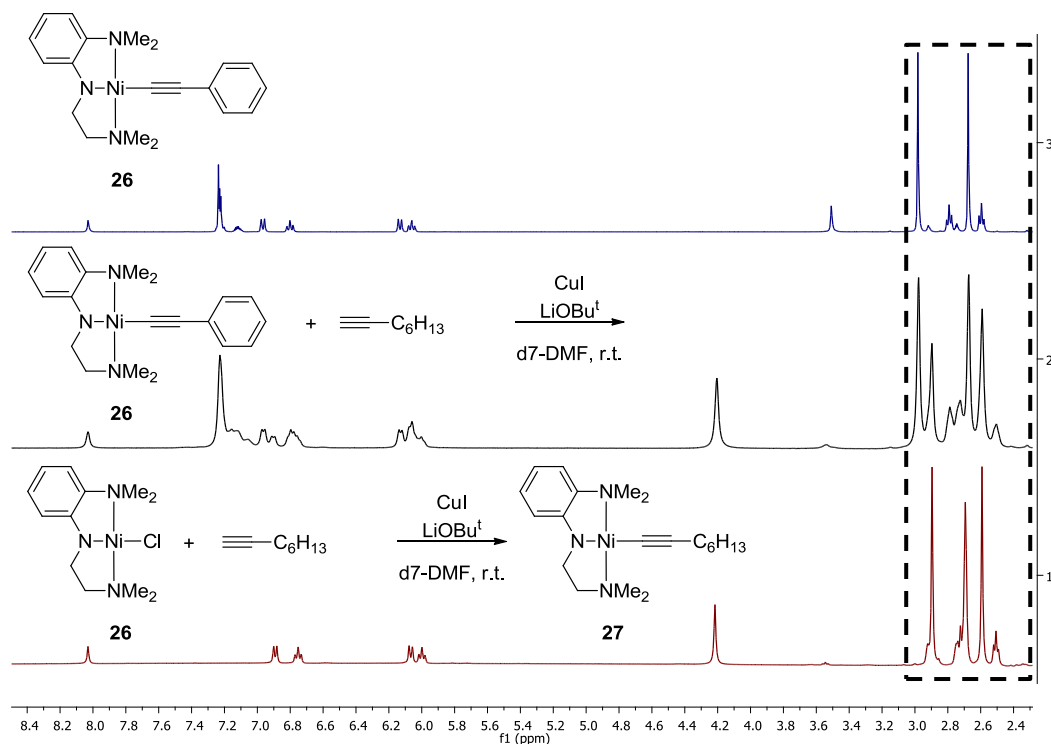
Figure 13. ^{1}H NMR study for alkyne exchange in nickel acetylde complexes. *Upper blue spectrum:* complex **26**. *Middle black spectrum:* Exchange reaction between phenylacetylene and oct-1-yne. *Lower red spectrum:* formation of a new acetylde nickel complex **27**. The amino methyl signals enclosed in a black dashed line clearly indicate an equal molar proportion of complexes **26** and **27**.

5.7 Tentative catalytic cycle

Based on the above results, a tentative catalytic cycle can be drawn (Fig. 14). Catalyst **25** is first transformed to the alkynyl complex **28**. A further alkynylation on **28** gives a Ni bis(alkynyl) complex **29** in which an alkynyl ligand is possibly coordinated to a Cu(I) ion as well. It is possible that the Cu-alkynyl moiety is coordinated to an amine donor of the pincer ligand rather than the Ni-center (not drawn). Recently Ni-Cu bimetallic alkynyl complexes in which Cu binds to the alkyne π-system were isolated as intermediates in Ni-catalyzed Sonogashira coupling of a vinyl iodide.[29] Complex **29** then undergoes a rate-determining decoordination of the labile amine donor to give a more active intermediate **30**. The Cu ion likely remains coordinated to one of the nitrogen donors of the pincer ligand because the reaction is 0th order on Cu. Reaction of **30** with alkyl halide then leads to the coupling product and regenerates complex **28**. As activation of alkyl halide and reductive elimination occur after the turnover determining step, the kinetic data do not provide information on these reactions. When the coupling was conducted in the presence of 1 equivalent of the radical inhibitor, TEMPO, the yield decreased to 5%, suggesting the involvement of radical

intermediates. A similar effect of TEMPO was observed in cross coupling reactions of alkyl halides catalyzed by complex **3**. Our recent studies show that for the latter reactions the activation of alkyl halides proceeds via an alkyl radical in a bimetallic oxidative addition mechanism.[26,27] Based on the similarity of catalysts and reactions, we propose that activation of alkyl halides in the current catalysis has an analogous radical mechanism.

The coupling reaction was monitored by NMR in an attempt to detect the resting state of the catalysis. Diamagnetic species **25**, **28**, and **30** were not detected, ruling them out as the resting states. The dominating Ni species is paramagnetic and due to interference of signals from other species present in the catalysis mixture, its identification by NMR is impossible. The formation of a paramagnetic resting state, on the other hand, is consistent with **29** being the resting state since this 5-coordinate species is expected to be paramagnetic.
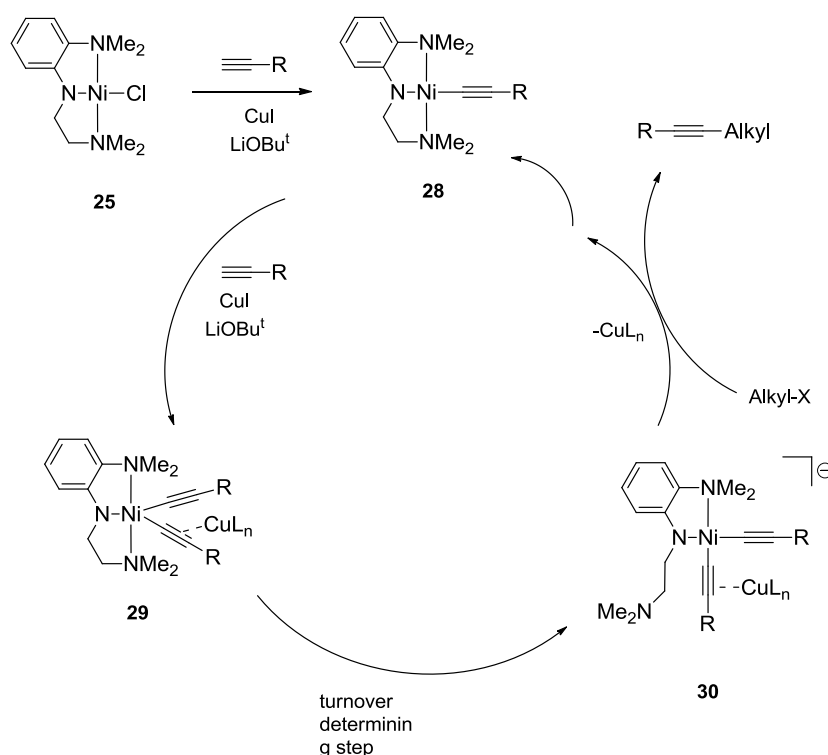
Figure 14. A simplified catalytic cycle highlighting the mechanistic information obtained from this study

5.8 Conclusion

A new Ni pincer complex has been developed for the direct alkylation of alkynes. This complex catalyzes the coupling of primary alkyl iodides and bromides with terminal alkynes at room temperature and with good scope and group tolerance. The mild reaction conditions and the well-defined nature of the catalyst have facilitated the first in-depth mechanistic study of this type of reaction. Kinetic measurements confirm the hemilabile nature of the new pincer ligand. The decoordination of an amine donor from a catalytic intermediate leads to the species that activates alkyl halides. Results of kinetics and inhibition studies are consistent with this decoordination step being the turnover determining step of the catalysis. A catalytic relevant Ni-alkynyl complex has been isolated and structurally characterized. This species is both chemically and kinetically competent for the catalytic process. The reactivity of this Ni-alkynyl species suggests an yet undetected Ni bis(alkynyl) species as the essential species to activate alkyl halide. The two alkynyl ligands in this species are exchangeable. The work provides significant mechanistic insights into the direct coupling of alkyl halides and alkynes which is an efficient and versatile method for the synthesis of alkyl-substituted alkynes.

5.9 Experimental Part

5.9.1 Chemicals and reagents

All manipulations were carried out under an inert $N_2(g)$ atmosphere using standard Schlenk or glovebox techniques. Solvents were purified using a two-column solid-state purification system (Innovative Technology, NJ, USA) and transferred to the glove box without exposure to air. Deuterated solvents were purchased from Cambridge Isotope Laboratories, Inc., and were degassed and stored over activated 3 Å molecular sieves. Unless otherwise noted, all other reagents and starting materials were purchased from commercial sources and used without further purification. Liquid compounds were degassed by standard freeze-pump-thaw procedures prior to use. The following chemicals were prepared according to literature procedure: 2-(pent-4-yn-1-yloxy)tetrahydro-2H-pyran[30] (Table 2, entry 5), 4-(hex-5-yn-1-yl)morpholine[12] (Table 1, entry 7), 2-(3-iodopropyl)furan[31] (Table 1, entry 8), 5-iodopentyl acetate[32] (Table 2, entry 9 and 10) and (4-(pent-4-yn-1-yloxy)phenyl)(phenyl)methanone[33] (Table 1, entry 11).

5.9.2 Physical methods

The ^{1}H and ^{13}C NMR spectra were recorded at 293 K on a Bruker Avance 400 spectrometer. ^{1}H NMR chemical shifts were referenced to residual solvent as determined relative to Me$_4$Si (δ = 0 ppm). The ^{13}C{^{1}H} chemical shifts were reported in ppm relative to the carbon resonance of CDCl$_3$ (77.0 ppm). GC-MS measurements were conducted on a Perkin-Elmer Clarus 600 GC equipped with Clarus 600T MS. HRESI-MS measurements were conducted at the EPFL ISIC Mass Spectrometry Service with a Micro Mass QTOF Ultima spectrometer.

5.9.3 Synthesis of complex 25

- *Synthesis of 2-(2-(dimethylamino)ethyl)-N,N-dimethylaniline (Me₂NNEtNMe₂)*
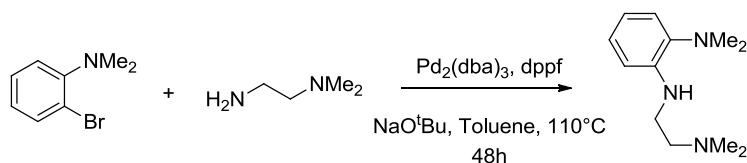
A 250 mL reaction vessel was charged with Pd$_2$(dba)$_3$ (0.68 g, 0.74 mmol), bis(diphenylphosphino)-ferrocene (DPPF) (0.82 g, 1.48 mmol), NaO^{t}Bu (4.70 g, 49.1 mmol) and toluene (50 mL) under a dinitrogen atmosphere. 2-Bromo-N,N-dimethylaniline (7.3 g, 36.4 mmol) and 2-(dimethylamino)ethylamine (6.42 g, 36.4 mmol) were added to the reaction mixture. The resulting brown solution was vigorously stirred for 2 days at 100 °C. The solution was then cooled to room temperature and filtered through Celite. Removal of the solvent yielded a black liquid which was then purified by flash chromatography (silica-gel, CHCl$_3$), and then was distilled under vacuum to afford the product as a light yellow oil. Yield: 5.10 g, 68%.

^{1}H NMR (400 MHz, CDCl$_3$): 6.98-7.04 (m, 2H), 6.68 (dt, *J* = 7.6, 1.2 Hz, 1H), 6.62 (d, *J* = 8.0 Hz, 1H), 4.95 (br. s, 1H), 3.21 (q, *J* = 6.4 Hz, 2H), 2.65 (s, 6H), 2.59 (t, *J* = 6.4 Hz, 2H), 2.28 (s, 6H).
^{13}C NMR (100 MHz, CDCl3): 143.1, 140.3, 124.5, 118.8, 116.3, 109.8, 58.6, 45.5, 43.8, 41.6.
HR-MS (ESI): calculated for (C$_{12}$H$_{21}$N$_3$, M+H), 208.1814; found, 208.1810.
Anal. Calcd for C$_{12}$H$_{21}$N$_3$: C , 69.52; H, 10.21; N, 20.27. Found: C, 69.73; H, 10.21; N, 20.09.

- *Synthesis of **25***

25
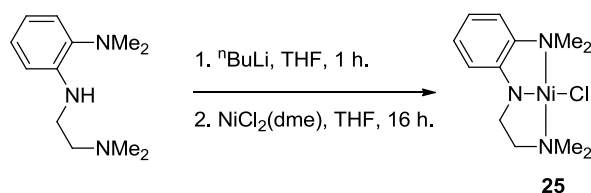
^{n}BuLi (16.3 mmol, 1.6 M in hexane) was slowly added to a THF solution (50 mL) of ligand Me$_2$NNEtNMe$_2$ (3.08 g, 14.85 mmol) at -10°C. The reaction mixture was stirred for 15 min, and for 1 h at room temperature. This solution was then added into a solution of NiCl$_2$(dme) (3.26 g, 14.85 mmol, dme = dimethoxyethane) in THF (50 mL). The resulting solution was stirred overnight and then evaporated in vacuum. The residue was extracted with CH$_2$Cl$_2$ (100 mL), and then was concentrated to ca. 5 mL. Addition of pentane (100 mL) afforded a brown precipitate, which was filtered, washed with additional pentane, and vacuum dried. Yield: 2.67 g (60%). Diffusion of pentane into a dichloromethane solution of **25** afforded brown crystals suitable for X-ray analysis.

^{1}H NMR (400 MHz, CDCl$_3$): 6.86 (dt, *J* = 7.8, 1.2 Hz, 1H), 6.78 (dd, *J* = 8.0, 0.8 Hz, 1H), 6.15-6.25 (m, 2H), 2.80 (s, 6H), 2.62 (t, *J* = 6.0 Hz, 2H), 2.50 (s, 6H). 2.37 (t, *J* = 6.0 Hz, 2H). **^{13}C NMR** (100 MHz, CDCl$_3$): 153.6, 144.2, 128.4, 119.3, 111.6, 109.5, 66.8, 50.6, 49.1, 44.1. **Anal. Calcd for C$_{12}$H$_{20}$ClN$_3$Ni :** C, 47.97; H, 6.71; N, 13.99 Found: C, 47.93; H, 6.82; N, 14.15.

5.9.4 Crystallographic data

- *Crystallographic details for complex **25***

A total of 28544 reflections ($-19 \leq h \leq 18$, $-9 \leq k \leq 11$, $-21 \leq l \leq 20$) were collected at T = 100(2) K of which 4625 were unique (Rint = 0.0771); Mo$_{K\alpha}$ radiation (λ= 0.71073 Å). The structure was solved by the direct methods. All non-hydrogen atoms were refined anisotropically, and hydrogen atoms were placed in calculated idealized positions. The residual peak and hole electron densities were 0.417 and –0.349 eA^{-3}, respectively. The absorption coefficient was 1.596 mm^{-1}. The least squares refinement converged normally with residuals of R(F) = 0.0367, wR(F2) = 0.0595 and a GOF = 1.077 (I>2σ(I)). C$_{12}$H$_{20}$ClN$_3$Ni, Mw = 300.47, space group P$_{ca}$2$_1$, Orthorhombic, a = 16.1973(14), b = 9.2551(7), c = 18.251(2) Å, α = 90°, β = 90°, γ = 90°, V = 2736.0(4) Å^3, Z = 8, ρ_{calcd} = 1.459 Mg/m^3

- *Crystallographic details for complex 26*

A total of 19221 reflections (-12 < h < 12, -19 < k < 18, -16 < l < 16) were collected at T = 100(2) K of which 4143 were unique (Rint = 0.0536); $Mo_{K\alpha}$ radiation (λ= 0.71073 Å). The structure was solved by the direct methods. All non-hydrogen atoms were refined anisotropically, and hydrogen atoms were placed in calculated idealized positions. The residual peak and hole electron densities were 0.462 and –0.651 eA^{-3}, respectively. The absorption coefficient was 1.075 mm^{-1}. The least squares refinement converged normally with residuals of R(F) = 0.0566, wR(F2) = 0.1115 and a GOF = 1.267 (I>2σ(I)). $C_{20}H_{25}N_3Ni$, Mw = 366.14, space group $P2_1/n$, Monoclinic, a = 9.7694(8), b = 14.6639(17), c = 12.8939(12) Å, α = 90°, β = 100.806(7)°, γ = 90°, V = 1814.4(3) $Å^3$, Z = 4, ρ_{calcd} = 1.340 Mg/m^3

5.9.5 Optimization of the catalysis

- *General procedure for the catalysis:*

5 mg of complex **25** (0.016 mmol, 3.5 mol %), 9 mg of CuI (0.047 mmol, 9 mol %), 56 mg of $LiOBu^t$ (0.7 mmol), 0.5 mmol of alkyl halide and 0.7 mmol of alkyne were placed in a vial and 2 mL (1 mL) of DMF were added. The reaction was stirred at room temperature during 16 hours. The reaction was quenched with 10 mL of water and extracted three times with 15 mL of ether each time. The organic phase was dried over anhydrous Na_2SO_4, filtered and the solvent was evaporated. The residue was purified by flash chromatography on silica-gel.

Table 4. Additional entries for the optimization of coupling conditions between 1-iodooctane and oct-1-yne.

Entry	Cu salt (9 mol %)	Base (1.4 equiv)	Solvent	Catalyst	Temperature [°C]	Yield[a] [%]
1	CuI	LiO^tBu	Dioxane	1	40	Traces
2	CuI	LiO^tBu	DMF	1	40	23
3	CuI	Cs_2CO_3	DMF	1	20	29
4	CuI	Et_3N	DMF	25	20	Traces
5	CuCl	LiO^tBu	DMF	25	20	11
6	CuI	LiO^tBu	THF	25	20	Traces
7	CuI	K_3PO_4	DMF	25	20	22
8	CuI	$LiOPr^i$	DMF	25	20	24

9	CuI	LiOPr^i	DMF	25	20	24
10	CuI	NaOBu^t	DMF	25	20	traces
11	CuI	KOPr^i	DMF	25	20	traces
12	CuI	LiOH	DMF	25	20	8

^{a} General reaction conditions: 0.5 mmol of 1-iodooctane and other reagent specified in Table 4 in 2 mL of solvent. ^{b} Yields are determined by GC and are relative to the alkyl halide.

5.9.6 Study of side reactions

1-tert-butoxyoctane was identified as a side-product by GC-MS analysis of the standard reaction. To understand its formation, the reaction of 1-iodooctane in the absence of an alkyne substrate was studied under relevant catalytic conditions (*vide supra*). Figure 15 shows the mass distribution of the substrates and the identified products involved in this reaction.

$$^nC_8H_{17}\text{-I} \quad + \quad 1.4 \text{ equiv LiOBu}^t \quad \xrightarrow[\text{DMF, r.t., 3 h}]{\text{conditions}} \quad ^nC_8H_{17}\text{—OBu}^t$$

Entry	CuI (mol %)	Complex 25 (mol %)	Yield 1-tert-butoxyoctane [%]
1	9	3.5	39
2	0	3.5	6
3	9	0	35
4	0	0	7

^{a} Yields were calculated by GC and are relative to 1-iodooctane
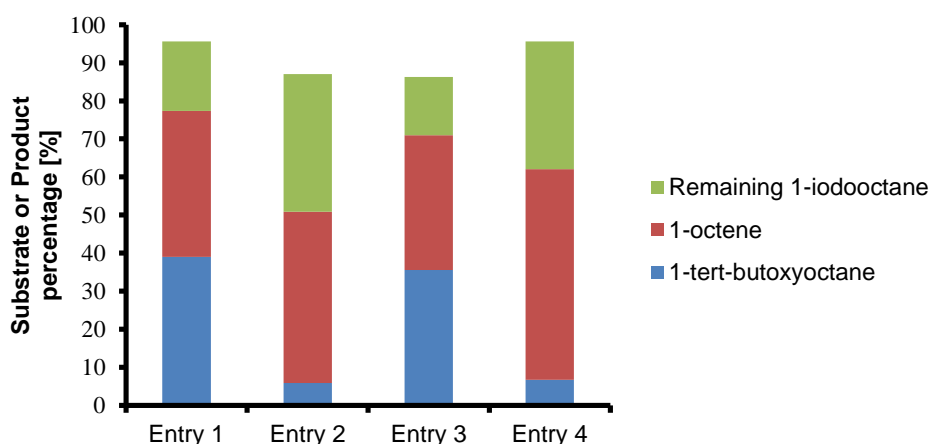
Figure 15. Species distribution of the reaction of 1-iodooctane under catalytic conditions in the absence of alkyne.

The reaction was stopped after three hours. In the presence of 9 mol% CuI and 3.5 mol% catalyst **25**, 1-tert-butoxyoctane was formed in a 39% yield. In the presence of 3.5 mol% **6** only, the yield was 6%. In the presence of 9 mol% CuI only, the yield was 35%. If neither CuI nor **25** was present, the yield was 7%. These results indicated that the reaction of 1-iodooctane with tert-butoxide to form 1-tert-butoxyoctane occurred without a catalyst, but this reaction was accelerated by CuI. The nickel catalyst **6** had little influence in the reaction. Another identified side-product was the 1-octene, which is likely formed by elimination process. The yields were all around 40% for the 4 entries. This product is likely formed by reaction of *tert*-butoxide with primary halides in an elimination process.

5.9.7 Total Kinetic profiles

- *General sampling procedure*

All the kinetic studies were set up under N_2 atmosphere. 2 mL of DMF as solvent and 60 μL (0.31 mmol) of decane as internal standard were used for all experiments. At every sampling time, an aliquot of 15 μL of the reaction mixture was taken and quenched in 1.5 mL of acetonitrile placed in a GC vial for further analysis.

- *Reaction profile for the coupling of 1-iodooctane with oct-1-yne (Figure 4)*

5 mg of complex **25** (0.016 mmol, 3.5 mol %), 9 mg of CuI (0.047 mmol, 9 mol %), 56 mg of LiOBu^t (0.7 mmol), 90 μL of 1-iodooctane (0.5 mmol) and 60 μL of decane (0.31 mmol) were placed in a vial and 2 mL of DMF were added. 100 μL of oct-1-yne (0.7 mmol) were added under magnetic stirring to the reaction mixture to start the coupling process. A reaction aliquot was then taken every 20 minutes during a period of 3 hours.

- *Reaction profile for the coupling process of 1-iodooctane with 1-phenylacetylene (Figure 5, GC yield)*

5 mg of complex **25** (0.016 mmol, 3.5 mol %), 9 mg of CuI (0.047 mmol, 9 mol %), 56 mg of LiOBu^t (0.7 mmol), 90 μL of 1-iodooctane (0.5 mmol) and 60 μL of decane (0.31 mmol) were placed in a vial and 2 mL of DMF were added. 75 μL of 1-phenylacetylene (0.7 mmol) were added under magnetic stirring to the reaction mixture to start the coupling process. A reaction aliquot was then taken every 5 minutes during a period of 1 hour.

- *Reaction profile for the coupling process of 1-iodooctane with 1-phenylacetylene (Figure 5, ^{1}H NMR yield)*

The experimental conditions were the same as described in the previous paragraph, but DMF was replaced by d7-DMF. The reaction mixture was placed in a NMR tube and a ^{1}H NMR spectrum was recorded at different times. Figure 16 shows the time-dependent NMR spectra of this process.
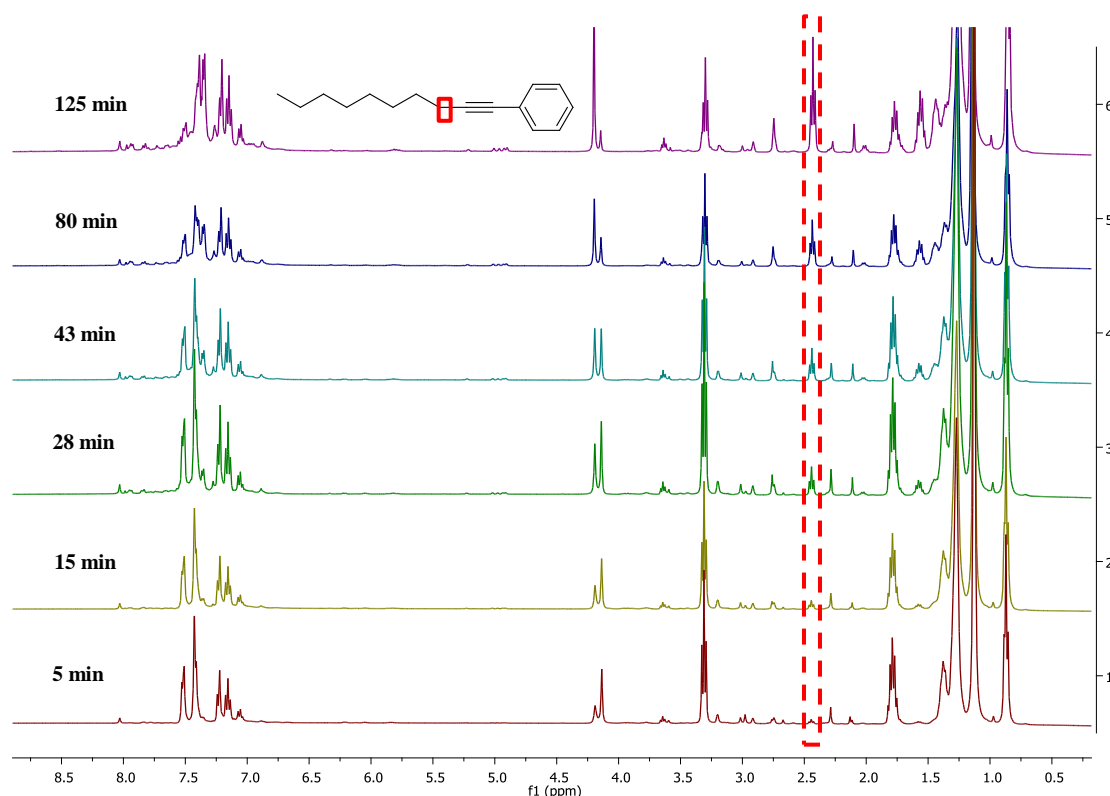
Figure 16. Time-dependent ^{1}H NMR spectra for the coupling of 1-iodooctane with 1-phenylacetylene. The signals of the methylene protons besides de triple bond are enclosed in a red dashed line.

5.9.8 Initial Rate analysis

The partial rate order of each one of the reaction's components was determined by the initial rate method. The data of the concentration of product vs. time plot was fitted linear with Excel. The obtained slope of the linear fitting represents the reaction rate. The order of the rate was then determined by the analysis of the plotting of the reaction rate vs. the initial concentration.

- *Rate order determination for the 1-iodooctane (Figure 6A)*

To determine the order of the reaction on 1-iodooctane, the initial kinetic profiles at different initial concentrations were recorded. The final data was obtained by averaging the results of three independent trials for each experiment.

Experiment	x µL of 1-iodooctane	Initial concentration [M]
1	90	0.25
2	110	0.30
3	130	0.36
4	150	0.42
5	200	0.55
6	300	0.83

Typical procedure: 5 mg of complex **25** (0.016 mmol, 3.5 mol %), 9 mg of CuI (0.047 mmol, 9 mol %), 56 mg of LiOBu^t (0.7 mmol), a specific quantity of 1-iodooctane according to the above table and 60 µL of decane (0.31 mmol) were placed in a vial and 2 mL of DMF were added. 100 µL of oct-1-yne (0.7 mmol) was added under magnetic stirring to the reaction mixture to start the coupling process. A reaction aliquot was then taken every five minutes during a period of one hour.

- *Rate order determination for the oct-1-yne (Figure 6B)*

To determine the order of the reaction on oct-1-yne, the initial kinetic profiles at different initial concentrations were recorded. The final data was obtained by averaging the results of three independent trials for each experiment.

Experiment	x µL of oct-1-yne	Initial concentration [M]
1	100	0.34
2	120	0.40
3	140	0.47
4	160	0.54

Typical procedure: 5 mg of complex **25** (0.016 mmol, 3.5 mol %), 9 mg of CuI (0.047 mmol, 9 mol %), 56 mg of LiOBu^t (0.7 mmol), 90 µL of 1-iodooctane (0.5 mmol) and 60 µL of decane (0.31 mmol) were placed in a vial and 2 mL of DMF were added. A specific quantity of oct-1-yne according to the above table was added under magnetic stirring to the reaction mixture to start the coupling process. A reaction aliquot was then taken every five minutes during a period of one hour.

- *Rate order determination for the CuI (Figure 6C)*

To determine the order of the reaction on copper iodide, the initial kinetic profiles at different initial concentrations were recorded. The final data was obtained by averaging the results of three independent trials for each experiment.

Experiment	x mg of CuI	Initial concentration [M]
1	4	0.011
2	9	0.0236
3	12	0.0315
4	16	0.042

Typical procedure: 5 mg of complex **25** (0.016 mmol, 3.5 mol %), a specific amount of of CuI according to the above table, 56 mg of LiO^{t}Bu (0.7 mmol), 90 µL of 1-iodooctane (0.5 mmol) and 60 µL of decane (0.31 mmol) were placed in a vial and 2 mL of DMF were added. 100 µL of oct-1-yne (0.7 mmol) were added under magnetic stirring to the reaction mixture to start the coupling process. A reaction aliquot was then taken every five minutes during a period of one hour.

- *Rate order determination for the catalyst **25** (Figure 6D)*

To determine the order of the reaction on catalyst **25**, the initial kinetic profile at different initial concentration were recorded. To assure the reproducibility of the data a standard solution of catalyst **25** in DMF was prepared (5 mg/200 µL). The final data was obtained by averaging the results of three independent trials for each experiment.

Experiment	x µL catalyst 25 standard solution	y µL of DMF	Initial concentration [M]
1	200	1800	0.0083
2	300	1700	0.0125
3	400	1600	0.0166
4	500	1500	0.0208

Typical procedure: 9 mg of CuI (0.047 mmol, 9 mol %), 56 mg of LiOBu^t (0.7 mmol), 90 µL of 1-iodooctane (0.5 mmol), 60 µL of decane (0.31 mmol) and certain amount of catalyst **25** (see table above) were placed in a vial and certain amount of DMF were added (see table above). 100 µL of oct-1-yne (0.7 mmol) were added under magnetic stirring to the reaction mixture to start the coupling process. A reaction aliquot was then taken every five minutes during a period of one hour.
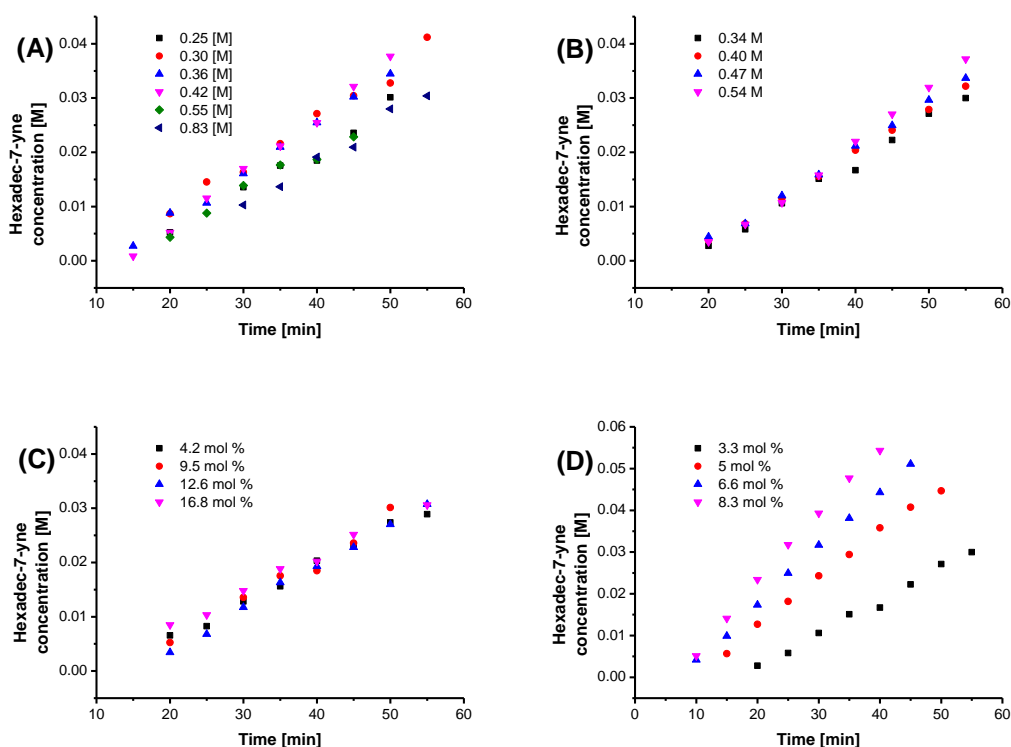
Figure 17 shows the time depending yields of all the above described experiments.

Figure 17: Time depending yields of coupling at different initial concentrations of : (A) 1-iodooctane, (B) oct-1-yne, (C) CuI and (D) Catalyst **25**.

- *Rate order influence of LiO^{t}Bu*

The influence of the loading of LiO^{t}Bu (1, 1.4 and 2 equiv.) on the rate of catalysis was studied under the general conditions of the catalysis: 5 mg of complex **25** (0.016 mmol, 3.5 mol %), 9 mg of CuI (0.047 mmol, 9 mol %), a certain amount of LiO^{t}Bu, 90 µL of 1-iodooctane (0.5 mmol) and 60 µL of decane (0.31 mmol) were placed in a vial and 2 mL of DMF were added. 100 µL of oct-1-yne (0.7 mmol) was added under magnetic stirring to the reaction mixture to start the coupling process. A reaction aliquot was then taken at defined times. Figure 18 shows the comparison of the reaction profile at three different LiO^{t}Bu loadings. The results suggest that the reaction rate is independent of the loading.
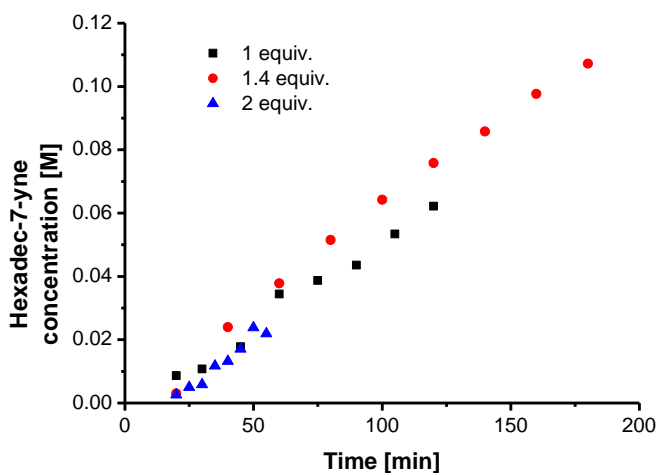
Figure 18. Comparison of kinetic profiles under different LiO^{t}Bu loadings.

5.9.9 Catalyst deactivation study

- *Reaction progress analysis, same excess experiments (Figure 7)*

In order to determine if the catalyst is deactivated along the reaction, the Reaction Progress Analysis at same excess conditions between the 1-iodooctane and the oct-1-yne was performed. The experiments were set-up under optimized catalytic conditions and the reaction profiles were measured applying the general methodology. The similar rates obtained for the experiments suggest that the active catalyst concentration remains unchanged during the coupling process.

- *Catalyst recycling experiment (Scheme 1)*

Reaction I: 5 mg of complex **25** (0.016 mmol, 3.5 mol %), 9 mg of CuI (0.047 mmol, 9 mol %), 56 mg of LiO^{t}Bu (0.7 mmol), 90 µL of 1-iodooctane (0.5 mmol), 100 µL of oct-1-yne and 60 µL of decane (0.31 mmol) were placed in a vial and 1 mL of DMF were added. The reaction was stirred at room temperature during 3.5 hours. A sample of 15 µL was taken from the reaction mixture and quenched in 1.5 mL of acetonitrile, the yield was then determined by GC analysis. *Reaction II:* 56 mg of LiO^{t}Bu (0.7 mmol), 90 µL of 1-iodooctane (0.5 mmol) and 100 µL of oct-1-yne (0.7 mmol) were then directly added to the reaction mixture. The reaction was stirred at room temperature overnight. The yield of reaction was determined by GC analysis.

5.9.10 Turnover determining step

- *General sampling procedure:*

All the kinetic studies were set up under N_2 atmosphere. A volume of 2 mL of DMF as solvent and 60 µL (0.31 mmol) of decane as internal standard were used for all the experiments. At every sampling time, an aliquot of 15 µL of the reaction mixture was taken and quenched in 1.5 mL of acetonitrile placed in a GC vial for further analysis. The data of the concentration of product vs. time plot was fitted linear with Excel. The obtained slope of the linear fitting represents the reaction rate.

- *Reaction profile for the coupling of 1-iodooctane with phenylacetylene:*

5 mg of complex **25** (0.016 mmol, 3.5 mol %), 9 mg of CuI (0.047 mmol, 9 mol %), 56 mg of LiO^{t}Bu (0.7 mmol), 90 µL of 1-iodooctane (0.5 mmol) and 60 µL of decane (0.31 mmol) were placed in a vial and 2 mL of DMF were added. 75 µL of phenylacetylene (0.7 mmol) were added under magnetic stirring to the reaction mixture to start the coupling process. A reaction aliquot was then taken every 5 minutes during a period of 1 hour. The final data was obtained by averaging the results of three independent trials for each experiment.

- *Reaction profile for the coupling of 1-iodooctane with 4-ethynylanisole:*

5 mg of complex **25** (0.016 mmol, 3.5 mol %), 9 mg of CuI (0.047 mmol, 9 mol %), 56 mg of LiO^{t}Bu (0.7 mmol), 90 µL of 1-iodooctane (0.5 mmol) and 60 µL of decane (0.31 mmol) were placed in a vial and 2 mL of DMF were added. 90 µL of 4-ethynylanisole (0.7 mmol) was added under magnetic stirring to the reaction mixture to start the coupling process. A reaction aliquot was then taken every 20 minutes during a period of 2 hours. The final data was obtained by averaging the results of three independent trials for each experiment.

- *Reaction profile for the coupling of 1-iodooctane with 4-ethynyl-α,α,α-trifluorotoluene:*

5 mg of complex **25** (0.016 mmol, 3.5 mol %), 9 mg of CuI (0.047 mmol, 9 mol %), 56 mg of LiO^{t}Bu (0.7 mmol), 90 µL of 1-iodooctane (0.5 mmol) and 60 µL of decane (0.31 mmol) were placed in a vial and 2 mL of DMF were added. 114 µL of 4-ethynyl-α,α,α-trifluorotoluene (0.7 mmol) was added under magnetic stirring to the reaction mixture to start the coupling process. A reaction aliquot was then taken every 15 minutes during a period of 2 hours. The final data was obtained by averaging the results of three independent trials for each experiment.

- *Reaction profile for the coupling of 1-iodooctane with 4-fluorophenylacetylene:*

5 mg of complex **25** (0.016 mmol, 3.5 mol %), 9 mg of CuI (0.047 mmol, 9 mol %), 56 mg of LiOBu^t (0.7 mmol), 90 µL of 1-iodooctane (0.5 mmol) and 60 µL of decane (0.31 mmol) were placed in a vial and 2 mL of DMF were added. 80 µL of 4-fluorophenylacetylene (0.7 mmol) was added under magnetic stirring to the reaction mixture to start the coupling process. A reaction aliquot was then taken every 15 minutes during a period of 2 hours. The final data was obtained by averaging the results of three independent trials for each experiment.
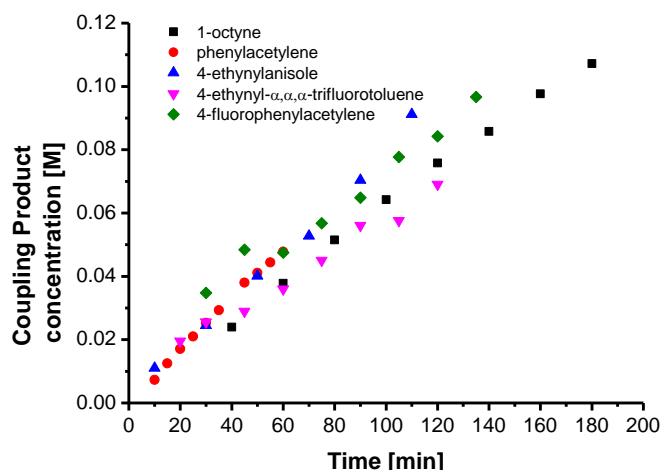
Figure 19 shows a comparison of time depending yields of coupling for different alkyne coupling partners.

Figure 19. Comparison of kinetic profiles when different alkynes are used as coupling partners.

- *Comparison of coupling rates in the presence of different exogenous ligands:*

5 mg of complex **25** (0.016 mmol, 3.5 mol %), 9 mg of CuI (0.047 mmol, 9 mol %), 56 mg of LiOBu^t (0.7 mmol), 90 µL of 1-iodooctane (0.5 mmol), 30 mol % of the exogenous ligand (Table 5) and 60 µL of decane (0.31 mmol) were placed in a vial and 2 mL of DMF were added. 100 µL of oct-1-yne (0.7 mmol) were added under magnetic stirring to the reaction mixture to start the coupling process. A reaction sample was then taken every 15-20 minutes during a period of 2 hours. Figure 20 shows a comparison of time depending yields of coupling in presence of different exogenous ligands.

Table 5. Mass or volumes quantities of exogenous ligand required for each experiment

Experiment[a]	Ligand	Quantity
1	TMDEA	24 μL
2	2,4-lutidine	18 μL
3	PPh$_3$	39 mg
4	Pyridine	14 μL
5	2,6-lutidine	18 μL
6	Hexadec-7-yne	33 mg
7	4-octyne	22 μL

[a] Each experiment was independently measured three times.
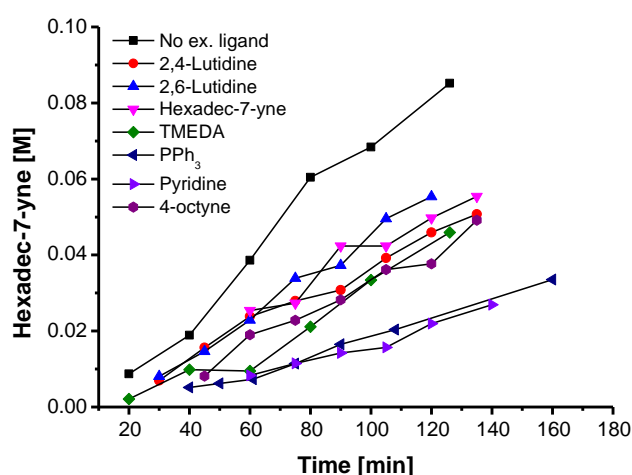
Figure 20. Comparison of kinetic profiles in the presence of different exogenous ligands.

5.9.11 Active species for alkynylation

- *Synthesis of intermediate 26 using Sonogashira coupling conditions*

225 mg of complex **25** (0.75 mmol), 142 mg of CuI (0.75 mmol), 76 mg of phenylacetylene (0.75 mmol) and 60 mg of LiOBu^t (0.75 mmol) were placed in a vial and 6 mL of DMF were added. The resulting solution was stirred during 16 hours. After evaporation of the solvent, the solid residue was dissolved in toluene and filtered through PTFE syringe filters. Then toluene was evaporated and the crude product was washed several times with pentane to give the desired product as a dark blue solid. Yield: 164 mg (60 %).

^{1}H NMR (400MHz, d7-DMF): 7.27 − 7.19 (m, 4H), 7.15 − 7.08 (m, 1H), 6.95 (dd, J = 8.0, 0.8 Hz, 1H), 6.80 (dt, J = 6.8, 1.2 Hz, 1H), 6.13 (dd, J = 7.6, 0.8 Hz, 1H), 6.06 (dt, J = 7.6, 0.8 Hz, 1H), 2.98 (s, 6H), 2.79 (t, J = 6.0 Hz, 2H), 2.68 (s, 6H), 2.60 (t, J = 6.0 Hz, 2H).

- *Synthesis of intermediate 26 using a Grignard reagent:*

Ph-C≡C-MgBr (1.07 mL, 0.7 M solution in THF, 0.75 mmol) was added dropwise to a THF (4 mL) solution of **25** (225 mg, 0.75 mmol) and O-TMEDA (170 µL, 0.89 mmol) at -40°C under N_2 atmosphere. The reaction mixture was slowly warmed up to room temperature. After evaporation of the solvent, the solid residue was dissolved in toluene and filtered through PTFE syringe filters. Then toluene was evaporated and the crude product was washed several times with pentane to give the desired product as a brown solid. Yield: 190 mg (70 %). Dark blue crystals suitable for X-ray diffraction analysis were obtained by slow diffusion of pentane into a concentrated toluene solution of **26**.

¹H NMR (400MHz, d7-DMF): 7.27 – 7.19 (m, 4H), 7.15 – 7.08 (m, 1H), 6.95 (dd, J = 8.0, 0.8 Hz, 1H), 6.80 (dt, J = 6.8, 1.2 Hz, 1H), 6.13 (dd, J = 7.6, 0.8 Hz, 1H), 6.06 (dt, J = 7.6, 0.8 Hz, 1H), 2.98 (s, 6H), 2.79 (t, J = 6.0 Hz, 2H), 2.68 (s, 6H), 2.60 (t, J = 6.0 Hz, 2H).
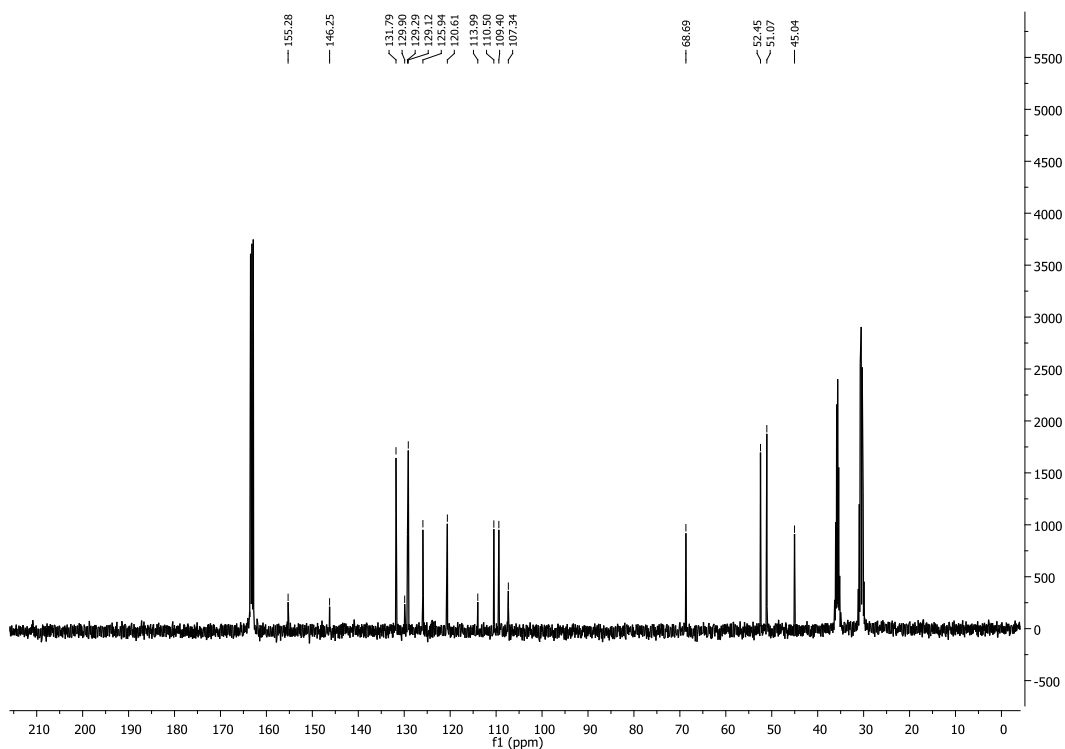**¹³C NMR** (100 MHz, d7-DMF): 155.28, 146.25, 131.79, 129.90, 129.29, 129.12, 125.94, 120.61, 113.99, 110.50, 109.40, 107.34, 68.69, 52.45, 51.07, 45.04
Elemental analysis calculated: C, 65.61; H, 6.88; N, 11.48; Found: C, 65.33; H, 6.64; N, 11.54

The ¹H and ¹³C NMR spectra of the purified complex are shown in Figures 21-22.
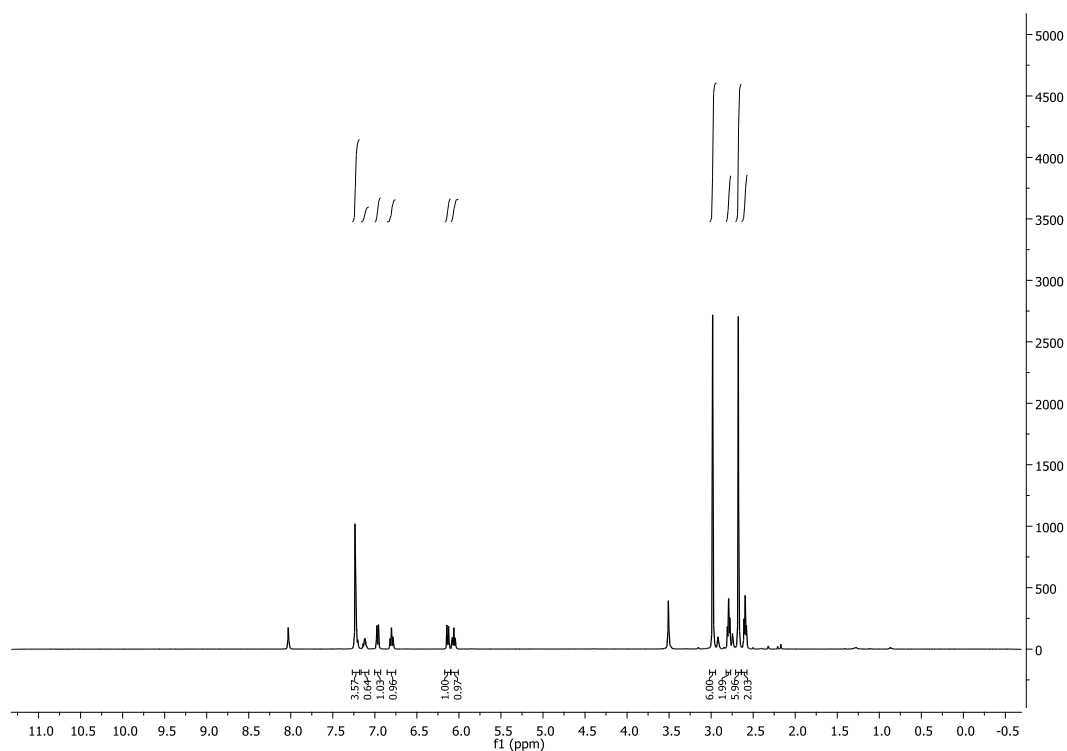
Figure 21. ¹H NMR spectrum of pure complex **26**.

Figure 22. ^{13}C NMR spectrum of pure complex **26**.

- *Reaction profile for the coupling process of 1-iodooctane with 1-phenylacetylene (^{1}H NMR profile, Figure 7):*

3 mg of complex **7** (0.008 mmol, 3.5 mol %), 5 mg of CuI (0.026 mmol, 10 mol %), 28 mg of LiOBu^{t} (0.35 mmol), 46 µL of 1-iodooctane (0.25 mmol) were placed in a vial and 1 mL of d7-DMF were added. 38 µL of 1-phenylacetylene (0.35 mmol) were added to the reaction mixture to start the coupling process. The reaction mixture was placed in a NMR tube and a ^{1}H NMR spectrum was recorded approximately every 15 min.

- *Reaction (2):*
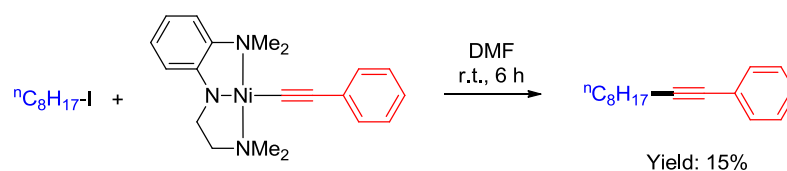
40 mg of complex **26** (0.109 mmol) and 20 µL of 1-iodooctane (0.109 mmol) were placed in a vial and 1 mL of DMF were added. The reaction was stirred at room temperature during 6

hours. The reaction was then quenched in water and extracted with ether. The coupling yield was calculated by GC analysis.

- *Reaction (3):*

40 mg of complex **26** (0.109 mmol), 2 mg of CuI (0.0105 mmol) and 20 µL of 1-iodooctane (0.109 mmol) were placed in a vial and 1 mL of DMF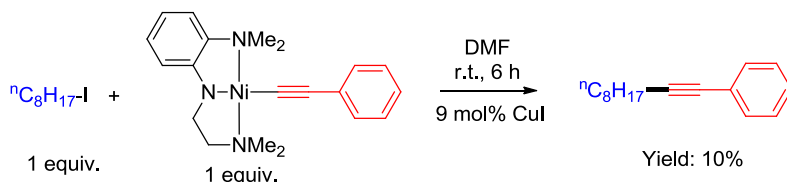 were added. The reaction was stirred at room temperature during 6 hours. The reaction was then quenched in water and extracted with ether. The coupling yield was calculated by GC analysis.

- *Reaction (4):*

40 mg of complex **26** (0.109 mmol), 2 mg of CuI (0.0105 mmol), 20 µL of 1-iodooctane (0.109 mmol),   12 µL of phenylacetylene (0.109 mmol) and 12 mg of LiO^{t}Bu (0.15 mmol) were placed in a vial and 1 mL of DMF were added. The reaction was stirred during 6 hours. The reaction was then quenched in water and extracted with ether. The coupling yield was calculated by GC analysis.

- *Reaction (5):*

40 mg of complex **26** (0.109 mmol), 2 mg of CuI (0.0105 mmol), 20 µL of 1-iodooctane (0.109 mmol), 12 µL of phenylacetylene (0.109 mmol), 16 µL of oct-1-yne (0.109 mmol) and 12 mg of LiOBu^t (0.15 mmol) were placed in a vial and 1 mL of DMF were added. The
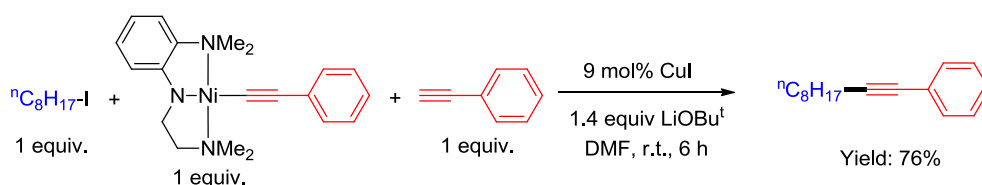
resulting solution was stirred during 6 hours. The reaction was then quenched in water and extracted with ether. The coupling yields were calculated by GC analysis.
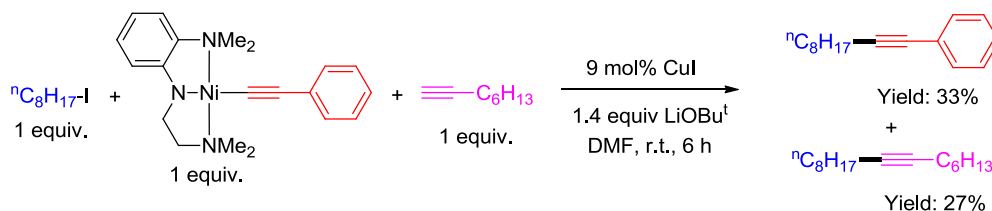
- *Reaction (6)*
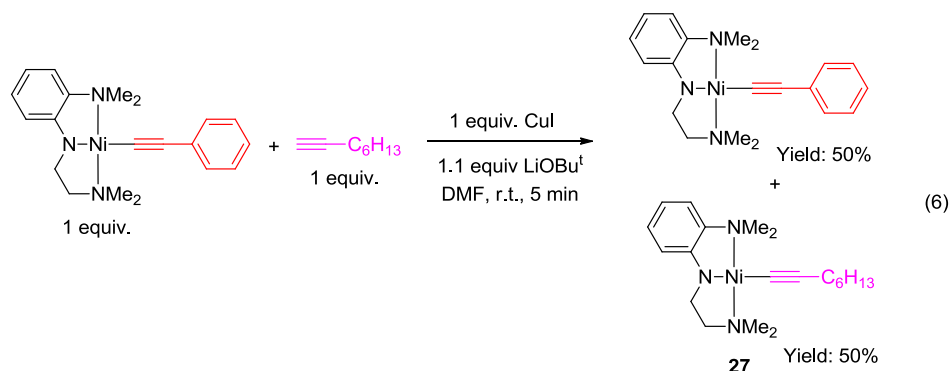
25 mg of complex **26** (0.068 mmol), 13 mg of CuI (0.068 mmol), 10 µL of oct-1-yne (0.068 mmol) and 6 mg of LiOBu^t (0.075 mmol) were placed in a vial and 0.6 mL of d7-DMF were added. The resulting solution was immediately placed in a NMR tube and the ^{1}H NMR spectrum was recorded. Figure 23 shows the NMR spectrum of the exchange process compared to spectrum of complex **26** and to spectrum of the product of the reaction between complex **25** and oct-1-yne. The areas of methyl signals indicate that two complexes formed are closely to equal proportion. The exchange reaction was fast (below 5 minutes); no significant further change of the ratios of was observed after 3 hours (Figure 23).
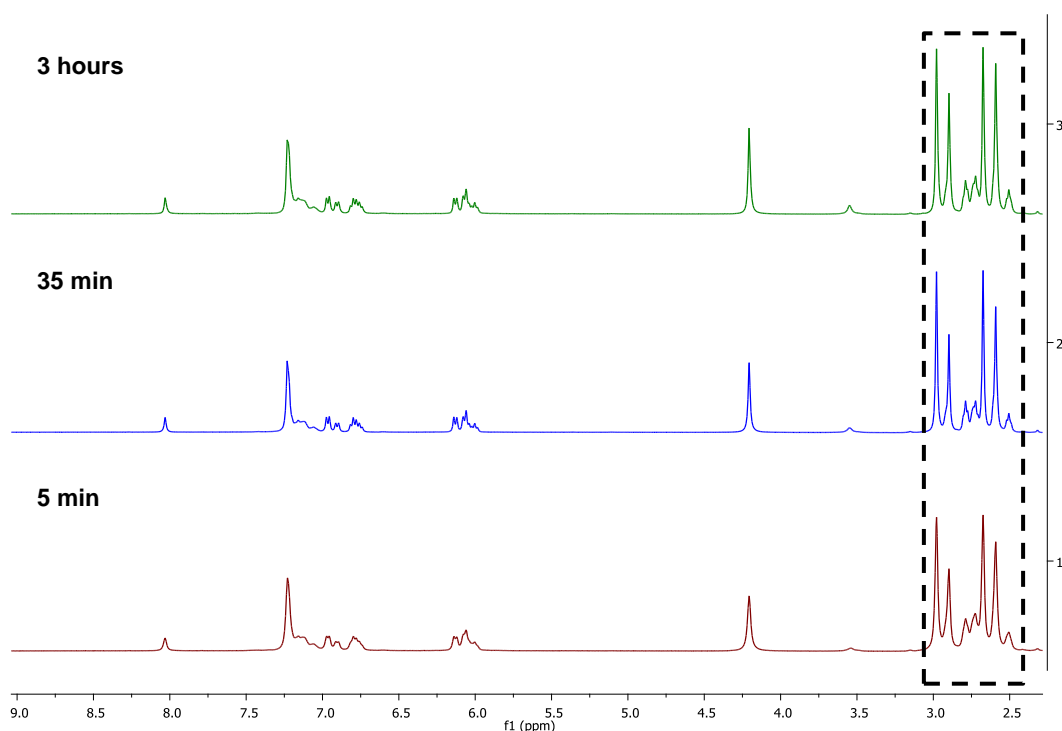
Figure 23. Time-depending NMR spectra for exchange process of complex **26** in presence of oct-1-yne.

- *Reaction of complex **25** with oct-1-yne:*

The synthesis of a pure alkyne complex was not possible using a 1:1 ratio of complex **25** and oct-1-yne. Nevertheless using an excess of oct-1-yne (21 equiv.), a major Ni-alkynyl complex was obtained. Th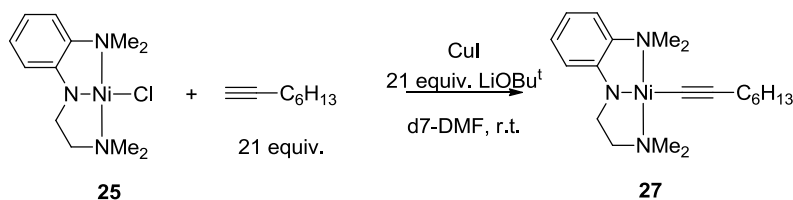e experimental conditions were the following: 5 mg of complex **25** (0.016 mmol), 4 mg of CuI (0.021 mmol), 50 µL of oct-1-yne (0.335 mmol) and 27 mg of LiO^{t}Bu (0.335 mmol) were placed in a vial and 0.6 mL of d7-DMF were added. The resulting solution was immediately placed in a NMR tube and the ^{1}H NMR spectrum was recorded (Figure 13, ^{1}H NMR red spectrum).

5.9.12 Detailed description for coupling products (Table 2)

hexadec-7-yne, entry 1

Purified by column (SiO$_2$, Hexane), 60% yield as a transparent liquid.
^{1}H NMR (400 MHz, CDCl$_3$): 2.13 (t, J = 6.9 Hz, 4H), 1.53 − 1.42 (m, 4H), 1.42 − 1.32 (m, 4H), 1.32 − 1.20 (m, 12H), 0.88 (td, *J* = 6.8, 2.8 Hz, 6H).
^{13}C NMR (100 MHz, CDCl$_3$): 80.36, 32.02, 31.55, 29.40, 29.31, 29.03, 28.70, 22.83, 22.74, 18.91, 14.24, 14.20.
MS-APPI: calculated for (C$_{16}$H$_{30}$, M), 222.2342; found, 222.2333.

dec-1-yn-1-ylbenzene, entry 2
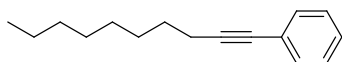
Purified by column (SiO$_2$, Hexane), 60% yield as a transparent liquid.
^{1}H NMR (400 MHz, CDCl$_3$): 7.45 − 7.41 (m, 2H), 7.36 − 7.22 (m, 3H), 2.44 (t, *J* = 7.1 Hz, 2H), 1.68 − 1.58 (m, 2H), 1.54 − 1.42 (m, 2H), 1.40 − 1.24 (m, 8H), 0.93 (t, *J* = 7.2 Hz, 3H).
^{13}C NMR (400 MHz, CDCl$_3$): 131.67, 128.30, 127.57, 124.24, 90.62, 80.67, 32.00, 29.37, 29.29, 29.09, 28.92, 22.82, 19.56, 14.27.
HRESI-MS: calculated for (C$_{16}$H$_{23}$, M+H), 215.1800; found, 215.1805.

dodec-1-yn-1-yltrimethylsilane, entry 3
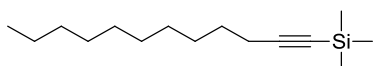
Purified by column (SiO$_2$, Hexane), 58% yield as a yellow liquid.
**^{1}H NMR** (400 MHz, CDCl$_3$): 2.20 (t, *J* = 7.2 Hz, 2H), 1.56 − 1.43 (m, 2H), 1.41 − 1.20 (m, 14H), 0.88 (t, *J* = 6.8 Hz, 3H), 0.14 (m, 9H).
^{13}C NMR (100 MHz, CDCl$_3$): 107.94, 84.35, 32.07, 29.71, 29.65, 29.48, 29.24, 28.96, 28.79, 22.84, 20.01, 14.27, 0.33.
Anal. Calcd for C$_{15}$H$_{30}$Si : C , 75.54; H, 12.68. Found: C, 75.36; H, 13.00.

2-(dec-1-yn-1-yl)-6-methoxynaphthalene, entry 4
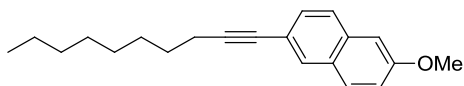
Purified by column (SiO$_2$, Hexane:EtOAc 95:5), 60% yield as a white solid.
^{1}H NMR (400 MHz, CDCl$_3$): 7.83 (s, 1H), 7.69 − 7.62 (m, 2H), 7.42 (dd, *J* = 8.4, 1.6 Hz, 1H), 7.13 (dd, *J* = 8.9, 2.5 Hz, 1H), 7.09 (d, *J* = 2.4 Hz, 1H), 3.91 (s, 3H), 2.44 (t, *J* = 7.1 Hz, 2H), 1.64 (dt, *J* = 14.7, 7.1 Hz, 2H), 1.53 − 1.42 (m, 2H), 1.39 − 1.24 (m, 8H), 0.89 (t, *J* = 7.2 Hz, 3H).

^{13}C NMR (100 MHz, CDCl$_3$): 158.09, 133.80, 130.97, 129.47, 129.26, 128.68, 126.76, 119.33, 119.18, 105.85, 90.21, 81.05, 55.45, 32.02, 29.38, 29.31, 29.13, 29.01, 22.83, 19.66, 14.28.
HRESI-MS: calculated for (C$_{21}$H$_{27}$O$_2$, M+H), 295.2062; found, 295.2058.

2-(tridec-4-yn-1-yloxy)tetrahydro-2H-pyran, entry 5
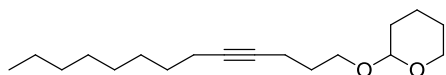
Purified by column (SiO$_2$, Hexane:EtOAc 90:10), 64% yield as a transparent liquid.
^{1}H NMR (400 MHz, CDCl$_3$): 4.59 (t, J = 4 Hz, 1H), 3.93 − 3.73 (m, 2H), 3.57 − 3.40 (m, 2H), 2.32 − 2.28-2.23 (m, 2H), 2.14-2.09 (m, 2H), 1.88 − 1.64 (m, 4H), 1.64 − 1.39 (m, 6H), 1.40 − 1.18 (m, 10H), 0.87 (t, J = 6.9 Hz, 3H).
^{13}C NMR (100 MHz, CDCl$_3$): 98.90, 80.74, 79.52, 66.23, 62.26, 32.00, 30.84, 29.48, 29.36, 29.28, 29.03, 25.66, 22.81, 19.66, 18.90, 15.80, 14.24.
HRESI-MS: calculated for (C$_{18}$H$_{32}$O$_2$Ag, M+Ag), 387.1453; found, 387.1459.

1-(piperidin-1-yl)tetradec-5-yn-1-one, entry 6
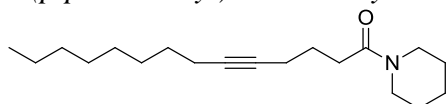
Purified by column (SiO$_2$, Hexane:EtOAc 90:10), 63% yield as a yellow liquid.
^{1}H NMR (400 MHz, CDCl$_3$): 3.52 (t, J = 5.6 Hz, 2H), 3.39 (t, J = 5.6 Hz, 2H), 2.41 (t, J = 1.3 Hz, 2H), 2.22 − 2.18 (m, 2H), 2.13 − 2.08 (m, 2H), 1.82 − 1.71 (m, 2H), 1.64 − 1.58 (m, 2H), 1.56 − 1.47 (m, 4H), 1.46 − 1.40 (m, 2H), 1.35 − 1.18 (m, 10H), 0.85 (t, J = 6.9 Hz, 3H).
^{13}C NMR (100 MHz, CDCl$_3$): 170.94, 81.13, 79.40, 46.72, 42.72, 32.12, 31.94, 29.22, 28.99, 26.64, 25.68, 24.86, 24.69, 22.74, 18.83, 18.55, 14.18.
HRESI-MS: calculated for (C$_{19}$H$_{34}$NO, M+H), 292.2640; found, 292.2648.

4-(tetradec-5-yn-1-yl)morpholine, entry 7
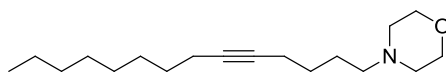
Purified by column (SiO$_2$, Hexane:EtOAc 90:10), 60% yield as a yellow liquid.
^{1}H NMR (400 MHz, CDCl$_3$): 3.73 − 3.64 (m, 4H), 2.45 − 2.36 (m, 4H), 2.31 (dd, J = 8.2, 6.6 Hz, 2H), 2.18 − 2.07 (m, 4H), 1.62 − 1.52 (m, 2H), 1.50 − 1.37 (m, 4H), 1.36 − 1.19 (m, 10H), 0.85 (t, J = 6.9 Hz, 3H).
^{13}C NMR (100 MHz, CDCl$_3$): 80.70, 79.81, 67.11, 58.70, 53.85, 31.95, 29.33, 29.24, 29.00, 27.11, 25.78, 22.77, 18.85, 18.79, 14.22.
HRESI-MS: calculated for (C$_{18}$H$_{34}$NO, M+H), 280.2640; found, 280.2641.

2-(undec-4-yn-1-yl)furan, entry 8
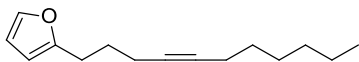
Purified by column (SiO$_2$, Hexane:EtOAc 90:10), 65% yield as a yellow liquid.
^{1}H NMR (400 MHz, CDCl$_3$): 7.20 (dd, *J* = 1.7, 0.7 Hz, 1H), 6.18 (dd, *J* = 3.0, 1.9 Hz, 1H), 5.90 (dd, *J* = 3.0, 1.9 Hz, 1H), 2.63 (t, *J* = 7.6 Hz, 2H), 2.12 – 2.02 (m, 4H), 1.72 (q, *J* = 7.2 Hz, 2H), 1.44 – 1.35 (m, 2H), 1.32 – 1.13 (m, 6H), 0.79 (t, *J* = 6.4 Hz, 3H).
^{13}C NMR (100 MHz, CDCl$_3$): 155.78, 140.99, 110.20, 105.17, 81.12, 79.43, 31.53, 29.26, 28.71, 27.68, 27.15, 22.73, 18.92, 18.42, 14.20
HRESI-MS: calculated for (C$_{15}$H$_{22}$OAg, M+Ag), 325.0722; found, 325.0716.

tridec-6-yn-1-yl acetate, entry 9
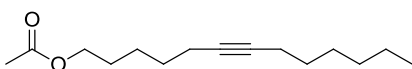
Purified by column (SiO$_2$, Hexane:EtOAc 90:10), 52% yield as a yellow liquid.
^{1}H NMR (400 MHz, CDCl$_3$): 4.06 (t, *J* = 6.7 Hz, 2H), 2.20 – 2.09 (m, 4H), 2.04 (s, 3H), 1.69 – 1.57 (m, 2H), 1.54 – 1.39 (m, 4H), 1.39 – 1.20 (m, 8H), 0.88 (t, *J* = 6.8 Hz, 3H).
^{13}C NMR (100 MHz, CDCl$_3$): 171.70, 81.05, 80.14, 64.94, 31.82, 30.16, 29.17, 29.01, 28.61, 25.59, 23.03, 21.48, 19.20, 19.11, 14.52.
HRESI-MS: calculated for (C$_{15}$H$_{26}$O$_2$Na, M+Na), 261.1830; found, 261.1834.

10-chlorodec-6-yn-1-yl acetate, entry 10
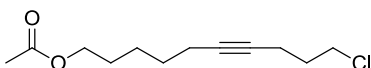
Purified by column (SiO$_2$, Hexane:EtOAc 90:10), 50% yield as a yellow liquid.
^{1}H NMR (400 MHz, CDCl$_3$): 4.06 (t, *J* = 6.7 Hz, 2H), 3.65 (t, *J* = 6.4 Hz, 2H), 2.38 – 2.31 (m, 2H), 2.18 - 2.12 (m , 2H), 2.05 (s, 3H), 1.98 – 1.85 (m, 2H), 1.69 – 1.59 (m, 2H), 1.57 – 1.37 (m, 4H).
^{13}C NMR (100 MHz, CDCl$_3$): 171.27, 81.07, 78.50, 64.57, 43.94, 31.87, 28.73, 28.29, 25.30, 21.17, 18.75, 16.33.
HRESI-MS: calculated for (C$_{12}$H$_{20}$ClO$_2$, M+H), 231.1152; found, 231.1154.

phenyl(4-(tridec-4-yn-1-yloxy)phenyl)methanone, entry 11
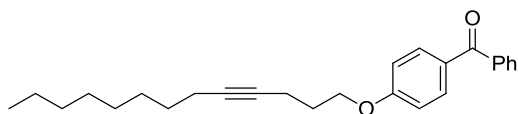
Purified by column (SiO$_2$, Hexane:EtOAc 90:10), 65% yield as a transparent liquid.
^{1}H NMR (400 MHz, CDCl$_3$): 7.85 − 7.79 (m, 2H), 7.78 − 7.73 (m, 2H), 7.59 − 7.53 (m, 1H), 7.49 - 7.44 (m, 2H), 6.99 − 6.94 (m, 2H), 4.15 (t, *J* = 6.2 Hz, 2H), 2.38 (tt, *J* = 6.7, 2.2 Hz, 2H), 2.14 (tt, *J* = 7.1, 2.3 Hz, 2H), 1.99 (p, *J* = 6.6 Hz, 2H), 1.52 − 1.41 (m, 2H), 1.39 − 1.32 (m, 2H), 1.30 − 1.12 (m, 8H), 0.87 (t, *J* = 6.8 Hz, 3H).
^{13}C NMR (100 MHz, CDCl$_3$): 195.67, 162.84, 138.45, 132.69, 131.97, 130.14, 129.84, 128.30, 114.15, 81.42, 78.73, 66.84, 31.96, 29.34, 29.24, 29.18, 29.02, 28.69, 22.78, 18.85, 15.56, 14.24.
HRESI-MS: calculated for (C$_{26}$H$_{33}$O$_2$, M+H), 377.2480; found, 377.2488.

1-(dec-1-yn-1-yl)-4-methoxybenzene, entry 12
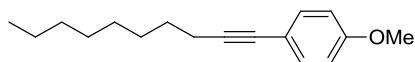
Purified by column (SiO$_2$, Hexane:EtOAc 90:10), 57% yield as a transparent liquid.
^{1}H NMR (400 MHz, CDCl$_3$): 7.35 − 7.30 (m, 2H), 6.83 − 6.78 (m, 2H), 3.80 (s, 3H), 2.38 (t, *J* = 7.1 Hz, 2H), 1.64 − 1.53 (m, 2H), 1.50 − 1.39 (m, 2H), 1.35 − 1.25 (m, 8H), 0.89 (t, *J* = 6.8 Hz, 3H).
^{13}C NMR (100 MHz, CDCl$_3$): 159.11, 132.98, 116.44, 113.93, 88.96, 80.36, 55.38, 32.01, 29.37, 29.30, 29.11, 29.04, 22.82, 19.57, 14.26.
HRESI-MS: calculated for (C$_{17}$H$_{25}$O, M+H), 245.1905; found, 245.1907.

tetradec-7-ynenitrile, entry 13
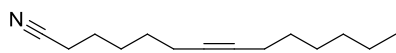
Purified by column (SiO$_2$, Hexane:EtOAc 85:15), 60% yield as a yellow liquid.
^{1}H NMR (400 MHz, CDCl$_3$): 2.35 (t, *J* = 7.1 Hz, 2H), 2.20 − 2.10 (m, 4H), 1.73 − 1.63 (m, 2H), 1.60 − 1.42 (m, 6H), 1.40 − 1.20 (m, 6H), 0.88 (t, *J* = 8.4 Hz, 3H).
^{13}C NMR (100 MHz, CDCl$_3$): 119.85, 81.07, 79.41, 31.50, 29.20, 28.70, 28.32, 27.96, 25.14, 22.72, 18.87, 18.63, 17.25, 14.21.
HRESI-MS: calculated for (C$_{14}$H$_{23}$NAg, M+Ag), 312.0881; found, 312.0878.

5.10 References

(1)   *Chemistry of Triple-Bonded Functional Groups*; Patai, S. ed.; Wiley: New York, 1994.
(2)   *Modern Acetylene Chemistry*; Stang, P. J.; Diederich, F. ed.; VCH: Weinheim, 1995.
(3)   *Handbook of Organopalladium Chemistry for Organic Synthesis*; Sonogashira K.; Negishi, E. ed.; Willey-Interscience: New York: 2002; Vol. 1.
(4)   Chinchilla, R.; Najera, C. *Chem. Soc. Rev.* **2011**, *40*, 5084.
(5)   Chinchilla, R.; Nájera, C. *Chem. Rev.* **2007**, *107*, 874.
(6)   Negishi, E.-i.; Anastasia, L. *Chem. Rev.* **2003**, *103*, 1979.
(7)   Cahiez, G.; Gager, O.; Buendia, J. *Angew. Chem. Int. Ed.* **2010**, *49*, 1278.
(8)   Thaler, T.; Guo, L.-N.; Mayer, P.; Knochel, P. *Angew. Chem. Int. Ed.* **2011**, *50*, 2174.
(9)   Cheung, C. W.; Ren, P.; Hu, X. *Org. Lett.* **2014**, *16*, 2566.
(10)   Hatakeyama, T.; Okada, Y.; Yoshimoto, Y.; Nakamura, M. *Angew. Chem. Int. Ed.* **2011**, *50*, 10973.
(11)   Ohmiya, H.; Yorimitsu, H.; Oshima, K. *Org. Lett.* **2006**, *8*, 3093.
(12)   Vechorkin, O.; Godinat, A.; Scopelliti, R.; Hu, X. *Angew. Chem. Int. Ed.* **2011**, *50*, 11777.
(13)   Eckhardt, M.; Fu, G. C. *J. Am. Chem. Soc.* **2003**, *125*, 13642.
(14)   Altenhoff, G.; Würtz, S.; Glorius, F. *Tetrahedron Lett.* **2006**, *47*, 2925.
(15)   Vechorkin, O.; Barmaz, D.; Proust, V.; Hu, X. *J. Am. Chem. Soc.* **2009**, *131*, 12078.
(16)   Yi, J.; Lu, X.; Sun, Y.-Y.; Xiao, B.; Liu, L. *Angew. Chem. Int. Ed.* **2013**, *52*, 12409.
(17)   Ren, P.; Vechorkin, O.; Csok, Z.; Salihu, I.; Scopelliti, R.; Hu, X. *Dalton Trans.* **2011**, *40*, 8906.
(18)   Ren, P.; Vechorkin, O.; Allmen, K. v.; Scopelliti, R.; Hu, X. *J. Am. Chem. Soc.* **2011**, *133*, 7084.
(19)   Ren, P., PhD. Thesis, Ecole Polytechnique Fédérale de Lausanne, 2012.
(20)   Csok, Z.; Vechorkin, O.; Harkins, S. B.; Scopelliti, R.; Hu, X. *J. Am. Chem. Soc.* **2008**, *130*, 8156.
(21)   Blackmond, D. G. *Angew. Chem., Int. Ed.* **2005**, *44*, 4302.
(22)   Hartwig, J. F. *Inorg. Chem.* **2007**, *46*, 1936.
(23)   Terao, J.; Kambe, N. *Acc. Chem. Res.* **2008**, *41*, 1545.
(24)   Jones, G. D.; McFarland, C.; Anderson, T. J.; Vicic, D. A. *Chem. Comm.* **2005**, 4211.
(25)   Hu, X. *Chem. Sci.* **2011**, *2*, 1867.
(26)   Breitenfeld, J.; Wodrich, M. D.; Hu, X. *Organometallics* **2014**, *33*, 5708.
(27)   Breitenfeld, J.; Ruiz, J.; Wodrich, M. D.; Hu, X. *J. Am. Chem. Soc.* **2013**, *135*, 12004.
(28)   Anderson, T. J.; Jones, G. D.; Vicic, D. A. *J. Am. Chem. Soc.* **2004**, *126*, 8100.
(29)   Gallego, D.; Brück, A.; Irran, E.; Meier, F.; Kaupp, M.; Driess, M.; Hartwig, J. F. *J. Am. Chem. Soc.* **2013**, *135*, 15617.
(30)   Renard, M.; Ghosez, L. A. *Tetrahedron* **2001**, *57*, 2597.
(31)   Gómez, G.; Rivera, H.; García, I.; Estévez, L.; Fall, Y. *Tetrahedron Lett.* **2005**, *46*, 5819.
(32)   Oku, A.; Harada, T.; Kita, K. *Tetrahedron Lett.* **1982**, *23*, 681.
(33)   Xu, T.; Cheung, C. W.; Hu, X. *Ang. Chem. Int. Ed.* **2014**, *53*, 4910.

Conclusions and Perspectives

This work was focused on the development and catalytic application of well-defined amido – amine nickel complexes. The research followed two directions: (i) the development of stereoselective cross coupling methodologies for non-activated secondary halides and (ii) the mechanistic studies of the Sonogashira coupling of alkyl halides at room temperature.

We extended the application of complex Nickamine **1** to the catalysis of diastereoselective Kumada coupling of 1,3- and 1,4-substituted cyclohexyl derivatives as well as for tetrahydropyranes. The coupling yields and the dr values of coupling products were very high. The stereoselectivity of the process was controlled by the bulky structure of **1** and by the chemical properties of the substituent on the cyclohexyl halide. Furthermore, we conducted mechanistic investigations that showed evidence that the activation of the cyclohexyl halide goes through a reverse radical process.

We synthesized well-defined nickel complex (*S*)-**8** having a bidentate chiral ligand derived from α-methylbenzylamine. The complex is an effective catalyst for the alkyl – alkyl Kumada coupling of secondary halides but it didn't show any asymmetric induction capacity. We believed that the structure of (*S*)-**8** in solution, is not rigid enough to efficiently transmit the chirality during the coupling process. Looking for a more rigid structure, we developed nickel pincer complex **23** having dimethyl amino and pyrrolidine donors. Complex **23** is an active catalyst for the coupling of acyclic and cyclic non-activated secondary halides with alkyl and aryl Grignard reagents. The structure of this complex constitutes an ideal molecular frame to include chirality. Our group is currently developing a new chiral amido – amine ligand having dimethyl amino and (2*R*,5*R*)-2,5-dimethylpyrrolidine donors. We expect that the corresponding pincer nickel complex will be able to catalyze stereoconvergent Kumada coupling reactions of secondary alkyl halides.

Finally, we succeed to catalyze the Sonogashira coupling of alkyl halides at room temperature using amido – bis(amine) nickel pincer complex **25** having a ligand with aryl dimethyl amino and ethylene dimethyl amino arms. We discovered that is the ethylene dimethyl amino arm that enhances the catalytic activity of the complex because of its hemilabile character. Moreover, we were able to fully characterize an alkynyl nickel intermediate. This mechanistic understanding is what it makes our system advantageous over the limited reported coupling methodologies of this process. In the future, the catalytic application of our system should be extended to the Sonogashira coupling of secondary alkyl halides.

Curriculum Vitae

Pablo Marcelo Pérez García

Birth Date: 12.11.1982 – Nationality: Bolivian

Professional experience

Swiss Federal Institute of Technology in Lausanne – EPFL, Switzerland   03/2011 – 08/2015
Research assistant.

- Developed multi-step organic synthesis of potential organic pincer ligands scaling-up from mg to grams.
- Conducted chemical product characterization by: NMR, GC-MS, TLC, chiral HPLC techniques.
- Improved free-oxygen synthetic methodologies for organometallic nickel complexes.
- Screened and optimized reaction conditions for cross-coupling process catalyzed by homogenous catalysts.
- Designed accurate chemical monitoring analytic protocols for kinetic studies to elucidate catalysis mechanisms.
- Coordinated the purchases of scientific equipment and managed the laboratory inventory.

Swiss Federal Institute of Technology in Lausanne – EPFL, Switzerland   03/2011 – 08/2015
Teaching assistant.

- Supervised two master research projects and the micro-reactor project for the chemical engineering laboratory.
- Supported the theoretical teaching and the final evaluation of the following courses: General Chemistry (200 students) and Coordination Chemistry (70 students).
- Trained two chemistry technicians during their professional stage.

Catholic University of Bolivia, Cochabamba – Bolivia.   07/2006 – 12/2010
Lecturer and experimental trainer at the Engineering Department.

American International School of Bolivia, Cochabamba – Bolivia.   10/2009 – 11/2010
Teacher of Physical Sciences.

Education

PhDc. in Chemistry and Chemical Engineering   03/2011 – 08/2015
Swiss Federal Institute of Technology in Lausanne – EPFL, Lausanne –Switzerland.
Director: Prof. Xile Hu – Laboratory of Inorganic Synthesis and Catalysis

Additional Semester in Chemical Engineering   03/2008 – 07/2008
Swiss Federal Institute of Technology in Lausanne – EPFL, Lausanne –Switzerland.
Relevant courses: chemical engineering laboratory, chemical reaction engineering, transfer phenomena, process control, biotechnology and legislation in laboratory work.

BSc. – MSc. Chemistry   09/2001 – 05/2006
University of Geneva, Geneva – Switzerland.

- Master Research Project: Improved the synthesis of quinine derived organic catalyst and screened its activity for enantioselective acylations.
    Director: Prof. E. P. Kündig
Scholarship: Simon I. Patiño Foundation – Best high school students from Bolivia.

Academic Presentations and Publications

European Symposium on Organic Chemistry, Marseille – France. $7^{th} – 12^{th}$ /07/2013
Poster presentation.

Conférence Universitaire de Suisse Occidentale, Geneva – Switzerland. $13^{th} – 14^{th}$ /12/2012
Oral presentation.

Publications:

E. P. Kündig, A. Enriquez Garcia, T. Lomberget, P. Perez Garcia, P. Romanens, "Truncated Cinchona alkaloids as catalysts in enantioselective monobenzoylation of meso-1,2-diols" *Chem. Commun.* **2008**, 3519 – 3521.

P. M. Perez Garcia, T. Di Franco, A. Orssino, P. Ren, X. L. Hu, "Nickel-catalyzed diastereoselective alkyl-alkyl Kumada coupling reactions" *Org. Lett.* **2012**, *14*, 4286 – 4289.

P. M. Perez Garcia, P. Ren, R. Scopelliti, X. L. Hu, "Nickel-Catalyzed Direct Alkylation of Terminal Alkynes at Room Temperature: A Hemilabile Pincer Ligand Enhances Catalytic Activity" *ACS Catal.* **2015**, *5*, 1164 – 1171.

IT Skills

MS Office: proficiency; **Matlab** (*engineering calculations*): intermediate level; **ChemOffice** (*molecular drawing*): proficiency; **OriginPro** (*scientific data treatment*): familiarity; **AQUASIM** (*chemical reaction modelling*): familiarity.

Languages

Spanish (*native*); **English** (*C1*); **French** (*DALF C1, November 2013*).